ESTIMATION OF GROUNDWATER RECHARGE ALONG A PRECIPITATION GRADIENT FOR SAVANNAH AQUIFERS IN NAMIBIA WITH SPECIAL EMPHASIS ON THE IMPACT OF VEGETATION

A DISSERTATION SUBMITTED IN FULFILMENT OF THE REQUIREMENTS FOR THE DEGREE OF

DOCTOR OF PHILOSOPHY IN SCIENCE (GEOLOGY)

OF

THE UNIVERSITY OF NAMIBIA

BY

SHOOPALA UUGULU

200326244

OCTOBER 2022

MAIN SUPERVISOR: Dr. Heike Wanke (Geography and Environmental Management Department, University of the West of England)

CO-SUPERVISOR: Dr. Paul Koeniger (Federal Institute for Geosciences and Natural Resources (BGR))

Abstract

The quantification of groundwater resources is essential especially in water scarce countries like Namibia as well as the assessment of the influence of vegetation on groundwater recharge for a better management and sustainability of savannah aquifers. This study has two specific objectives which are firstly to identify groundwater recharge processes and quantify such along a precipitation gradient in Namibian savannah aquifers. Secondly, to determine the influence of savannah vegetation on groundwater recharge by determining the active root depth and source water sources for *S. mellifera* and *B. albitrunca.* The study was carried out along a precipitation gradient at three sites namely: Tsumeb; Waterberg and Kuzikus/Ebenhaezer.

The chloride mass balance (CMB) method and water stable isotope methods were used in determining groundwater recharge rates at the three sites. Precipitation samples from Tsumeb and Waterberg were collected during the rainy season from 2017 to 2018, while Kuzikus/Ebenhaezer samples were collected between 2014 and 2015. Groundwater samples were collected before, during and after rainy seasons from 2016 to 2017. A deuterium tracer was inserted at different plots with varying depths in December 2016 in order to assess the active root depths for both *S. mellifera* and *B. albitrunca* at Ebenhaezer farm. Both woody plants were sampled for the xylem and transpired water.

A scattered distribution of rain sample isotopic ratios along the global meteoric water line in the areas was attributed to a seasonal effect. Local meteoric water line equations for Tsumeb, Waterberg and Kuzikus/Ebenhaezer were obtained as: δ^2H = 7.78 $\delta^{18}O$ + 6.74, (R^2 = 0.95); δ^2H = 7.37 $\delta^{18}O$ + 5.77, R^2 = (0.97); δ^2H = 7.16 $\delta^{18}O$ +

9.88, (R^2 = 0.96) respectively. All the slopes obtained from three study sites are all lower than that of a global meteoric water line equation. A lower slope indicates that the local precipitation has experienced some sub cloud evaporation, leading to enrichment of heavy isotopes.

Waterberg groundwater plots on the GMWL which indicates little or absence of evaporation. Tsumeb groundwater plots on/close to the GMWL with an exception of groundwater from the karst Lake Otjikoto which is showing evaporation. Groundwater from Kuzikus/Ebenhaezer shows an evaporation effect. All groundwater isotopic values from three sites match those of precipitation depleted in heavy stable isotopes, which indicates that recharge only take place during January, February and March where the precipitation is highest and depleted in heavy stable isotopes. CMB method revealed that savannah aquifers are recharged at low rates, mostly below 10% of the annual precipitation

The analysis of woody plant water isotopes at Ebenhaezer farm revealed their source water and the active root depth for *S. mellifera*. Of 49 transpired water samples, only one *S. mellifera* sample showed a high deuterium content of 515.9 ‰ where the tracer was inserted at 2.5 m soil depth. Elevated deuterium contents were observed in two *S. mellifera* xylem samples where the tracer was applied at 2.5 m and 3 m, a possible sign of the active root depth for *S. mellifera*. However, the active root depth of *B. albitrunca* could not be determined due to the absence of the tracer in the sampling depths used. *S. mellifera* $\delta^{18}O$ values indicate that it is using both groundwater and soil water while *B. albitrunca* $\delta^{18}O$ values show that it is mainly using groundwater. Groundwater recharge rates from this study can be used to guide policy makers on decisions regarding safe yields for the sustainability of the aquifers.

List of Publication(s)/Conference(s) proceedings

Peer reviewed articles

1. **Uugulu, S**. and Wanke, H., **2021** Determination of local meteoric water lines along a precipitation gradient, Namibia. *International Science and Technology Journal Namibia*

2. **Uugulu, S**. and Wanke, H., **2020**. Estimation of groundwater recharge in savannah aquifers along a precipitation gradient using chloride mass balance method and environmental isotopes, Namibia. *Physics and Chemistry of the Earth, Parts A/B/C*, p.102844.

Co-authorship of a peer reviewed article related to this study

3. Geißler, K., Heblack, J., **Uugulu, S.,** Wanke, H. and Blaum, N., **2019**. Partitioning of water between differently sized shrubs and potential groundwater recharge in a semiarid savannah in Namibia. *Frontiers in Plant Science*, *10*, p.1411.

Manuscript to be submitted to a peer reviewed journal

4. **Uugulu, S.** and Wanke, H., **(2022)**. Estimation of water sources and active root depth of woody plants using deuterium tracer at the savannah site in Namibia. *Journal of Ecohydrology and hydrobiology.*

Conference abstracts (oral presentations)

5. **Uugulu, S.** and Wanke (22th – 26th November **2020**). An isotopic study of groundwater at Waterberg, Namibia, 3rd SADC Groundwater Conference. Online

6. **Uugulu, S.** and Wanke, H. (13th – 14th November **2019**). Determination of local meteoric water lines along a precipitation gradient, Namibia. Book of Abstracts, 7th Science Annual Research Conference, UNAM. Windhoek, Namibia

7. **Uugulu, S.** and Wanke, H. (30th October – 1st November **2019**). Determination of active root depth and water sources of woody plants using deuterium tracer, Ebenhaezer, Namibia. Oral presentation at the 20th WaterNet/WARFSA/GWP-SA Symposium. Johannesburg, South Africa

8. **Uugulu, S.** and Wanke, H. (25th – 27th of October **2017**). Estimation of groundwater recharge using chloride mass balance method and isotopic composition along a precipitation gradient, Namibia Oral presentation at the 18th WaterNet/WARFSA/GWP-SA Symposium. Swakopmund, Namibia

9. **Uugulu, S.**, Wanke, H., Taapopi, J. (26th – 28th October **2016**). Estimation of groundwater recharge using chloride mass balance method and isotopic composition along a precipitation gradient, Namibia Oral presentation at the 17th WaterNet/WARFSA/GWP-SA Symposium. Gaborone, Botswana

Table of Contents

List of Tables

List of Figures

List of Abbreviations and/or Acronyms

BGR	Federal Institute for Geosciences and Natural Resources
BMBF	Federal Ministry for Economic Cooperation and Development
B. albitrunca	*Boscia albitrunca*
CEB	Cuvelai-Etosha Basin
CMB	Chloride mass balance
DEA	Directorate of Environmental Affairs
DEM	Digital Elevation Model
DWA	Department of Water Affairs
EC	Electric Conductivity
EU	European Union
Eq	Equation
JICA	Japan International Cooperation Agency
GMWL	Global Meteoric Water Line
GNIP	Global Network of Isotopes in Precipitation
GSN	Geological Survey of Namibia
Lat.	Latitude
LiCl	Lithium Chloride
LMWL	Local Meteoric Water Line

Long. Longitude

MAWRD Ministry of Agriculture, Water and Rural Development

NAMWATER Namibia Water Corporation Ltd

NAU Namibia Agricultural Union

NWR Namibia Wildlife Resorts

OPTIMASS Options for sustainable geo-biosphere feedback management in savannah systems under regional and global change

ORP Redox Potential

pers. comm personal communication

SADC Southern African Development Community

SASSCAL Southern African Science and Service Centre for Climate Change Adaptive Land Management and Land use

S. mellifera *Senegalia mellifera*

SPACE II Science Partnerships for the Adaptation to Complex Earth System Processes in the Southern Africa II

SRTM Shuttle Radar Topography Mission

Subsp. Subspecies

TDS Total Dissolved Solids

US United States

UNAM	University of Namibia
V-SMOW	Vienna Standard Mean Ocean Water
WHO	World Health Organization
ZFP	Zero-flux plane

Acknowledgements

“In all your ways acknowledge Him; And He shall direct your paths” Proverbs 3:6. Firstly I would like to acknowledge my Heavenly Father, His Holy Son Jesus Christ and the Holy Spirit for directing my paths in making this work possible. Secondly, let me express my sincere gratitude to the OPTIMASS Project for giving me this precious opportunity to carry out this research by funding it; I will always be grateful for that. I would like to acknowledge all individuals that supported me during my PhD study at the University of Namibia.

I would like to express my sincere gratitude to my main supervisor Dr. Heike Wanke for her invaluable guidance, support and encouragement throughout the study. I acknowledge the exchange of ideas and synergy of expertise with her that led to the realisation of this study. I cannot thank her enough.

I would like to thank my second supervisor Dr. Paul Koeniger for his guidance during laboratory work especially with the extraction and analysis of both xylem and soil water. I am thankful to his comments and corrections that have improved the quality of this work.

I would like to thank Dr. Rosemary Shikangalah and Prof. Benjamin Mapani for their words of encouragement and support.

I would like to express my gratitude to the entire Geology Department for the support, especially to Dr. Josefina Hamutoko for her guidance and Mr. Gabriel Nghikongelwa for escorting me on some of the field trips.

My heartfelt thanks go to my family and friends for their prayers, moral support and their words of encouragement during the course of my study.

Dedication

In loving memory of my maternal grandmother Rauha Nkondo Nahole-Nendongo who passed on just two hours before I gave a research proposal presentation for this work. I will always cherish the words of wisdom, prayers and also the good moments I have shared with GwaNahole.

Declarations

I, Shoopala Uugulu, hereby declare that this study is my own work and is a true reflection of my research, and that this work, or any part thereof has not been submitted for a degree at any other institution.

No part of this dissertation may be reproduced, stored in any retrieval system, or transmitted in any form, or by means (e.g. electronic, mechanical, photocopying, recording or otherwise) without the prior permission of the author, or The University of Namibia on behalf.

I, Shoopala Uugulu, grant The University of Namibia the right to reproduce this dissertation in whole or in part, in any manner or format, which The University of Namibia may deem fit.

....

Name of Student Signature Date

CHAPTER 1

INTRODUCTION

1.1 Background of the study

Water is one of the precious resources needed for living. In the past centuries, water scarcity has become a global phenomenon and by the year 2000, close to 80% of the global population was found to be living in high water stress regions (Vörösmarty et al., 2010; Zarch et al., 2015) and water use doubled in the second half of the twentieth century (MEA), 2005). The scarcity of water is mostly felt in arid and semi-arid regions due to the effects of climate change (Sharafatmandrad and Mashizi, 2021; Singh and Chudasama, 2021). Several studies have shown evidence of the occurrence of climate variation in the form of a rise in temperatures, low annual mean precipitation, sporadic rainfall, high seasonal and inter-annual variation (Allen et al., 2018; Gupta and Jain, 2018; Ramarao et al., 2019; Singh and Chudasama, 2021). The changes impact negatively on various natural resources resulting in extreme hydroclimatic events (floods and droughts), reduction of biodiversity and environmental degradation, reduction in agricultural productivity (Treut et al., 2007; Zarch et al., 2015), and also impact on groundwater systems through increase in temperature and potential evapotranspiration, decrease in precipitation, temperature, and changes in the composition of vegetation (Aguilera and Murillo, 2009; Haidu and Nistor, 2020; Meixner et al., 2016; Taylor et al., 2013).

Understanding and quantifying recharge of groundwater systems has never been more important in Africa than now and for the future as groundwater forms the basis of water supply to many African communities. As such, groundwater recharge is a fundamental factor for sustaining groundwater systems and the use of such systems to ensure community development and survival at large, especially under the factors of rapid population increase with subsequent demand on water supply and food production. There is often not an adequate, or sustainable, level of recharge in arid and semi-arid regions to keep groundwater supplies in line with demand.

Namibia is one of the driest countries in sub-Saharan Africa. More than 92% of the country is characterised by aridity (22% as hyper-arid (desert), 33% as arid, 37% as semi-arid, and only 8% is sub-humid) (Shanyengana et al., 2004; Shikangalah, 2020). Long-term temperature records from weather stations in Namibia have shown a mean decadal increase of 0.2 °C which is roughly three times the global mean temperature increase reported for the 20th century (Reid et al., 2007). It is also predicted that temperature increases in Namibia will be ranging from 2°C to 6 °C by the year 2100 (Reid et al., 2007) while evaporation rates are also exceedingly high, where mean annual evaporation from open water surfaces in western catchments is measured to be six times higher than the mean annual rainfall and 100 times higher in the arid parts of the country (Jacobson et al., 1995; Seely et al., 2003). Despite the harsh conditions, groundwater remains the most important source of water supply in Namibia. Over the past century, over 100,000 boreholes were drilled to supply water to around 80% of the country for industrial, municipal and rural water supply and consequently provide water to human population in both urban and rural areas for domestic and agricultural activities, for livestock and game, irrigation systems and also for tourism activities, industries and mining activities (NamWater, 2012). Water demand for such activities is estimated to increase from 416.1 million m^3/a in 2015 to about 572.5 m^3/a in 2025, while rural domestic use is estimated to slightly increase from 10.6 million m^3/a in 2015 to 10.9 million m^3/a in 2025 (NDP5, 2017).

One of the thematic areas in the SADC Regional Water Policy adopted in 2005 is water resources information and management. Information on water resources in the SADC region is often scarce and can only be made available by carrying out investigations on water resources in the respective countries (SADC, 2005). According to MAWRD (2000), one of the constraints of Namibia's water resources is the limited and sporadic annual recharge of groundwater. MAWRD (2000) further states that understanding aquifers recharge, aquatic ecology and groundwater flows is essential for the management of the water resources. At present there appear to be imbalances between the information and knowledge available, and the needs of those trying to manage the resource base in the interests of all Namibians. It is therefore fundamental to understand groundwater recharge in order to use available groundwater resources effectively and sustainably.

Vegetation is one of the main factors influencing groundwater. Within the context of global climate change, changes in precipitation patterns will have an important influence on water sources, water utilisation strategies and vegetation distributions of individual plant species (Ma et al., 2021; Pan et al., 2020). Moreover, global warming leads to excessive evapotranspiration forcing plants to use more soil bound water (Ma et al., 2021). However this is only possible if there is sufficient precipitation to replenish soil bound water and therefore the utilisation of groundwater by vegetation is likely to be intensified in the future due to climate change (Ma et al., 2021). Groundwater uptake by plants in water limited environments is either underestimated or disregarded because of limited knowledge about that phenomenon (Lubczynski, 2009). It is therefore important to investigate plants in particular their source water and the rooting depth they extract such water. Woody plants are efficient in finding soil moisture and hence reducing groundwater recharge (Geißler et al., 2019; Lubczynski, 2009). In dry areas like Namibia where water is a limiting factor, some plants adapt by developing tap roots (Lubczynski, 2009) and it is therefore important to know the active root depth at which plants are finding soil moisture. Such information is useful integrated into groundwater recharge models. The rooting depth is a useful parameter that can be integrated in groundwater recharge models such as soil water balance models. The rooting depth was identified as a high sensitive parameter to the soil water balance model (Finch, 1998).

This study addresses the knowledge gap of understanding groundwater recharge processes and their quantification, of understanding precipitation-groundwater relationships and of understanding the influence of woody plants in these processes in the savannah areas of Namibia. The study was carried out along a precipitation gradient in the savannah ecosystem with focus on three sites namely Tsumeb, Waterberg and Kuzikus /Ebenhaezer (Figure 1-1). The study areas indicate a precipitation gradient with the Tsumeb area within the Cuvelai-Etosha Basin, having the highest annual precipitation rate of about 600 mm/a and an annual potential evapotranspiration rate between 2000 to 3000 mm/a. Waterberg area within the Omatako Basin has a mean annual precipitation of about 450 mm/a and a potential evapotranspiration of about 2800 mm/a. Kuzikus/Ebenhaezer farm lies in the south-eastern part of Namibia within the Stampriet Basin, where the mean annual precipitation within the basin ranges between 175 mm/a to 240 mm/a from South to

North, with a potential evaporation varying from 3000 mm/a in the North to 3500 mm/a in the South (DWA, 1988).

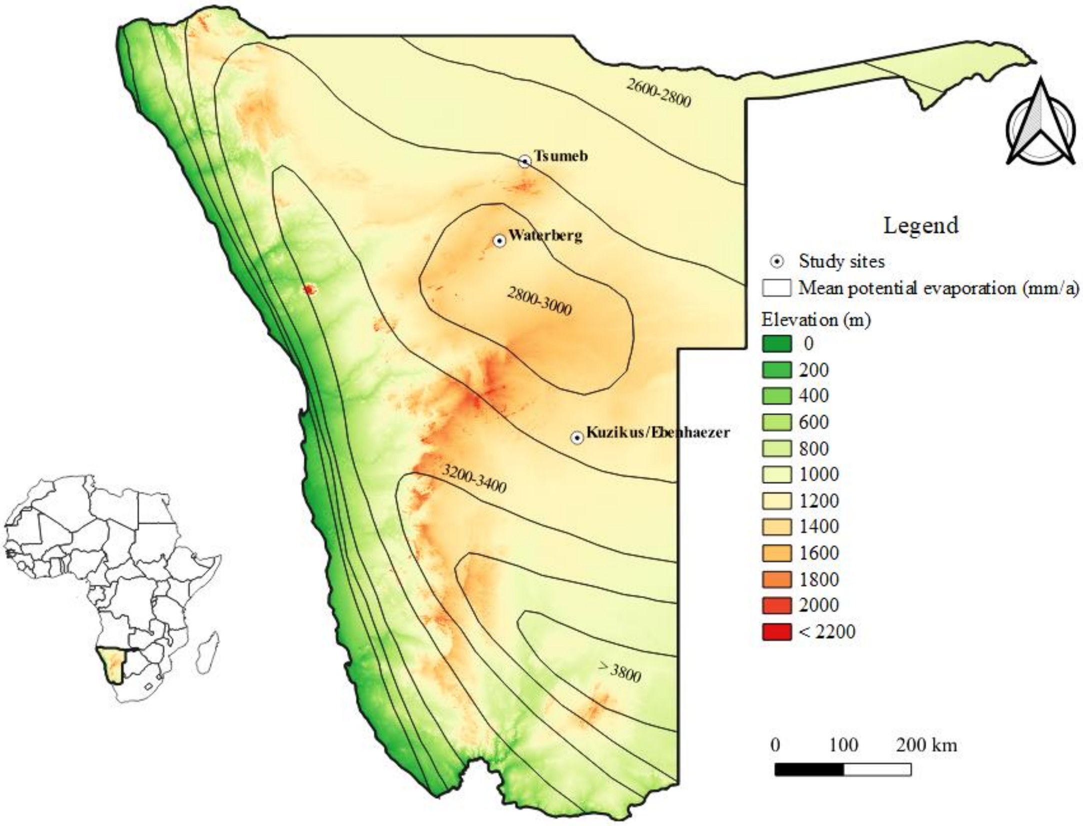

Figure 1-1: Location of the study areas and SRTM DEM (Data source:EarthExplorer); mean potential evaporation (Data source:DEA 2002).

1.2 Statement of the problem

Effective management of groundwater resources is necessary to ensure sustainability of aquifers but this is only possible when groundwater systems are fully understood, including the understanding of recharge processes, the influence of precipitation gradients as well as the impact of woody plants on water resources in a savannah system. No groundwater recharge studies have been carried out along a wide precipitation gradient before in Namibia. Moreover, the influence of woody plants on groundwater recharge in semi-arid regions like in Namibia is insufficiently studied;

thus water sources and active root depths of *S. mellifera* and *B. albitrunca* have not been investigated before.

1.3 Objectives of the study

The study was carried out under the following two main objectives:

- To identify groundwater recharge processes and quantify groundwater recharge rates along a precipitation gradient in Namibian savannah aquifers. This objective is addressed in Chapter 3 and Chapter 4.
- To determine the influence of savannah woody plants on groundwater recharge along a precipitation gradient. This objective is addressed in Chapter 5.

1.4 Hypotheses of the study

- It is hypothesised that groundwater recharge rates increase along a precipitation gradient in savannah aquifers of Namibia, thus Tsumeb with annual precipitation of 600 mm is expected to have a higher groundwater recharge rate, followed by Waterberg with annual precipitation of 450 mm and lastly Kuzikus/Ebenhaezer with the lowest annual precipitation of 240 mm.
- The presence of the woody plants in a savannah reduces groundwater recharge, owing to water uptake in the unsaturated zone, hence shallowly rooted woody plants such as *S. mellifera* use soil water while deep rooted woody plants such as *B. albitrunca* use groundwater.
- There is a seasonal variation in source water, especially with *S. mellifera* that can develop tap roots.

1.5 Significance of the study

The study increases the understanding of hydrological dynamics in terms of feedback between water and vegetation. Specifically, the study assesses groundwater recharge mechanisms, estimated groundwater recharge rates, thus providing a quantification of available groundwater resources along a precipitation gradient. The outcome of this study will contribute to a better management of groundwater resources in the study areas, especially a recommendation of a sustainable yield to ensure that farmers are not abstracting more than what the aquifers are recharged with. The research also helps in identification of the source water and active root depth of *S. mellifera* and *B. albitrunca*. A known root depth helps in improving groundwater recharge models in order to avoid overestimation of recharge estimates.

1.6 Limitation of the study

An independent verification of the results from the used methods is difficult for the reason that long term data, ideally for 30 years to verify, are only available for very limited sites in Namibia. Another limitation was access to some of the boreholes. About 98% of the boreholes are privately owned. Tsumeb in particular where an official agreement was not signed with all the farmers in the area, access to farms was only granted after a negotiation with farm owners who agreed for their boreholes to be sampled. Another limitation is the uniformity of sites in terms of hydrogeology and soil hydraulic difference between sites.

1.7 Dissertation structure

This dissertation is structured into 6 chapters. Chapter 1 begins with the orientation, the research problem, objectives, hypothesis, significance and limitations of the study. Chapter 2 gives a literature review to set context and give an overview of groundwater recharge and the influence of woody plants on groundwater. Chapter 3 addresses the local meteoric water lines along a precipitation gradient. Stable isotope composition of precipitation serves as a fingerprint in tracing the origin of groundwater; hence the stable isotope composition of groundwater in Chapter 4 will be compared to the findings of this chapter in order to trace its origin. Chapter 3 is published in *International Science and Technology Journal of Namibia* and can be retrieved from http://journals.unam.edu.na/index.php/ISTJN/article/view/1568.

Chapter 4 looks at the estimates of potential groundwater recharge rates in savannah aquifers along a precipitation gradient using chloride mass balance method. Moreover, recharge mechanisms and the tracing of the origin of groundwater is looked at using stable isotopes by comparing the isotopic compositions of groundwater to that of precipitation obtained in Chapter 3. This chapter is published in *Physics and Chemistry of the Earth, Parts A/B/C* under the https://doi.org/10.1016/j.pce.2020.102844.

Chapter 5 covers the influence of woody plants on groundwater recharge. The active root depth and source water for woody plants are determined using a deuterium tracer at Ebenhaezer farm. This chapter links to potential groundwater recharge rates estimated in Chapter 4 as plant's water root uptake reduces groundwater recharge. Futhermore, the active root depth is a needed parameter for groundwater models that estimate net groundwater recharge rates. This chapter will be submitted to the *Journal of Ecohydrology and Hydrobiology.*

The last chapter (Chapter 6) covers the overall conclusion and recommendations. A summary of these chapters are outlined in Figure 1-2 below.

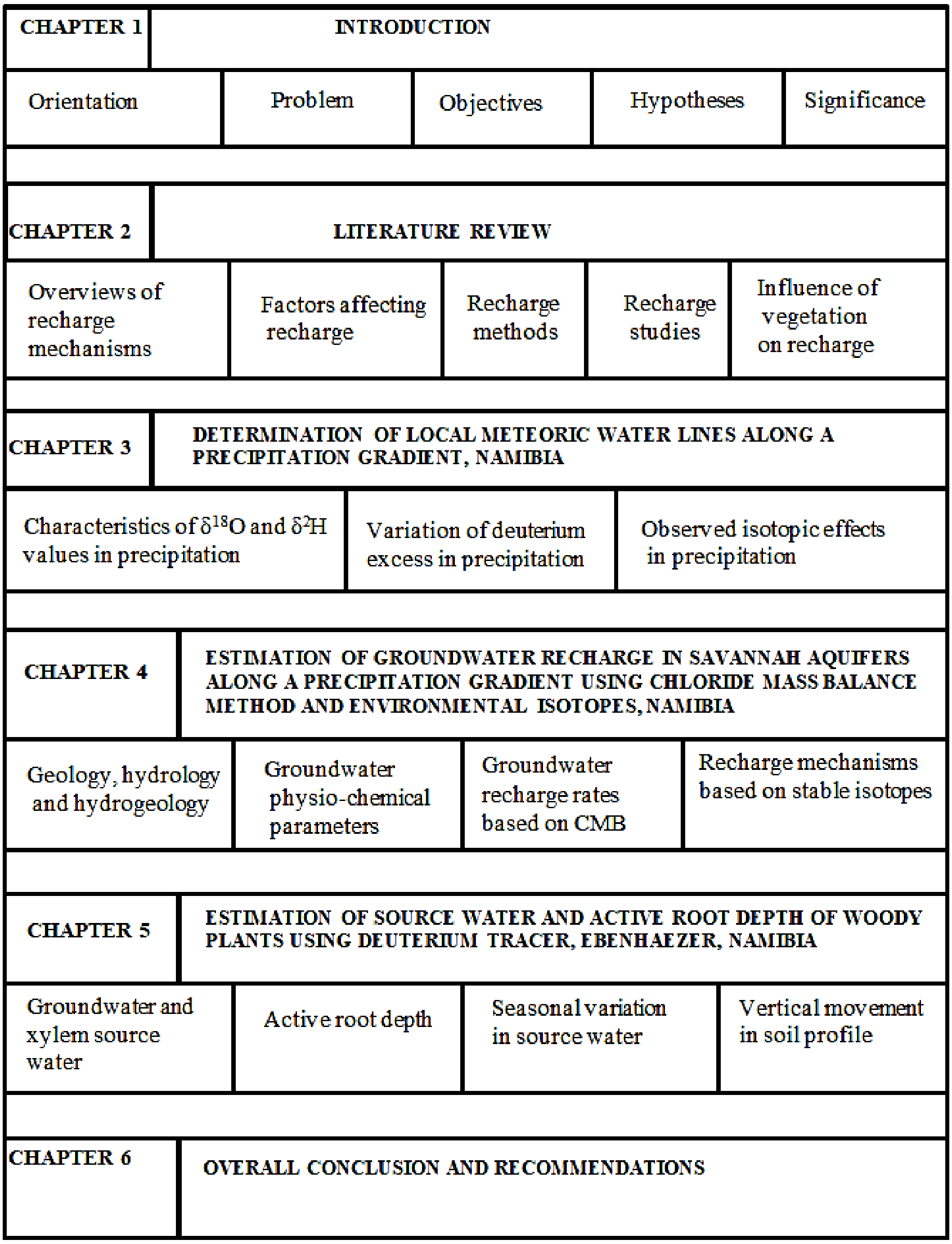

Figure 1-2: A schema outlining a summary of the chapters in the dissertation.

CHAPTER 2

LITERATURE REVIEW

2.1 General overview of groundwater recharge mechanisms

Groundwater recharge is the amount of surface water which reaches the permanent water table either by direct contact in the riparian zone or by downward percolation through the unsaturated zone (Hiscock and Bense, 2014). Beekman and Xu (2018) conceptualises different modes of recharge according to the origin of water, flow mechanisms through the unsaturated zone, areas on which it acts as illustrated in Figure 2-1. Although evapotranspiration flux is illustrated in Figure 2-1, it only covers the unsaturated zone, hence the figure is modified to cater for potential groundwater evaporation or groundwater evapotranspiration flux (brown arrow). There are three principal recharge mechanisms that are based on the origin of water, thus direct recharge, indirect recharge and localised recharge (Beekman and Xu, 2018; Cuthbert et al., 2019; De Vries and Simmers, 2002).

Beekman and Xu (2018) define these terminologies as follow:

- Direct, autogenic/diffuse recharge: direct infiltration of precipitation and subsequent percolation through the unsaturated zone to a groundwater body, i.e. water added to the groundwater reservoir in excess of soil-moisture deficits and evapotranspiration.
- Indirect, allogenic/non-diffuse recharge: percolation to the water table through depressions and fault zones.
- Localised/focused recharge: accumulation of precipitation in surface-water bodies, and subsequently concentrated infiltration and percolation through the unsaturated zone to a groundwater body.

Furthermore, Beekman and Xu (2018) propose two flow mechanisms through the unsaturated zone as follows:

- Piston/translatory flow: precipitation which stored in the unsaturated zone is displaced downwards by the next infiltration/percolation event without disturbance of the moisture distribution.
- Preferential flow: flow via preferred pathways/macro-pores, which are sites (e.g. abandoned root channels, burrows, fissures) or zones (e.g. stream beds) in the unsaturated zone with a relatively high infiltration and/or percolation capacity.

Several studies have indicated that groundwater recharge can occur to some extent in arid and semi arid regions, even where annual potential evapotranspiration exceeds annual precipitation (Allison et al., 1994; Döll and Fiedler, 2008; Gee and Hillel, 1988; Hamutoko et al., 2019; Scanlon et al., 2006; Stephens, 1993; Uugulu and Wanke, 2020; Verhagen et al., 1974). In such regions, direct recharge is likely to become less important than localised and indirect recharge, in terms of total aquifer replenishment (Alsaaran, 2005; De Vries and Simmers, 2002). In most cases, such groundwater recharge only occurs episodic as a result of heavy precipitation events, thus such a rapid inflow is protected from further evaporation as it passes the unsaturated zone through preferential paths (Lewis and Walker, 2001; Rathay et al., 2018; van Wyk et al., 2012).

Moreover, an analysis of multidecadal groundwater hydrographs across sub-Saharan Africa has indicated that the levels of aridity dictate the predominant recharge processes (Figure 2-2) (Cuthbert et al., 2019). The dominant recharge process in hyper-arid and arid regions is a focused recharge which mainly occur episodically in arid regions, while sub-humid to humid regions are predominated by diffuse recharge processes that occurs inter-annually and seasonally (Cuthbert et al., 2019; MacDonald et al., 2021).

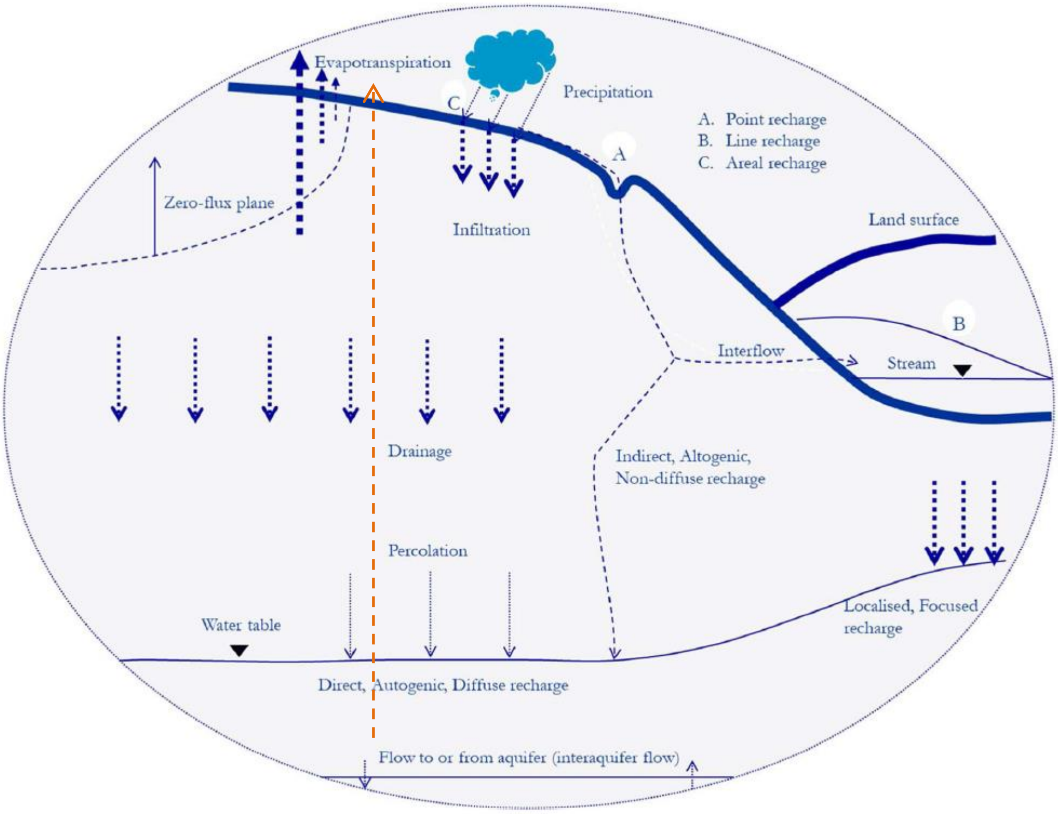

Figure 2-1: Recharge mechanisms (after Healy, 2010; modified by Beekman and Xu, 2018).

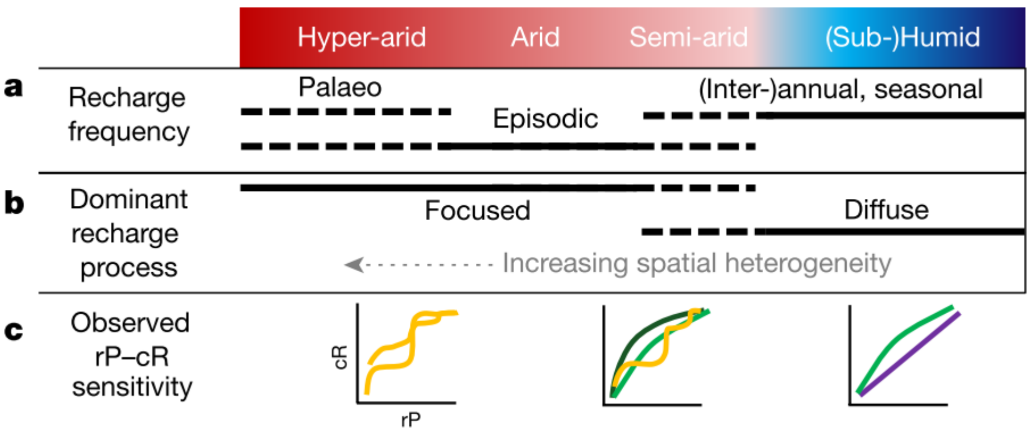

Figure 2-2: Synthesis of controls on recharge variations and processes in sub-saharan africa (Cuthbert et al., 2019).

2.2 Factors influencing groundwater recharge

Groundwater recharge is controlled by several factors. The key factors are climate, soils and geology, vegetation types, land use and land cover, topography (Bean et al., 2003; Foster et al., 1994; Healy and Scanlon, 2010; Maitre et al., 1999; Sanford, 2002; Sophocleous, 2004). These factors are outlined and only summarised in Table 2-1 below.

Table 2-1: Key factors influencing groundwater recharge.

Factors	**Description**
1. *Climate*	Regions with relatively arid climates, the climate controls the rate of recharge whereas in humid climates, other factors such as geologic framework control the rate of recharge. Precipitation is the main source of natural groundwater recharge, hence temporal distribution; frequency, duration and intensity of individual precipitation affect recharge processes.
2. *Soils and geology*	The permeability of geological materials affects recharge processes. Soils allow water to infiltrate to the water table; a deeper geologic framework provides the permeability necessary for deeper flow. Recharge is more likely to occur in areas with high permeable units that allow high infiltration rates to take place.
3. *Vegetation type*	Vegetated areas have higher evapotranspiration rates compared to unvegetated areas, hence less water available for recharge. Deep rooted vegetation such as woody plants are capable of drawing moisture from depths of several metres or more while shallow rooted plants can only access moisture in upper layers. Vegetation has an impact on infiltration both by providing

	canopy and litter cover to protect the soil surface from raindrop impacts and by producing organic matter which binds soil particles and increases its porosity Roots generate preferential flow paths of water through the unsaturated zone to the water table, particularly in low-permeability soils, thereby increasing recharge. Extraction of soil water in the unsaturated zone by plant roots, to feed transpiration, reduces the amount of water available for potential groundwater recharge.
4. *land use and land cover*	For land use, activities such as irrigation enhance groundwater recharge especially in arid or semi-arid regions. On the other hand, urbanisation tends to reduce groundwater recharge due to impervious structures such as roads and pavements.
5. *Topography*	Areas with gentle slopes are favoured for groundwater recharge as compared to areas with steep slopes whereby the surface runoff is high. Surface water runs towards depressions, hence infiltration from depression can lead to groundwater recharge.

2.3 Groundwater recharge estimation methods

There are several methods that can be used to estimate groundwater recharge in both unsaturated and saturated zones. Allison et al. (1994) reviewed these methods for the unsaturated zone in arid and semi-arid regions and classified them into physical and chemical methods. The authors further classified physical methods into direct and indirect physical methods. The direct physical methods mainly include lysimetry while the indirect physical methods include the soil water balance, zero-flux plane and estimation of water fluxes.

The chemical methods involve both natural tracers as well as applied tracers. The natural tracers that are commonly used in recharge studies are tritium, carbon-14, chlorine-36, chloride, oxygen-18 and deuterium, nitrate and carbon-13 (Allison et al., 1994). Applied tracers that have been successfully used are oxygen-18, deuterium, tritium, bromide and dye solutions (Allison et al., 1994; Koeniger et al., 2016; Sharma et al., 1985). Moreover, Scanlon et al. (2002) indicated that tracers can also be used to estimate groundwater recharge in arid and semi-arid regions. There are other techniques that can be used to estimate groundwater recharge such as hydrogeological (water table fluctuation method) and composite techniques such as groundwater modelling. These methods are described in detail below; with an exemption of carbon-14, chlorine-36, nitrate and carbon-13.

2.3.1 Physical methods

Lysimetry is a direct physical method that can be used to estimate groundwater recharge in the unsaturated zone. Lysimeters consist of containers that are filled with either disturbed or undisturbed soil, with or without vegetation, that are hydrologically disconnected from the surrounding soils (Scanlon et al., 2002). The components of the water balance such as precipitation, evapotranspiration and water storage are measured in such containers and recharge is estimated based on that (Allison et al., 1994; Scanlon et al., 2002). In order to avoid recharge rate overestimations, the base of the lysimeter should be deeper than the root zone when measuring drainage fluxes (Scanlon et al., 2002). This method is rarely used to estimate groundwater recharge because it is expensive, difficult to install as this can easily disturb the unsaturated zone conditions in the process, and have high maintenance requirements (Allison et al., 1994; Scanlon et al., 2002).

Zero-flux plane (ZFP) method is an indirect physical method used to estimate groundwater recharge. ZFP represents the plane where the vertical hydraulic gradient is zero (Allison et al., 1994; Scanlon et al., 2002). Water moves in the upward direction above this plane and moves downward below it (Khalil et al., 2003). Recharge is estimated by summation of the changes in water content below the plane during a time interval (Allison et al., 1994). High infiltration results in a positive hydraulic gradient downward throughout the profile and making it difficult to use the method (Scanlon et al., 2002). This method is relatively expensive in terms of instruments required as well as the amount of data collection required.

Estimation of water fluxes is an indirect physical method that uses either Darcy's law or Richards's equation to estimate soil water flux for a period of time (Allison et al., 1994). This method involves the determination of hydraulic conductivity and hydraulic potential (Allison et al., 1994; Sanford, 2002). If the water flux is calculated at a depth in the profile where no further extraction of water by roots occurs, then the flux is equated to groundwater recharge as given by Equation 2.1:

$$\mathrm{R} = \mathrm{K}(\theta)\Delta\mathrm{H_t} \qquad Eq\ 2.1$$

Where $\mathrm{K}(\theta)$ = hydraulic conductivity and $\Delta\mathrm{H_t}$ = the total head gradient. It is difficult and time consuming to determine hydraulic conductivity both in the field and in the laboratory and usually uncertainty increases with soil dryness (Allison et al., 1994).

2.3.2 Chemical methods

2.3.2.1 The chloride mass-balance (CMB) method

The CMB method is used to estimate groundwater recharge both in unsaturated and saturated zones. Evapotranspiration takes place before a proportion of precipitation infiltrates below the zone of recycling whereby the chloride concentration increases proportional to the loss of water due to evapotranspiration (Figure 2-3) (Stone and Edmunds, 2016). The method is based on the law of conservation of mass, where chloride is considered as a conservative tracer, hence the concentration of chloride in the evapotranspiration water is assumed to be virtually zero (Sibanda et al., 2009).

The input of chloride deposition by both dry and wet deposition is assumed to balance the output of chloride concentration by infiltration and mineralisation as given by Equation 2.2 (Edmunds et al., 1988):

$$F_N + F_D = F_S + F_M \quad \text{Eq 2.2}$$

Where F_N= Input by wet deposition, F_D = Input by dry deposition; F_S = Output by infiltration and; F_M = Output by mineralisation, adsorption. For CMB in Kalahari, Equation 2.2 is simplified to Equation 2.3 as input by dry deposition is considered negligible (Gieske et al., 1995):

$$F_N = F_S \quad \text{Eq 2.3}$$

Equation 2.3 can further be written as Equation 2.4:

$$R = \frac{(P - A) * Cl_p}{Cl_{sw}} \quad \text{Eq 2.4}$$

Where P = precipitation (mm); A = surface runoff; Cl_p = Chloride concentration in precipitation (mg/l); Cl_{sw} = Chloride concentration in soil water (mg/l) and R =

Recharge (mm). This method further assumes that there is no surface runoff or if there is, its flux can be accounted for (Sibanda et al., 2009). Wanke et al. (2013) integrated surface runoff in their water balance model to estimate direct groundwater recharge in north-eastern Namibia and the scenario did not improve the modelling results. Hence very little surface runoff can be neglected and recharge computation is justified in semi-arid regions (Sibanda et al., 2009).

In the saturated zone, Equation 2.4 is modified to use Cl_{gw} instead of Cl_{sw} where Cl_{gw} is chloride concentration in the groundwater. Slightly higher recharge rates can be estimated using chloride in groundwater than in soil water due to the fact that extraction of water from the soil generally requires additional dilution (Scanlon et al., 2002). Additional dilution during the extraction of water from the soil can cause the measured chloride to approach the analytical detection limits and thus give rise to additional uncertainties in reported chloride concentrations (Gee et al., 2005). It is therefore recommended that minimum soil water dilutions be used when measuring chloride concentrations in soil water in order to reduce the impact of analytical errors (Gee et al., 2005).

The CMB method is widely used because of its low cost and time integrating properties (Scanlon et al., 2006; Wood, 1999). It has been successfully applied in several studies to estimate groundwater recharge rates in semi-arid areas (Gebru and Tesfahunegn, 2019; Gieske et al., 1990; Hamutoko et al., 2019; Klock, 2001; Marei et al., 2010; Schmidt et al., 2013; Sharma and Hughes, 1985; Subyani, 2004; Ting et al., 1998). Sharma and Hughes (1985) estimated groundwater recharge using CMB in the deep coastal sands of Western Australia, Gieske et al., (1990) in south eastern

Botswana and Subyani (2004) in Saudi Arabia with 15, 2.5 and 11 % of the average annual precipitation, respectively.

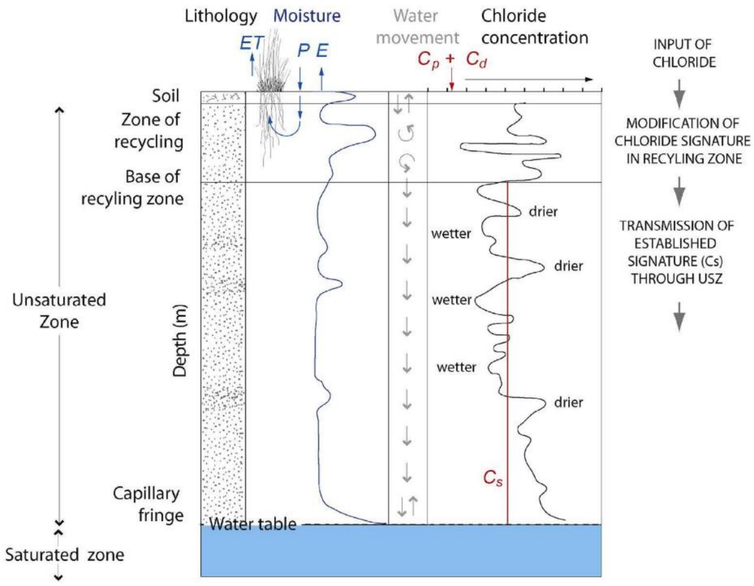

Figure 2-3: A schema showing the behaviour of pore water and dissolved chloride in the unsaturated zone (Stone and Edmunds, 2016).

2.3.2.2 Oxygen-18 and Deuterium

Water stable isotopes are widely used as tracers to comprehend hydrogeological processes such as precipitation, groundwater recharge, groundwater-surface water and vegetation interaction. Stable isotopes of water are used to estimate groundwater recharge both in the unsaturated and saturated zones. Koeniger et al. (2016) reviewed water isotope-based groundwater recharge estimation methods in the unsaturated zone. The authors identified two approaches that can be used to estimate groundwater recharge based on the natural stable isotopes of water. The first approach involves seasonal variations of stable isotopes in precipitation that are caused by temperature driven Rayleigh-type fractionation processes that can be used to follow soil water displacement. In this approach the mean soil water content is determined as an average of observed soil water content below the root zone (Gehrels et al., 1998). Recharge is then estimated by integrating soil water content over the displacement of the tracer peak over a certain time period using Equation 2.5 (Leibundgut et al., 2009):

$$R = \frac{\int_{Z_0}^{Z_n} \theta(z).\,dz}{T} \quad Eq\ 2.5$$

Where Z_0 and Z_n represent the soil depths of the tracer peak after t = 0 and at a time period T respectively; θ represent the volumetric water content. A peak displacement technique (PDT) was successfully used in humid and semi-arid environments to estimate groundwater recharge (e.g. Barbecot et al., 2018; Beyer et al., 2015; Boumaiza et al., 2020). Recharge can also be calculated using a mass balance method whereby the mass of the tracer within the soil profile is related to the mass of the entering tracer, assuming a constant tracer source using Equation 2.6 (Koeniger et al., 2016):

$$R = \frac{P.\,C_P}{C_{UZ}} \quad Eq\ 2.6$$

Where P is precipitation and C_P and C_U are average concentrations of tracer in precipitation and in the unsaturated zone, respectively.

The second approach involves evaluating stable isotope evaporation signals. Stable isotopic compositions are not conservative and are subject to fractionation by evaporation (De Vries and Simmers, 2002). Fractionation due to evaporation complicates the use of isotopes to trace the origin of groundwater recharge because the isotopic composition of groundwater can be considerably modified from that of local precipitation (Clark and Fritz, 1997; Jasechko, 2019). However, the characteristic stable isotope patterns imparted by fractionation is useful in understanding groundwater recharge mechanisms as well as estimating groundwater recharge rates (Clark and Fritz, 1997; Koeniger et al., 2016). A parallel shift method which takes into account evaporative isotopic enrichment has been developed to quantify groundwater recharge was first developed by Allison et al. (1985) and later modified by Clark and Fritz (1997) to give Equation 2.7 and Equation 2.8:

$$\mathrm{R} = \left[\frac{22}{\delta^{2}\mathrm{H}_{\mathrm{shift}}}\right]^{2} \qquad Eq\ 2.7$$

$$\mathrm{R} = \left[\frac{3}{\delta^{18}\mathrm{O}_{\mathrm{shift}}}\right]^{2} \qquad Eq\ 2.8$$

Where R = Recharge; $\delta^{2}H_{shift}$ is a displacement of $\delta^{2}H$ from a local meteoric water line (LMWL) and $\delta^{18}O_{shift}$ is a displacement of $\delta^{18}O$ from a LMWL. In this method, an assumption of constant evaporative demand and uniform rain events in terms of intensity is made, whereby the δ-value shift can be shown to be proportional to the reciprocal of the square root of the annual recharge. The method was used by Gaj et al., (2016) to estimate groundwater recharge rates using in situ unsaturated zone water stable isotope measurements in northern Namibia. However, the parallel shift method and its accuracy have been debated by some studies (Barnes and Allison, 1988; Herczeg and Leaney, 2011). For the saturated zone, it is believed to give crude estimates of groundwater recharge (Clark and Fritz, 1997; JICA, 2002), hence, there is a need for it to be used alongside other groundwater recharge estimation methods such as the CMB method.

2.3.2.3 Tritium

Tritium (^{3}H) is a common radioisotope which is used to identify the presence of modern recharge. The distribution of bomb-pulse tritium in the unsaturated zone can be used to estimate groundwater recharge using either the peak displacement method or mass balance method (Allison, 1988; Clark and Fritz, 1997; Koeniger et al., 2016). Equation 2.5 and Equation 2.9 are used to calculate groundwater recharge using tritium as a chemical tracer. Bomb-pulse tritium is now found at great depths (>20 m) or even in groundwater, hence making it not practical to be used in the unsaturated zone (Koeniger et al., 2016). Moreover, bomb-pulse tritium concentrations have greatly reduced due to radioactive decay (Scanlon et al., 2002). However tritium can be used as an applied tracer in the unsaturated zone but it should be injected at the bottom of the root zone to prevent the immediate loss of the tracer (Koeniger et al., 2016). Groundwater recharge rate in the saturated zone using tritium is estimated by determining the age of groundwater using Equation 2.9 (Scanlon et al., 2002):

$$t = -\frac{1}{\lambda}\ln\left[1 + \frac{{}^{3}_{2}He}{{}^{3}_{1}H}\right] \qquad Eq\ 2.9$$

Where λ is the decay constant (ln 2/t ^{½}), $t^{1/2}$ is the tritium half life (12.43 years), and Helium is tritiogenic. A closed system which is characterised by piston flow is assumed when using this equation (Scanlon et al., 2002). Determination of groundwater age should be done at several points in a vertical profile, the groundwater velocity is then calculated by inverting the age gradient, and multiplying the velocity by the porosity for the depth interval in order to get a groundwater recharge rate (Scanlon et al., 2002).

2.3.3 Other techniques

The *Water-table fluctuation method* is used in the estimation of groundwater recharge rates for unconfined aquifers only (Scanlon et al., 2002). This method requires continuous monitoring of groundwater level and the determination of specific yield by pumping tests and grain size analysis at the level fluctuation area.

The Water-table fluctuation method is based on the fact that rises in groundwater levels in unconfined aquifers are due to recharge water arriving at the water table (Healy and Cook, 2002; Sibanda et al., 2009).

Recharge is calculated using Equation 2.10:

$$R = S_y * \frac{dh}{dt} = S_y * \frac{\Delta h}{\Delta t} \qquad \text{Eq 2.10}$$

Where R is aquifer recharge, S_y is specific yield, *h* is elevation of the hydraulic head, and *t* is time. Equation 2.10 assumes that water arriving at the water table goes immediately into storage. Equation 2.10 can be applied over longer time intervals (seasonal or annual) to produce an estimate of change in subsurface storage. This value is referred to as “net” recharge by Healy and Cook (2002). However, interference with pumping should be accounted for by knowing the pumping rates or the amount abstracted in the study areas. Fan et al. (2014) determined groundwater recharge rates under three vegetation covers in a coastal sandy aquifer of subtropical Australia, ranging between 21% to 56% of the annual precipitation.

Soil water balance model method assumes that when stored water in the soil exceeds the field capacity, excess water percolate downward beyond the rooting depths, such excess water is assigned to groundwater recharge, even though it may take months or years to actually reach the water tabler (Hiscock and Bense, 2014).The method has been successfully applied in the north eastern Namibia and north western Botswana by Wanke et al. (2013) and determined a mean annual recharge of 2.6% of the annual precipitation.

Groundwater modelling involves modelling groundwater flow to predict the aquifer piezometry under various groundwater stress situations (Bean et al., 2003). A threedimensional groundwater flow equation is solved through numerical modelling for various complex flow configurations and recharge is then estimated based on the known hydraulic head, hydraulic conductivity and specific storage values, and other inflow into and outflow from the aquifer (Bean et al., 2003; Beekman and Xu, 2018; Scanlon et al., 2002).

2.4 Selected Research methods for this study

The methods used in this study are chemical methods, thus natural tracers and an applied tracer were used. The CMB method was selected based on the budget; availability of the data as well as the aridity/ semi-aridity of the study sites. The CMB method is inexpensive, easy and simple to apply (Beekman and Xu, 2018) as compared to other methods. This method was used in quantification of groundwater recharge and it is addressed in Chapter 4 of the dissertation. Oxygen-18 and deuterium were used to trace the isotopic fingerprints of both precipitation in Chapter 3 as well as in Chapter 4 to understand groundwater recharge mechanisms. This method was chosen based on its simplicity as well as the availability of the measuring equipment at the University of Namibia. An applied tracer thus deuterium was used in understanding the water uptake for woody plants in Chapter 5. Deuterium tracer was chosen because it is chemically stable, non-reactive, easy to handle and cost-effective (Koeniger et al., 2016) and it is becoming increasingly popular in hydrology (Beyer et al., 2016).

2.5 Groundwater recharge studies on a global scale and continental scale

Several groundwater recharge studies have been carried out across the globe (De Vries and Simmers, 2002; Döll and Fiedler, 2008; Moeck et al., 2020; Scanlon et al., 2006; Tögl, 2010). Most of these studies demonstrated that groundwater recharge is highly dependent on climate, geology, morphology and vegetation. A study by Tögl (2010) considered analysis of texture, hydrogeology and vegetation/ land cover and could not give complete explanations for the discrepancies from the groundwater recharge measurements methods causing underestimations. Döll and Fiedler (2008) estimated a global groundwater recharge of 12,666 km^3/a for the climate normal 1961 - 1990, thus 32% of the total renewable water resources.

For semi-arid and arid regions, groundwater recharge accounts for a lower fraction of total runoff, making such regions to be more vulnerable to seasonal and inter-annual precipitation (Döll and Fiedler, 2008). As for arid regions, extreme local variability in recharge, with rates of about 720 mm/a are a result of focused recharge and preferential flow paths especially in fractured systems (Scanlon et al., 2006).

At a continental scale estimates of groundwater recharge have concentrated predominantly on semi-arid regions of Africa with around 60 studies (Figure 2-4b) (MacDonald et al., 2021). This is most likely driven by the scarcity of water or absence of permanent or reliable surface water in those regions and the reliance on groundwater for water supply requiring this information for water resources management. According to MacDonald et al. (2021) (Figure 2-4), the CMB is the dominant method used in estimating groundwater recharge in Africa, especially in arid to semi-arid regions. The CMB method is considered to be an easy, inexpensive, and most universal method and widely used for recharge estimation (Allison et al., 1994; Sophocleous, 2004) as compared to physical methods that are challenging when soil moisture content values are low, such that the resolution and precision of estimates is compromised.

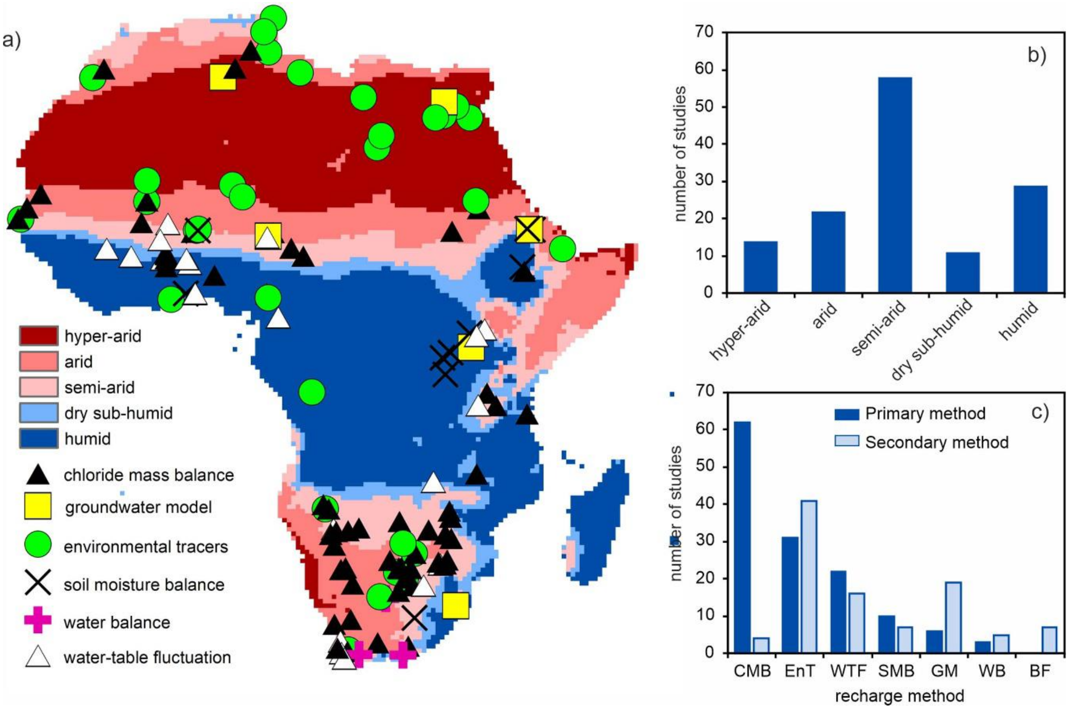

Figure 2-4: Locations of groundwater recharge studies in Africa (MacDonald et al., 2021).

2.6 Groundwater recharge at a Namibian scale

2.6.1 Aquifers in Namibia

The hydrogeological map (Figure 2- 5) by DWA & GSN, 2001 shows that the main aquifers in Namibia are porous and fractured, fissured or karstified aquifers of moderate to high groundwater potential. The porous aquifers are mainly unconsolidated to semi-consolidated sand and gravel as well as sandstones while fractured, fissured or karstified aquifers are non-porous clastic rocks, crystalline rocks including both igneous and metamorphic rocks (Christelis and Struckmeier, 2011). Significant portions of the country are covered by rock bodies with little groundwater potential (Figure 2-5). These rock types are mainly dune sand, fine grained clastic rocks, unkartistified carbonates and crystalline rocks (igneous and metamorphic) (Christelis and Struckmeier, 2011).

2.6.2 Groundwater recharge studies in Namibia

A total of 40 groundwater recharge studies in Namibia are collated in Table 2-2. The studies compiled in Table 2-2 particularly focus on those that have estimated recharge values and excluded those that dealt with groundwater recharge mechanisms only. Figure 2-5 shows a spatial distribution of groundwater recharge studies in Namibia whereby most of the studies concentrate on porous aquifers especially on Kalahari beds. Most of the studies undertaken on porous aquifers mainly covered Cuvelai-Etosha Basin, Kalahari catchment, western catchments and Stampriet Basin (Figure 2-5).

Studies on perched aquifers in the Cuvelai-Etosha Basin using CMB method have indicated that groundwater recharge is lower in sand fields and higher in depressions, pans and ephemeral rivers (Hamutoko, 2018; Hamutoko et al., 2019; Wanke et al., 2014). Such high recharge rates are attributed to preferential flow paths formed by cracks and fissures in the calcrete surface (Hamutoko et al., 2019). Recharge studies have also been carried out on the regional aquifer in the Cuvelai-Etosha Basin using a peak displacement and soil water balance methods (Beyer et al., 2015; Gaj et al., 2016).

Groundwater recharge studies have also been carried out in the Kalahari catchment of north eastern Namibia. Evidence from radiocarbon and tritium tracers has shown that the main recharge mechanism in this area is direct recharge from precipitation (Verhagen et al., 1974). Recharge rates in this area depend both on the precipitation and on surface materials, whereby areas covered by sandy soils have very low recharge rates in comparison to areas covered by karstified hard rocks (Klock et al., 2001). These recharge rates were estimated as point recharge values using a CMB method. However, a groundwater balance method revealed lower recharge values assuming an equal distribution of such recharge values across the entire catchment (Klock and Udluft, 2002).

Alluvial aquifers in the western catchments of Namibia are associated with ephemeral rivers and play a major role in sustaining numerous settlements and ecological systems in Namibia (Sarma and Xu, 2017; Shikangalah and Mapani, 2021). The few recharge studies that have been carried out on these alluvial aquifers have demonstrated that they are usually recharged through infiltration during flash floods, hence an indirect recharge mechanism (Matengu, 2020; Sarma and Xu, 2017). The dynamic processes governing flood water infiltration and groundwater recharge of Kuiseb alluvial aquifer were investigated (Dahan et al., 2008; Morin et al., 2009). Infiltration that leads to groundwater recharge mainly takes place in the river channel, which is made of sandy materials, while there is a reduced infiltration in the floodplain due to the presence of thin alternating layers of sand and silt-clay (Dahan et al., 2008). A study undertaken by Crerar et al., (1988) on Swakop River identified silt deposited during a flood event as one of the extremely important factors controlling groundwater recharge in unconsolidated alluvium underlying ephemeral rivers by inhibiting recharge at relatively high flow velocities.

Groundwater recharge estimates have been carried out in the Stampriet Basin too (JICA, 2002; Stone and Edmunds, 2012). Stone and Edmunds (2012) estimated groundwater recharge in the Stampriet Basin using CMB method in the unsaturated zone of the Kalahari beds. Their study indicated recent direct recharge with soil profiles representing 10 to 30 years of precipitation infiltration. JICA (2002) investigated groundwater recharge in Kalahari, Auob and Nossob aquifers in the Stampriet Basin using CMB, stable isotope, water level fluctuation and water balance methods. Auob aquifer is indirectly recharged through the Kalahari aquifer where there are no impermeable layers (JICA, 2002). For the Nossob aquifer, water is regarded as fossil water since there is no direct recharge from precipitation (JICA, 2002). Radiocarbon-derived age of groundwater from the Nossob aquifer is typically more than 30 000 year-old (Heaton et al., 1983), which is evidence that this aquifer is not part of the active hydrological cycle.

Despite fractured, fissured or karstified aquifers being classified as moderate to high groundwater potential rock bodies in Figure 2-5, Only few studies (Bäumle, 2003; Kambinda, 2014; Mukendwa, 2009) are done on these aquifers. There is therefore a need to study fractured, fissured or karstified aquifers in Namibia.

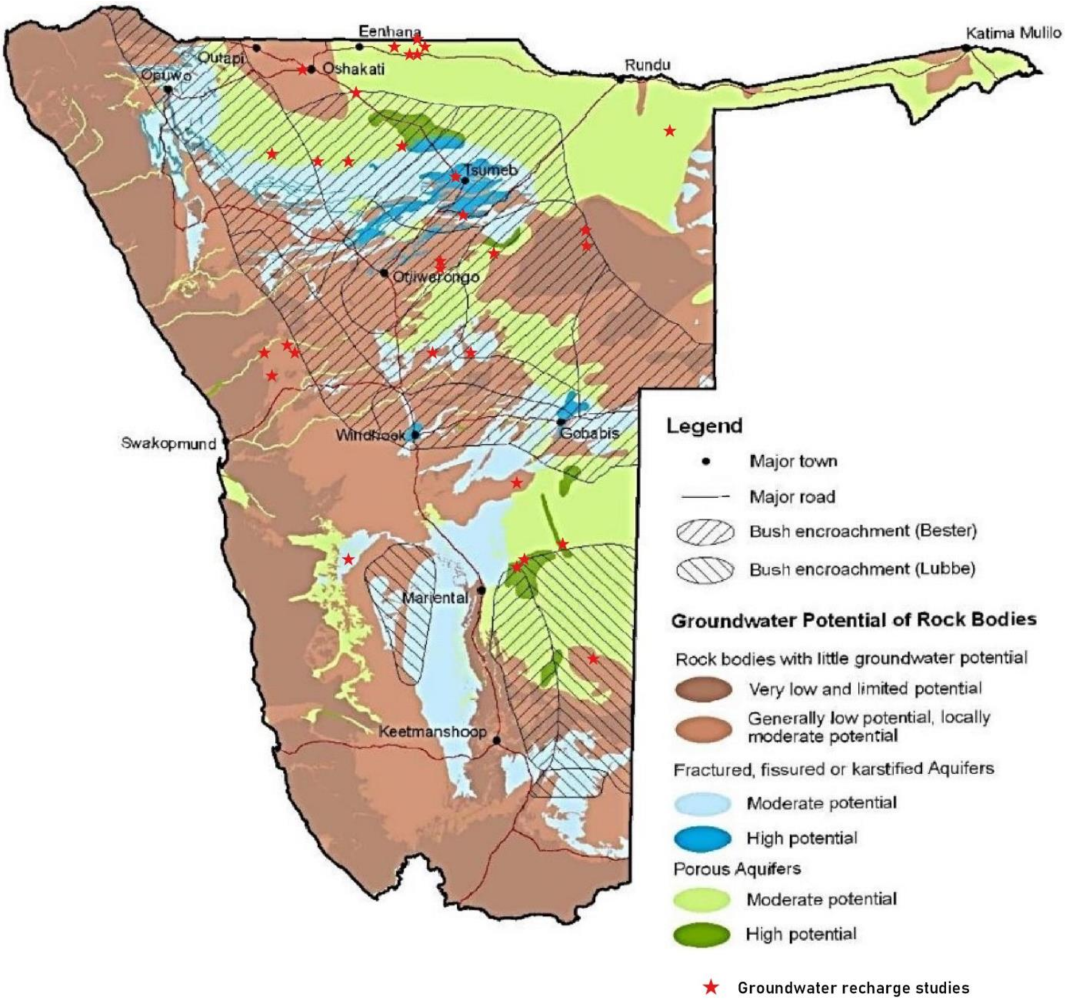

Figure 2-5: Hydrogeological map of Namibia superimposed by bush encroached areas. Hydrogeological map by (DWA & GSN, 2001). Bush encroachment map by (Bester, 1996) with additions by Lubbe (pers. comm to Colin Christian and Associates CC environmental Consultants (NAU, 2010). The map is overlaid with Groundwater recharge studies presented in Table 2-2.

Table 2-2: A summary of groundwater recharge estimations in Namibia (adopted, updated and modified from (Abiye, 2016; Andjamba, 2016; Hamutoko, 2018; MacDonald et al., 2021).

CMB = Chloride Mass Balance; GM = Groundwater Model; WTF = Water Table Fluctuation; PDT = Peak Displacement Technique; SWB = Soil Water Balance; WSI = Water Stable Isotopes; SVF = Saturated Volume Fluctuation

Source	**Location**		**Recharge method**	**Mean precipitation (mm/a)**	**Mean recharge value (mm/a)**	**Aquifer type**
	Lat.	**Long.**				
Amutenya, 2020 (A-A')	-18.1	16.3	CMB	450	0.08	Porous
Amutenya, 2020 (A-A')	-18.1	16.3	WSI	450	3.24	Porous
Amutenya, 2020 (B-B')	-18.8	16.9	CMB	450	0.53	Karst; porous
Amutenya, 2020 (B-B')	-18.8	16.9	WSI	450	46.72	Karst;porous
Amutenya, 2020 (C-C')	-19	16.2	CMB	400	0.40	Karst
Amutenya, 2020 (C-C')	-19	16.2	WSI	400	11.48	Karst
Amutenya, 2020 (D-D')	-19	15.8	CMB	300	1.56	Karst
Amutenya, 2020 (E-E')	-18.9	15.2	CMB	300	1.22	Karst
Amutenya, 2020 (E-E')	-18.9	15.2	WSI	300	3.11	Karst

Amutenya, 2020 (F-F’)	-17.8	15.6	CMB	400	0.03	Porous
Bäumle, 2003	-19.2	17.6	SVF	525	11.4	Karst
Beyer et al., 2015	-17.5	16.8	WSI	450	43	Porous (dune sand)
Beyer et al., 2015	-17.5	16.8	PDT	450	29	Porous (dune sand)
Beyer et al., 2015	-17.5	16.8	WSI	450	29	Porous (dune sand)
David, 2013	-17.6	17.0	Physical Water Balance Model (MODBIL)	450	39.4	Porous (dune sand)
Gaj et al., 2016	-17.5	16.8	SMB	450	4.5	Porous (dune sand)
Hamutoko, 2018	-17.6	17.1	CMB	450	92.5	Porous
JICA, 2002	-24.3	18.4	WTF	200	6.5	Porous (sand)
Kambinda, 2014	-24.2	16.2	CMB	150	12.4	Karst
Klock, 2001	-19.9	19.3	CMB	409	1.5	Porous (dune sand)
Klock, 2001	-19.9	19.3	GM	409	1.5	Porous (dune sand)

Külls, 2000	-21.5	17.3	CMB	370	8.3	Porous
Külls, 2000	-20.2	18.1	CMB	450	20	Porous
Külls, 2000	-20.2	18.1	SMB	450	5	Porous
Mainardy, 1999	-20.3	17.4	CMB	375	20	Fractured
Mainardy, 1999	-20.3	17.4	GM	375	20	Fractured
Matengu, 2020	-21.5	15.1	CMB	125.1	1.2	Porous (alluvial)
Matengu, 2020	-21.4	15.4	CMB	117.1	10.8	Porous (alluvial)
Matengu, 2020	-21.8	15.2	CMB	125.1	0.2	Porous (alluvial)
Matengu, 2020	-21.5	15.5	CMB	161.5	1.2	Porous(alluvial)
Mukendwa, 2009	-19.7	17.7	WTF	525	20	Karst (Kombat)
Mukendwa, 2009	-19.7	17.7	GM	525	20	Karst (Kombat)
Nghipandulwa, 2018	-17.4	17.1	WSI	450	31	Porous (dune sand)

Nghipandulwa, 2018	-17.4	17.1	WTF	450	30.2	Porous
Nghipandulwa, 2018	-17.4	17.1	CMB	450	79.9	Porous
Peck, 2010	-25.5	19.4	GM	225	2.3	Porous
Schwartz, 2006	-24	19	CMB	225	3	Porous
Schwartz, 2006	-24	19	GM	225	3	Porous
Stone and Edmunds, 2012	-24.2	18.5	CMB	207.5	24	Porous (dune sand)
Uugulu and Wanke, 2020	-19.2	17.6	CMB	600	34.8	Karst
Uugulu and Wanke, 2020	-20.4	17.4	CMB	450	45.1	Porous (sandstone)
Uugulu and Wanke, 2020	-23.2	18.4	CMB	240	10.4	Porous (dune sand)
Wanke et al., 2008	-20.1	19.31	Physical Water Balance Model (MODBIL)	409	8	Porous
Wanke et al., 2013	-18.6	20.4	GM	450	11.5	Porous
Wanke et al., 2018a	-17.5	17.2	CMB	450	33	Porous (dune sand)

Wrabel, 1999	-21.5	17.8	CMB	425	28	Fractured

2.6.3 Comparative plots for annual groundwater recharge and precipitation in Namibia

The relationship between mean annual precipitation and mean annual recharge is illustrated in Figure 2-6, and shows a weak positive correlation. The GM gives stronger correlations than the CMB with $R^2 = 0.45$. Most of the groundwater models try to include the nature of the aquifer hence the degree of weathering and occurrence of porosity within the aquifer and vegetation or land cover (Abiye, 2016; Tögl, 2010). On the other hand, the CMB method primarily depends on climatic and chemical data regardless of the nature of the aquifer (Abiye, 2016). Thus, higher recharge values from the CMB are observed especially in fracture, karstified aquifers Figure 2-6b. The flow mechanism in these aquifers is preferential through the secondary porosity rather than piston flow, and that there is no loss of water, which would increase the Chloride concentration in the remaining water. The slopes in Figure 2-6a – c range from 0.05 to 0.14 and this means in general 5% to 14% of the precipitation become groundwater recharge in areas with mean annual precipitation between 150 to 600 mm/a in Namibia

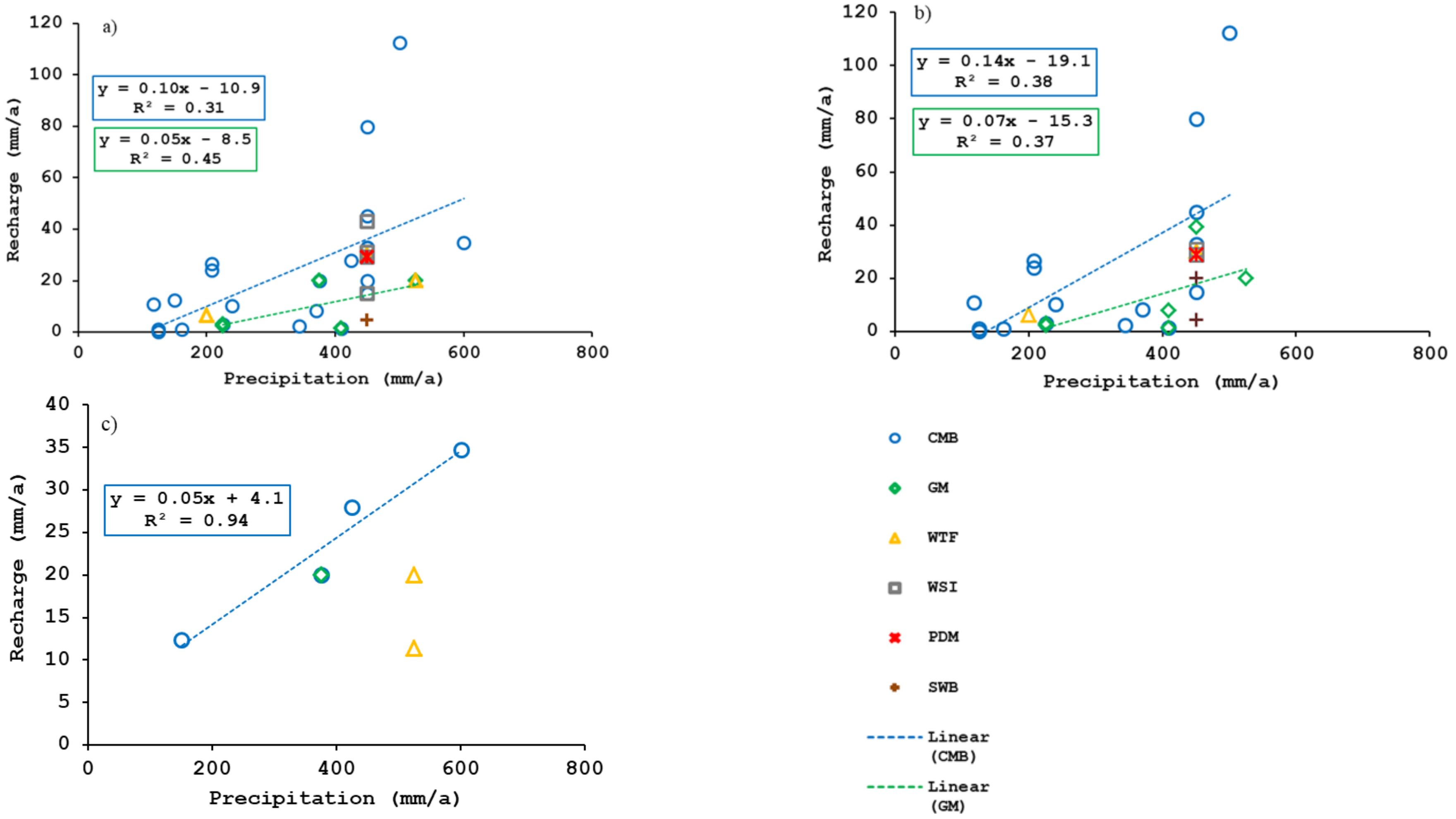

Figure 2-6: a) A comparative plot for annual recharge and precipitation in Namibia. b) Based on porous and c) Based on fractured, fissured or karstified aquifers; based on compilation in Table 2-2 and references therein. CMB = Chloride Mass Balance; GM = Groundwater Model; WTF = Water Table Fluctuation; WSI = Water Stable Isotope.

2.7 The effect/influence of woody plants on groundwater recharge

Ecohydrology is concerned with at least two issues: the importance of hydrological processes in ecosystems and the effects of plants on hydrological processes (Roberts, 2000). Plants play key roles in the interactions between groundwater and surface-water systems, because of its direct and indirect influence on recharge and because of the dependence of plant communities on groundwater (Maitre et al., 1999). Plants may uptake either soil water or groundwater, or both, depending on their rooting depths. Rooting depth and distribution defines the depth to or volume from which plants can potentially extract these water sources (Schulze et al., 1996; Zencich et al., 2002). Shrub's roots tend to be shallow and mainly distributed in the shallow soil as compared to trees that generally have deep root systems. As a result, shrubs utilise more soil water as compared to trees that utilise more groundwater (Ma et al., 2021; Pan et al., 2020) (Figure 2-7). Water stable isotope composition can be used to distinguish such source water by comparing the isotope signature of water in plant xylems to that of groundwater, soil water and precipitation in the respective focal study areas. Studies have been carried out to determine active root depths as well as to determine plant's source water using water stable isotopes (Beyer et al., 2016; Lubczynski, 2009; Lubis et al., 2014; Ma et al., 2021; Obakeng, 2007; Pan et al., 2020).

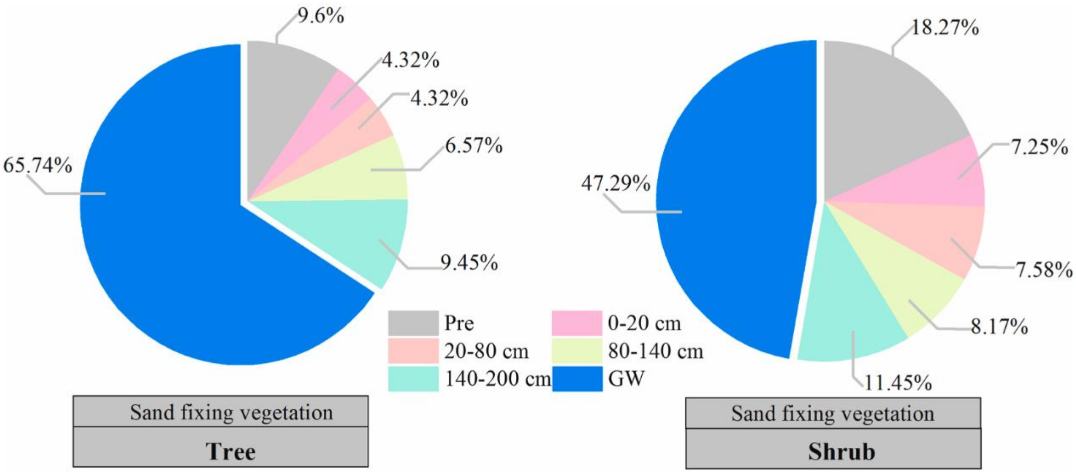

Figure 2-7: The contributions of different water sources to trees and shrubs water use in the sandy lands of northern China. Pre and GW represent precipitation and groundwater as water sources. The tree species examined included Pinus sylvestris, Haloxylon ammodendron, and Populus euphratica. Shrubs included Artemesia ordosica, Caragana korshinskii, and Tmarix ramosissima (Ma et al., 2021).

2.7.1 The effect of woody plant encroachment on groundwater

Woody plant encroachment is defined as an increase in density, cover, and biomass of shrubs and trees into areas where they were not present previously (Acharya et al., 2018; Van Auken, 2009). Bush encroached areas in Namibia are mapped by Bester (1996) and Lubbe 2010 through pers. comm to Colin Christian and Associates CC environmental Consultants, (2010) as shown in Figure 2-4. One of the parameters affected by woody plant encroachment is groundwater. Woody plant encroachment alters soil hydrological properties and reduces downward flux of water (Acharya et al., 2018, 2017). As a result water available for groundwater recharge is reduced due to the plant root uptake. Another effect of woody plant encroachment is an increase in transpiration rates as a result of an increase in woody plants (Acharya et al., 2018; Huxman et al., 2005). Although evapotranspiration is an underestimated component (Lubczynski, 2016), the estimated amount of water lost by woody plant encroachers through transpiration is around 12 million m^3 on a 10 000 ha (NAU, 2010; Shikangalah and Mapani, 2020). Barbeta and Peñuelas (2017) targeted studies evaluating the contributions of groundwater use by plants using stable isotope techniques and sampled the broadest geographical scale possible. Ma et al. (2021) also undertook a study looking at variations in water use strategies of plants along a precipitation gradient in northern China. Both Barbeta and Peñuelas (2017) and Ma et al. (2021) revealed that groundwater is most likely used by plants in areas with lower precipitation and during dry seasons. Plants tend to use groundwater during dry seasons when surface soils are dry due to lack of precipitation (Barbeta and Peñuelas, 2017). Moreover, the use of groundwater by plants is expected to intensify in the future due to climate change (Ma et al., 2021). The global average surface temperature rose at a rate of 0.12℃/a from 1951 to 2012 (Stocker and Plattner, 2014). An increase in average ambient temperature will thus result in high transpiration rates forcing plants to use more soil water provided that there is sufficient precipitation for replenishment, if not, groundwater will be used to a greater extent (Ma et al., 2021).

2.7.2 General description of Senegalia mellifera (S. mellifera)

S. mellifera subsp. *detinens* (Black Thorn) is listed among the main species that are causing the encroachment problem in Namibia (Bester, 1999; De Klerk, 2004) and it is the most widely distributed encroacher species in Namibia (De Klerk, 2004). *S. mellifera* has a bush-like form with branches just above the root crown. *S. mellifera* is believed to have a shallow but extensive root system which radiates from the root crown, whereby many of the roots extend 8 to 15 m from the stem, parallel to the surface and a depth of 25 cm (Figure 2-8a) (Adams, 1967). Moreover, an example of the extensive root system of *S. mellifera* in the upper layer of the soil layers is presented in Figure 2-8b. Such an extensive root system makes it easier for *S. mellifera* to effectively compete with other plants and have effect on water balance by extraction of soil water that could be available for groundwater recharge (NAU, 2010). Studies have also indicated that *S. mellifera* can develop a tap root in addition to its shallow extensive root system (Britz and Ward, 2007; O'Donnell et al., 2015). According to Bester (1999), Ebenhaezer Farm (where the deuterium tracer experiment was carried out) falls under the demarcations of commercial farming areas whereby *S. mellifera* has a bush density of 2000/ha, hence the farm to falls under encroached areas.

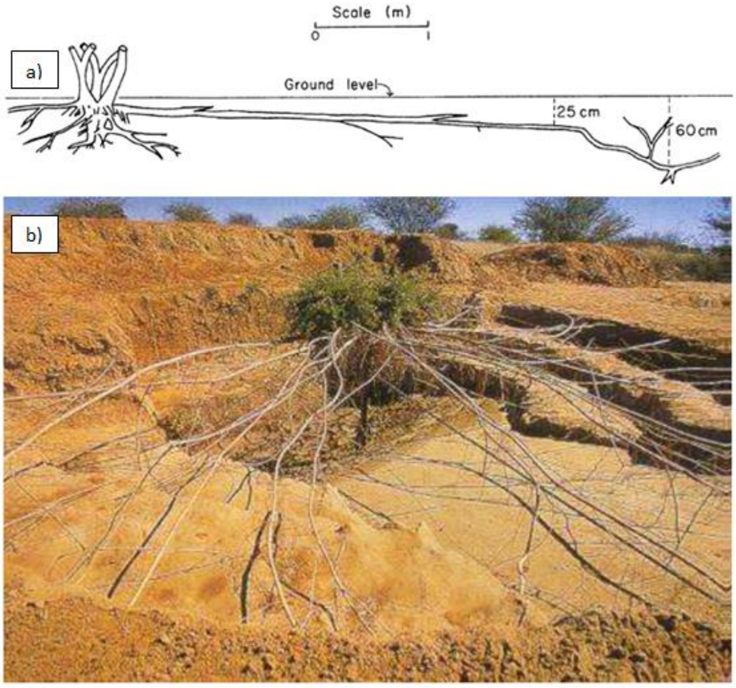

Figure 2-8: a) The root system of S. mellifera after G.E Wickens cited by Adams (1967). b) An example of the extensive root system of S. mellifera in the upper layers of the soil. Source: Nico Smit, University of the Free State, South Africa, cited by NAU (2010).

2.7.3 General description of Boscia albitrunca (B. albitrunca)

B. albitrunca (Shepherd's tree) is an evergreen tree with only one stem usually. *B. albitrunca* is classified as deep-rooted (Burke, 2006; Canadell et al., 1996). The distribution of the lateral biomass above 1.5 m depth is depicted in Figure 2- 9; whereby the root biomass increases with an increase in depth. Deep-rooted plants have the ability to abstract water from deep aquifers. Jennings (1974) discovered living tree roots from a depth of 68 m from an unused borehole in the Central Kalahari. However, Alias et al., (2003) stated that the effect of water extraction from groundwater sources on *B. albitrunca* is not known, but assumed that there could be a lowering of the water table that could result in large-scale mortality. Moreover, the environmental envelope for this plant covers the entire country (Burke, 2006).

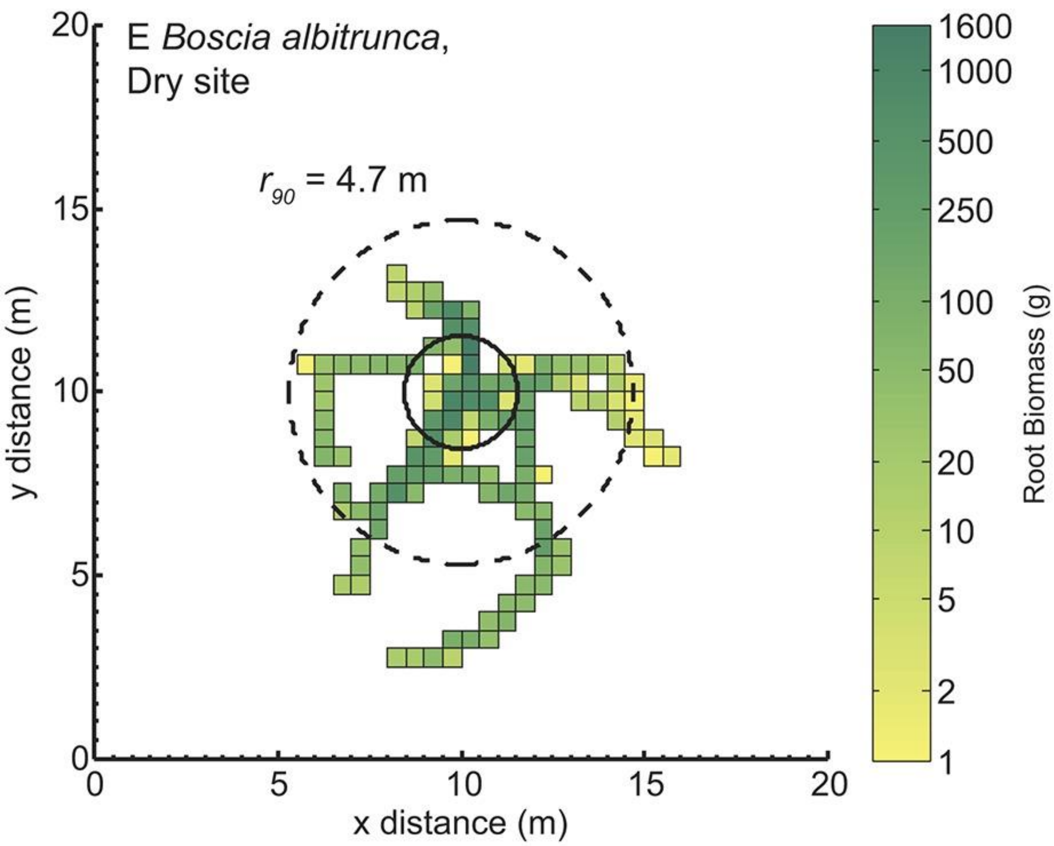

Figure 2-9: Distribution of lateral root biomass above 1.5 m of B. albitrunca excavated by O'Donnell et al. (2015). A Solid circle shows the outline of the canopy. The dashed circle shows the r_{90} (the radius of a circle that encompasses 90% of the root biomass to describe the lateral extent of a root system).

2.8 Identified knowledge gaps from the literature review

All the Namibian groundwater recharge studies collated in this chapter are either at a local scale or regionalised to the groundwater basin scale and thus covering only the precipitation gradient within that particular basin. Hence, there is a need to understand recharge processes and quantify such along a much larger precipitation gradient. Although the spatial distribution of these studies in Table 2-2 covers a wider range of precipitation gradient, they were carried out at different times. Therefore this study covers a wider precipitation gradient in three different groundwater basins with the same temporal resolution. The integrated temporal aspect makes it easier to compare results from these three particular sites. This addresses the first objective as well as tests the first hypothesis of the study.

Although a good number of groundwater recharge studies listed in Table 2-2 have been carried out in Namibia, only very few studies (Beyer et al., 2016, 2015; Geißler, 2019; Kanyama, 2017) have incorporated the effect of vegetation on groundwater recharge. Vegetation type is identified as one of the key factors influencing groundwater recharge (Table 2-1), it is of importance to determine the influence of woody plants on groundwater recharge in Namibia. Active root depth and comparisons of source water for both *S. mellifera* and *B. albitrunca* have never been studied in Namibia, hence this study addresses the two issues by attaining the second objective and proving the second hypothesis of the study. Furthermore, a seasonal variation in source water for these woody plants is assessed in order to test the third hypothesis of the study.

CHAPTER 3

DETERMINATION OF LOCAL METEORIC WATER LINES ALONG A PRECIPITATION GRADIENT, NAMIBIA

This chapter is published as: Uugulu, S., & Wanke, H. (2021). Determination of local meteoric water lines along a precipitation gradient, Namibia. *International Science and Technology Journal of Namibia*, *14*, 63-72.

3.1 Abstract

Precipitation is the main input parameter in the hydrological balance and plays an important role in groundwater recharge. Isotopic fingerprints are a tool to trace this component. In this study, isotopic composition of precipitation was determined along a precipitation gradient at three sites namely: Tsumeb (600 mm/a precipitation; Waterberg (450 mm/a) and Kuzikus/Ebenhaezer (240 mm/a precipitation). Precipitation samples from Tsumeb and Waterberg were collected during the rainy season from 2017 to 2018, while Kuzikus/Ebenhaezer samples were collected between 2014 and 2015. A total number of 83 precipitation samples were collected. Precipitation samples were analysed using a Los Gatos water stable isotope spectro-analyser at the University of Namibia. Precipitation isotopic values for $\delta^{18}O$(‰) range from -9.08 to 5.19 for Tsumeb, -15.96 to 5.09 for Waterberg and -12.54 to 4.75 for Kuzikus/Ebenhaezer, while $\delta^{2}H$(‰) isotopic values for Tsumeb, Waterberg and Kuzikus/Ebenhaezer range from -73.30 to 46.70; -117.50 to 40.60 and -82.50 to 47.80, respectively. Scattering of rain samples along the global meteoric water line in the areas could be attributed to a seasonal effect. Local meteoric water line equations for Tsumeb, Waterberg and Kuzikus/Ebenhaezer were obtained using a linear regression method and are $\delta^2H = 7.78\ \delta^{18}O + 6.74$, $R^2 = 0.95$; $\delta^2H = 7.37\ \delta^{18}O + 5.77$, $R^2 = 0.97$; $\delta^2H = 7.16\ \delta^{18}O + 9.88$, $R^2 = 0.96$ correspondingly. All the slopes obtained from three study sites are lower than that of a global meteoric water line equation. A lower slope could be an indication that the local precipitation has experienced some subcloud evaporation, leading to enrichment of heavy isotopes. The effect is more pronounced at Kuzikus/Ebenhaezer where the slope is 7.16. Our findings could serve as a baseline for these three study sites with regards to further isotopic investigations in the study areas especially in tracing the origin of groundwater.

Keywords: Local meteoric water line; precipitation gradient; isotopic values; Tsumeb; Waterberg; Kuzikus/Ebenhaezer

3.2 Introduction

Precipitation is the main input parameter in the hydrological cycle and plays a major role in groundwater recharge. To understand the process of groundwater recharge based on its isotopic fingerprint, it is important to first understand the isotopic composition of precipitation that serves as the parent source of groundwater through recharge processes. Craig (1961) derived Equation 3.1 for the Global Meteoric Water Line (GMWL) based on meteoric water from many places around the world as follows:

$$\delta^2\text{H} = 8\ \delta^{18}\text{O} + 10‰\ \text{SMOW} \quad \text{Eq 3.1}$$

where δ^2H is the concentration of deuterium relative to protium in unit of per mill (‰) of a sample compared to a standard; δ^{18}O is the concentration of oxygen-18 relative to oxygen-16 in unit of per mill (‰) of a sample compared to a standard, and the standard is SMOW (Standard Mean Ocean Water).

Isotopic composition of precipitation (δ^2H and δ^{18}O) is controlled by factors and processes such as meteorological conditions that are controlling evaporation of water from the ocean; rainout mechanisms, which influence the fraction of precipitable water; second-order kinetic effects such as snow formation or evaporation below cloud base and admixture of recycled water from evapotranspiration over the continents (Araguás-Araguás et al., 2000; Gat, 2000; Gibson et al., 2008). Variations in δ^2H and δ^{18}O values of precipitation water result from both equilibrium and kinetic fractionations depending on many factors and processes. These processes include conditions of air moisture source areas, air moisture transport trajectories, precipitation histories, weather systems leading to precipitation, and subcloud processes (Guan et al., 2013).

A meteoric water line is characterised by two parameters, i.e. slope and intercept which is a deuterium excess (d-excess). The slope and d-excess for the meteoric water line depend on hydrological parameters (Singh, 2017). Generally, the slope of a meteoric water line should be close to 8 which is the theoretic Craig slope under equilibrium conditions. However, the slope value could be lower than 8 during non-equilibrium processes such as evaporation or be greater than 8 for condensation (Dansgaard, 1964). The d-excess equation (Equation 3.2) was first formulated by Dansgaard (1964) as:

$$d = \delta^{2}H - 8\ \delta^{18}O \qquad \text{Eq 3.2}$$

where d is the d-excess, δ^2H and $\delta^{18}O$ stand for the deuterium and oxygen-18 abundance relative to VSMOW (Vienna Standard Mean Ocean Water). It is used to constrain the source of precipitation as well as the conditions during vapour transport to the precipitating site (Aemisegger et al., 2014; Bershaw, 2018; Pang et al., 2011; Pfahl and Sodemann, 2014; Uemura et al., 2008). The d-excess parameter has been shown to be a diagnostic tool for measuring the contribution of evaporated moisture to the downwind atmosphere (Gat et al., 1994). Craig (1961) derived the global d-excess value from the GMWL as 10‰. Lower d-excess values than 10‰ are likely due to enhanced subcloud evaporation of raindrops which is common in arid regions (Bershaw, 2018; Wang et al., 2016). Higher d-excess of vapour is observed when relative humidity is low over evaporating water bodies. The more kinetic fractionation that occurs, the higher the d-excess is observed in vapour (Bershaw, 2018).

Although studies have been carried out to determine local precipitation lines such as those of Kaseke et al. (2016) and Wanke et al. (2018), these studies focused on particular areas but have not identified a correlation between local meteoric water lines and the precipitation gradient in Namibia. Therefore a gap is identified to determine local meteoric water lines along a precipitation gradient. In this study, the δ^2H and $\delta^{18}O$ values of precipitation samples that were collected from Tsumeb, Waterberg and Kuzikus/Ebenhaezer are investigated with the main objective of determining local meteoric water lines along a precipitation gradient, and to understand isotopic variations.

3.3 General descriptions of study sites

The study was carried out along a precipitation gradient from Tsumeb in the northern part of Namibia, Waterberg in the central region and Kuzikus/Ebenhaezer in south-eastern Namibia. The study sites show a precipitation gradient from about 600 mm/a to 200 mm/a (Figure 3-1). Tsumeb area lies within the south-eastern part of Cuvelai-Etosha Basin. The area receives exceptionally high annual precipitation compared to the rest of the country with an annual precipitation rate of about 600 mm/a and an annual potential evaporation rate ranging between 2000 to 3000 mm/a (DWA, 1988). The Tsumeb area is known for its intensive agricultural activities as well as mining activities. The Waterberg area is found in the south-western part of Omatako Basin. The area receives an annual precipitation of about 450 mm/a and has a potential evaporation of about 2800 mm/a. (DWA, 1988). The study area is part of the Waterberg Plateau National Park which is distinguished by flowing springs at the foot of the plateau and game. The Kuzikus/Ebenhaezer area falls within the northern part of the Stampriet Basin, where the annual precipitation ranges between 175 mm to 240 mm, with potential evaporation varying from 3000 mm/a to 3500 mm/a (DWA, 1988). The study area is associated with cattle and game farming activities.

The rainy season in Namibia starts in October and ends in April of the following year. Mean annual precipitation isohyets are presented in Figure 3-1a). Long-term climatic conditions thus mean monthly precipitation and mean monthly temperatures were obtained from nearest weather stations to the sites namely: Tsumeb station (for the Tsumeb site); Okakarara station (for the Waterberg site) and Leonardville station (for the Kuzikus/Ebenhaezer site). A summary of these climatic conditions are presented in Figure 3-1 b).

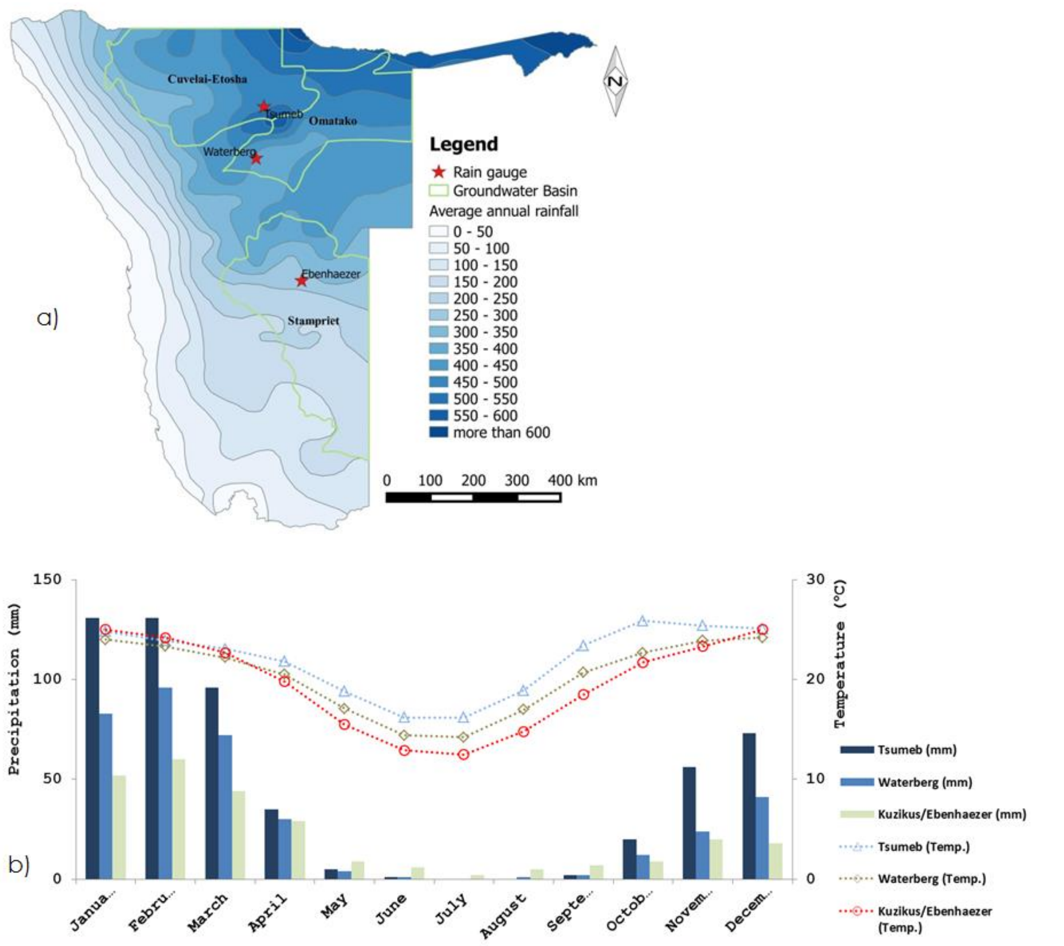

Figure 3-1: Climatic conditions: a) precipitation gradient (Data source: DEA, 2002); b) mean monthly precipitation and temperature for Tsumeb, Waterberg and Kuzikus/Ebenhaezer from 1982 -2012 (Data source: climate-data.org, 2018).

3.4 Material and Methods

Precipitation stations were set up at respective study areas whereby a rain gauge was mounted to a pole about 2 m long. Precipitation events were collected and tightly sealed in 50 ml clear glass bottles as soon as the rain stopped to prevent evaporation.

Precipitation samples from Tsumeb and Waterberg were collected during the rainy season from 2017 to 2018, while Kuzikus/Ebenhaezer samples were collected between 2014 and 2015. A total number of 83 precipitation event samples were collected (20 samples from Tsumeb, 29 samples from Waterberg, 34 samples from Ebenhaezer). Precipitation event samples were analysed using Los Gatos Research Inc., LGR DLT 100 laser spectrometer at the hydro-lab, University of Namibia whereby the mean values of each sample were obtained. All isotope ratios were reported in δ-notation (‰) relative to the international Vienna Standard Mean Ocean Water (VSMOW) standard as indicated in Equation 3.3:

$$\delta \text{ sample } (‰) = \left(\mathrm{R_{sample}} - \frac{\mathrm{R_{VSMOW}}}{\mathrm{R_{VSMOW}}}\right) * 1000 \quad \text{Eq 3.3}$$

where δ sample is the deviation of the isotope ratio of a sample relative to that of the VSMOW, R_{sample} is the ratio of ^{18}O to ^{16}O atoms or $^{2}H/^{1}H$ atoms in the sample, and R_{vsmow} is the ratio of ^{18}O to ^{16}O atoms or $^{2}H/^{1}H$ atoms in the VSMOW standard.

D-excess values for each sample were obtained using Equation 3.2 by (Dansgaard, 1964). The mean weighted isotopic values for $\delta^{2}H$ and $\delta^{18}O$ were obtained by multiplying isotope values by the precipitation amount added together and divided by the total precipitation amount. The arithmetic mean was obtained by adding isotopic values and then divided by the total number of samples. Local Meteoric Water Lines (LMWs) were generated using linear regressions for all precipitation samples collected at the specific site. Coefficients of determination of the regression lines have been determined as R^2. Annual arithmetic $\delta^{18}O$ means have been calculated based on events and used in the plots for *altitude, latitude and continental effects*.

3.5 Results and Discussion

3.5.1 Characteristics of $\delta^{18}O$ and $\delta^{2}H$ values in precipitation

Precipitation isotopic values for $\delta^{18}O$(‰) range from -9.08 to 5.19 for Tsumeb, -15.96 to 5.09 for Waterberg and -12.54 to 4.75 for Kuzikus/Ebenhaezer, while $\delta^{2}H$(‰) isotopic values for Tsumeb range from -73.30 to 46.70, Waterberg -117.50 to 40.60 and Kuzikus/Ebenhaezer -82.50 to 47.80 (See Appendix 6 for a full dataset). These isotopic values are scattered along the GMWL (Figure 3-2). The scattering of isotopic values along a GMWL could be attributed to a seasonal effect.

A seasonal fluctuation of the stable isotope ratios is observed as a result of temperature effects, different trajectory of air masses, and varying fractionation processes in the source area of atmospheric moisture (Külls, 2000). A comparison of weighted mean values of both $\delta^{18}O$ and $\delta^{2}H$ (Table 3-1) to the precipitation isotopic isoscapes of Namibia by Kaseke et al. (2016) indicates that the mean values obtained in these study areas fall mainly within the $\delta^{18}O$ and $\delta^{2}H$ range values of their globally fitted isoscape model with an exception of Waterberg $\delta^{2}H$ mean value that falls within the ranges of their cokriging isoscape model. Kaseke et al. (2016) have indicated a progressive isotopic depletion from east to west of Namibia which is attributed to the modification of the water vapour from the Indian Ocean along its trajectory. Furthermore, as marine air parcels move into the continents, they tend to mix and homogenise resulting in the scattering of isotopic values along meteoric water lines (Gat, 1996).

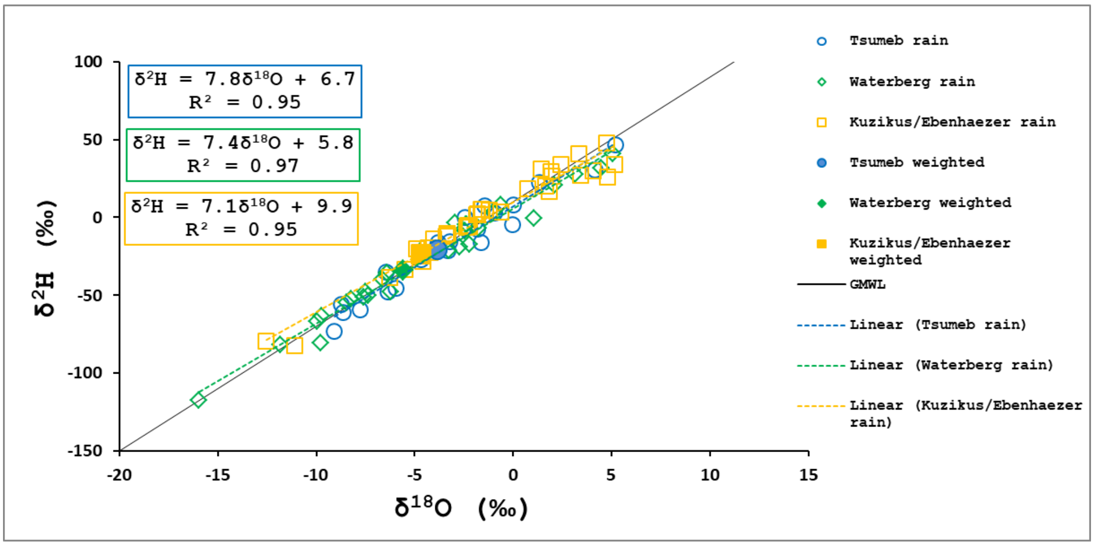

Figure 3-2: Dual plot of stable isotopes for Tsumeb, Waterberg and Kuzikus/Ebenhaezer.

Table 3-1: A summary of isotopic values in precipitation events

Site	Long. (⁰)	Lat. (⁰)	Altitude (m)	Arithmetic Mean $\delta^{18}O$ (‰)	Arithmetic Mean $\delta^{2}H$(‰)	Weighted mean $\delta^{18}O$ (‰)	Weighted mean $\delta^{2}H$(‰)
Tsumeb	17.58215	-19.20610	1313	-2.99	-17.61	-3.88	-21.14
Waterberg	17.39876	-20.39602	1475	-4.36	-26.36	-5.60	-34.30
Ebenhaezer	18.45601	-23.21571	1340	-1.40	0.025	-4.67	-23.57

3.5.2 Slopes of the local meteoric lines

LMWL equations for Tsumeb, Waterberg and Kuzikus/Ebenhaezer were obtained using a linear regression method and are: $\delta^2H = 7.78\ \delta^{18}O + 6.74$, $R^2 = 0.95$; $\delta\ ^2H = 7.37\ \delta^{18}O + 5.77$, $R^2 = 0.97$; $\delta^2H = 7.07\ \delta^{18}O + 9.94$, $R^2 = 0.96$ correspondingly. Slopes of the defined LMWs are noted to be decreasing along a precipitation gradient, whereby Tsumeb has the highest slope and Kuzikus/Ebenhaezer the lowest (see Figure 3-2). All the slopes obtained from the three study sites are lower than that of the GMWL which is 8. The effect is most pronounced at Kuzikus/Ebenhaezer (slope =7.07).

A slope which is less than 8 is usually attributed to evaporation from the falling rain that results in the enrichment of the heavy isotopes in the remnant drop along the so-called evaporation line (Gat, 1996). Kuzikus/Ebenhaezer site having the lowest slope correlates well with a higher potential evaporation value in the study area in comparison to Tsumeb and Waterberg; hence a pronounced evaporation effect. Our slopes are within the ranges of slopes that have been determined in Namibia by Kaseke et al. (2016) (GNIP based LMWL and observed LMWL both with a slope of 7.20, Wanke et al. (2018) (LMWL slope for CEB as 7.20) and JICA (2002) (LMWL for Stampriet basin with a slope of 7.10) where they indicated that such a low slope implies a degree of dryness. Wanke et al. (2018) compiled slopes from 22 different sources in southern Africa whereby the minimum slope of 5.60 is from Lake Sibayi catchment, South Africa, and the highest value of 8.70 from central Mozambique. All in all, the average slope value from these 22 sources is 7.13 and comparable to our results. On a global scale, lower slopes were also found for the semi-arid region of the US Great Plains (Harvey and Welker, 2000) and an arid region in northwest China (Pang et al., 2011).

3.5.3 Variation of Deuterium Excess in Precipitation

D-excess obtained from the LMWL equations are as follows: 6.74‰ for Tsumeb; 5.77‰ for Waterberg and 9.94‰ for Kuzikus/Ebenhaezer (see Figure 3-2). D-excess value for Kuzikus/Ebenhaezer is very close to that defined by Craig (1961) which is

10. However, the same cannot be said for Tsumeb and Waterberg as they have lower d-excess values. Deuterium excess obtained from each sample plotted against $\delta^{18}O$ (Figure 3-3) shows an insignificant negative correlation for all three sites with R^2 values of 0.02; 0.20 and 0.26 for Tsumeb, Waterberg and Kuzikus/Ebenhaezer, respectively.

The fact that d-excess values from the LMWLs for all the three sites are lower than that of GMWL, could be a result of subcloud secondary evaporation which also leads to enrichment of heavy isotopes in precipitation (Crawford et al., 2017; Wang et al., 2016). On the other hand, most of the d-excess values obtained from each sample are slightly higher than 10‰ and usually, the evaporated moisture's isotope composition is characterised by larger d-excess values, so precipitation derived from an air mass into which the re-evaporated moisture is admixed is also characterised by a large d-excess (Dansgaard, 1964; Gat, 1996).

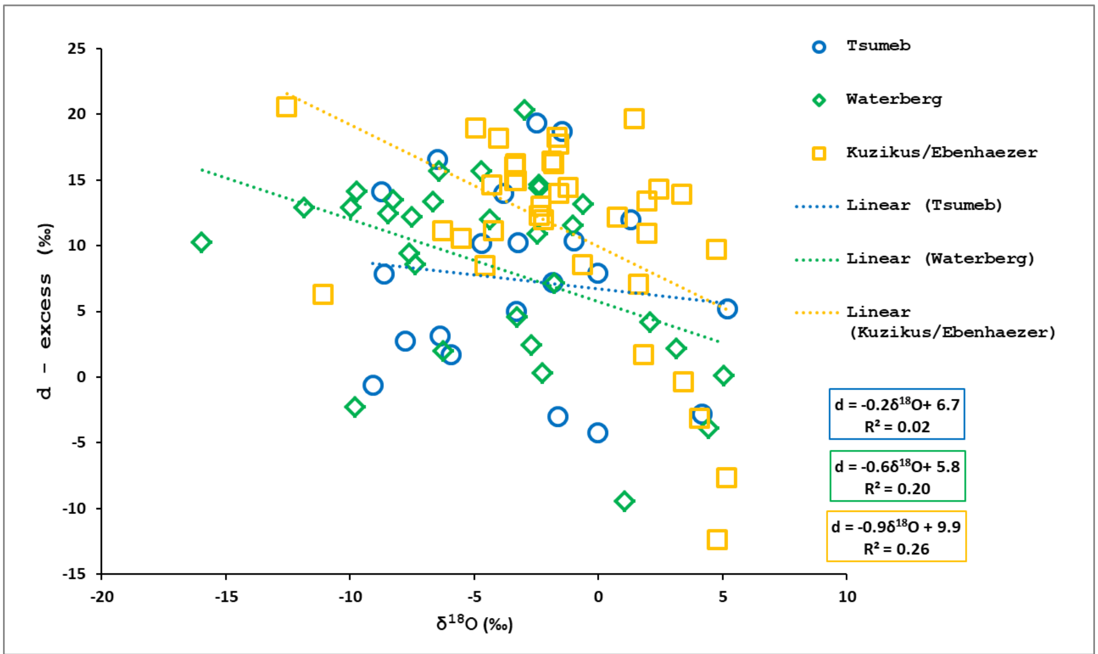

Figure 3-3: D-excess variations observed at Tsumeb, Waterberg and Kuzikus/Ebenhaezer.

3.5.4 Observed Isotopic Effects in Precipitation

3.5.4.1 Amount Effects

R^2 derived from regression lines were as follows: R^2 = 0.08 for Tsumeb; R^2 = 0.09 for Waterberg; R^2 = 0.52 for Kuzikus/Ebenhaezer (Figure 3-4). Very low R^2 values for both Tsumeb and Waterberg (0.08 and 0.09 respectively) is an indication that precipitation amount is not a controlling factor of the isotopic composition of precipitation at these two sites. It correlates well with findings by Wanke et al. (2018) and Crawford et al. (2017). However, the same cannot be said for Kuzikus/Ebenhaezer where R^2 value (0.52) shows that there is a moderate correlation between $\delta^{18}O$ and the amount of precipitation. Evaporation from falling rain drops and fractionation by isotopic exchange tend to enrich small amounts of rain in heavy isotopes (Dansgaard, 1964). A slightly pronounced amount effect at Kuzikus/Ebenhaezer could be attributed to such factors, especially that this area has the highest potential evapotranspiration and lowest monthly precipitation averages in comparison to the other two study areas.

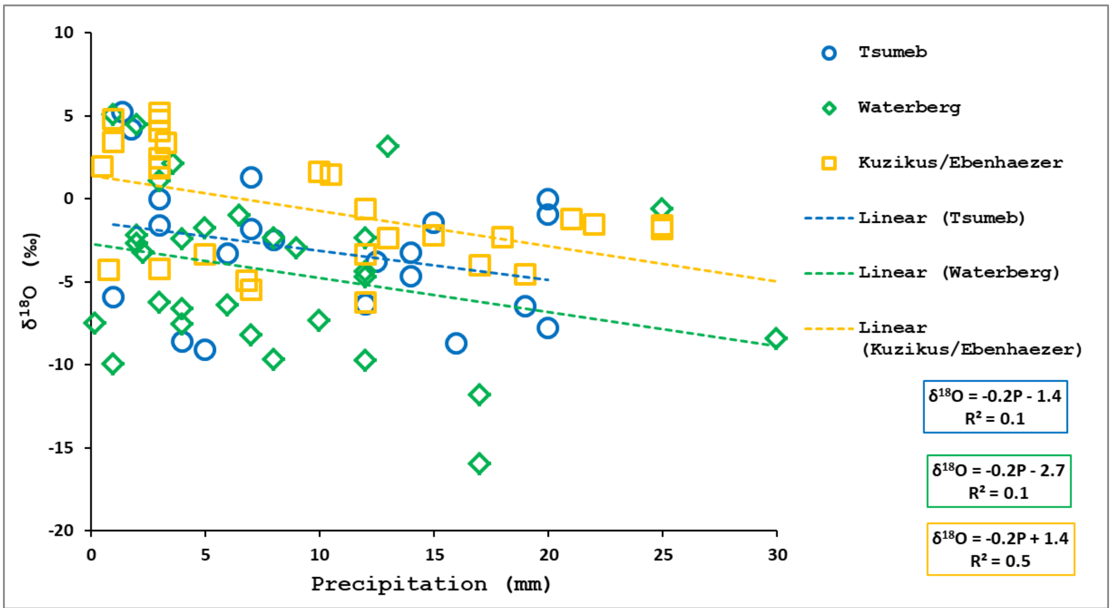

Figure 3-4: Amount effects observed at Tsumeb, Waterberg and Kuzikus/Ebenhaezer.

3.5.4.2 Altitude, Latitude, Continental and Seasonal Effect

For the altitude effect, there is a strong linear correlation with R^2 = 0.90 (Figure 3-5a). However, there is no correlation for latitude and continental effects as their R^2 values are 0.06 and 0.04, respectively (Figure 3-5b and 3-5c). A pronounced altitude effect could be attributed to the fact that the lowering of temperature with increasing elevation in mountainous regions usually leads to enhanced condensation and as a result to a progressive depletion in heavy isotopes of precipitation with altitude (Araguás-Araguás et al., 2000). Dansgaard (1964) also indicated that heavy isotope concentrations in fresh water decrease with increasing altitude.

For the seasonal effect, the general trend for the three sites is that $\delta^{18}O$ values are varying with months (Figure 3-5d). Values are enriched in $\delta^{18}O$ at the beginning of the rainy season (October to January) and progressively become depleted during the rainy season. The most $\delta^{18}O$ depleted value is from Kuzikus/Ebenhaezer of -10.79‰ in April followed by Waterberg with -10.35‰ in March. Kuzikus/Ebenhaezer received two heavy rain events thus 55 mm and 65 mm with more depleted $\delta^{18}O$ values of -11.10‰ and -12.54‰ respectively. The heaviest rain event at Waterberg was recorded in March of 30 mm with $\delta^{18}O$ values of -8.44‰ and the most depleted $\delta^{18}O$ value of -15.96‰ in the same month is associated with a 17 mm rain event. High rain intensities are usually associated with depleted isotope compositions (Gat et al., 2000).

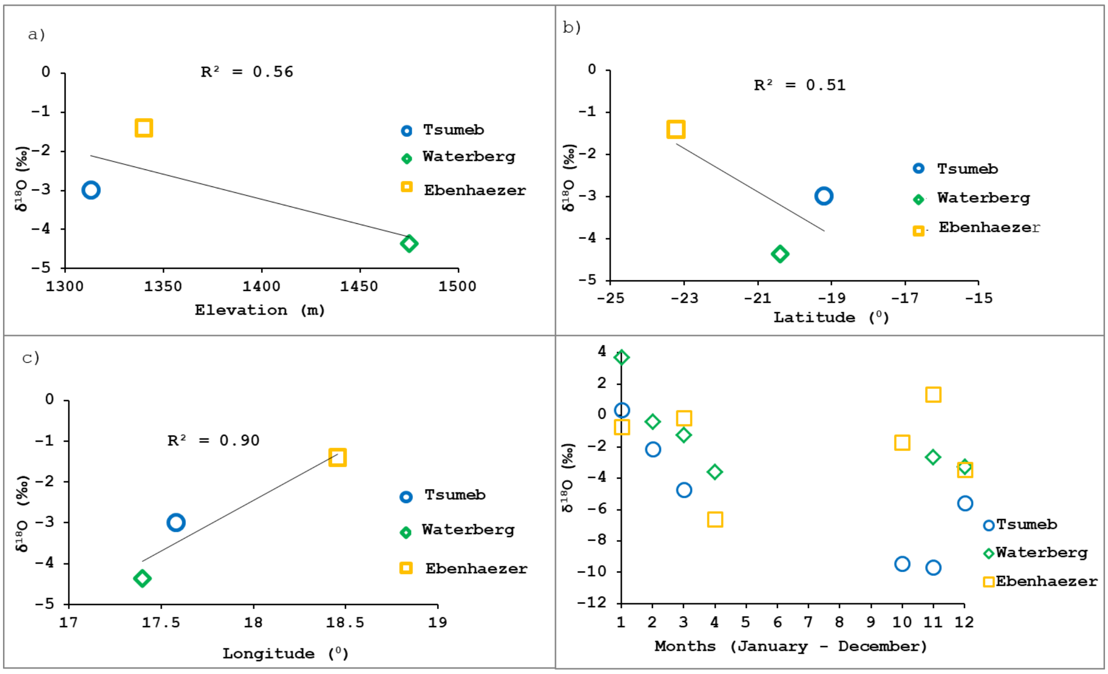

Figure 3-5: Effects across a precipitation gradient in Namibia: a) altitude effect; b) latitude effect; c) longitude effect; d) seasonal effect (based on weighted means $\delta^{18}O$ values) observed at Tsumeb, Waterberg and Kuzikus/Ebenhaezer.

3.6 Conclusion

The study has determined and shown local meteoric water lines that are varying along a precipitation gradient and their slopes were noted to be decreasing along a precipitation gradient. Such findings could be of importance for future studies along the precipitation gradient in between the study sites as one could use our generalised findings by extrapolations to give insight for the distribution across the entire country. Additionally, these findings serve as a baseline for those three study sites with regards to further isotopic investigations in the study areas especially in tracing the origin of groundwater since much of the isotopic composition of precipitation recharging groundwater is retained provided that there is no evaporation. However, this study was done for a yearlong period only and it would be ideal to record such measures over periods of at least one decade and obtain long term annual averages. It would also be more accurate to collect samples at the same time for the three sites for a longer period as this will be interesting to understand the impact of climate change over time.

3.7 Acknowledgements

The study was carried out under the framework of OPTIMASS Project (01LL1302A) and fully funded by the German Federal Ministry of Education and Research (BMBF). Authors would like to thank Mr Hiskia Uugulu, Mr Arsenio Nambuli and OPTIMASS students for assisting in collecting precipitation events at Tsumeb, Waterberg and Kuzikus/Ebenhaezer.

3.8 Declaration of conflict of Interest

The authors declare that there are no conflicts of interest.

CHAPTER 4

ESTIMATION OF GROUNDWATER RECHARGE IN SAVANNAH AQUIFERS ALONG A PRECIPITATION GRADIENT USING CHLORIDE MASS BALANCE METHOD AND ENVIRONMENTAL ISOTOPES, NAMIBIA

This chapter is published as: Uugulu, S., and H. Wanke. "Estimation of groundwater recharge in savannah aquifers along a precipitation gradient using chloride mass balance method and environmental isotopes, Namibia." *Physics and Chemistry of the Earth, Parts A/B/C* 116 (2020): 102844. https://doi.org/10.1016/j.pce.2020.102844

4.1 Abstract

The quantification of groundwater resources is essential especially in water scarce countries like Namibia. The chloride mass balance (CMB) method and isotopic composition were used in determining groundwater recharge along a precipitation gradient at three sites, namely: Tsumeb (600 mm/a precipitation); Waterberg (450 mm/a precipitation) and Kuzikus/ Ebenhaezer (240 mm/a precipitation). Groundwater and rainwater were collected from 2016 to 2017. Rainwater was collected monthly while groundwater was collected before, during and after rainy seasons. Rainwater isotopic values for $\delta^{18}O$ and $\delta^{2}H$ range from -10.70 to 6.10 and from -72.7 to 42.1 respectively. Groundwater isotopic values for $\delta^{18}O$ range from -9.84 to -5.35 for Tsumeb; from -10.85 to -8.60 for Waterberg and from -8.24 to -1.56 for Kuzikus/Ebenhaezer, while that for $\delta^{2}H$ range from -65.6 to -46.7 for Tsumeb; -69.4 to -61.2 for Waterberg and -54.2 to -22.7 for Kuzikus/Ebenhaezer. Rainwater scatters along the GMWL. Rainwater collected in January, February and March are more depleted in heavy isotopes than those in November, December, April and May. Waterberg groundwater plots on the GMWL which indicates absence of evaporation.

Tsumeb groundwater plots on/close to the GMWL with an exception of groundwater from the karst Lake Otjikoto which is showing evaporation. Groundwater from Kuzikus/Ebenhaezer shows an evaporation effect. All groundwater from three sites plot in the same area with rainwater depleted in stable isotopic values, an indication that recharge only takes place during January, February and March. CMB method revealed that Waterberg has the highest recharge rate ranging between 39.1 mm/a and 51.1 mm/a (8.7% - 11.4% of annual precipitation), Tsumeb with rates ranging from 21.1 mm/a to 48.5 mm/a (3.5% - 8.1% of annual precipitation), and lastly Kuzikus/Ebenhaezer from 3.2 mm/a to 17.5 mm/a (1.4% - 7.3% of annual precipitation). High recharge rates in Waterberg could be related to fast infiltration and absence of evaporation as indicated by the isotopic ratios. Differences in recharge rates cannot only be attributed to the precipitation gradient but also to the evaporation rates and the presence of preferential flow paths. Recharge rates estimated for these three sites can be used in managing the savannah aquifers especially at Kuzikus/Ebenhaezer where evaporation effect is observed that one can consider rain harvesting.

Key words*: Chloride Mass Balance; Groundwater recharge; Isotopic values; Precipitation gradient*

4.2 Introduction

Namibia is a dry sub-Saharan country with limited surface water resources due to the fact that all rivers inside Namibia are ephemeral and all perennial rivers are shared with neighbouring countries. Groundwater is therefore the main source of water in the country both for domestic and agricultural purposes.

Estimating groundwater recharge in arid and semi-arid regions like Namibia can be difficult, because such regions are characterised by generally low recharge compared to the average annual rainfall or evapotranspiration, and thus making it difficult to quantify precisely (Bridget R; Scanlon et al., 2002). Recharge occurs to some extent in even the most arid regions and, as aridity increases, direct recharge is likely to become less important than localised and indirect recharge, in terms of total aquifer replenishment (Alsaaran, 2005) (De Vries and Simmers, 2002).

Accurate quantification of recharge rates is vital for proper management and protection of valuable groundwater resources. For proper management systems the recharge to the aquifer cannot be easily measured directly but usually estimated by indirect means (Lerner et al., 1990).

The Chloride mass balance (CMB) method and environmental isotopes have been commonly used in water resource development and management (Subyani, 2004). The CMB method is based on the law of conservation of mass, where chloride is considered as a conservative tracer. The input of chloride deposition by both dry and wet deposition is assumed to balance out the output of chloride concentration by infiltration and mineralisation.

The CMB method has been successfully applied in several studies to estimate groundwater recharge rates in semi-arid areas. Sharma and Hughes (1985) estimated groundwater recharge using the CMB method in the deep coastal sands of Western Australia, (Gieske et al., (1990) in south eastern Botswana and Subyani (2004) in Saudi Arabia with 15, 2.5 and 11 % of the average annual precipitation respectively.

Environmental isotopes are widely used as tracers to understand hydrogeological processes such as precipitation, groundwater recharge, groundwater-surface water and vegetation interaction. A comparison of the $\delta^{18}O$ and $\delta^{2}H$ isotopic compositions of precipitation and groundwater provides an excellent tool for evaluating the recharge mechanism (Yeh et al., 2014). This method can only be used to understand groundwater recharge processes rather than quantifying groundwater recharge, and therefore needs to be used hand in hand with other groundwater recharge estimation methods such as CMB.

Vogel and Van Urk (1975) compared the $\delta^{18}O$ content of the precipitation at Grootfontein with the $\delta^{18}O$ content of the groundwater from the Etosha National Park, assuming a north western discharge of groundwater from the Grootfontein district. His conclusion was the recharge only takes place under exceptional circumstances, when precipitation tends to have lower heavy isotope content. Hoad (1993) considers that recharge to the confined Kalahari aquifer occurs by through flow from the unconfined Kalahari aquifer. The unconfined aquifer between Namutoni Gate and Otjikoto Lake is defined as the recharge area where direct diffuse recharge is thought to be the dominant recharge mechanism to the unconfined Kalahari aquifer. Groundwater recharge estimation using the saturated volume fluctuation approach revealed annual recharge ranging between 0.33% and 4% of the mean annual precipitation for both Kalahari and Otavi dolomite aquifers (Bäumle, 2003).

Mainardy (1999) estimated groundwater recharge rates based on the chloride method and on fracture aperture measurements. Recharge amounts ranging between 3.2 to 4.8% of the mean annual precipitation were determined for bare, fractured sandstone in the western part of the Waterberg. Much lower recharge values of 0.2 to 1.8% of the mean annual rainfall in the area were derived for quartzite outcrops of the Nossib Group and for meta-sediments belonging to the Damara Sequence.

Külls (2000) estimated groundwater recharge in the north-eastern part of the Omatako Basin ranging between 0.1 to 2.5 % using a water balance model. He also used the CMB method that gave recharge values ranging between 2% and 3.3% of the mean annual rainfall.

Külls (2000) observed only little isotopic enrichment by evaporation in the western part of the Waterberg area. However, the isotopic composition of groundwater from the secondary aquifers in the Damara Sequence north of the Waterberg indicates some evaporative enrichment due to shallower depths to the water table.

Taapopi (2015) estimated groundwater recharge rates in the unsaturated zone at Ebenhaezer farm in the Stampriet Basin using CMB. Her findings ranged from 0.18% to 0.71% of the mean annual precipitation. Stone and Edmunds (2012) estimated groundwater recharge rates in the Kalahari dune field, Stampriet Basin using CMB method in the unsaturated zone. Their findings indicated recharge values between 4% and 20% of the mean annual precipitation, with chloride profiles representing between 10 years and 30 years of rainfall infiltration. JICA (2002) determined groundwater recharge rates of the Auob aquifer system, Stampriet Basin and found out that the recharge is 1% of the long-term mean annual precipitation.

Although groundwater recharge studies have been carried out in Namibia, a seasonal sampling along a precipitation gradient has not been carried. This study thus aims at identifying groundwater recharge rates as well as processes using a CMB method and water stable isotopes $\delta^{2}H$ and $\delta^{18}O$ along a precipitation gradient in the savannah aquifers, therefore from Tsumeb area in the north, Waterberg in the central part and Kuzikus/Ebenhaezer further south of Namibia.

4.3 Description of the study areas

4.3.1 Location

The study was carried out along a precipitation gradient in the following areas: Tsumeb, Waterberg and Kuzikus/Ebenhaezer. The study areas indicate a precipitation gradient (Figure 4-1). Tsumeb area lies within the south-eastern part of Cuvelai-Etosha Basin, having the highest annual precipitation rate of about 600 mm/a and an annual potential evaporation rate ranging between 2000 to 3000 mm/a. The Waterberg area lies within the south-western part of Omatako Basin. The area receives an annual precipitation of about 450 mm and has a potential evaporation of about 2800 mm/a. Kuzikus/Ebenhaezer area is part of the Stampriet Basin, where the annual precipitation within the basin ranges between 175 mm to 240 mm, with potential evaporation varying from 3000 mm/a to 3500 mm/a (DWA, 1988).

Both Tsumeb and Kuzikus/Ebenhaezer study areas are flat-lying areas while the Waterberg area has a southern slope where springs emerge from the Etjo sandstone. All three study areas are characterised by a savannah vegetation zone which is mainly dominated by thorn trees and bushes. Common vegetation species that are found at all three study areas are: *Senegalia mellifera, Senegalia erioloba, Dichrostachys cinerea, Boscia Albitrunca.*

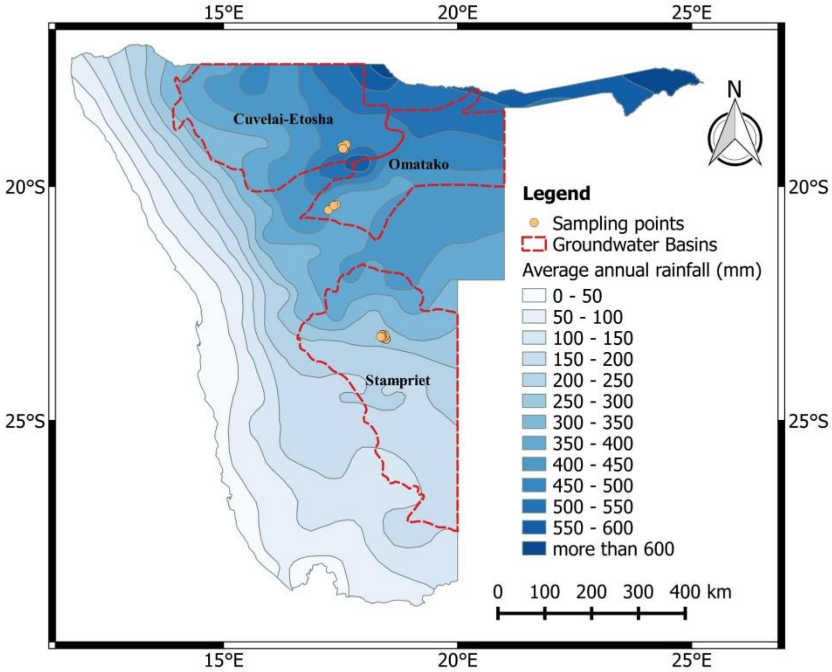

Figure 4-1: Location of the study areas, data source Acacia Project E1 database.

4.3.2 Geology, Hydrology and Hydrogeology

4.3.2.1 Tsumeb area

Tsumeb area is located within the Otavi Mountain Land of northern Namibia, which forms part of the Northern Carbonate Platform of the Pan African Orogen. Rocks of the Damara Supergroup are unconformably deposited on the Grootfontein basement rocks. The oldest Damara sediments are the volcanics and clastic rocks of the Nosib Group. These are unconformably overlain by rocks of the Otavi Group which are composed of Carbonates initially deposited on a stable marine shelf (Miller, 2008). Sandstone of the young Mulden Group overlays the Otavi Group rocks (Figure 4-2).

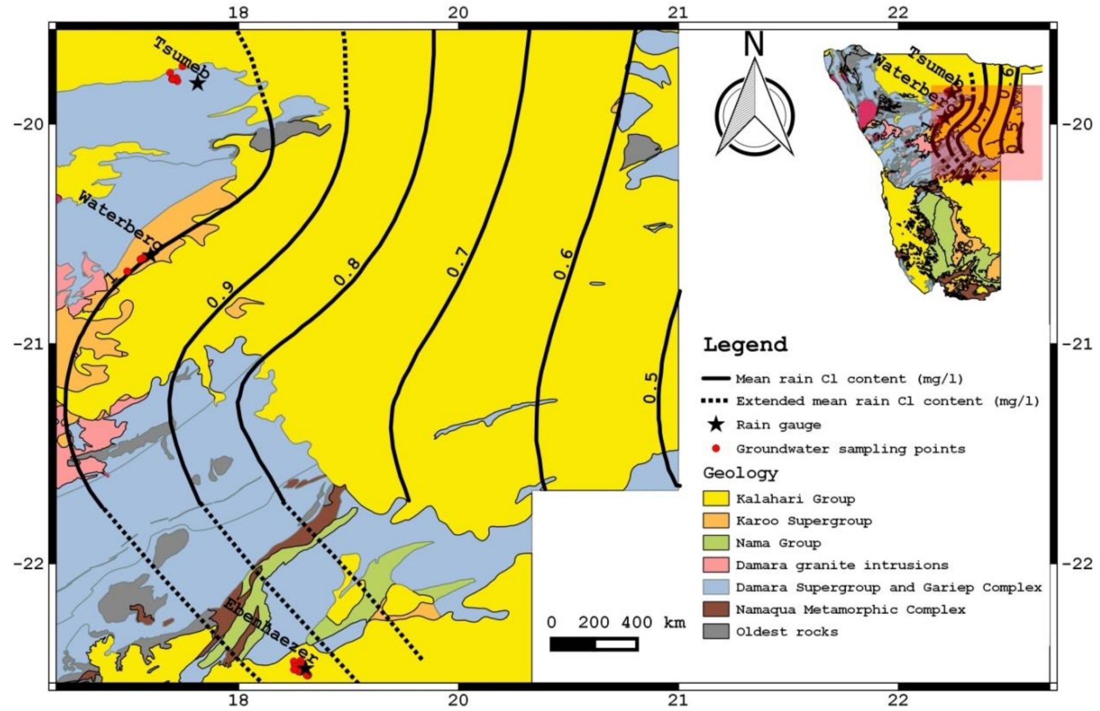

Figure 4-2: Geology of the study areas, Data source E1, Acacia Project database overlain by the mean chloride concentration in precipitation isolines obtained from Klock (2001).

In general, the Otavi Mountain Land, within which the Tsumeb area lies, has a watershed draining westwards into the Ugab River catchment, northwards into the Etosha Pan, south and eastwards into the Omatako Omuramba, a tributary of the Okavango River (Christelis and Struckmeier, 2011).

Groundwater in the Tsumeb area is contained in two principal aquifers: the Tsumeb Karst Aquifer (TKA) in the north and the Grootfontein Karst Aquifer (GKA) in the south. According to Van Vuuren (2011) these two aquifer systems are divided by the low transmissivity rocks of the Nosib group and therefore there is little groundwater flow between them. The GKA drains water towards the south, in the direction of the Omatako Omuramba whilst the TKA drains towards the north (Van Vuuren, 2011).

Due to the karstic nature of the TKA, the groundwater potential in the study area is relatively high with a few areas that are locally having low potential probably where karstic features are not well pronounced (Figure 4-3).

Borehole information from the SADC Groundwater Information Portal (SADC-GIP) shows a wide range of the borehole depths in the TKA. Some boreholes are as shallow as 18 m while some are as deep as 120 m. Depth to groundwater in the study area varies, with static water level as low as 6 m and the deepest at 25 m.

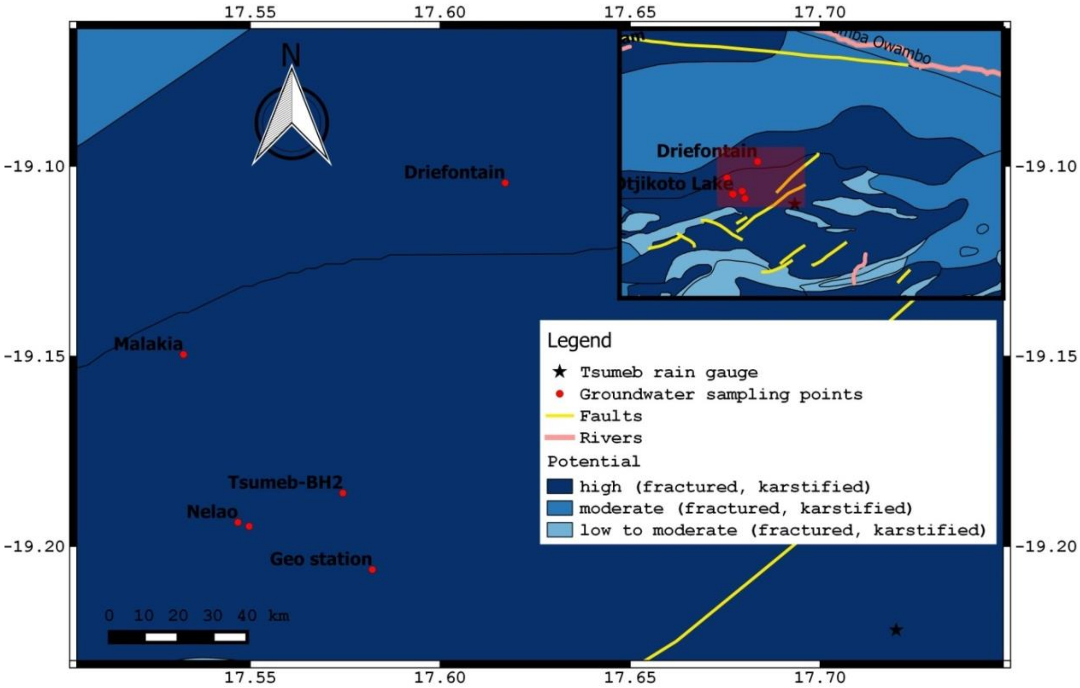

Figure 4-3: Hydrogeological map of the Tsumeb area, data source Department of Water Affairs of Namibia and BGR (2001).

4.3.2.2 Waterberg area

Waterberg area is covered by Kalahari sediments of less than 10 m thick that overlay the Etjo formation (Sandstone) of the Karoo group in the western part of the area and the secondary aquifers in the Damara sequence north of the Waterberg (Külls, 2000) (Figure 4-2).

The Waterberg area forms part of the Brandberg, Erongo and Waterberg Hydrogeological Region of Namibia (Christellis and Struckmeier, 2011). The area has no permanent rivers, except for small ephemeral rivers which may carry water for very short periods after heavy rain. Generally, the Omatako Omuramba drains towards the east and finally to the north-east while the Ugab and several smaller rivers drain towards the west (Figure 4-4). Almost all water in the region comes from the underground, pumped from boreholes or via free flowing springs.

In this region, the Waterberg plateau forms a major hydrogeological structure containing a series of contact fountains that drain water from the porous sandstone layers of the Etjo Formation (Christellis and Struckmeier, 2011). In addition to that, a number of springs emerge on the southern slope of the Waterberg. Groundwater in the study area occurs predominantly in hard rock bodies and porous alluvial aquifers, as shown in Figure 4-4. The hard rock bodies (sandstone) and the porous alluvial aquifers (Kalahari sand) have generally low but locally moderate groundwater potential whilst in areas where the hard rock bodies are fractured or fissured, the potential for groundwater is relatively high (Figure 4-4).

SADC Groundwater Information portal (SADC-GIP) reveals borehole depth in the study area ranging from 50 m to 150 m and with an average depth to groundwater of 20 m.

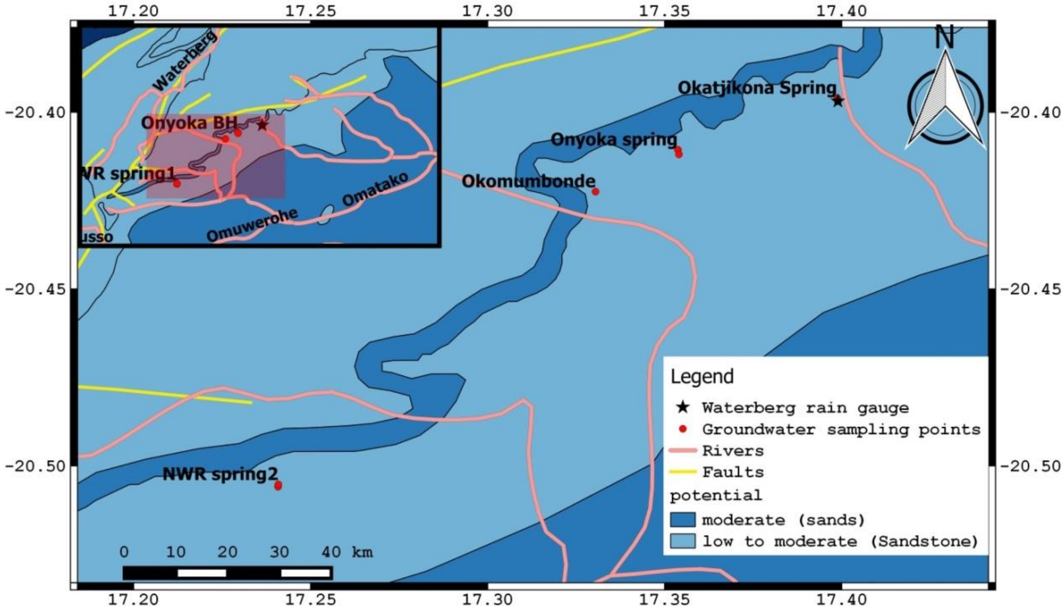

Figure 4-4: Hydrogeological map of the Waterberg area, Data source Department of Water Affairs of Namibia and BGR (2001).

4.3.2.3 Kuzikus/Ebenhaezer area

Kuzikus/Ebenhaezer, which lies in the north-western parts of the Stampriet Basin (Figure 4-1), is characterised by rocks of the Karoo Sequence, Nama group rocks as well as the Damara Sequence (Figure 4-2). These are overlain by young Kalahari sequence deposits (Miller, 2008).

There are no permanent rivers flowing through the basin except for the ephemeral Auob River and Nossob River, which are the only evidence of surface water flow during wetter climates in the past (Christellis and Struckmeier, 2011). The entire basin therefore relies on groundwater.

Groundwater in the basin occurs in three main aquifers (Figure 4-5): the Auob sandstone; the Nossob sandstone and the Kalahari beds (Alker, 2009; Christellis and Struckmeier, 2001). The Auob aquifer and the Nossob aquifer lie in the Ecca Group of the Lower Karoo Sequence. These aquifers are confined and may be free-flowing (artesian) in some parts of the basin such as in the Auob valley and downstream of the Stampriet settlement as well as in the Nossob valley around Leonardville.

Elsewhere in the basin, groundwater is sub-artesian.

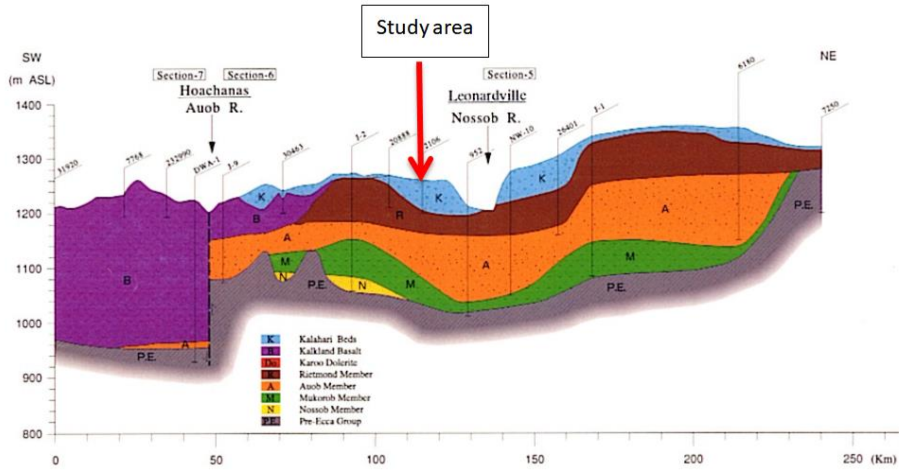

Figure 4-5: Geological cross section of JICA Section 1 (the section closer to the sampling points) in the Stampriet Basin (JICA, 2002).

According to JICA (2002), small, shallow depressions caused by calcrete dissolution become karstic sinkholes where local runoff concentrates and sinks into permeable layers or structures below. Furthermore, fractures also act as preferential flow paths for groundwater recharge to these confined aquifers. Such geological features exist in the west, northwest and southwest of the basin; as a result there is low or non-existence of isotopic evaporation of the water in these aquifers. On the other hand, the water in the unconfined Kalahari layers in the central part of the basin has a very definite isotopic evaporation signal, indicating that a substantial proportion of rainfall evaporates and consequently does not recharge the aquifer (Alker, 2009).

Groundwater in the Kuzikus/Ebenhaezer area is contained in porous aquifers, thus the hard rock bodies as well as in porous alluvium layers (Figure 4-6). The groundwater potential in these layers ranges between low to moderate potential. An average measured depth to groundwater in the study area is 36.5 m.

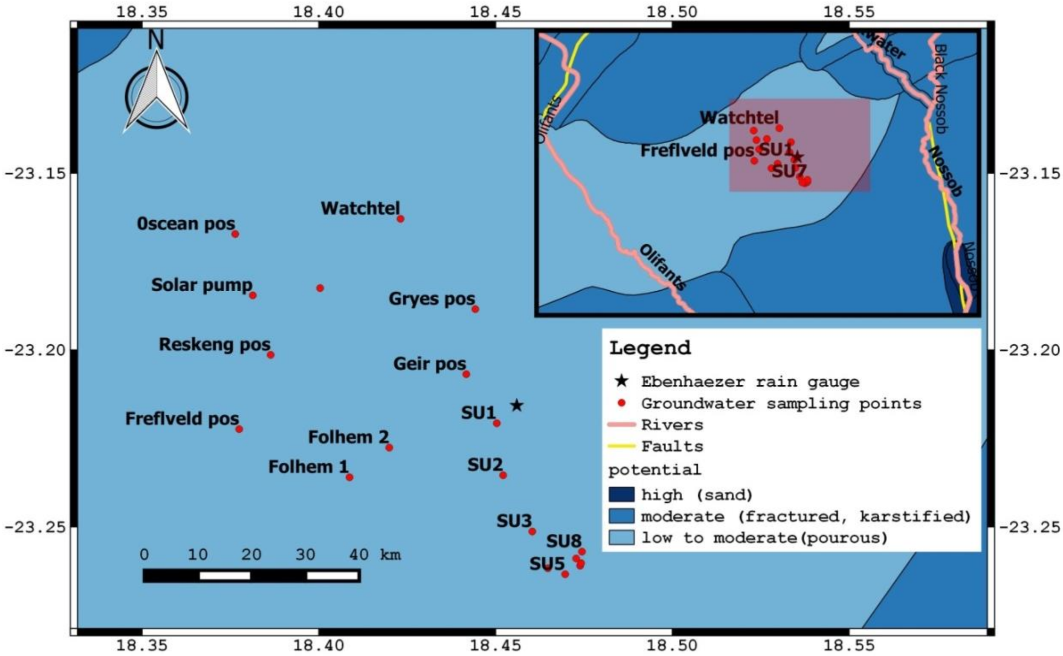

Figure 4-6: Hydrogeological map of the Kuzikus/Ebenhaezer area, Data source Department of Water affairs of Namibia and BGR (2001).

4.4 Materials and Methods

Seasonal field campaigns were carried out between 2016 and 2017 for Tsumeb, Waterberg and Kuzikus/Ebenhaezer areas. A total of 20 rainwater samples were collected monthly throughout the rainy seasons using a rain collector at all three study sites. Groundwater sampling was done before the rainy season (around November), during the rainy season (March), and after the rainy season (June). As a result, a total of 28, 25 and 58 groundwater samples were collected from boreholes in Tsumeb Karst Aquifer, Tsumeb; boreholes and springs in the Etjo sandstone, Waterberg; and boreholes in the unconfined Kalahari sand, Kuzikus/Ebenhaezer respectively. Accessibility to boreholes in the Kuzikus/Ebenhaezer area enabled us to collect more samples compared to the other two study sites.

Onsite parameters such as electrical conductivity, pH, redox potential and temperature were measured using Hach field portable instruments (pH metre, conductivity metre, multimeter for the redox potential). TDS was determined from the electrical conductivity values where the conversion factors (k_e) for the study areas were determined from SADC-GIP borehole data. Average k_e values of 0.66 for Tsumeb, 0.71 for Waterberg and 0.64 for Kuzikus/Ebenhaezer were used.

50 ml glass bottles were used to collect groundwater samples. Chloride content for 27 groundwater samples from the three study sites was determined using an ion-selective electrode by measuring 25 ml of the sample into a beaker with a chloride ionic strength adjuster, and then placed on a magnetic stirrer to homogenise the solution.

The long term averages for annual precipitation amounts from DWA (1988) were used for each of the sites to estimate groundwater recharge. An annual precipitation amount of 600 mm/a was used for Tsumeb, 450 mm/a for Waterberg and an average annual precipitation amount of 240 mm/a for the Leonardville weather station close to the Kuzikus/Ebenhaezer area.

Average chloride concentrations in precipitation were obtained from Klock (2001). For Waterberg, the rain collector falls on the 1 mg/l average chloride concentration isoline. Furthermore, average chloride concentrations isolines were extended to obtain values for both Tsumeb and Kuzikus/Ebenhaezer as indicated in Figure 4-2, where a 1.05 mg/l and 0.95 mg/l were determined for Tsumeb and Kuzikus/Ebenhaezer respectively.

Groundwater recharge rates were determined using the CMB method. For CMB in Kalahari, the input by dry deposition is small when compared to the wet deposition

(Gieske, 1992) and for that reason it is assumed negligible and therefore Equation 4.1 can be used to estimate groundwater recharge:

$$R = \frac{\left((P-A)*Cl_p\right)}{Cl_{gw}} \qquad \text{Eq 4.1}$$

Where P = Precipitation (mm); A = surface runoff; Cl_p = Chloride concentration in precipitation (mg/l); Cl_{gw} = Chloride concentration in groundwater (mg/l) and R = Recharge (mm). There is no sign of surface runoff at the study sites as there are no stream close to sites, hence very little surface runoff can be neglected and recharge computation is justified in semi-arid regions (Sibanda et al., 2009).

Both rainwater and groundwater isotopic contents were measured using the Laser Absorption Spectrometry measurements LGR DLT 100. Results are reported in ‰ versus VSMOW standard (Vienna–Standard Mean Ocean Water). Typical analytical uncertainty of the reported isotopic values is about ±0.2 ‰ for $\delta^{18}O$ and ±0.14‰ for $\delta^{2}H$. Both Chloride and isotopic content analyses were carried out at the University of Namibia hydro-laboratories.

4.5 Results

4.5.1 Groundwater physio-chemical parameters

Groundwater pH ranges between 6.0 to 7.2 for Tsumeb; 5.4 to 8.4 for Waterberg; and 6.2 to 8.0 for Kuzikus/Ebenhaezer, thus groundwater in these areas is slightly acidic to slightly alkaline in nature with an exception of Onyoka spring in the Waterberg area which is mildly acidic, covered by algae and not captured due to its low yield. With an exception of Onyoka spring in Waterberg, pH for all sites are within a range of 6 – 9 therefore, groundwater at all three study areas can be classified as of class A according to Namibian drinking water guidelines.

The electrical conductivity values for Tsumeb range from 630 to 1763 µS/cm; 17 to 311 µS/cm for Waterberg; and 347 to 994 µS/cm for Kuzikus/Ebenhaezer. Groundwater samples from the Tsumeb area show elevated electric conductivities during the rainy season and after the rainy season in comparison to values before rainy the season as indicated in Figure 4-7. Electrical conductivities for both Waterberg and Kuzikus/Ebenhaezer are below 1500 µS/cm and therefore the water quality is classified as of type A which is an excellent quality according to Namibian drinking water guidelines. All other groundwater points sampled in Tsumeb have class A water quality with an exception of Driefontein where the electrical conductivity is 1763 µS/cm during the rainy season, making the water quality to be of class B, hence water with acceptable quality.

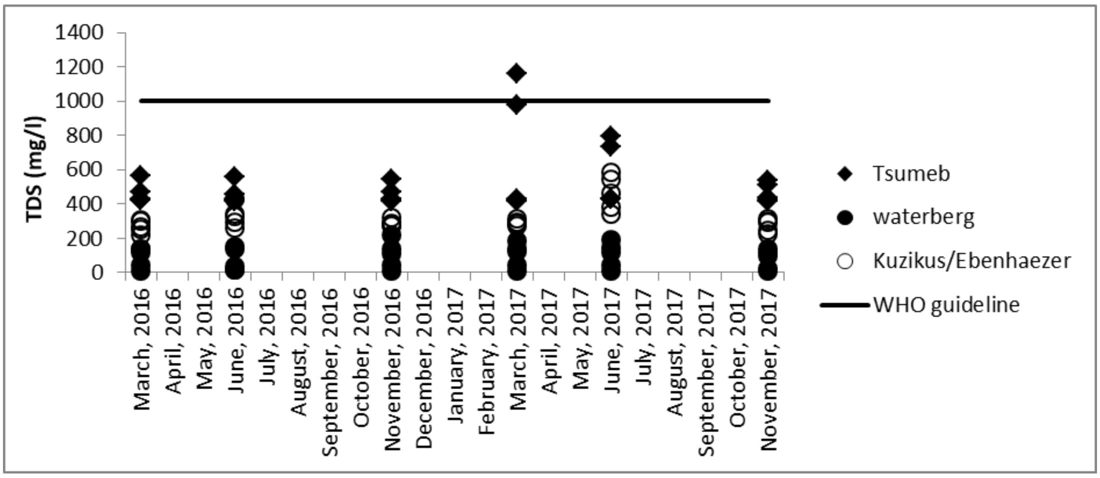

Figure 4-7: TDS for the three sites.

Total dissolved solids (TDS) at Waterberg and Kuzikus/Ebenhaezer sites are all within the World Health Organization (WHO) guidelines for safe drinking water (Figure 4-7). However, Tsumeb has one sampling point (Driefontein) where the TDS is above WHO guidelines during the rainy season (March 2017).

The average redox potential values for Tsumeb, Waterberg and Kuzikus/Ebenhaezer areas are 138.5 mV, 126.8 mV and 131.0 mV respectively. Such values are typical for an oxidising environment. Groundwater sampled during the rainy season has a higher redox potential especially those from Kuzikus/Ebenhaezer area (Figure 4-8) compared to those collected at the end of the rainy season. A summary of groundwater physical parameters is given below in Table 4-1.

Table 4-1: Summary of physical parameters for all three seasons.

Kuzikus/Ebenhaezer				
Parameter	Minimum	Maximum	Median	Average
pH	6.2	8.0	7.0	7.1
EC (µS/cm)	347.0	1792.0	470.5	555.2
Temp (^{o}C)	17.2	39.7	26.3	26.6
Eh (mV)	-3.6	423.0	121.0	131.0
Waterberg				
Parameter	Minimum	Maximum	Median	Average
pH	5.4	8.4	6.6	6.7
EC (µS/cm)	17.0	311.0	158.2	123.8
Temp (^{o}C)	18.3	35.7	23.7	24.1
Eh (mV)	25.4	204.6	126.4	126.8
Tsumeb				
Parameter	Minimum	Maximum	Median	Average
pH	6.0	7.2	6.6	6.7
EC (µS/cm)	630.0	1763.0	649.0	778.6
Temp (^{o}C)	14.9	31.4	27.8	27.1
Eh (mV)	46.7	195.2	136.7	138.5

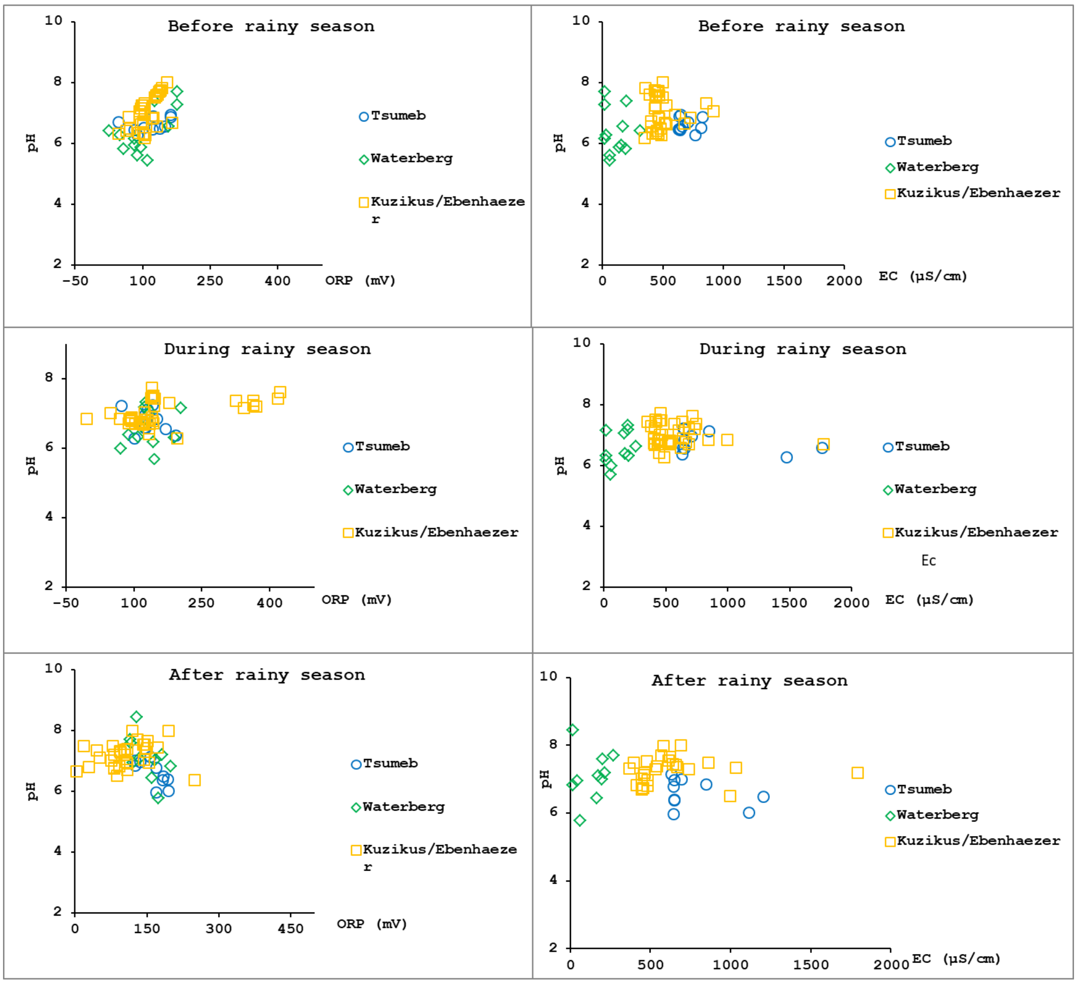

Figure 4-8: Redox Potential (ORP), Electrical Conductivity (EC) and pH for the groundwater samples from Tsumeb, Waterberg and Kuzikus/Ebenhaezer areas.

4.5.2 Chloride mass balance method

Groundwater recharge rates in the Tsumeb area vary between 21.1 and 48.5 mm/a (3.5 – 8.1% of annual precipitation) (see Table 4-2). Waterberg recharge rates range between 39.1 mm/a to 51.1 mm/a (8.7- 11.45% of annual precipitation) while rates from Kuzikus/Ebenhaezer are between 3.2 mm/a to 17.5 mm/a (1.3 – 7.3% of annual precipitation). On average, Waterberg has the highest recharge rate of 43.1 mm/a (9.6 % of annual precipitation), followed by Tsumeb with a rate of 36.4 mm/a (6.1%

of annual precipitation) and lastly Kuzikus/Ebenhaezer with an average rate of 9.8 mm/a (4.1 % of annual precipitation). See Appendix 7 for a full dataset.

Table 4-2: Groundwater recharge values based on chloride content

Tsumeb	Minimum	Maximum	Median	Average
Chloride in Groundwater (mg/l)	13.0	29.8	14.2	18.1
Recharge values (mm/a)	20.1	46.2	42.3	36.4
Recharge values (%)	3.4	7.7	7.0	6.1
Waterberg	Minimum	Maximum	Median	Average
Chloride in Groundwater (mg/l)	8.8	11.5	10.7	10.5
Recharge values (mm/a)	39.1	51.1	42.3	43.1
Recharge values (%)	8.7	11.4	9.4	9.6
Kuzikus/Ebenhaezer	Minimum	Maximum	Median	Average
Chloride in Groundwater (mg/l)	13.0	71.4	26.9	31.5
Recharge values (mm/a)	3.4	18.5	8.9	9.8
Recharge values (%)	1.4	7.7	3.7	4.1

4.5.3 Water stable isotopes

Rainwater samples show isotopic contents ranging from –10.70 to 6.10‰ vs. VSMOW for $\delta^{18}O$ and –72.7 to 42.1‰ vs. V-SMOW for $\delta^{2}H$. Rainwater samples are scattered along the global meteoric water line (GMWL) Figure 4-8. A seasonal effect is indicated by more enriched samples collected in April, May, November and December while samples collected in January, February, and March are more depleted in heavy isotopes (Figure 4-9).

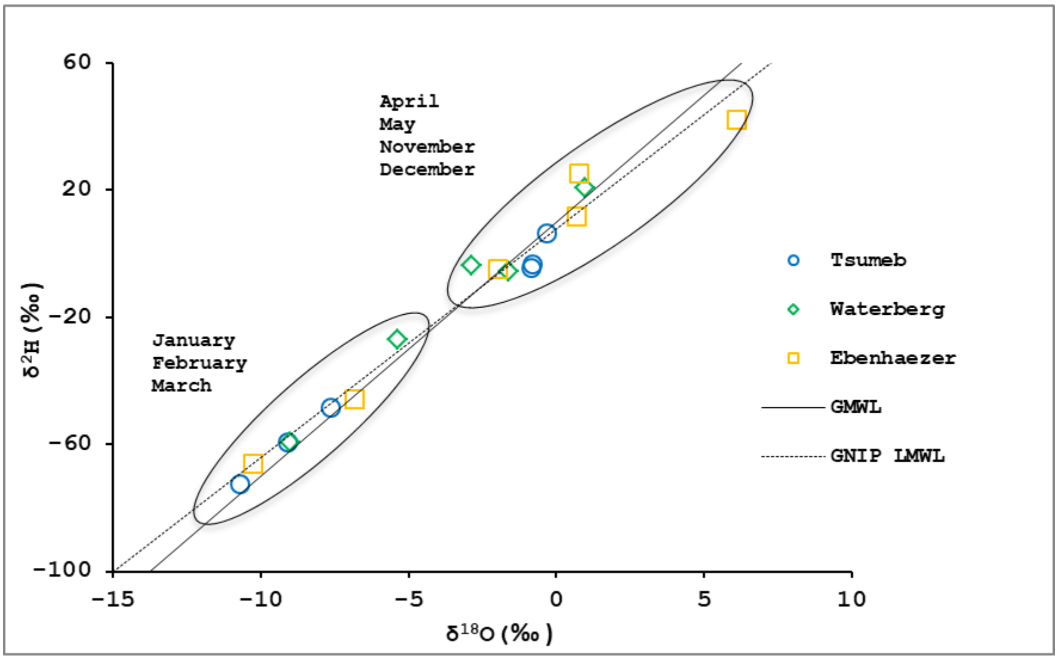

Figure 4-9: Isotopic values for monthly rain samples collected at Tsumeb, Waterberg and Kuzikus/Ebenhaezer areas.

Groundwater samples show isotopic values ranging from –9.9 to –1.1‰ vs. V-SMOW for δ^{18}O and –65.6 to –32.3‰ vs. V-SMOW for δ^{2}H for Tsumeb area; –10.9 to –8.6‰ vs. V-SMOW for δ^{18}O and –70.7 to –61.2‰ vs. V-SMOW for δ^{2}H for Waterberg and –8.2 to –1.3‰ vs. V-SMOW for δ^{18}O and –59.0 to –21.3‰ vs. V-SMOW for δ^{2}H for Kuzikus/Ebenhaezer.

Groundwater samples from the Tsumeb area are plotted on the GMWL, with an exemption of a few that are plotting slightly below and above the GMWL (Figure 4-10). Groundwater from Waterberg area is plotting on the GMWL, with an exemption of few samples that are plotting slightly above the GMWL (Figure 4-10) but on the Global Network of Isotopes in Precipitation local meteoric water line for Windhoek (GNIP LMWL). Few groundwater samples collected at Kuzikus/Ebenhaezer are plotting on the GMWL while the majority of the samples are plotting below the GMWL. Samples that are plotting directly on the GMWL at Kuzikus/Ebenhaezer are mainly collected during the rainy season. In general, groundwater isotopic compositions from these three study sites are similar to that of rain water occurring in January, February and March (Figure 4-9 and Figure 4-10).

Groundwater sampled during rainy season shows a trendline of $\delta^2H = 3.8\ \delta^{18}O - 28.1$ with a $R^2 = 0.7$) for Tsumeb; $\delta^2H = 3.2\ \delta^{18}O - 34.4$ with a $R^2 = 0.6$ for Waterberg; and $\delta^2H = 5.0\ \delta^{18}O - 16.6$ with a $R^2 = 1.0$ for Kuzikus/Ebenhaezer. Samples taken after the rainy season has a $\delta^2H = 4.4\ \delta^{18}O - 24.2$ with a $R^2 = 0.9$ for Tsumeb; $\delta^2H = 4.5\ \delta^{18}O - 23.3$ with a $R^2 = 0.5$ for Waterberg; and $\delta 2H = 5.7\ \delta^{18}O - 14.7$ with a $R^2 = 0.9$ for Kuzikus/Ebenhaezer. Groundwater collected before the rainy season shows a trend line of $\delta^2H = 3.8\ \delta^{18}O - 28.2$ with a $R^2 = 1.0$ for Tsumeb; $\delta^2H = 3.5\ \delta^{18}O - 32.1$ with a $R^2 = 0.6$ for Waterberg; and $= 4.8\ \delta^{18}O - 17.7$ with a $R^2 = 1$ for Kuzikus/Ebenhaezer. Groundwater collected at the beginning of the rainy season at Tsumeb and Waterberg areas show trend lines of $\delta^2H = 4.3\ \delta^{18}O - 23.3$ with $R^2 = 1.0$ and $\delta^2H = 7.5\ \delta^{18}O + 7.1$ with a $R^2 = 0.9$ respectively.

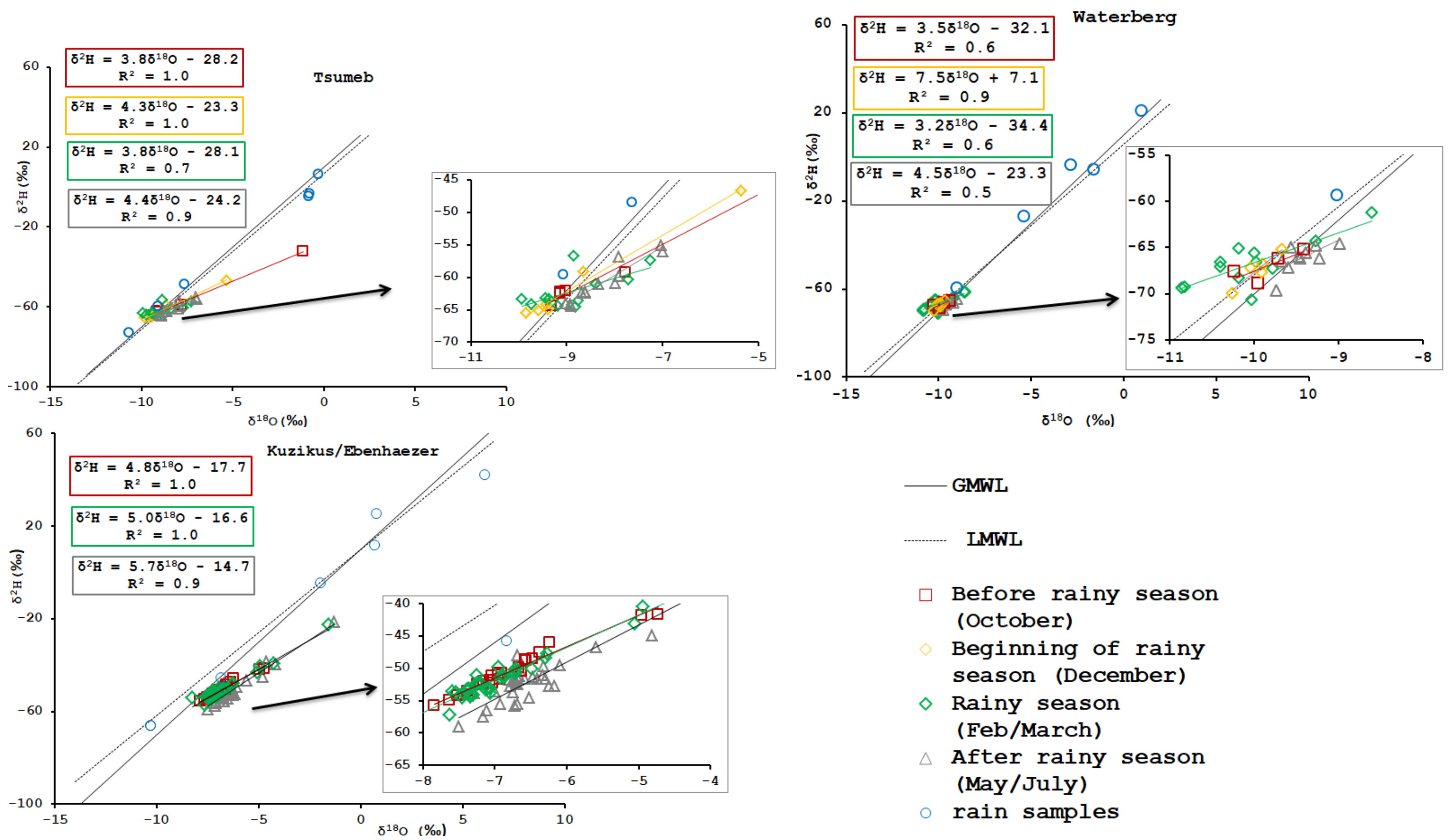

Figure 4-10: Dual isotope plots of both precipitation and groundwater from Tsumeb, Waterberg and Kuzikus/Ebenhaezer areas.

4.6. Discussion

4.6.1 Groundwater physio-chemical parameters

Groundwater samples from Onyoka spring in the Waterberg area are mildly acidic due to the presence of algae. The presence of algae in water reduces its pH due to the fact that the pH of the water is lowered during respiration, where carbon dioxide is produced and hydroxide levels decrease (Assmy and Smetacek, 2012).

Waterberg groundwater having the lowest electrical conductivity and followed by Kuzikus/Ebenhaezer can be explained by the fact that groundwater at these two study sites are hosted in Karoo sandstone and Kalahari sand respectively where dissolution is limited in comparison to Tsumeb groundwater which is hosted in a karst aquifer (TKA). Consequently, this explains why Tsumeb area show elevated electric conductivities during rainy and after rainy seasons in comparison to values before rainy season which is due to rock-water interaction therefore dissolution of the carbonate minerals at Tsumeb especially at the Driefontein farm where TDS exceeded WHO drinking water guideline during 2017 rainy season. This is further supported by the study carried out by Li et al. (2018) in the western part of the Cuvelai - Etosha Basin where authors identified dissolution of carbonates as the main hydrochemical process responsible for an increase in total dissolved solids.

Groundwater sampled during the rainy season has a higher redox potential especially at Kuzikus/Ebenhaezer area compared to other seasons due to rainwater that enters the groundwater system with a higher redox potential as a result of its exposure to atmospheric oxygen (Freeze and Cherry, 1979). This indicates that groundwater systems at all three study sites are under oxic conditions.

4.6.2 Chloride mass balance method

The chloride mass balance method revealed that the Waterberg area has a higher recharge rate compared to all other study sites although the Tsumeb area has the highest annual precipitation amount. This is an indication that groundwater recharge at these three study sites is not only necessarily controlled by the mean annual amount of precipitation at each site but probably by other factors too.

A synthesis on groundwater recharge in Southern Africa done by Abiye (2016) revealed that the presence of permeable geological cover plays a role in groundwater recharge in the region which however is not captured by most of the recharge estimate methods. Based on Abiye (2016) study, this would mean that Waterberg has more preferential paths compared to the other savannah aquifers since the area is fractured and faulted. Our recharge rates are however slightly higher compared to the previous studies in the study areas. For example, in the Tsumeb area, Bäumle (2003) estimated the rate to range between 0.33 to 4 % of the annual precipitation. This could be an indication that groundwater recharge rates probably vary in the Tsumeb Karst Aquifer depending on the degree of karstification.

Both Stone and Edmunds (2012) and Taapopi (2015) estimated groundwater recharge rates in the Stampriet basin using the same method but in the unsaturated zone where Taapopi (2015) findings are lower compared to ours. However, our groundwater recharge rates fall under the range estimated by Stone and Edmunds (2012).

Other factors that influence groundwater recharge in an arid to semi-arid environment are vegetation cover, slope and aspect and surface runoff. However these factors play an insignificant role in groundwater recharge variations since they are relatively uniform to the study sites.

4.6.3 Water stable isotopes

Scattering of rainwater samples along the GMWL/GNIP LMWL indicates a seasonal effect whereby samples collected in April, May, November and December have more enriched isotopic values while samples collected in January, February, and March are depleted in isotopic values. April, May, November and December are generally dry months where rain amounts are small in Namibia. Gat et al. (2000) stated that dry months are associated with partially evaporated rain which is characterised by relatively higher $\delta^{18}O$ values and hence enriched isotopic values in these months.

Groundwater isotopic values similar to isotopic values of rainwater collected in January, February and March at all three study sites, could be an indication that groundwater recharge generally occurs during those months. Külls (2000) pointed out that the potential for direct recharge is highest in February followed by January and March in the upper Omatako Basin using a daily water balance method which correlates to our findings. Moreover, our findings correlate with the conclusion made by Vogel and Van Urk (1975) that recharge in Grootfontein only takes place when precipitation has lower heavy isotope content.

Figure 4-11 shows groundwater level fluctuation over the years 1987 to 2009, water levels rise generally from January and drop during June. A rise in the water level during these months could be attributed to groundwater recharge, hence supporting our findings.

Groundwater from the Waterberg area plotting right on the GMWL/GNIP LMWL suggests that there is fast infiltration of rainwater with the absence of evaporation, probably via preferential path flows. Such path flows could be faults or fractures since the Etjo sandstone formation is documented to be synsedimentary faulted (Mountney et al., 1998).

Groundwater samples from the Tsumeb area plotting on the GMWL/GNIP LMWL, with an exemption of a few that are plotting slightly below and above the GMWL also indicated fast infiltration of rainwater through karstic features, and probably slowed infiltration rates in areas that are not less karstified. Groundwater from Otjikoto Lake, which is a karst sinkhole, shows an evaporation effect due to the fact that it is open to the atmosphere.

Gibson et al. (1993) stated that meteoric waters that have undergone evaporation display systematic enrichment in both $\delta^{18}O$ and $\delta^{2}H$, resulting in divergence from the meteoric water line along evaporation lines having slopes of less than 8, often in the range of 4 to 6. Groundwater samples collected from the Kuzikus/Ebenhaezer area have a slope ranging between 4.8 to 5.7 during all field campaigns, therefore indicate an evaporation effect which is observed at all field campaigns, thus during, before and after rainy seasons. It is therefore suggested that evaporation probably takes place during infiltration of rainwater to the Kalahari beds, a typical isotopic evaporation signal for the unconfined Kalahari aquifer in the study area according to Alker (2009).

Furthermore, isotopic values showing evaporation effect at Kuzikus/Ebenhaezer area compared to the other two sites corresponds to higher potential evaporation in that area in relation to potential evaporation rates at both Waterberg and Tsumeb areas (DWA, 1988).

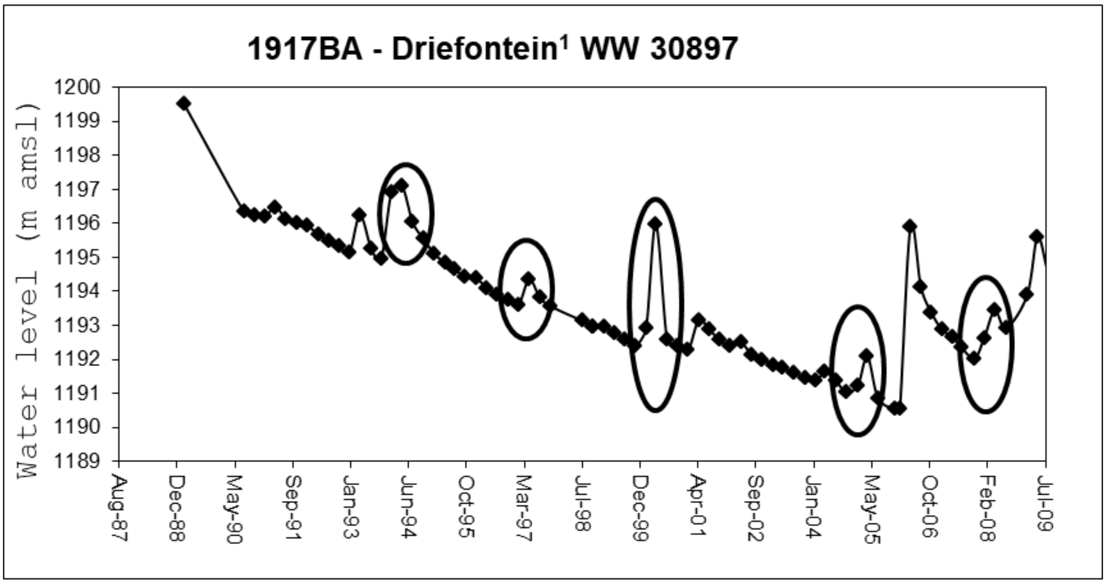

Figure 4-11: water level fluctuation in Tsumeb (Driefontein) data source Department of Water Affairs of Namibia

4.7 Conclusion

The water quality assessment based on the onsite parameters show that groundwater at all three sites is mostly safe for human consumption. The Chloride Mass Balance method revealed that Waterberg area has the highest recharge rate compared to the other two study sites despite Tsumeb having a higher mean annual precipitation amount, followed by Tsumeb area and Kuzikus/Ebenhaezer area having the lowest. High recharge rates in the Waterberg can be related to the absence of evaporation as indicated by the isotopic ratios due to fast infiltration of rainwater possibly through preferential flow paths. Groundwater from the Kuzikus/Ebenhaezer area indicated that evaporation takes place during infiltration of rainwater. Differences in recharge rates at these three study sites can not only be attributed to the precipitation gradient but also to the potential evaporation rates and the preferential paths at each study site.

The identified groundwater recharge rates and recharge mechanisms revealed by chloride mass balance method and stable isotope composition provide useful information for groundwater management for example groundwater users in the Stampriet Basin where recharge values are very low due to evaporation during infiltration of rainwater can explore options such as roof rainwater harvesting.

4.8 Acknowledgements

Authors would like to thank the OPTIMASS project for funding this research. We would like to also acknowledge and thank all the farmers who allowed us to sample their private boreholes. Special thanks go to the maintenance team at NWR Waterberg for field assistance in sampling their springs.

CHAPTER 5

ESTIMATION OF SOURCE WATER AND ACTIVE ROOT DEPTH OF WOODY PLANTS USING DEUTERIUM TRACER AT A SAVANNAH SITE IN THE NORTH OF THE STAMPRIENT BASIN IN NAMIBIA

This chapter is to be submitted to a peer reviewed journal as: Uugulu, S., Wanke, H & Koeniger, P. (2022) Estimation of source water and active root depth of woody plants using deuterium tracer at a savannah site in Namibia

5.1 Abstract

Woody plants as part of the ecosystem play a major role in the global water cycle, through water uptake by roots, evapotranspiration and determining groundwater recharge. Enriched deuterium was used as a tracer to assess the active root depths for both *Senegalia mellifera (S. mellifera)* and *Boscia albitrunca (B. albitrunca)* at a savannah site in Namibia from December 2016 to May 2017. The tracer was inserted at different soil depths (at 0.5 m; 1 m; 2.5 m; 3 m; 3.5 m and 4 m) early December 2016. Xylem cores were obtained using an increment borer and transpired water was collected using transpiration bags that were zipped around leaves from both plant species. Groundwater was collected from boreholes around the study site where the average depth to groundwater is around 32 m. Soil samples were collected only after the rainy season using a hand auger. Xylem and soil water were extracted using a cryogenic vacuum extraction method and were analysed for stable water isotopes at the BGR laboratory, Hannover while groundwater and transpired water were analysed at UNAM laboratory, Windhoek. Out of 49 samples from transpired water, only one *S. mellifera* sample showed a high deuterium content of 515.9‰ where the tracer was inserted at 2.5 m soil depth. *B. albitrunca* transpired samples lead to a

slope of 2.43, R^2 = 0.62 while *S. mellifera* lead to a slope of 4.13, R^2 = 0.64. Elevated deuterium contents were observed in two *S. mellifera* xylem samples were the tracer was applied at 2.5 m and 3 m (34.94‰ and 30.61‰ respectively), a possible sign of the active root depth for *S. mellifera*. The average values for $\delta^{18}O$ values for May 2017 for groundwater and soil water are -5.72‰ and -2.47‰, respectively. Average $\delta^{18}O$ value for *B. albitrunca* for May 2017 is -6.15‰ and is similar to that of groundwater while for *S. mellifera* is -2.47‰, i.e. in-between soil water and groundwater. This could be an indication that *S. mellifera* is using both soil water and groundwater while *B. albitrunca* is using only groundwater. A vertical movement both upward and downward of the tracer was observed in all soil profiles, indicating evaporation and infiltration/percolation over time.

***Key words**: S. mellifera; B. albitrunca; stable water isotopes; deuterium tracer*

5.2 Introduction

Woody plants as part of the ecosystem play a fundamental role within the global water cycle, and particularly when with respect to water uptake by roots, evapotranspiration and groundwater recharge. Plants may uptake either soil water or groundwater or both depending on their rooting depths. Vertical niche separation model studies have demonstrated that woody plants uptake water from both shallower and deeper depths (Case et al., 2020; Scanlon et al., 2005). The model suggests that the competition soil moisture among woody plants and grasses would be minimal, as they rely on soil water occurring at different soil depths, which allows niche separation to take place (Walter, 1939) The depth from which plants can potential extract source water sources is defined by the rooting depth and distribution (Kulmatiski et al., 2020; Zencich et al., 2002). Plants in environments with low moisture balance often experience water stress. And as a result, they adapt by developing root morphologies that include both shallow lateral roots and deep groundwater-tapping roots (Lubczynski, 2009).

In this study two woody species were studied namely Senegalia mellifera subsp. detien *(S.mellifera)* and Boscia albitrunca *(B. albitrunca). S. mellifera* was chosen because it is considered to be one of the main bush encroacher species and it is widely distributed in Namibia (Bester, 1999; De Klerk, 2004; Rothauge, 2017; Shikangalah and Mapani, 2020). Woody plant encroachment has an impact on the sustainable management of groundwater in water limited environments like Namibia (NAU, 2010; Stafford et al., 2017). One of the impacts of woody plant encroachment is that it results in a decrease of groundwater recharge (Acharya et al., 2018; NAU, 2010). Many bush encroacher species in arid and semi-arid environments have shallow, spreading root systems that are used to capture infiltrating water, and extract water by roots, thereby decreasing recharge through the unsaturated zone (Lubczynski, 2009; NAU, 2010). As bush vegetation cover increases, root uptake and plant transpiration at a site increases, which leads to a reduction in groundwater levels, both by reducing unsaturated zone recharge, and by any direct use of groundwater by roots. Table 5-1 shows the mean relative transpiration for 8 hour day, per plant, for the two species studied, using data from the Molopo region of South Africa (Donaldson, 1969, as cited by NAU, 2010).

S. mellifera appears to have primarily shallow and straight roots. *S. mellifera* was observed to have an extensive root system in the upper layers of the soil, thus extending uniformly from its stem as shown in Figure 2-8. Due to the concentration of roots in the upper soil layers, this species has the advantage of receiving water from even low precipitation events (Geißler et al., 2019; Sala et al., 1992). *S. mellifera* has also been demonstrated to be capable of developing a tap root with a depth of more than 30 m, for a plant observed at the farm Aiams in the Otavi district, Namibia (NAU, 2010). As a result, the species may be adapted to seek out groundwater while exploiting soil water with an extensive lateral root system, either to support growth until groundwater is reached or to absorb water moved to the surface by hydraulic redistribution (Burgess et al., 1998; Scott et al., 2008).

An evergreen species *B. albitrunca* was chosen because it is documented to have deep roots and that it is also widely distributed in Namibia (Curtis and Mannheimer, 2005). Jennings (1974) encountered *B. albitrunca* roots at about 70 m depth in borehole cores in the Kalahari sands. A deep rooted *B. albitrunca* can easily access groundwater and hence has an effect on groundwater resources. *B. albitrunca* has a strategy of extending individual roots at much greater depths than *S. mellifera*; *B. albitrunca* with deep-rooted, sinuous roots shows a different distribution of lateral root biomass with depth, with hardly any roots in the upper soil layers (O'Donnell et al., 2015). Kalahari trees with extremely deep roots reach groundwater and remain green throughout the dry season which is a case for *B. albitrunca* (Obakeng, 2007).

Table 5-1: Size, leaf area and relative transpiration of S. mellifera and B. albitrunca (after NAU, 2010).

Woody plant species	Height (m)	Crown diameter (m)	Canopy area (m^2)	Total leaf area (m^2)	Mean-relative transpiration per 8 hour day per plant (L)
S. mellifera	2.5	2.8	6.0	55.68	64.80
B. albitrunca	1.2	1.5	2.0	13.58	13.84

Water stable isotopic composition can be used to distinguish source water by comparing such compositions from plant xylems to those of groundwater, of soil water, and within precipitation in the same study site (Geißler et al., 2019; Huxman et al., 2005; von Freyberg et al., 2020). In order to trace the isotopic composition of the precipitation from which plant xylem water originated, intersection points of local plant xylem evaporation lines with local meteoric water lines (LMWLs) are calculated using Equations 5.1 and 5.2 to derive a plant xylem source values (Evaristo et al., 2015).

$$\delta^2H_{\text{intercept}} = \delta^2H - m\,\delta^{18}O \quad \text{Eq 5.1}$$

$$\delta^{18}O_{\text{intercept}} = (\delta^2H_{\text{intercept}} - b)/a \quad \text{Eq 5.2}$$

Whereby *m* is the slope of the evaporation line, *a* is the LMWL slope, and b is the LMWL intercept. However, Equation 5.1 was revised by Javaux et al. (2016) to Equation 5.3:

$$\delta^2H_{\text{intercept}} = \delta^2H - m\,(\delta^{18}O - \delta^{18}O_{\text{intercept}}) \quad \text{Eq 5.3}$$

Alternatively, the point on the local meteoric water line (LMWL) where the plant xylem water evaporation line intersects, can provide a good approximation of the mean isotopic value of plant xylem source precipitation (Evaristo et al., 2015). Plant xylem water is preferred over transpired water for determining the water source, because fractionation that occurs at a leaf level causes a more enriched isotope value (Beyer et al., 2016; Evaristo et al., 2015; Flanagan et al., 2019; Kulmatiski and Forero, 2021). Nevertheless, there are new approaches that account for fractionation processes by using the Craig and Gordon model to map leaf water back to its individual precipitation event water sources (Benettin et al., 2021).

Lubis et al. (2014) determined plant water sources using stable water isotopes in Riau, Indonesia. Their study found out that oil palms absorb water from depth of 0 - 50 cm, which corresponds to the most active root of oil palm that absorbs nutrients, water and oxygen. Zencich et al. (2002) studied seasonal water sources for species growing on a coastal dune system that overlies a shallow sandy aquifer in south-western Australia. The authors found out that during the wet winter, plants use more water from the upper layers of the soil profile. A study carried out by Beyer et al. (2016) using deuterium as artificial tracer to investigate rooting depths in a semiarid environment in northern Namibia suggest the primary root zone ended between 2 and 2.5 m below the ground surface.

Knowledge of the influence of vegetation, especially bush encroacher species, on groundwater recharge in semi-arid regions, such as Namibia, remains limited (with one preliminary report in the grey literature for Namibia (NAU, 2010). The objective of this study is thus to determine the influence of woody plants on groundwater recharge at a farm site Ebenhaezer, in the Stampriet Basin region of southeast

Namibia, using two species, namely *S. mellifera* and *B. albitrunca*, by determining their effective root depths and source water.

5.3 Materials and Methods

5.3.1 Study area

The study site is located in the Ebenhaezer area in the northern part of the Stampriet Basin in Namibia (Figure 5-1). The mean annual precipitation within the basin ranges between 175 mm to 240 mm and the mean potential evaporation is varying between 3000 mm/a to 3500 mm/a (DWA, 1988). The study area is generally flat with an elevation of about 1200 m amsl and it is flanked by ephemeral rivers, the Nossob River to the East and Olifants River to the West (Figure 5-1). The area is covered by Kalahari dune sands that are partially underlain by calcrete (Mendelsohn et al., 2002). The vegetation is classified as mixed tree and shrub savannah (Christelis and Struckmeier, 2011). Biogeographically, the study area is characterised as Kalahari shrubland within the Central Kalahari Camelthorn Savannah (Geißler et al., 2019; Mendelsohn et al., 2002).

The spatial distribution of both *S. mellifera* and *B. albitrunca* ranges from common to abundant (Figure 5-2) (Curtis and Mannheimer, 2005). The distribution of each species was determined from the records collected for each quarter-degree square for a period of six years (Curtis and Mannheimer, 2005). Such observations were entered into a Tree Atlas Project database. Abundance was then estimated visually and assigned it to one of four categories. Rare category is given if only one specimen had been observed in the quarter-degree square, in spite of spending some time looking; an uncommon category was assigned if more than one specimen seen, but not very many; a common category was given if quite a few specimens scattered between other species and an abundant category is given if many species were observed (Curtis and Mannheimer, 2005).

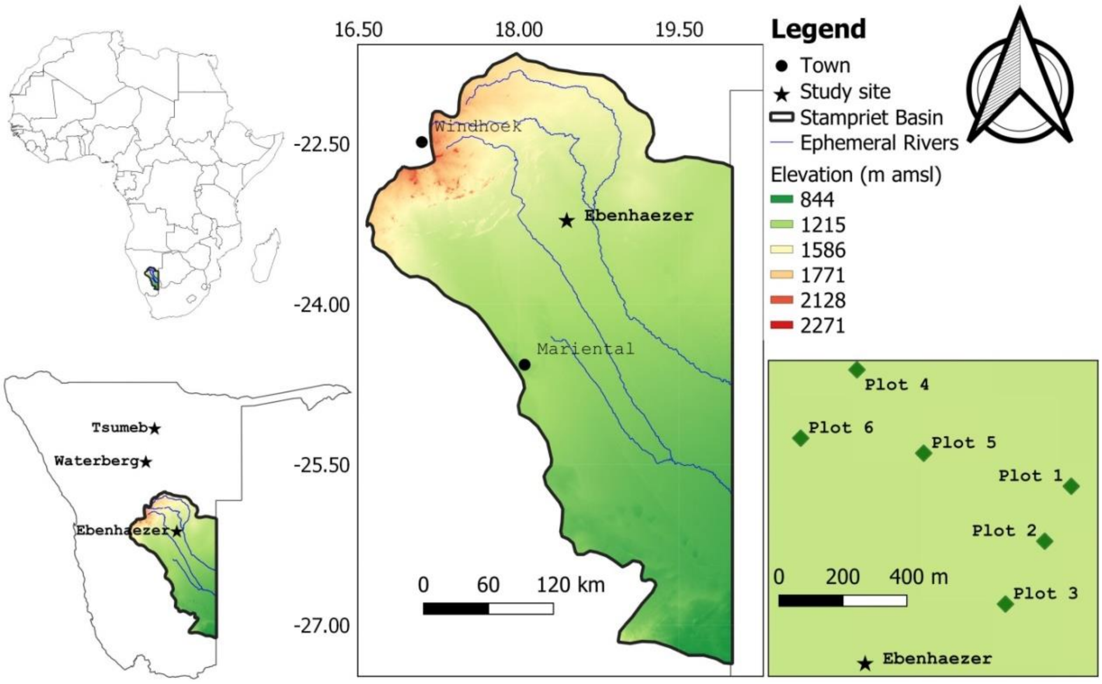

Figure 5-1: Digital elevation model (DEM) and drainage network of the Stampriet basin. The study site (Ebenhaezer) is located in the northern part of the basin. Diamond-shapes represent the spatial distribution of plots used in this study. Precipitation and xylem samples collected at Tsumeb and Waterberg are considered for water sources in this study as discussed in the following.

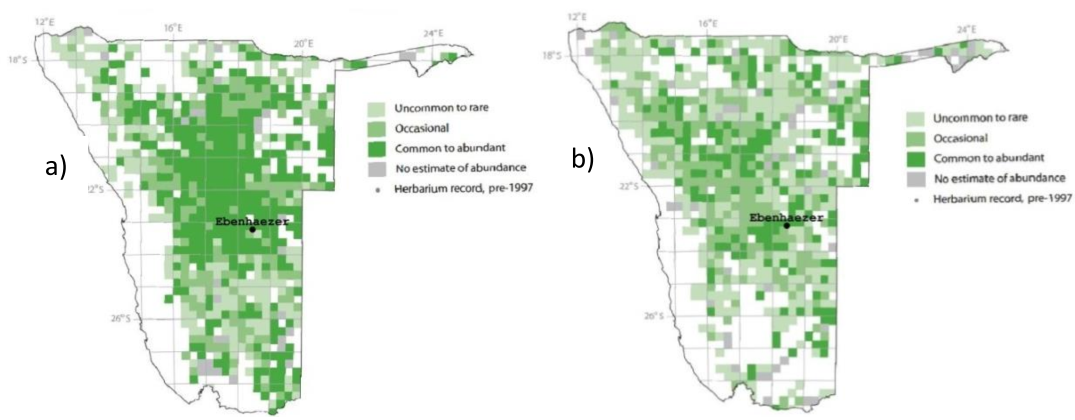

Figure 5-2: The spatial distribution of species: a) S. mellifera subsp. detien; b) B. albitrunca and location of the study area modified (modified from Curtis and Mannheimer, 2005).

5.3.2 Demarcation of plots, tracer injection and sampling

Field campaigns were carried out in December 2016, March and May 2017. In December 2016, *S. mellifera* and *B. albitrunca* were sampled for both xylem cores and transpired water to get the background isotopic values before injection of a deuterium tracer (tracer). Xylem core samples were obtained using an increment borer. Transpired water samples were obtained using transpiration bags that were zip locked in place around the leaves in the mornings, with the transpire water collected in the evenings.

The deuterium tracer (input concentration of the tracer is 30% ^2H_2O) was injected at different target depths at 6 plots (see Figure 5-1 for the spatial distribution of the plots) using the similar procedures as outlined by Beyer et al. (2016). The deuterium tracer was inserted at 0.5 m for plot 5; 1 m for plot 4; 2.5 m for plot 2; 3 m for plot 3; 3.5 m for plot 6 and 4 m for plot 1. Three holes that are 1 metre apart were drilled at each plot until the target depth using a hand auger. Each hole was inserted with five small balloons filled with a 30% deuterium tracer with a capacity of about 65 ml each. The balloons were attached to a thin cord and then inserted into the holes. The balloons were busted at the target depth using a sharp object. The distance from the injected holes to the traced woody plants is illustrated in Appendix 3. Both transpired water samples and xylem cores were collected once per day for four days following the injection of the tracer.

Detailed descriptions of the trees were conducted by estimating height, crown diameter and thickness of the stem. A total of 15 woody plants were selected, at least one *S. mellifera* and one *B. albitrunca* per plot. Appendix 4 presents biometric characteristics of the sampled woody plants.

Soil samples were collected during the second field campaign in May 2017. A new hole was drilled at the centre of the earlier plots 2, 3, 4 and 5 in order to collect soil samples at 1, 1.5, 2, 2.5 and 3 m depth to assess the vertical movement of the tracer within the soil profile after the rainy season.

5.3.3 Xylem and soil water extraction and analysis

Water was extracted from both xylem cores and soil samples using a cryogenic vacuum distillation method, following Koeniger et al. (2011) and Gaj et al. (2016). A sample was inserted into a capped exetainer vial and connected to an empty vial using a capillary tube. The soil sample within was frozen with liquid nitrogen to prevent loss of water vapour during evacuation. The connected and frozen vials were subsequently evacuated using a syringe needle that was connected to an evacuation system. A frozen sample was placed in an aluminium vial holder over a hot plate (180 °C) while the tip of the empty vial was inserted in a Dewar flask containing liquid nitrogen and ensuring that the flask was completely filled with liquid nitrogen during the entire extraction process.

After 30 minutes of the extraction process, the water sample was removed, recapped to prevent evaporation and stored in a fridge until measurement for stable water isotopes using a Picarro L2120-i cavity-ring down spectrometer at the isotope hydrology laboratory at BGR in Hanover, Germany. Results obtained from analysis were checked with ChemCorrect©, a software package that identifies and flags contamination from a broad range of organics, providing confidence in the accuracy of isotope ratios reported.

Groundwater and transpired water was analysed at the University of Namibia using a Los Gatos Research Inc., LGR DLT 100 laser spectrometer at the hydro-lab. All isotope ratios were reported in δ notation given in ‰ relative to the international Vienna Standard Mean Ocean Water (VSMOW) standard as shown in Equation 5.4:

$$\delta = \frac{(R_{sample} - R_{VSMOW})}{R_{VSMOW}} * 1000 \quad \text{Eq 5.4}$$

Where δ-value is the deviation of the isotope ratio of a sample relative to that of VSMOW, R_{sample} is the isotope ratio of $^{2}H/H$ or $^{18}O/^{16}O$ in the sample, and R_{vsmow} is the isotope ratio of $^{2}H/H$ or $^{18}O/^{16}O$ of VSMOW standard.

Analytical errors involved with stable isotope analyses are usually given as better than 0.1 and 1‰ for $\delta^{18}O$ and $\delta^{2}H$ of pure water samples respectively. For xylem and soil water extractions analytical errors of up to 5 times higher should be considered, depending mainly on clay contents of the soils. For measurements of highly enriched deuterium samples analytical errors can be higher than 10‰ due to memory effects, depending on degree of enrichment (Koeniger et al., 2011).

5.3.4 Estimation of source water

An estimation of source water for *S. mellifera* and *B. albitrunca* was conducted by using an approach of determining source water from xylem water rather than from transpired water. To trace the isotopic composition of precipitation from which xylem water originated, intersection points of local xylem evaporation lines with LMWLs were determined on $\delta^{18}O$ vs. $\delta^{2}H$ plots. LMWLs determined by Uugulu and Wanke (2021) for Ebenhaezer ($\delta^{2}H = 7.16\ \delta^{18}O + 9.88$, $R^2 = 0.96$), Waterberg ($\delta^{2}H = 7.37\ \delta^{18}O + 5.77$, $R^2 = 0.97$) and Tsumeb ($\delta^{2}H = 7.78\ \delta^{18}O + 6.74$, $R^2 = 0.95$) were used. Xylem water sources for *S. mellifera* and *B. albitrunca* were determined at Ebenhaezer and compared to those at Tsumeb and Waterberg sites.

5.4 Results

5.4.1 Isotopic description of groundwater and xylem water and estimation of their source water

Figure 5-3 shows stable isotope values for groundwater, *S. mellifera* and *B. albitrunca* xylem water for Ebenhaezer (Figure 5-3a) in comparison to Waterberg (Figure 5-3b) and Tsumeb (Figure 5-3c). The groundwater samples plot close to the LMWL of Waterberg and Tsumeb but not as close to Ebenhaezer LMWL. Regression lines for all stable isotope data are compiled in Table 5-2. The slope of the regression lines for both groundwater and *B. albitrunca* range between 4.0 and 4.8 for the three sites. *S. mellifera* slope variations are larger (2.1 to 8.7) and show lower R^2 values, hence the data does not fit the linear regression model as compared to B. albitrunca. At Waterberg, groundwater samples are plotted directly on the LMWL with a regression line of $\delta^2H=7.5\ \delta^{18}O + 7.1$, $R^2 = 0.89$. As for *S. mellifera* in Tsumeb, a regression line equation of $\delta^2H = 8.7\ \delta^{18}O + 0.7$, $R^2 = 0.99$ is derived which is almost parallel to the LMWL.

Intersects between species-specific isotope regression lines and groundwater with LMWLs for all three sites are shown in Table 5-3. Intersects for *B. albitrunca* are relatively similar between all three sites. *B. albitrunca* intersects are similar to the groundwater intersects at Waterberg and Ebenhaezer, but *B. albitrunca* intersects lower than groundwater at Tsumeb. Intersects for *S. mellifera* are above those for groundwater and *B. albitrunca* at Ebenhaezer and Waterberg, but could not be determined for Tsumeb as the regression line is parallel to the LMWL). Moreover, there is a greater divergence in the intersection values (22 ‰ different for δ^2H) for *S. mellifera* for the two sites as compared to *B. albitrunca*.

Table 5-2: Summary of regression parameters for groundwater and xylem water for Ebenhaezer in comparison to Waterberg and Tsumeb.

Sites	Equations for the regression lines		
	Groundwater	S. *mellifera*	*B. albitrunca*
Ebenhaezer	δ^2H=4.8 $\delta^{18}O$ - 17.7; R^2 = 0.97	δ^2H=2.1 $\delta^{18}O$ - 25.5; R^2 = 0.20	δ^2H = 4.0 $\delta^{18}O$ - 25.8; R^2 = 0.54
Waterberg	δ^2H=7.5 $\delta^{18}O$ + 7.1; R^2 = 0.89	δ^2H = 3.2 $\delta^{18}O$ – 32.7; R^2 = 0.34	δ^2H = 4.7 $\delta^{18}O$ - 21.5; R^2 = 0.59
Tsumeb	δ^2H = 4.2 $\delta^{18}O$ – 24.7; R^2 = 0.97	δ^2H = 8.7 $\delta^{18}O$ + 0.7; R^2 = 0.99	δ^2H = 4.2 $\delta^{18}O$ – 30.7; R^2 = 0.85

Table 5-3: Sources water/intersects LMWL and regression line for groundwater and xylem water at Ebenhaezer in comparison to Waterberg and Tsumeb.

Sites	Intersect of regression lines with the LMWL					
	S. mellifera (Xylem)		*B. albitrunca* (Xylem)		*Groundwater*	
	$\delta^{18}O$	δ^2H	$\delta^{18}O$	δ^2H	$\delta^{18}O$	δ^2H
Ebenhaezer	-6.9‰	-40‰	-11.4‰	-70‰	-11.7‰	-74‰
Waterberg	-9.2‰	-62‰	-10.2‰	-71‰	-10‰	-67‰
Tsumeb	-	-	-10.4‰	-75‰	-8.8‰	-63‰

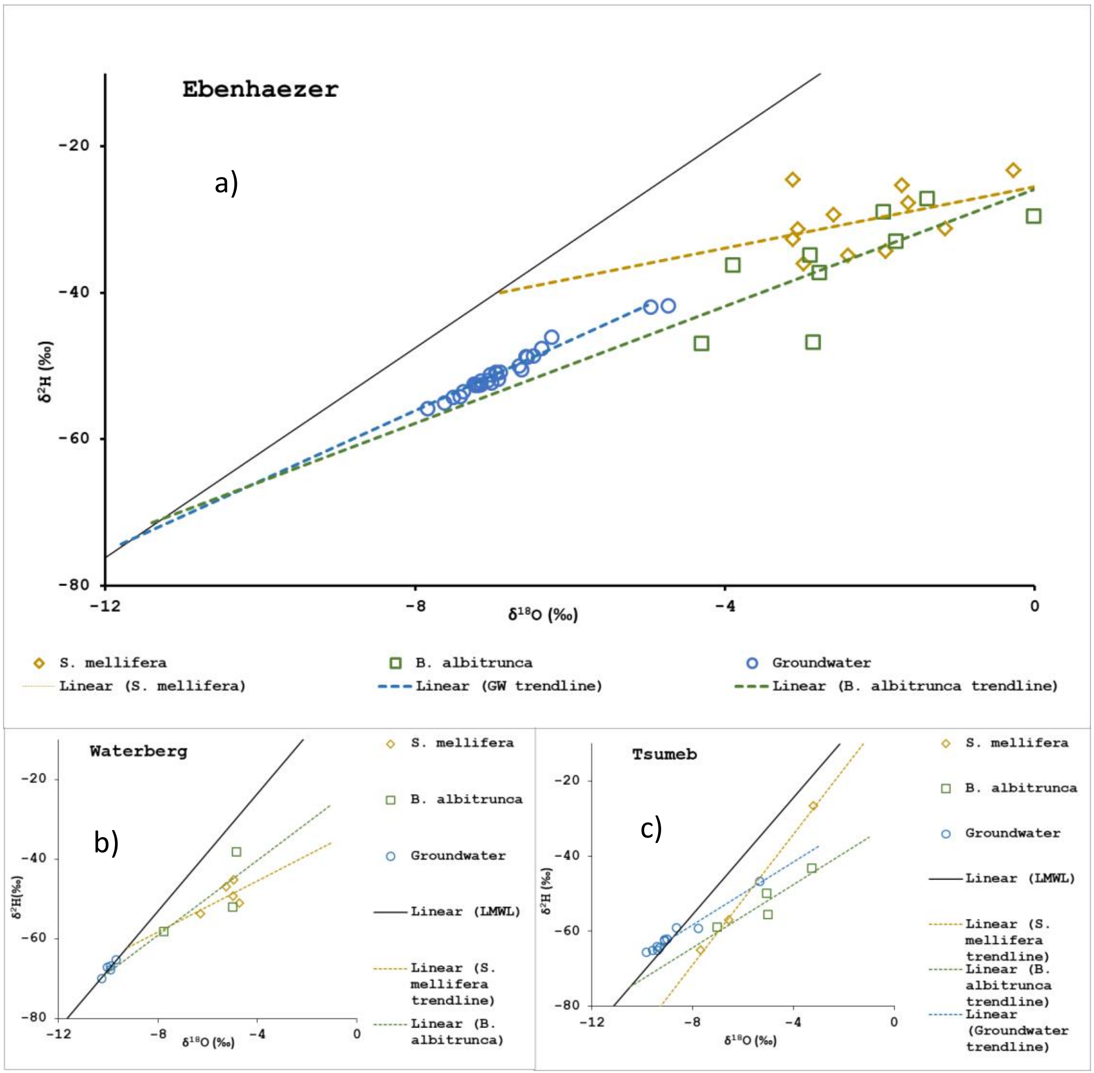

Figure 5-3: Estimation of source water at a) Ebenhaezer in comparison to b) Waterberg and c) Tsumeb. Data collected during November/December 2016.

5.4.2 Results of the deuterium tracer experiment at Ebenhaezer

5.4.2.1 Active root depth

This section presents results of the deuterium tracer experiment which was only carried out at Ebenhaezer. Figure 5-4a shows stable isotope values for groundwater, *S. mellifera* xylem and transpiration water from Ebenhaezer. Regression lines equations and the range of stable isotope values for xylem and transpiration water are compiled in Table 5-4 (See Appendix 8 for a full dataset). Groundwater plots close to the LMWL. *S. mellifera* xylem sampled after the deuterium tracer was inserted show more negative isotope values (represented as squares in Figure 5-4a). These values seem to have become more negative during the sampling campaign in comparison to the first day of sampling representing natural background values. Ranges for all isotope values are presented in Table 5-4. Only 2 xylem samples that are plotting clearly above LMWL show elevated deuterium contents (34.94‰ and 30.61‰); these 2 samples are from plots where the deuterium tracer was applied at 2.5 m and 3 m respectively. *S. mellifera* shrubs' isotopic composition is varying from enriched to depleted values in heavy isotopes and demonstrates a regression line of $\delta^2H = 3.77 \delta^{18}O - 75.67$, $R^2 = 0.92$.

Figure 5-4b shows isotopic data for groundwater, *B. albitrunca* xylem and transpiration water from Ebenhaezer. Regression line equations and isotopic value ranges for xylem and transpiration water are compiled in Table 5-4. *B. albitrunca* xylem water appears to plot close to groundwater with less variation in comparison to *S mellifera* in Figure 5-4a. There is no evidence of a tracer being picked up by *B. albitrunca* as all the xylem isotopic values are below 0‰ δ^2H. The only *B. albitrunca* shrub xylem which was sampled during the last two days of the campaign indicates more negative isotope values as compared to that of groundwater and *B. albitrunca* xylem (Figure 5-4b). Not much variation is visible in *B. albitrunca* xylem water isotope composition in comparison to that of *S. mellifera*.

5.4.2.2 Transpiration

Regression lines of isotopic composition for transpiration water are presented in Table 5-5, along with the range in isotopic values observed for each species. Out of 49 transpired samples, only one *S. mellifera* sample showed a clearly enriched deuterium signal of 515.9‰. This particular sample was taken from plot 2 where the deuterium tracer was inserted at 2.5 m depth (Figure 5-4a). Transpiration water for *S. mellifera* is enriched in heavy isotopes as compared to xylem water with a regression line of δ^2H = 4.70 $\delta^{18}O$ -20, (R^2 = 0.70). Groundwater, *S. mellifera* transpiration water and *S. mellifera* xylem samples taken before the deuterium tracer was introduced plot along one regression line (Figure 5-4a).

Transpiration water isotope values for *B. albitrunca* are also enriched in heavy isotopes as compared to xylem water. *B. albitrunca* transpiration samples show a regression line of δ^2H = 3.03x -19.6, (R^2 = 0.63). A similar trend to that of *S. mellifera* is observed for *B. albitrunca* whereby groundwater, *B. albitrunca* transpiration water and *B. albitrunca* xylem taken before the deuterium tracer was inserted appear on one regression line (Figure 5-4b). Two transpiration water samples show slightly enriched deuterium values of 11.4‰ δ^2H (plot 2) and 12.8‰ δ^2H (plot 3) (Figure 5-4 b). The only *B. albitrunca* shrub which was sampled during the last two days of the campaign indicates more negative isotope values compared to that of groundwater, xylem and transpiration water isotope compositions (Figure 5-4).

Table 5-4: Regression lines and isotopic value ranges at Ebenhaezer.

Site (Ebenhaezer)		*S. mellifera* transpiration		*S. mellifera* post-tracer (xylem)		*S. mellifera* shrubs (xylem)		*B. albitrunca* Transpiration		*B. albitrunca* post-tracer (xylem)
Regression lines		δ^2H = 4.70 $\delta^{18}O$ -20, R^2 = 0.70		δ^2H = 6.99 $\delta^{18}O$ -14.03, R^2 = 0.71		δ^2H = 3.77 $\delta^{18}O$- 75.67, R^2 = 0.92		δ^2H = 3.03x - 19.6, R^2 = 0.63		δ^2H = 2.84x -44.42, R^2 = 0.11
Ranges	$\delta^{18}O$ (‰)	Min -0.55	Max -5.96	Min -15.17	Max -1.69	Min -17.64	Max 5.5	Min -1.86	Max 8.64	
	δ^2H (‰)	-16.3	14.6	-116.4	34.9	-147.6	-54.9	-28.6	12.8	

5.4.2.3 Seasonal variation in source water

Figure 5.5 shows xylem water composition (and in one sampling interval also transpiration water), compared to groundwater. This appears to indicate a seasonal variation in source water and/or isotopic fractionation processes within these species.

In December, 2016, the xylem samples from both species overlap with groundwater samples, and each other, and both have a wider range of values (or wider distribution) than groundwater (Figure 5-5a). In comparison, the transpiration samples for both species have more positive (isotopically enriched) values, with their interquartile ranges above 0‰.

In March, 2017, the pattern was different, with xylem values from both species being more negative (isotopically depleted) compared to groundwater, although with some overlap with groundwater for *B. albitrunca* (Figure 5-5b). The range of values is larger, and the mean values are more negative for *S. mellifera* than *B. albitrunca*.

In May, 2017 (which was shortly after the rainy season), *S. mellifera* xylem samples have more positive values (enriched) than groundwater, whilst *B. albitrunca* overlaps that of groundwater (with a wider range) (Figure 5-5c). Soil water samples also sampled during this interval contain more enriched (positive) values, and these overlap with *S. mellifera* xylem samples (Figure 5-5c). Overall, it can be seen that *S. mellifera* xylem $\delta^{18}O$ composition is more variable through time than *B. albitrunca*.

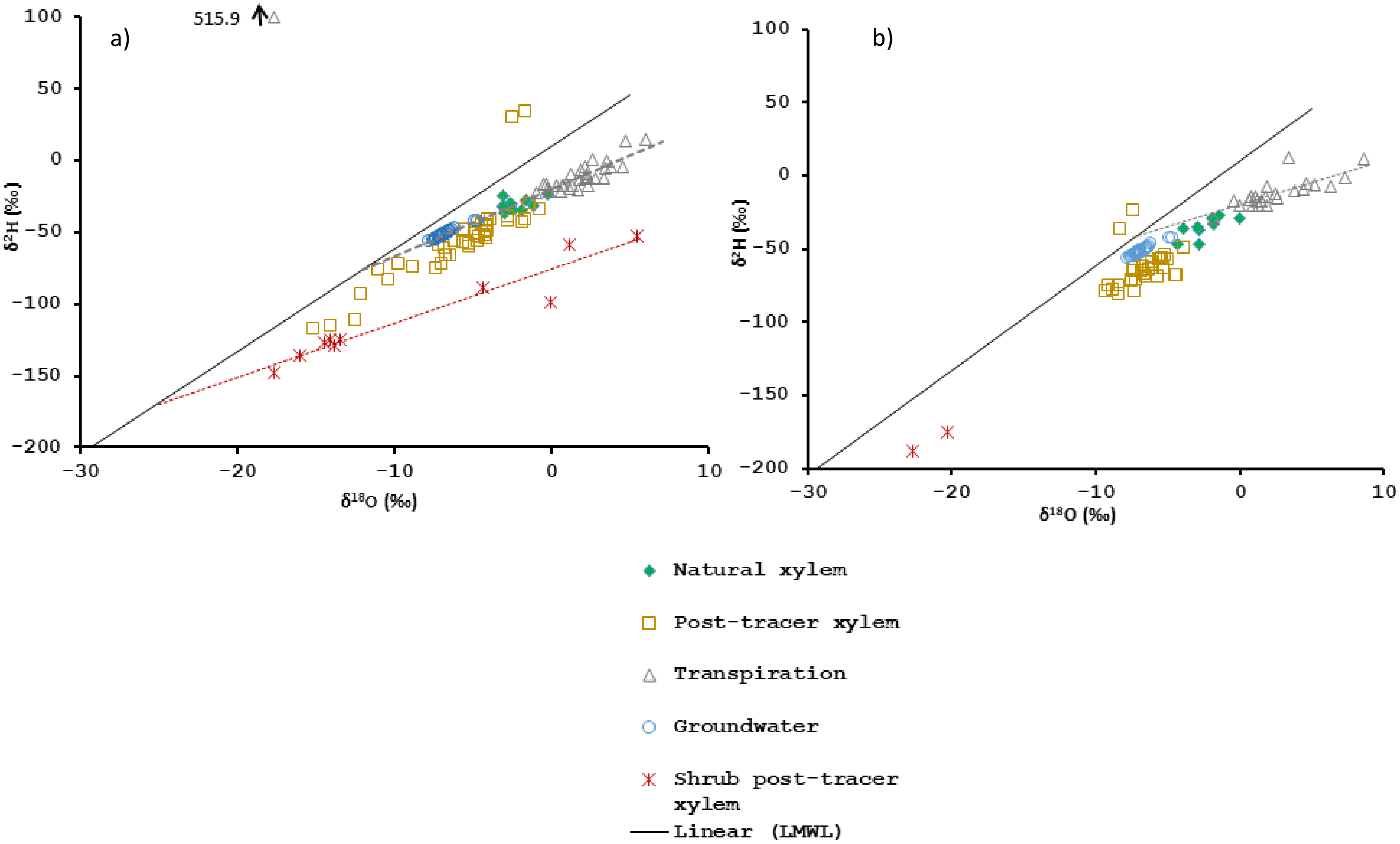

Figure 5-4: Dual isotope plot for a) S. mellifera and b) B. albitrunca transpired and xylem water December 2016 at Ebenhaezer. Natural xylem samples were taken before the deuterium tracer was inserted; post-tracer xylem samples were taken after the deuterium tracer was introduced.

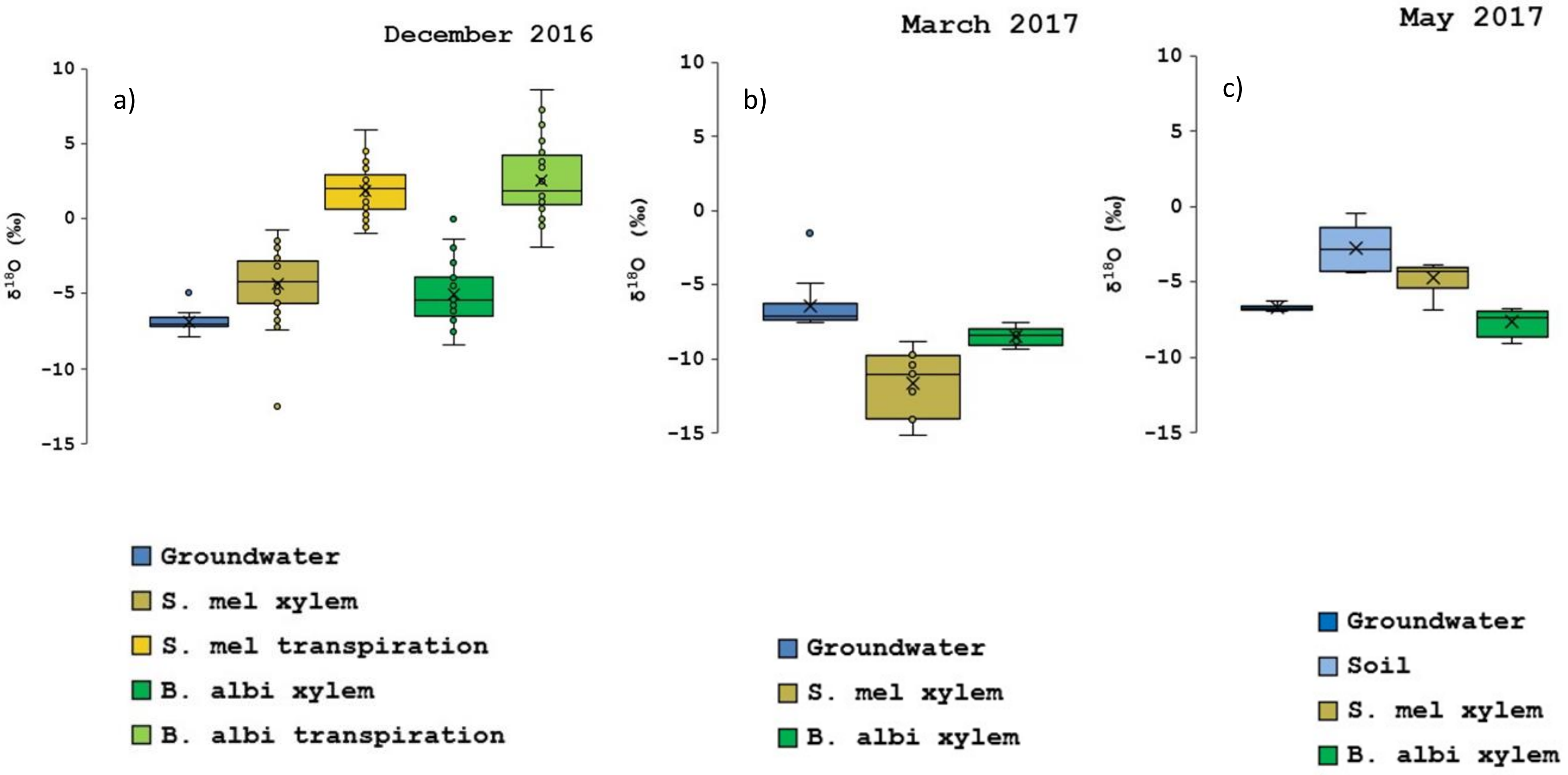

Figure 5-5: $\delta^{18}O$ values for S. mellifera and B. albitrunca, soil water and groundwater a) December 2016, b) March 2017 and c) May 2017.

5.4.2.4 Vertical movement in soil profile

Figure 5-6 shows soil profiles for plot 2, 4 and 5 and the depth at which the deuterium tracer was inserted for each plot is shown on the legend. A vertical movement both upward and downward of the deuterium tracer was observed in all soil profiles (Figure 5-6). At plot 2 where the tracer was inserted at 2.5 m, the upward movement was observed at 1 m with a value of 2‰ δ^2H while the downward movement was observed at 3 m with a value of 14554‰ δ^2H. The δ^2H content increases with an increase in the depth at which the deuterium tracer was inserted, thus plot 5 has the lowest δ^2H content and plot 2 has the highest δ^2H content despite the same δ^2H content initially applied to each plot. Generally, plot 4 and plot 5 where the deuterium tracer was inserted at shallower depths indicate a larger downward displacement of the tracer in comparison to plot 2 where the tracer is inserted at a deeper level. In general, the tracer front did not move noticeable as the highest deuterium concentrations are observed at depths where the tracer was inserted.

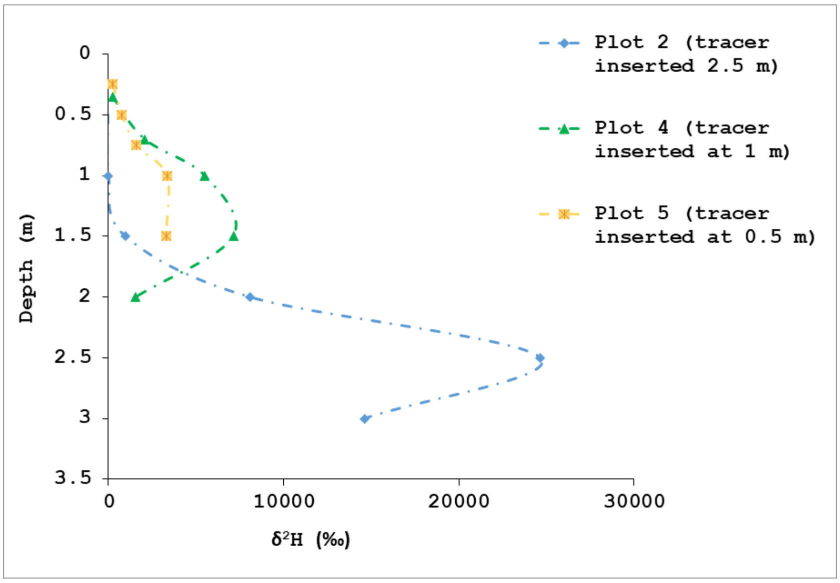

Figure 5-6: Vertical soil profiles showing deuterium concentrations for plots 2, 4 and 5 recorded in May 2017, 145 days after tracer application on 8th December 2016.

5.5 Interpretation and Discussion

5.5.1 Groundwater and xylem water isotopic compositions, sources and processes

The groundwater isotopic regression line at Ebenhaezer, shows there is an evaporative enrichment of groundwater compared to its LMWL (Figure 5-3a, 5-4a), in comparison to the Tsumeb and Waterberg sites where groundwater isotopic composition is comparable to their LMWLs (Figure 5-3b, 5-3c). A similar trend is seen for xylem water at Ebenhaezer (Figure 5-3 a), and together this indicates a strong kinetic isotope effect due to evaporation (Craig, 1961; Evaristo et al., 2015; Uugulu and Wanke, 2020). Such kinetic effects produce a systematic deviation of isotopic compositions of a pool of water from the LMWL that evolves along an evaporation line (Bowen et al., 2018). The slopes of the regression line equations for both groundwater and *B. albitrunca* are typical evaporation slope lines. Slopes around 5 indicate evaporation being the dominant factor governing the isotopic relationship (Craig, 1961). Therefore this is an indication that the deep rooted *B. albitrunca* is tapping evaporated source water. Subsequently, it has been demonstrated that an isotopic enrichment of water in the woody plants can also occur and hence this has an implication on the interpretation of plant source water (Dawson and Ehleringer, 1993). However, this enrichment was mainly observed in younger stems that are not yet suberized to prevent gaseous exchange (both carbon dioxide and water vapour) with the atmosphere while mature stems showed little or no isotopic enrichment (Dawson and Ehleringer, 1993).

S. mellifera showing a wide range of slopes ranging from 2.1 to 8.7 suggests that it is tapping from a range of evaporated to non-evaporated source water. The ability to switch among different source water puts a plant at an advantage if competition for water occurs within the ecosystem (Ehleringer and Dawson, 1992). Isotopic composition of source water of *S. mellifera* and *B. albitrunca* being different is an indication that these woody plants are exploiting different source water at different active rooting zones and hence a large variation in isotope composition. For Waterberg, *S. mellifera* seems to be using soil water which is traced back to some smaller precipitation events while *B. albitrunca* traces back to groundwater and hence using groundwater. As for Ebenhaezer, *S. mellifera* uses soil water which is traced back to some smaller precipitation events while *B. albitrunca* traces back to the same source as groundwater.

The source water for *S. mellifera* and *B. albitrunca* in this study was inferred based on the assumption that stable water isotopes are largely conservative tracers (with the primary exception of evapotranspiration), thus the isotopic composition of xylem water remains constant despite other physical and chemical transformations undergone by the water as it moves into roots and up through the plant (Bowen et al., 2018; Dawson and Ehleringer, 1993). Furthermore, some studies have demonstrated that there is little or no isotopic fractionation occurring between the soil water pool and the plant during root uptake (Chen et al., 2020; Dawson and Ehleringer, 1993; Lubis et al., 2014; Walker and Richardson, 1991; White et al., 1985). On the contrary, some studies have demonstrated that there is fractionation that takes place during root water uptake (Ellsworth and Williams, 2007; von Freyberg et al., 2020). Hence the source water identified in this study should be used as an approximation because of the fractionation effect that creates uncertainty.

5.5.2 Results of the deuterium experiment at Ebenhaezer

5.5.2.1 Active root depth

More negative isotope values observed (Figure 5-4) especially for shrubs and some *S. mellifera* xylem samples at Ebenhaezer are probably reflecting isotope composition of heavy precipitation events. Such negative isotope values could be explained by higher monthly rainfall, stronger precipitation events, the contribution of recycled moisture to precipitation or a combination of those (Callow et al., 2014; Wanke et al., 2018b). It has to be noted, that it rained during the second day of sampling (8th December 2016) and the closest SASSCAL weather station to Ebenhaezer (SASSCAL station Sandveld; ID 31198) recorded a precipitation amount of 9.2 mm. *S. mellifera* develop a dense network of roots extending uniformly from the tree stem in the upper soil layers at dry sites (O'Donnell et al., 2015). It could be that *S. mellifera* and shrubs used their extensive lateral root system in the upper layers of the soil to scavenge water from that precipitation event that could have been available for groundwater recharge.

Elevated deuterium contents observed in two *S. mellifera* xylem samples where the tracer was applied at 2.5 m and 3 m are a possible indication of the active root depth for *S. mellifera*. The possible active root depth determined in this study is similar to that of Beyer et al., (2016). Although different species were used (*C. collinum, S. erioloba, B. plurijuga, T. sericea and S. luebertii*), they determined an end of primary root zone of between 2 – 2.5 m using a deuterium tracer in the northern Namibia. Also, *S. mellifera* being known for its extensive lateral root system (NAU, 2010; O'Donnell et al., 2015), makes it ideal to access soil water at such depths. The active root depth for *B. albitrunca* could not be determined due to the absence of the deuterium tracer in *B. albitrunca* xylem water. However a study by Obakeng (2007) using LiCl tracer concluded that *B. albitrunca* in Kalahari Basin, Botswana is one of the species that are extracting water at a depth of more than 3 m, thus below the main root zone of shrubs and grasses.

S. mellifera xylem water having a high isotopic composition variation in Figure 5-4a could be an indication that it is using a mixture of both groundwater and soil water. An extensive root system not only gives *S. mellifera* an advantage to access soil water but also reduces infiltration to groundwater levels (NAU, 2010). Ebenhaezer having a general depth to groundwater around 34 m, makes it likely for *S. mellifera* to access groundwater using its tap roots since it is demonstrated to develop a tap root of more than 30 m. Kanyama (2017) indicated that woody plants at Ebenhaezer are using both groundwater and soil water which correlates well with our findings for *S. mellifera*. Moreover, a study on *S. mellifera* tree ring growth formation by Shikangalah et al. (2020) indicated that there is a variation in water supply throughout the growth period, whereby *S. mellifera* uses less water during drier seasons. As a result, *S. mellifera* may be adapted to seek out groundwater while exploiting surface water with an extensive lateral root system, either to support growth until groundwater is reached or to absorb water moved to the surface by hydraulic redistribution (Lubczynski, 2009; O'Donnell et al., 2015; Scott et al., 2008).

B. albitrunca xylem isotopic composition is similar to that of groundwater, although it is slightly depleted in $\delta^{18}O$ and $\delta^{2}H$ (Table 5-1 and Figure 5-3 & 5-4b). This suggests that *B. albitrunca* is mainly utilising groundwater but the possibility of using soil water cannot be ruled out either especially for the *B. albitrunca* shrubs. *B. albitrunca* mainly using groundwater could be explained by the fact that there is barely root on the upper soil layer, thus the species extending its roots to much greater depths (O'Donnell et al., 2015). Deep roots of this species were encountered at about 70 m depth in boreholes cores in the Kalahari sands (Jennings, 1974). The presence of such deep roots makes it easier for *B. albitrunca* to easily access groundwater and hence a similar isotopic composition of source water with that of groundwater. Slightly depleted isotopic values of the source water can be attributed to very few roots in the upper soil layers that are tapping soil water (Figure 5-4b).

As noted, both groundwater and *B. albitrunca* xylem water have similar regression line slopes values that are higher than that of *S. mellifera*. A lower slope value indicates a higher evaporation effect (Craig, 1961; Gat et al., 2000). The evaporation effect is usually more pronounced at shallow depths than at deeper depths. As a result, soil profiles normally have heavier isotopic ratios at shallow depths and lighter isotope ratios at greater depths (Barnes and Allison, 1984; von Freyberg et al., 2020). A lower slope value for *S. mellifera* could probably be attributed to a portion of soil water which is being tapped by its dense extensive shallow root system. Kalahari profiles indicated an isotopic enrichment of soil moisture in the upper unsaturated zone of about less than 5 m due to a direct evaporation (Lubczynski, 2009). Furthermore, it was demonstrated that with bulk soil water showing greater levels of evaporative enrichment near the surface and gradually declining with depth (Gokool et al., 2021).

A slight variation of the intersects of regression lines with LMWLs across a precipitation gradient is observed whereby the isotopic composition of source water is decreasing along a precipitation gradient; Tsumeb has the highest values and Ebenhaezer having lowest values (Table 5-4). This is in contrast to the evaporation factor because a site with a higher evaporation rate is expected to be enriched in heavier isotopic values. Furthermore, Kanyama (2017) found a lack of correspondence between plant source water and precipitation amount, thus along a precipitation gradient in Namibia. The study collected woody species (*V. erioloba, C. mopane, R. trichotomum, S. mellifera, T. sericea, B. albitrunca and A. hebeclada*) covering 11 sites along a precipitation gradient.

5.5.2.2 Transpiration

A high deuterium content of 515‰ in transpired water of a *S. mellifera* sample where the tracer was inserted at 2.5 m soil depth indicates an active root depth for *S. mellifera or* a possible contamination due to the fact that such high deuterium content is only observed in one sample. Slightly elevated deuterium contents in *B. albitrunca* transpired water at plot 2 and plot 3 could be attributed to either fractionation at a leaf level or it could be attributed to the tapping of soil water by its rare roots that are found in the upper soil layer.

Transpired water for both species being enriched in heavy isotopes composition could be attributed to the fractionation that occurs at leaf level. When a plant is transpiring, water vapour molecules containing the lighter isotopic composition escape from the leaf more readily than heavier ones, resulting in transpired water to be enriched with heavy isotope composition (Dongmann and Nürnberg, 1974; Flanagan and Ehleringer, 1991). As a result, all linear regression lines fitted to transpired water samples for *B. albitrunca* have a lower slope (slope =3.03) in comparison to those fitted from xylem water samples (slope = 4) in Figure 4. However, the same cannot be said for *S. mellifera* as the slope of the transpiration line (slope = 4.7) is higher than that derived from xylem water (slope =2.1). This is an indication that *S. mellifera* is using different source waters. Water extracted from the upper layers of a soil has been found to produce slopes in the range 2 - 5, with lowest slopes generally produced by drier soils (Barnes and Allison, 1984).

5.5.2.3 Seasonal variation in source water

Both *S. mellifera* and *B. albitrunca* xylem having similar boxplots of $\delta^{18}O$ is an indication that these two species used more or less the same source water in December 2016, at the beginning of rainy season (Figure 5-5a). *S. mellifera* and *B. albitrunca* xylem $\delta^{18}O$ values overlapping with those of groundwater indicates that groundwater is one of the main source water to these woody plants. Both *S. mellifera* and *B. albitrunca* transpired water are enriched in $\delta^{18}O$ values as compared to xylem water due to fractionation as an evaporative enrichment of stable isotopes occurs in the leaves (Allison et al., 1985; Dongmann and Nürnberg, 1974; Sheshshayee et al., 2005; Wang and Yakir, 2000).

In March 2017 (Figure 5-5b), during the rainy season, *S. mellifera* made a substantial shift in source water, probably using soil water from large precipitation events indicated by negative $\delta^{18}O$ values usually associated with such precipitation events which eventually also contribute to groundwater recharge (Geißler, 2019). Generally, it is observed that there is a positive relationship between the amount of precipitation and the negative isotopic composition of that precipitation (Dansgaard, 1964; Flanagan and Ehleringer, 1991). In May 2017 (Figure 5-5c), *S. mellifera* used both groundwater and soil water and positive $\delta^{18}O$ values are attributed to evaporated soil water at Ebenhaezer. Evaporative processes in the soil water usually result in the surface layers becoming isotopically enriched (Zencich et al., 2002). *B. albitrunca* xylem water on the other hand has not shown a significant variation. The fact that its isotopic composition falls within that of groundwater is an indication that *B. albitrunca* is mainly using groundwater.

5.5.2.4 Vertical movement in Soil Profile

The observed upward movement of the tracer can be attributed to evaporation, causing some of the deuterium tracer to escape to the atmosphere (Figure 5-6). A similar observation of the tracer transport towards the ground surface was observed by Beyer et al., (2016) in northern Namibia and attributed it to the upward water vapour transport. Moreover, a study on soil water movement in an eastern Amazonian forest by Romero-Saltos et al. (2005) attributed the upward movement through soil pores to a significant water potential gradient which is caused by evaporation. A study by Scanlon et al. (1997) in the south western United States also indicated that the upward movement in the unsaturated zone was due to water potentials whereby the total potential gradients are upward. All soil profiles have shown a displacement of the peak downward that could be attributed to dilution by infiltration. The downward movement is mainly regulated by precipitation input (Romero-Saltos et al., 2005). The deuterium tracer front did not move noticeably in May is an indication that precipitation did not reach the depth of 2.5 m and did thus not cause a displacement of the tracer front downward.

5.6 Conclusion

An investigation to assess the influence of woody plants on groundwater recharge was carried out at Ebenhaezer farm. A deuterium tracer was inserted in December 2016 at different depths at each of the six plots in order to determine the source water and active root depth of both *S. mellifera* and *B. albitrunca*. This was done by measuring δ^2H and δ^{18}O compositions for groundwater, soil water, xylem water and transpired water. The source water for the woody plants was compared to those obtained at Tsumeb and Waterberg. This work indicates that *S. mellifera* does not exclusively use groundwater but also water from the unsaturated zone via its extensive root system. *S. mellifera* roots capturing water from the unsaturated zone could influence groundwater recharge. As for *B. albitrunca,* $\delta^{18}O$ and $\delta^{2}H$ compositions revealed that it is mainly using groundwater due to its deep rooted system. The study allowed the estimation of the effective root depth for *S. mellifera* is between 2.5 m and 3 m. However the effective root depth for *B. albitrunca* could not be determined due to the absence of a tracer in both its xylem and transpiration water. The estimation of the effective root depth helps to better identify and quantify groundwater use by vegetation and also to improve groundwater recharge models. This knowledge helps in improving hydrological modelling by incorporating the influence of woody plants on groundwater recharge into such models. Further experimental studies focusing on woody plants and groundwater recharge are necessary especially along a precipitation gradient as the impact of woody plants on groundwater resources is essential for long-run planning of water resources in arid and semi arid countries.

5.7 Acknowledgements

The authors would like to acknowledge the OPTIMASS Project (01LL1302A) fully funded by the German Federal Ministry of Education and Research (BMBF) for funding this study. Authors thank Job Nghipandulwa and Lucas Shifeeleni for their assistance in the field especially drilling the holes at Ebenhaezer farm.

CHAPTER 6

OVERALL CONCLUSION AND RECOMMENDATIONS

6.1 Overall conclusion

The main aim of this study was to identify groundwater recharge processes and quantifying such along a precipitation gradient in savannah aquifers, thus at Tsumeb, Waterberg and Kuzikus/Ebenhaezer. The literature review revealed that aquifers in Namibia are mainly recharged directly from precipitation. Most of the groundwater recharge studies in Namibia excluded the influence of vegetation on groundwater despite it being one of the key factors influencing groundwater recharge. Hence the study also determined the influence of savannah vegetation on groundwater recharge along a precipitation gradient.

Precipitation being the main source of recharge to aquifers, its stable isotopic composition was determined along a precipitation gradient. The study determined local meteoric water lines along a precipitation gradient in order to understand isotopic variations. The range of slopes for the study area is 7.16 – 7.78, whereby Tsumeb has the highest slope and Kuzikus/Ebenhaezer has the lowest slope, thus slope values decreased with a decrease in annual precipitation amount. LMWL slopes lower than that of GMWL (slope is 8) is typical for semi-arid environments. With an exception of the altitude effect, other effects such as latitude, longitude and seasonal effect have revealed no correlation. These findings are important for future investigations, especially in tracing the origin of groundwater or source water for the vegetation in these study areas.

In addition, the study identified groundwater recharge rates along a precipitation gradient using CMB method. The highest mean recharge value was observed at Waterberg (9.6% of the mean annual precipitation), Tsumeb (6.1% of the mean annual precipitation) and the lowest value was at Kuzikus/Ebenhaezer (4.1% of the mean annual precipitation). Clearly this does not support the first hypothesis of this study that groundwater recharge rates increase along a precipitation gradient in savannah aquifers in Namibia. This indicates that there are other key factors apart from precipitation, such as soils and geology that are influencing groundwater recharge at these study sites. Thus higher groundwater recharge rates at Waterberg were attributed to faults and fractures within the Etjo sandstone aquifer acting as preferential flow paths. The dry deposition can be a source of uncertainty in the calculations of the obtained groundwater recharge rates since it was considered negligible in this study. There are very limited studies done on dry deposition. A study by Wanke (2005) carried out in central Namibia indicated that dry deposition contributes 22 – 83% of the total chloride deposition. Moreover, Selaolo (1998) have shown that dry chloride deposition contributes between 14 and 59% to the total chloride deposition in Botswana. Hence, these recharge values could have an uncertainty in that range.

Water stable isotopes revealed recharge mechanisms in the study areas with Waterberg having fast infiltration of precipitation due to absence of evaporation effect in its groundwater isotopic composition. These findings are essential for the management of the water resources in these study sites, especially at Kuzikus/Ebenhaezer where the recharge rates are lower, groundwater resources should be used effectively and sustainably.

The study further examined the influence of savannah vegetation on groundwater recharge. The study used a bush encroacher, *S. mellifera* and a deep-rooted non-encroacher *B. albitrunca*, to determine source water along a precipitation gradient using water stable isotopes. The study demonstrated that even though both woody plants are well distributed across Namibia, their water up taking mechanism differs.

The active root depths of these woody plants were traced at Ebenhaezer farm using a deuterium tracer. 2 xylem samples showed elevated deuterium contents (34.94‰ and 30.61‰); these 2 samples are from plots where the deuterium tracer was applied at 2.5 m and 3 m respectively. Hence, the active root depth for *S. mellifera* can be inferred to be between 2.5 – 3 m. However, the active root depth of *B. albitrunca* could not be conclusively determined due to the absence of the tracer in the sampling depths used.

S. mellifera did not exclusively take up groundwater but made extensive use of water sourced from the unsaturated zone which is well inline of expectation considering the nature of its extensive shallow root system while the isotopic composition of *B. albitrunca* falls mainly within that of groundwater, indicating the direct use of groundwater. The $\delta^{18}O$ median values (e.g May 2016) for *B. albitrunca* and groundwater are close to each other (-7.43‰ and -6.75‰ respectively) while that of *S. mellifera* is -4.36‰; the values falls between that of soil water (-2.89‰) and groundwater. These findings prove the second hypothesis of the study that shallowly rooted woody plants use water available for groundwater recharge. Furthermore, a seasonal variation in source water is observed in *S. mellifera* and that proves the third hypothesis of the study to be true.

The findings of this part of the dissertation demonstrated the influence of vegetation on groundwater recharge in savannah aquifers of Namibia. Hence, it is of utmost importance to incorporate a vegetation component in future groundwater recharge studies in Namibia. Additionally, this knowledge should be integrated into future groundwater recharge models for example the active root depth for *S. mellifera* in such models can be taken as 3 m inorder to avoid overestimations of groundwater recharge values. A technique of utilising a deuterium tracer proved useful to investigate effective rooting depth for shallow rooted woody plants. The developed knowledge is also helpful in terms of managing different types of vegetation in groundwater basins, especially bush encroachers.

Furthermore, both SADC and Namibia water policies highlight that there is a lack of information and understanding of groundwater systems and hence encourage investigations of water resources in the respective countries or at a national level in the case of Namibia. This study has responded to that highlight by narrowing the gap of groundwater resources data scarcity in Namibia. Groundwater recharge rates from the three study sites are all below 10% of the annual precipitation; hence these rates are relatively low. Policy makers should take into account these findings when determining safe yields for these study sites to ensure sustainability of groundwater use. Moreover, with climate change resulting in low annual mean precipitation, studies of this nature are vital in quantification of limited groundwater resources in semi-arid regions like Namibia.

Overall, the study has contributed to knowledge by determining LMWLs along a precipitation gradient which has never been done before in Namibia. This is an initial step for future isotope hydrology studies in the three study areas. Groundwater recharge rates along a precipitation gradient using the same methodology with the same temporal resolution were determined. The integrated temporal aspect made it easier to compare results from these three study sites along a precipitation gradient. The estimated groundwater recharge rates can help to predict water availability under scenarios of climate change. Furthermore, the study emphasised on the impact of vegetation on groundwater recharge. The study investigated the active root depths for both *S. mellifera* and *B. albitrunca* which was never examined before. The influence of vegetation on groundwater recharge in dry lands is not well understood; hence more studies of this nature are required to develop a true picture.

6.2 Recommendations

- The results of the research in this study together with the most complete compilation of groundwater recharge up to date in the literature review of this dissertation (Chapter 2) should be taken up in a thorough GIS based regionalisation of aquifer recharge that is not only based on precipitation amounts, but rather Hydrological Response Units that integrate vegetation, soil, hydrology and hydrogeology.

- Local meteoric water lines presented in Chapter 3 are based on a yearlong period only and it would be ideal to record such measures over periods of at least one decade and obtain long term annual averages. This could be achieved by training local people at these sites on how to collect precipitation events and get such samples analysed at the University of Namibia. Moreover, precipitation stations could be set up along a wider precipitation gradient. Obtained results could then be integrated in a worldwide isotope monitoring network of hydrogen and oxygen isotopes in precipitation (the

Global Network of Isotopes in Precipitation (GNIP)). This will also be interesting to understand the impact of climate change on isotopic composition in precipitation over time and help for example to identify trajectories and sources.

- Application of water stable isotope methods in groundwater recharge studies should be used in drylands especially in the saturated zone as more understanding of important recharge processes can be derived in comparison to studies that only use the CMB method to estimate groundwater recharge rates only.

- Although the CMB method is widely used successfully in semi-arid regions, the negligence of chloride dry deposition and using mean annual precipitation amounts that were measured more than 20 years ago should be treated with extreme care. It would be highly useful, if in the future someone could verify these data and improve input data for the CMB method.

- In areas where a higher evaporation effect is observed in groundwater, i.e. Kuzikus/Ebenhaezer in this study, methods that capture and protect rainwater from evaporation are recommended. This should include rain water harvest and flood water harvesting in covered tanks and reservoirs.

- It is recommended for future groundwater recharge studies in Namibia to incorporate a vegetation component since it has been demonstrated here that *S. mellifera* is using up soil water which is available for groundwater recharge. This could be done through the determination of the active root depth of bush encroachers and other species along a precipitation gradient and integrate such active root depths into groundwater recharge models as this will help to improve rates from potential groundwater recharge rates to net groundwater recharge rates that are more accurate.

- The use of statistics to interrogate the comparison between stable isotopes of the xylem water and source water is recommended for Chapter 5. It would be good to interrogate variability within the dataset and across stable isotopes within different woody plant species. Moreover, observation of time series of change in plant uptake through time and see how variable it is is recommended.

- Bush encroachers such as *S. mellifera* should be controlled and monitored as they have an effect on groundwater recharge. Such encroachers can be harvested for economic purposes. e.g. for charcoal production. Harvesting of these woody plants will reduce their water uptake which is available for groundwater recharge and as a result groundwater levels would rise.

REFERENCES

Abiye, T., 2016. Synthesis on groundwater recharge in Southern Africa: A supporting tool for groundwater users. Groundwater for Sustainable Development 2–3, 182–189. https://doi.org/10.1016/j.gsd.2016.10.002

Acharya, B.S., Hao, Y., Ochsner, T.E., Zou, C.B., 2017. Woody plant encroachment alters soil hydrological properties and reduces downward flux of water in tallgrass prairie. Plant and Soil 414, 379–391. https://doi.org/10.1007/s11104-016-3138-0

Acharya, B.S., Kharel, G., Zou, C.B., Wilcox, B.P., Halihan, T., 2018. Woody plant encroachment impacts on groundwater recharge: A review. Water (Switzerland) 10, 1–26. https://doi.org/10.3390/w10101466

Adams, M.E., 1967. A Study of the Ecology of Acacia mellifera, A. seyal and Balanites aegyptiaca in Relation to Land-Clearing. The Journal of Applied Ecology 4, 221. https://doi.org/10.2307/2401420

Aemisegger, F., Pfahl, S., Sodemann, H., Lehner, I., Seneviratne, S.I., Wernli, H., 2014. Deuterium excess as a proxy for continental moisture recycling and plant transpiration. Atmospheric Chemistry and Physics 14, 4029–4054. https://doi.org/10.5194/acp-14-4029-2014

Aguilera, H., Murillo, J.M., 2009. The effect of possible climate change on natural groundwater recharge based on a simple model: A study of four karstic aquifers in SE Spain. Environmental Geology 57, 963–974. https://doi.org/10.1007/s00254-008-1381-2

Alias, D., Milton, S., Herrmann, E., Seymour, C., 2003. A collation and overview of research information on Boscia albitrunca (shepherd’s tree) and identification of relevant research gaps to inform protection of the species.

Alker, M., 2009. The Stampriet Artesian Aquifer Basin A case study for the research project ”Transboundary groundwater management in Africa”. Bonn.

Allen, M., Dube, O., Solecki, W., 2018. Climate Change: Framing and Context. IPCC Specail Report: Global Warming of 1.5 °C.

Allison, G.B., 1988. A Review of Some of the Physical, Chemical and Isotopic Techniques Available for Estimating Groundwater Recharge. Estimation of Natural Groundwater Recharge 49–72. https://doi.org/10.1007/978-94-015-7780-9_4

Allison, G.B., Gat, J.R., Leaney, F.W.J., 1985. The relationship between deuterium and oxygen-18 delta values in leaf water. Chemical Geology: Isotope Geoscience Section 58, 145–156. https://doi.org/10.1016/0168-9622(85)90035-1

Allison, G.B., Gee, G.W., Tyler, S.W., 1994. Vadose-Zone Techniques for Estimating Groundwater Recharge in Arid and Semiarid Regions. Soil Science Society of America Journal. https://doi.org/10.2136/sssaj1994.03615995005800010002x

Alsaaran, N.A., 2005. Using environmental isotopes for estimating the relative contributions of groundwater recharge mechanisms in an arid basin, central Saudi Arabia. The Arabian Journal for Science and Engineering 31.

Amutenya, S., 2020. Improving Groundwater Recharge Estimates and Groundwater Management for the Cuvelai-Etosha Basin, University of Namibia, Windheok.

https://doi.org/10.13140/RG.2.2.26198.88644

Andjamba, P., 2016. A groundwater recharge map for Namibia based on the chloride mass balance method. University of Namibia.

Araguás-Araguás, L., Froehlich, K., Rozanski, K., 2000. Deuterium and oxygen-18 isotope composition of precipitation and atmospheric moisture. Hydrological Processes 14, 1341–1355. https://doi.org/10.1002/1099-1085(20000615)14:8<1341::AID-HYP983>3.3.CO;2-Q

Assmy, P., Smetacek, V., 2012. Algal Blooms. In Environmental Microbiology and Ecology. Edited by Schaechter, M 32, 435–449.

Barbecot, F., Guillon, S., Pili, E., Larocque, M., Gibert-Brunet, E., Hélie, J.-F., Noret, A., Plain, C., Schneider, V., Mattei, A., Meyzonnat, G., 2018. Using Water Stable Isotopes in the Unsaturated Zone to Quantify Recharge in Two Contrasted Infiltration Regimes. Vadose Zone Journal 17, 170170. https://doi.org/10.2136/vzj2017.09.0170

Barbeta, A., Peñuelas, J., 2017. Relative contribution of groundwater to plant transpiration estimated with stable isotopes. Scientific Reports 7, 1–10. https://doi.org/10.1038/s41598-017-09643-x

Barnes, C.., Allison, G.B., 1984. The distribution of deuterium and 18O in dry soils: 3. Theory for non-isothermal water movement. Journal of Hydrology 74, 119–135. https://doi.org/https://doi.org/10.1016/0022-1694(84)90144-6

Barnes, C.J., Allison, G.B., 1988. Tracing of water movement in the unsaturated zone using stable isotopes of hydrogen and oxygen. Journal of Hydrology 100, 143–176. https://doi.org/10.1016/0022-1694(88)90184-9

Bäumle, R., 2003. Geohydraulic Characterisation of Fractured Rock Flow Regimes. Regional Studies in Granite (Lindau, Black Forest, Germany) and Dolomite (Tsumeb Aquifers, Northern Namibia). Universität Karlsruhe (TH).

Bean, J., Beekman, H.E., Braune, E., Bredenkamp, D., Cave, L., Gieske, A., Hughes, G., Lerner, D., Lorentz, S., Kirchner, J., Maclear, L., Pitman, W., Sami, K., Schulze, R., Selaolo, E., van Tonder, G., Vegter, J., Verhagen, B., de Vries, J., Weaver, J., Wu, Y., Xu, Y., 2003. Groundwater Recharge Estimation in Southern Africa, UNESCO IHP. ed. UNESCO Paris, Paris.

Beekman, H.E., Xu, Y., 2018. Review: Groundwater recharge estimation in arid and semi-arid southern Africa. Hydrogeology Journal 27, 929–943.

Benettin, P., Nehemy, M.F., Cernusak, L.A., Kahmen, A., McDonnell, J.J., 2021. On the use of leaf water to determine plant water source: A proof of concept. Hydrological Processes. https://doi.org/10.1002/hyp.14073

Bershaw, J., 2018. Controls on deuterium excess across Asia. Geosciences (Switzerland) 8. https://doi.org/10.3390/geosciences8070257

Bester, F., 1999. Major problem-bush species and densities in Namibia. Agricola 10, 1–3.

Bester, F., 1996. Bush encroachment: A thorny problem. Namibian Environment 175–177.

Beyer, M., Gaj, M., Hamutoko, J.T., Koeniger, P., Wanke, H., Himmelsbach, T., 2015. Estimation of groundwater recharge via deuterium labelling in the semi-arid Cuvelai-Etosha Basin, Namibia. Isotopes in Environmental and Health Studies 51, 533–552. https://doi.org/10.1080/10256016.2015.1076407

Beyer, M., Koeniger, P., Gaj, M., Hamutoko, J.T., Wanke, H., Himmelsbach, T., 2016. A deuterium-based labeling technique for the investigation of rooting depths, water uptake dynamics and unsaturated zone water transport in semiarid environments. Journal of Hydrology 533, 627–643. https://doi.org/10.1016/j.jhydrol.2015.12.037

Boumaiza, L., Chesnaux, R., Walter, J., Stumpp, C., 2020. Assessing groundwater recharge and transpiration in a humid northern region dominated by snowmelt using vadose-zone depth profiles. Hydrogeology Journal 28, 2315–2329. https://doi.org/10.1007/s10040-020-02204-z

Bowen, G.J., Putman, A., Brooks, J.R., Bowling, D.R., Oerter, E.J., Good, S.P., 2018. Inferring the source of evaporated waters using stable H and O isotopes. Oecologia 187, 1025–1039. https://doi.org/10.1007/s00442-018-4192-5

Britz, M.L., Ward, D., 2007. Dynamics of woody vegetation in a semi-arid savanna, with a focus on bush encroachment. African Journal of Range and Forage Science 24, 131–140. https://doi.org/10.2989/AJRFS.2007.24.3.3.296

Burgess, S.S.O., Adams, M.A., Turner, N.C., Ong, C.K., 1998. The redistribution of soil water by tree root systems. Oecologia 115, 306–311. https://doi.org/10.1007/s004420050521

Burke, A., 2006. Savanna trees in Namibia — Factors controlling their distribution at the arid end of the spectrum. Flora 201, 189–201. https://doi.org/10.1016/j.flora.2005.06.011

Callow, N., McGowan, H., Warren, L., Speirs, J., 2014. Journal of Geophysical Research : Atmospheres. Journal of Geophysical Research 119, 2966–2989.

https://doi.org/10.1002/2013JD020710.Received

Canadell, J., Jackson, R.B., Ehleringer, J.R., Mooney, H.A., Sala, O.E., Schulze, E.D., 1996. Maximum rooting depth of vegetation types at the global scale. Oecologia 108, 583–595. https://doi.org/10.1007/BF00329030

Case, M.F., Nippert, J.B., Holdo, R.M., Staver, A.C., 2020. Root-niche separation between savanna trees and grasses is greater on sandier soils. Journal of Ecology 108, 2298–2308. https://doi.org/10.1111/1365-2745.13475

Chen, Y., Helliker, B.R., Tang, X., Li, F., Zhou, Y., Song, X., 2020. Stem water cryogenic extraction biases estimation in deuterium isotope composition of plant source water. Proceedings of the National Academy of Sciences of the United States of America 117, 33345–33350. https://doi.org/10.1073/PNAS.2014422117

Christelis, G., Struckmeier, W.F., 2011. Groundwater in Namibia, Second. ed, Water.

Clark, I.D., Fritz, P., 1997. Environmental Isotopes in Hydrogeology, Environmental Isotopes in Hydrogeology. CRC Press. https://doi.org/10.1201/9781482242911

Climate-Data.Org [WWW Document], 2018. URL https://en.climate-data.org/africa/namibia-89

Craig, H., 1961. Isotopic Variations in Meteoric Waters. Science 133, 1702 LP – 1703. https://doi.org/10.1126/science.133.3465.1702

Crawford, J., Hollins, S.E., Meredith, K.T., Hughes, C.E., 2017. Precipitation stable isotope variability and subcloud evaporation processes in a semi-arid region.

Hydrological Processes 31, 20–34. https://doi.org/10.1002/hyp.10885

Crerar, S., Fry, R.G., Slater, P.M., van Langenhove, G., Wheeler, D., 1988. An unexpected factor affecting recharge from ephemeral river flows in SWA/Namibia, in: Estimation of Natural Groundwater Recharge. https://doi.org/10.1007/978-94-015-7780-9_2

Curtis, B., Mannheimer, C., 2005. Tree Atlas of Namibia. National Botanical Research Institute, Ministry of Agriculture, Water and Forestry, Windhoek, Namibia.

Cuthbert, M.O., Taylor, R.G., Favreau, G., Todd, M.C., Shamsudduha, M., Villholth, K.G., MacDonald, A.M., Scanlon, B.R., Kotchoni, D.O.V., Vouillamoz, J.M., Lawson, F.M.A., Adjomayi, P.A., Kashaigili, J., Seddon, D., Sorensen, J.P.R., Ebrahim, G.Y., Owor, M., Nyenje, P.M., Nazoumou, Y., Goni, I., Ousmane, B.I., Sibanda, T., Ascott, M.J., Macdonald, D.M.J., Agyekum, W., Koussoubé, Y., Wanke, H., Kim, H., Wada, Y., Lo, M.H., Oki, T., Kukuric, N., 2019. Observed controls on resilience of groundwater to climate variability in sub-Saharan Africa. Nature 572, 230–234. https://doi.org/10.1038/s41586-019-1441-7

Dahan, O., Tatarsky, B., Enzel, Y., Kulls, C., Seely, M., Benito, G., 2008. Dynamics of flood water infiltration and ground water recharge in hyperarid desert. Ground Water 46, 450–461. https://doi.org/10.1111/j.1745-6584.2007.00414.x

Dansgaard, W., 1964. Stable isotopes in precipitation. Tellus 16, 436–468. https://doi.org/10.3402/tellusa.v16i4.8993

David, A., 2013. Groundwater recharge estimation for perched aquifers in the

Ohangwena Region based on soil water balance modeling and chloride mass balance. Journal of Chemical Information and Modeling. University of Namibia.

Dawson, T.E., Ehleringer, J.R., 1993. Isotopic enrichment of water in the "woody" tissues of plants: Implications for plant water source, water uptake, and other studies which use the stable isotopic composition of cellulose. Geochimica et Cosmochimica Acta 57, 3487–3492. https://doi.org/10.1016/0016-7037(93)90554-A

De Klerk, J.., 2004. Bush encroachment in Namibia. Report on Phase 1 of the Bush encroachment, monitoring and management project. Windhoek, Namibia.

De Vries, J., Simmers, I., 2002. Groundwater recharge: an overview of processes and challenges. Hydrogeology 5–17.

Directorate of Environmental Affairs (DEA), M. of E. and T., 2002. Digital Atlas of Namibia [WWW Document]. Acacia Project E1. URL https://www.uni-koeln.de/sfb389/e/e1/download/atlas_namibia/main_namibia_atlas.html

Döll, P., Fiedler, K., 2008. Global-scale modeling of groundwater recharge. Hydrology and Earth System Sciences 12, 863–885. https://doi.org/10.5194/hess-12-863-2008

Donaldson, C.H., 1969. Bush encroachment with special reference to the Blackthorn problem of the Malopo area. Pretoria.

Dongmann, G., Nürnberg, H.W., 1974. On the Enrichment of H2180 in the Leaves of Transpiring Plants. Radiation and Environmental Biophysics 52, 41–52.

DWA, 1988. Evaporation map for Namibia. Windhoek.

DWA & GSN, 2001. Groundwater in Namibia. An explanation to the Hydrogeological map, First. ed. Windhoek, Namibia.

E1, A.P., n.d. No Title [WWW Document]. URL http://www.uni-koeln.de/sfb389/e/e1/index.htm

EarthExplorer, n.d. https://earthexplorer.usgs.gov/ [WWW Document].

Edmunds, W.M., Darling, W.G., Kinniburgh, D.G., 1988. Solute profile techniques for recharge estimation in semi-arid and arid terrain, in: Simmers, I. (Ed.), Estimation of Natural Groundwater Recharge. Springer, Dordrecht, pp. 139–157. https://doi.org/https://doi.org/10.1007/978-94-015-7780-9_9

Ehleringer, J.R., Dawson, T.E., 1992. Water uptake by plants: perspectives from stable isotope composition. Plant, Cell & Environment. https://doi.org/10.1111/j.1365-3040.1992.tb01657.x

Ellsworth, P.Z., Williams, D.G., 2007. Hydrogen isotope fractionation during water uptake by woody xerophytes. Plant and Soil 291, 93–107. https://doi.org/10.1007/s11104-006-9177-1

Evaristo, J., Jasechko, S., McDonnell, J.J., 2015. Global separation of plant transpiration from groundwater and streamflow. Nature 525, 91–94. https://doi.org/10.1038/nature14983

Fan, J., Oestergaard, K.T., Guyot, A., Lockington, D.A., 2014. Estimating groundwater recharge and evapotranspiration from water table fluctuations under three vegetation covers in a coastal sandy aquifer of subtropical Australia.

Journal of Hydrology 519, 1120–1129. https://doi.org/10.1016/j.jhydrol.2014.08.039

Finch, J.W., 1998. Estimating direct groundwater recharge using a simple water balance model - Sensitivity to land surface parameters. Journal of Hydrology 211, 112–125. https://doi.org/10.1016/S0022-1694(98)00225-X

Flanagan, L.B., Ehleringer, J.R., 1991. Stable Isotope Composition of Stem and Leaf Water: Applications to the Study of Plant Water Use. Functional Ecology 5, 270. https://doi.org/10.2307/2389264

Flanagan, L.B., Orchard, T.E., Tremel, T.N., Rood, S.B., 2019. Using stable isotopes to quantify water sources for trees and shrubs in a riparian cottonwood ecosystem in flood and drought years. Hydrological Processes 33, 3070–3083. https://doi.org/10.1002/hyp.13560

Foster, S.S.D., Morris, B.L., Lawrence, A.R., 1994. Effects of urbanization on groundwater recharge. Groundwater problems in urban areas 43–63. https://doi.org/10.1680/gpiua.19744.0005

Freeze, R., Cherry, J., 1979. Groundwater. Prentice Hall, Englewood cliffs.

G Christelis W.Struckmeier, 2011. Groundwater in Namibia: an Explanation to the Hydrogeological Map, second. ed. HYMNAM, Windhoek.

Gaj, M., Beyer, M., Koeniger, P., Wanke, H., Hamutoko, J., Himmelsbach, T., 2016. In situ unsaturated zone water stable isotope (2H and 18O) measurements in semi-arid environments: A soil water balance. Hydrology and Earth System Sciences 20, 715–731. https://doi.org/10.5194/hess-20-715-2016

Gat, J.R., 2000. Atmospheric water balance-the isotopic perspective. Hydrological Processes 14, 1357–1369. https://doi.org/10.1002/1099-1085(20000615)14:8<1357::AID-HYP986>3.0.CO;2-7

Gat, J.R., 1996. Oxygen and Hydrogen Isotopes in the Hydrologic Cycle. Annual Review of Earth and Planetary Sciences 24, 225–262. https://doi.org/10.1146/annurev.earth.24.1.225

Gat, J.R., Mook, W.G., Meijer, H.A.J., 2000. VOLUME II - Atmospheric Water. Environmental Isotopes in the Hydrological Cycle Principles and Applications 114.

Gebru, T.A., Tesfahunegn, G.B., 2019. Chloride mass balance for estimation of groundwater recharge in a semi-arid catchment of northern Ethiopia. Hydrogeology Journal 27, 363–378. https://doi.org/10.1007/s10040-018-1845-8

Gee, G.W., Hillel, D., 1988. Groundwater recharge in arid regions: Review and critique of estimation methods. Hydrological Processes 2, 255–266. https://doi.org/10.1002/hyp.3360020306

Gee, G.W., Zhang, Z.F., Tyler, S.W., Albright, W.H., Singleton, M.J., 2005. Chloride Mass Balance: Cautions in Predicting Increased Recharge Rates. Vadose Zone Journal 4, 72–78. https://doi.org/10.2113/4.1.72

Gehrels, J.C., Peeters, J.E.M., De Vries, J.J., Dekkers, M., 1998. The mechanism of soil water movement as inferred from 18O stable isotope studies. Hydrological Sciences Journal 43, 579–594. https://doi.org/10.1080/02626669809492154

Geißler, K., 2019. Partitioning of Water Between Differently Sized Shrubs and Potential Groundwater Recharge in a Semiarid Savanna in Namibia. frontiers in

Plant Science 10, 1–13. https://doi.org/10.3389/fpls.2019.01411

Geißler, K., Heblack, J., Uugulu, S., Wanke, H., Blaum, N., 2019. Partitioning of Water Between Differently Sized Shrubs and Potential Groundwater Recharge in a Semiarid Savanna in Namibia. Frontiers in Plant Science 10, 1–13. https://doi.org/10.3389/fpls.2019.01411

Gibson, J.J., Birks, S.J., Edwards, T.W.D., 2008. Global prediction of δA and δ2H-δ18O evaporation slopes for lakes and soil water accounting for seasonality. Global Biogeochemical Cycles 22, 1–12. https://doi.org/10.1029/2007GB002997

Gibson, J.J., Edwards, T.W.D., Bursey, G.G., 1993. Estimating Evaporation Using Stable Isotopes : Quantitative Results and Sensitivity Analysis for Two Catchments in Northern Canada. Nordic Hydrology 24, 79–94. https://doi.org/10.2166/nh.1993.006

Gieske, A., 1992. Dynamics of groundwater: a case study in semi-arid Eastern Botswana. University of Twente.

Gieske, A., Selaolo, E., McMullan, 1990. Groundwater recharge through the unsaturated zone of southeastern Botswana: a study of chlorides and environmental isotopes, in: Proceedings of the Ljubljana Symposium. IAHS, pp. 33–44.

Gieske, A., Selaolo, E.T., Beekman, H.E., 1995. Tracer interpretation of moisture transport in a Kalahari sand profile. Application of tracers in arid zone hydrology (United Kingdom) 373–382.

Gokool, S., Moody, J.E., Nippert, J., Swemmer, A., Chetty, K.T., Magombeyi, M., Riddell, E.S., 2021. A preliminary evaluation of ecohydrological separation in a semi-arid riparian area. Ecohydrology and Hydrobiology 21, 271–279. https://doi.org/10.1016/j.ecohyd.2021.01.002

Guan, H., Zhang, X., Skrzypek, G., Sun, Z., Xu, X., 2013. Deuterium excess variations of rainfall events in a coastal area of south Australia and its relationship with synoptic weather systems and atmospheric moisture sources. Journal of Geophysical Research Atmospheres 118, 1123–1138. https://doi.org/10.1002/jgrd.50137

Gupta, V., Jain, M.K., 2018. Investigation of multi-model spatiotemporal mesoscale drought projections over India under climate change scenario. Journal of Hydrology 567, 489–509. https://doi.org/10.1016/j.jhydrol.2018.10.012

Haidu, I., Nistor, M.M., 2020. Long-term effect of climate change on groundwater recharge in the Grand Est region of France. Meteorological Applications 27, 1–17. https://doi.org/10.1002/met.1796

Hamutoko, J.T., 2018. Groundwater recharge of perched aquifers in the Cuvelai-Etosha basin, Namibia. University of Namibia.

Hamutoko, J.T., Post, V.E.A., Wanke, H., Beyer, M., Houben, G., Mapani, B., 2019. The role of local perched aquifers in regional groundwater recharge in semi-arid environments: evidence from the Cuvelai-Etosha Basin, Namibia. Hydrogeology Journal 27, 2399–2413. https://doi.org/10.1007/s10040-019-02008-w

Harvey, F.E., Welker, J.M., 2000. Stable isotopic composition of precipitation in the semi-arid north-central portion of the US Great Plains. Journal of Hydrology

238, 90–109. https://doi.org/https://doi.org/10.1016/S0022-1694(00)00316-4

Healy, R.W., 2010. Estimating groundwater recharge. University Press, Cambridge.

Healy, R.W., Cook, P.G., 2002. Using groundwater levels to estimate recharge. Hydrogeology Journal 10, 91–109. https://doi.org/10.1007/s10040-001-0178-0

Healy, R.W., Scanlon, B.R., 2010. Estimating groundwater recharge. Cambridge Unversity Press, United Kingdom.

Heaton, T.H.E., Talma, A.S., Vogel, J.C., 1983. Origin and history of nitrate in confined groundwater in the western Kalahari. Journal of Hydrology 62, 243–262. https://doi.org/10.1016/0022-1694(83)90105-1

Herczeg, A.L., Leaney, F.W., 2011. Review: Environmental tracers in arid-zone hydrology. Hydrogeology Journal 19, 17–29. https://doi.org/10.1007/s10040-010-0652-7

Hipondoka, M.H.T., Aranibar, J.N., Chirara, C., Lihavha, M., Macko, S.A., 2003. Vertical distribution of grass and tree roots in arid ecosystems of Southern Africa: Niche differentiation or competition? Journal of Arid Environments 54, 319–325. https://doi.org/10.1006/jare.2002.1093

Hiscock, K. m., Bense, V.F., 2014. Hydrogeology Principles and Practice, Second. ed. John Wiley & Sons Ltd, West Sussex.

Hoad, N., 1993. An overview of Groundwater Investigations in the Tsumeb and Oshivelo Areas. Windhoek.

Huxman, T.E., Wilcox, B.P., Breshears, D.D., Scott, R.L., Snyder, K.A., Small, E.E., Hultine, K., Pockman, W.T., Jackson, R.B., 2005. Ecohydrological implications of plant encroachment. Ecology 86, 308–319. https://doi.org/https://doi.org/10.1890/03-0583

Jacobson, P., Jacobson, K., Seely, M., 1995. Ephemeral rivers and their catchments.

Jasechko, S., 2019. Global Isotope Hydrogeology―Review. Reviews of Geophysics 57, 835–965. https://doi.org/10.1029/2018RG000627

Javaux, M., Rothfuss, Y., Vanderborght, J., Vereecken, H., Brüggemann, N., 2016. Isotopic composition of plant water sources. Nature 536, E1–E3. https://doi.org/10.1038/nature18946

Jennings, C.M.H., 1974. The Hydrogeology of Botswana. University of Natal.

JICA, 2002. The study on the the groundwater potential evaluation and management plan in the southeast Kalahari (Stampriet) artesian Basin in the Republic of Namibia. Windhoek.

Kambinda, W.N., 2014. Hydrogeological investigation of the Naukluft mountains, southwest Namibia. University of Namibia.

Kanyama, C.M., 2017. A study of isotopic composition of xylem water of woody vegetation and groundwater along a precipitation gradient in Namibia. University of Namibia.

Kaseke, K.F., Wang, L., Wanke, H., Turewicz, V., Koeniger, P., 2016. An Analysis of Precipitation Isotope Distributions across Namibia Using Historical Data. PloS one 11, e0154598. https://doi.org/10.1371/journal.pone.0154598

Khalil, M., Sakai, M., Mizoguchi, M., Miyazaki, T., 2003. Current and Prospective Applications of Zero Flux Plane (ZFP) Method. Journal of the Japanese Society of Soil Physics 95, 75–90.

Klock, H., 2001. Hydrogeology of the Kalahari in north-eastern Namibia with special emphasis on groundwater recharge, flow modelling and hydrochemistry. Julius-Maximilians-University of Würzburg.

Klock, H., Külls, C., Udluft, P., 2001. Estimating recharge values using hydrochemical and geological data: A case study from the semiarid Kalahari catchment of northern Namibia, IAHS-AISH Publication.

Klock, H., Udluft, P., 2002. Mapping groundwater recharge and discharge zones in the Kalahari: A remote sensing approach.

Koeniger, P., Gaj, M., Beyer, M., Himmelsbach, T., 2016. Review on soil water isotope-based groundwater recharge estimations. Hydrological Processes 30, 2817–2834. https://doi.org/10.1002/hyp.10775

Koeniger, P., Marshall, J.D., Link, T., Mulch, A., 2011. An inexpensive, fast, and reliable method for vacuum extraction of soil and plant water for stable isotope analyses by mass spectrometry. Rapid Communications in Mass Spectrometry 25, 3041–3048. https://doi.org/10.1002/rcm.5198

Külls, C., 2000. Groundwater of the North-Western Kalahari, Namibia: Estimation of recharge and quantification of the flow systems. Julius-Maximilian University of Würzburg.

Kulmatiski, A., Beard, K.H., Holdrege, M.C., February, E.C., 2020. Small differences in root distributions allow resource niche partitioning. Ecology and Evolution 10, 9776–9787. https://doi.org/10.1002/ece3.6612

Kulmatiski, A., Forero, L.E., 2021. Bagging: a cheaper, faster, non-destructive transpiration water sampling method for tracer studies. Plant and Soil. https://doi.org/10.1007/s11104-021-04844-w

Leibundgut, C., Maloszewski, P., Külls, C., 2009. Tracers in hydrology. Wiley-Blackwell, Oxford, UK. https://doi.org/doi: 10.1002/9780470747148

Lerner, D.N., Issar, A.S., Simmers, I., 1990. Groundwater recharge. A Guide to Understanding and Estimating Natural Recharge.

Lewis, F.M., Walker, G.R., 2001. Assessing the potential for significant and episodic recharge in southwestern Austarlia using rainfal data.pdf. Hydrogeology Journal 10, 229–237.

Li, Z., Wang, G., Wang, X., Wan, L., Shi, Z., Wanke, H., Uugulu, S., Uahengo, C.I., 2018. Groundwater quality and associated hydrogeochemical processes in Northwest Namibia. Journal of Geochemical Exploration 186, 202–214. https://doi.org/10.1016/j.gexplo.2017.12.015

Lubczynski, M.W., 2016. Groundwater evapotranspiration , an underestimated component of a groundwater balance in a semi-arid environment Groundwater evapotranspiration – underestimated component of the groundwater balance in a semi-arid environment – Serowe case ,.

Lubczynski, M.W., 2009. The hydrogeological role of trees in water-limited environments. Hydrogeology Journal 17, 247–259. https://doi.org/10.1007/s10040-008-0357-3

Lubis, M.E.., Harahap, I.Y., Hidayat, T.C., Pangaribuan, Y., Sutarta, E.S., Rahman, Z.A., Teh, C., Hanafi, M.M., 2014. Stable Oxygen and Deuterium Isotope

Techniques to Identify Plant Water Sources. Journal of Water Resource and Protection 06, 1501–1508. https://doi.org/10.4236/jwarp.2014.615137

Ma, X., Zhu, J., Wang, Y., Yan, W., Zhao, C., 2021. Variations in water use strategies of sand-binding vegetation along a precipitation gradient in sandy regions, northern China. Journal of Hydrology 600, 126539. https://doi.org/10.1016/j.jhydrol.2021.126539

MacDonald, A.M., Lark, R.M., Taylor, R.G., Abiye, T., Fallas, H.C., Favreau, G., Goni, I.B., Kebede, S., Scanlon, B., Sorensen, J.P.R., Tijani, M., Upton, K.A., West, C., 2021. Mapping groundwater recharge in Africa from ground observations and implications for water security. Environmental Research Letters 16. https://doi.org/10.1088/1748-9326/abd661

Mainardy, H.., 1999. Grundwasserneubildung in der Übergangszone zwischen Festgesteinsrücken und Kalahari-Lockersedimentüberdeckung (Namibia). HU-Forschungsergebnisse aus dem Bereich Hydrogeologie und Umwelt 1–145.

Maitre, D.C. Le, Scott, D.F., Colvin, C., 1999. A review of information on interactions between vegetation and groundwater. Water SA 25, 137–152.

Marei, A., Khayat, S., Weise, S., Ghannam, S., Sbaih, M., Geyer, S., 2010. Estimation de la recharge hydrogéologique par la méthode du bilan massique des chlorures en Cisjordanie, Palestine. Hydrological Sciences Journal 55, 780–791. https://doi.org/10.1080/02626667.2010.491987

Matengu, B.M., 2020. Groundwater assessment and sustainable management of the coastal alluvial aquifers in Namib Desert , Namibia : Omdel Aquifer as case study. University of the Western Cape.

MAWRD, 2000. National Water Policy White Paper - Policy Framework for Equitable, Efficient, and Sustainable Water Resources Management and Water Services. Ministry of Agriculture, Water and Rural Development 45.

MEA (Millennium Ecosystem Assessment), 2005. Ecosystems and human well-being: sythesis., Island Press. Washington D.C.

Meixner, T., Manning, A.H., Stonestrom, D.A., Allen, D.M., Ajami, H., Blasch, K.W., Brookfield, A.E., Castro, C.L., Clark, J.F., Gochis, D.J., Flint, A.L., Neff, K.L., Niraula, R., Rodell, M., Scanlon, B.R., Singha, K., Walvoord, M.A., 2016. Implications of projected climate change for groundwater recharge in the western United States. Journal of Hydrology 534, 124–138. https://doi.org/10.1016/j.jhydrol.2015.12.027

Mendelsohn, J., Jarvis, A., Roberts, C., Robertson, T., 2002. The Atlas of Namibia. David Philip Publishers, Cape Town.

Miller, R., 2008. The geology of Namibia. Geological Survey of Namibia 3, 16.1-28.1.

Moeck, C., Grech-Cumbo, N., Podgorski, J., Bretzler, A., Gurdak, J.J., Berg, M., Schirmer, M., 2020. A global-scale dataset of direct natural groundwater recharge rates: A review of variables, processes and relationships. Science of the Total Environment 717, 137042. https://doi.org/10.1016/j.scitotenv.2020.137042

Morin, E., Grodek, T., Dahan, O., Benito, G., Kulls, C., Jacoby, Y., Langenhove, G. Van, Seely, M., Enzel, Y., 2009. Flood routing and alluvial aquifer recharge along the ephemeral arid Kuiseb River, Namibia. Journal of Hydrology 368, 262–275. https://doi.org/10.1016/j.jhydrol.2009.02.015

Mountney, N., Howell, J., Flint, S., Jerram, D., 1998. Aeolian and alluvial deposition within the Mesozoic Etjo Sandstone formation, northwest Namibia. Journal of African Earth Sciences 27, 175–192. https://doi.org/https://doi.org/10.1016/50899-5363(98)00056-6

Mukendwa, H.M., 2009. The Groundwater Flow Regime of the Kombat Aquifer, Namibia. University of the Free State.

Namibia Agricultural Union (NAU), 2010. The Effect of Bush Encroachment on Groundwater Resources in Namibia: a Desk Top Study. Windhoek, Namibia.

Namibia Water Corporation, 2012. Hydrological Services.

NDP5, 2017. Namibia's 5th national development plan. Namibia's 5th National Development plan (NDP5).

Nghipandulwa, J.N., 2018. Interpretation of hydrographs and establishment of rates and timing of recharge from shallow Kalahari perched aquifers in Ohangwena Region, Namibia. University of Namibia.

O'Donnell, F.C., Caylor, K.K., Bhattachan, A., Dintwe, K., D'Odorico, P., Okin, G.S., 2015. A quantitative description of the interspecies diversity of belowground structure in savanna woody plants. Ecosphere 6, 1–15. https://doi.org/10.1890/ES14-00310.1

Obakeng, O.T., 2007. Soil moisture dynamics and evapotranspiration at the fringe of the Botswana Kalahari, with emphasis on deep rooting vegetation, ITC Dissertation;141.

Pan, Y.X., Wang, X.P., Ma, X.Z., Zhang, Y.F., Hu, R., 2020. The stable isotopic composition variation characteristics of desert plants and water sources in an artificial revegetation ecosystem in Northwest China. Catena 189, 104499. https://doi.org/10.1016/j.catena.2020.104499

Pang, Z., Kong, Y., Froehlich, K., Huang, T., Yuan, L., Li, Z., Wang, F., 2011. Processes affecting isotopes in precipitation of an arid region. Tellus, Series B: Chemical and Physical Meteorology 63, 352–359. https://doi.org/10.1111/j.1600-0889.2011.00532.x

Peck, H., 2010. The preliminary study of the Stampriet transboundary aquifer in the south east Kalahari/Karoo basin. University of the Western Cape.

Pfahl, S., Sodemann, H., 2014. What controls deuterium excess in global precipitation? Climate of the Past 10, 771–781. https://doi.org/10.5194/cp-10-771-2014

Ramarao, M.V.S., Sanjay, J., Krishnan, R., Mujumdar, M., Bazaz, A., Revi, A., 2019. On observed aridity changes over the semiarid regions of India in a warming climate. Theoretical and Applied Climatology 136, 693–702. https://doi.org/10.1007/s00704-018-2513-6

Rathay, S.Y., Allen, D.M., Kirste, D., 2018. Response of a fractured bedrock aquifer to recharge from heavy rainfall events. Journal of Hydrology 561, 1048–1062. https://doi.org/10.1016/j.jhydrol.2017.07.042

Reid, H., Sahlen, L., MacGregor, J., Stage, J., 2007. The economic impact of climate change in Namibia, IIED. https://doi.org/10.15678/znuek.2019.0982.0406

Roberts, J., 2000. The influence of physical and physiological characteristics of vegetation on thier hydrological response. Hydrological Processes 14, 2885–2901. https://doi.org/10.1002/1099-1085(200011/12)14:16/17<2885::AID-HYP125>3.0.CO;2-Z

Romero-Saltos, H., Sternberg, L.D.S.L., Moreira, M.Z., Nepstad, D.C., 2005. Rainfall exclusion in an eastern Amazonian forest alters soil water movement and depth of water uptake. American Journal of Botany 92, 443–455. https://doi.org/10.3732/ajb.92.3.443

Rothauge, A., 2017. Bush Control Manual. AgriConsult Namibia.

SADC, 2005. SADC Regional water policy. Sadc 1–77.

SADC Grounwater Information Portal [WWW Document], n.d. URL https://www.un-igrac.org/special-project/sadc-groundwater-information-portal-gip

Sala, O.E., Lauenroth, W.K., Parton, W.J., 1992. Long-term soil water dynamics in the shortgrass steppe. Ecology 73, 1175–1181.

Sanford, W., 2002. Recharge and groundwater models: An overview. Hydrogeology Journal 10, 110–120. https://doi.org/10.1007/s10040-001-0173-5

Sarma, D., Xu, Y., 2017. Le processus de recharge dans des bandes aquifères alluviales en Namibie aride et son implication pour la recharge artificielle. Hydrogeology Journal 25, 123–134. https://doi.org/10.1007/s10040-016-1474-z

Scanlon, Bridget R;, Healy, R.W., Cook, P.G., 2002. Choosing appropriate techniques for quantifying groundwater recharge. Hydrogeology Journal 10, 18–39. https://doi.org/https://doi.org/10.1007/s10040-001-0176-2

Scanlon, Bridget R., Healy, R.W., Cook, P.G., 2002. Choosing appropriate techniques for quantifying groundwater recharge. Hydrogeology Journal 10, 18–39. https://doi.org/10.1007/s10040-001-0176-2

Scanlon, B.R., Keese, K.E., Flint, A.L., Flint, L.E., Gaye, C.B., Edmunds, W.M., Simmers, I., 2006. Global synthesis of groundwater recharge in semiarid and arid regions. Hydrological Processes 30, 3335–3370. https://doi.org/10.1002/hyp

Scanlon, B.R., Tyler, S.W., Wierenga, P.J., 1997. Hydrologic issues in arid, unsaturated systems and implications for contaminant transport. Reviews of Geophysics 35, 461–490. https://doi.org/10.1029/97RG01172

Scanlon, T.M., Caylor, K.K., Manfreda, S., Levin, S.A., Rodriguez-Iturbe, I., 2005. Dynamic response of grass cover to rainfall variability: Implications for the function and persistence of savanna ecosystems. Advances in Water Resources 28, 291–302. https://doi.org/10.1016/j.advwatres.2004.10.014

Schmidt, S., Geyer, T., Marei, A., Guttman, J., Sauter, M., 2013. Quantification of long-term wastewater impacts on karst groundwater resources in a semi-arid environment by chloride mass balance methods. Journal of Hydrology 502, 177–190. https://doi.org/10.1016/j.jhydrol.2013.08.009

Schulze, E.D., Mooney, H.A., Sala, O.E., Jobbagy, E., Buchmann, N., Bauer, G., Canadell, J., Jackson, R.B., Loreti, J., Oesterheld, M., Ehleringer, J.R., 1996. Rooting depth, water availability, and vegetation cover along an aridity gradient in Patagonia. Oecologia 108, 503–511. https://doi.org/10.1007/BF00333727

Schwartz, M.O., 2006. Numerical modelling of groundwater vulnerability: The example Namibia. Environmental Geology 50, 237–249. https://doi.org/10.1007/s00254-006-0204-6

Scott, R.L., Cable, W.L., Hultine, K.R., 2008. The ecohydrologic significance of hydraulic redistribution in a semiarid savanna. Water Resources Research 44, 1–12. https://doi.org/10.1029/2007WR006149

Seely, M., Henderson, J., Heyns, P., Jacobson, P., Nakale, T., Nantanga, K., Schachtschneider, K., 2003. Ephemeral and endoreic river systems: Relevance and management challenges. … Rivers, Sovereignty … 187–212.

Selaolo, E.T., 1998. Tracer studies and groundwater recharge assessment in the eastern fringe of the Botswanan Kalahari. Vrige Universiteit.

Shanyengana, E.S., Seely, M.K., Sanderson, R.D., 2004. Major-ion chemistry and ground-water salinization in ephemeral floodplains in some arid regions of Namibia. Journal of Arid Environments 57, 211–223. https://doi.org/10.1016/S0140-1963(03)00095-8

Sharafatmandrad, M., Mashizi, A.K., 2021. Temporal and Spatial Assessment of Supply and Demand of the Water-yield Ecosystem Service for Water Scarcity Management in Arid to Semi-arid Ecosystems. Water Resources Management 35, 63–82. https://doi.org/10.1007/s11269-020-02706-1

Sharma, M.L., Cresswell, I.D., Watson, J.D., 1985. Estimates of natural groundwater recharge from the depth distribution of an applied tracer. in: Iahr Preprint. Proc. 21St Congress, Volume 1, Theme a, Subsurface Flow, Pollutant Transport, and Salinity, 85, 64–70.

Sharma, M.L., Hughes, M.W., 1985. Groundwater recharge estimation using chloride, Deuterium and Oxygen-18 profiles in the deep coastal sands of western Australia. Journal of Hydrology 93–109.

Sheshshayee, M.S., Bindumadhava, H., Ramesh, R., Prasad, T.G., Lakshminarayana, M.R., Udayakumar, M., 2005. Oxygen isotope enrichment (Δ18O) as a measure of time-averaged transpiration rate. Journal of Experimental Botany 56, 3033–3039. https://doi.org/10.1093/jxb/eri300

Shikangalah, R., Mapani, B., Mapaure, I., Herzschuh, U., Musimba, A., Tabares, X., 2020. Growth ring formation of Dichrostachys cinerea and Senegalia mellifera in arid environments in Namibia. Dendrochronologia 59, 125661. https://doi.org/10.1016/j.dendro.2019.125661

Shikangalah, R.N., 2020. The 2019 drought in Namibia: An overview. Journal of Namibian Studies 27, 37–58.

Shikangalah, R.N., Mapani, B.S., 2021. Ephemeral river systems and their ecosystem provisions to the local populations: A review of the Huab and Ugab Rivers, Namibia. Int. Sci. Technol. J. Namibia Shikangalah & Mapani/ISTJN 2021 14, 46–62.

Shikangalah, R.N., Mapani, B.S., 2020. A review of bush encroachment in Namibia: From a problem to an opportunity? Journal of Rangeland Science 10, 251–266.

Sibanda, T., Nonner, J.C., Uhlenbrook, S., 2009. Comparison of groundwater recharge estimation methods for the semi-arid Nyamandhlovu area , Zimbabwe. Hydrogeology Journal 17, 1427–1441. https://doi.org/10.1007/s10040-009-0445-z

Singh, B.P., 2017. Original isotopic composition of water in precipitation by different methods. Applied Water Science 7, 3385–3390. https://doi.org/10.1007/s13201-016-0500-6

Singh, P.K., Chudasama, H., 2021. Pathways for climate change adaptations in arid and semi-arid regions. Journal of Cleaner Production 284.

Sophocleous, M., 2004. Groundwater - Volume I. EOLSS Publications.

Stafford, W., Birch, C., Etter, H., Blanchard, R., Mudavanhu, S., Angelstam, P., Blignaut, J., Ferreira, L., Marais, C., 2017. The economics of landscape restoration: Benefits of controlling bush encroachment and invasive plant species in South Africa and Namibia. Ecosystem Services 27, 193–202. https://doi.org/10.1016/j.ecoser.2016.11.021

Stephens, D.B., 1993. A Perspective on Diffuse Natural Recharge Mechanisms in Areas of Low Precipitation. Soil Science Society of America Journal 48, 40–48.

Stocker, T.F., Plattner, G.-K., 2014. Rethink IPCC reports. Nature 5–7.

Stone, A.E.C., Edmunds, W.M., 2016. Unsaturated zone hydrostratigraphies: A novel archive of past climates in dryland continental regions. Earth-Science Reviews 157, 121–144. https://doi.org/10.1016/j.earscirev.2016.03.007

Stone, A.E.C., Edmunds, W.M., 2012. Sand, salt and water in the Stampriet basin, Namibia: Calculating unsaturated zone (Kalahari dunefield) recharge using the chloride mass balance approach. Water SA 38, 367–378. https://doi.org/10.4314/wsa.v38i3.2

Subyani, A.M., 2004. Use of chloride-mass balance and environmental isotopes for evaluation of groundwater recharge in the alluvial aquifer, Wadi Tharad, western Saudi Arabia. Environmental Geology 741–749.

Taapopi, J., 2015. Application of the chloride mass balance method to determine groundwater recharge in the area of farm Ebenhaezer. University of Namibia.

Taylor, R.G., Scanlon, B., Döll, P., Rodell, M., Van Beek, R., Wada, Y., Longuevergne, L., Leblanc, M., Famiglietti, J.S., Edmunds, M., Konikow, L., Green, T.R., Chen, J., Taniguchi, M., Bierkens, M.F.P., Macdonald, A., Fan, Y., Maxwell, R.M., Yechieli, Y., Gurdak, J.J., Allen, D.M., Shamsudduha, M., Hiscock, K., Yeh, P.J.F., Holman, I., Treidel, H., 2013. Ground water and climate change. Nature Climate Change 3, 322–329. https://doi.org/10.1038/nclimate1744

Ting, C.S., Kerh, T., Liao, C.J., 1998. Estimation of groundwater recharge using the chloride mass-balance method, Pingtung Plain, Taiwan. Hydrogeology Journal 6, 282–292. https://doi.org/10.1007/s100400050151

Tögl, A.C., 2010. Global groundwater recharge : Evaluation of modeled results on the basis of independent estimates. Goethe-Universität, Frankfurt am Main.

Treut, H. Le, Somerville, R., Cubasch, U., Ding, Y., Mauritzen, C., Mokssit, A., Peterson, T., Prather, M., 2007. Historical Overview of Climate Change; The Physical Science Basis. Contribution of Working Group I to the Fourth Assessment Report of the Intergovernmental Panel on Climate Change. Climate Change 2007 2008, 94–127.

Uemura, R., Matsui, Y., Yoshimura, K., Motoyama, H., Yoshida, N., 2008. Evidence of deuterium excess in water vapor as an indicator of ocean surface conditions. Journal of Geophysical Research Atmospheres 113, 1–10.

https://doi.org/10.1029/2008JD010209

Uugulu, S., Wanke, H., 2021. Determination of local meteoric water lines along a precipitation gradient, Namibia. International science and technology journal of Namibia 14, 63–72.

Uugulu, S., Wanke, H., 2020. Estimation of groundwater recharge in savannah aquifers along a precipitation gradient using chloride mass balance method and environmental isotopes, Namibia. Physics and Chemistry of the Earth 116, 102844. https://doi.org/10.1016/j.pce.2020.102844

Van Auken, O.W., 2009. Causes and consequences of woody plant encroachment into western North American grasslands. Journal of Environmental Management 90, 2931–2942. https://doi.org/10.1016/j.jenvman.2009.04.023

Van Vuuren, O., 2011. Groundwater. A Namibian perspective.

van Wyk, E., van Tonder, G., Vermeulen, D., 2012. Characteristics of local groundwater recharge cycles in South African semi-arid hard rock terrains: Rainfall-groundwater interaction. Water SA 38, 747–754. https://doi.org/10.4314/wsa.v38i5.14

Verhagen, B.T., Mazor, E., Sellschop, J.P.F., 1974. Radiocarbon and tritium evidence for direct rain recharge to ground waters in the northern Kalahari. Nature 249 (5458), 643–644. https://doi.org/https://doi.org/10.1038/249643a0

Vogel, J.C., Van Urk, H., 1975. Isotopic composition of groundwater in semi-arid regions of southern Africa. Journal of Hydrology 23–36.

von Freyberg, J., Allen, S.T., Grossiord, C., Dawson, T.E., 2020. Plant and root-zone water isotopes are difficult to measure, explain, and predict: Some practical recommendations for determining plant water sources. Methods in Ecology and Evolution 11, 1352–1367. https://doi.org/10.1111/2041-210X.13461

Vörösmarty, C.J., McIntyre, P.B., Gessner, M.O., Dudgeon, D., Prusevich, A., Green, P., Glidden, S., Bunn, S.E., Sullivan, C.A., Liermann, C.R., Davies, P.M., 2010. Global threats to human water security and river biodiversity. Nature 467, 555–561. https://doi.org/10.1038/nature09440

Walker, C.D., Richardson, S.B., 1991. The use of stable isotopes of water in characterising the source of water in vegetation. Chemical Geology: Isotope Geoscience Section 94, 145–158. https://doi.org/10.1016/0168-9622(91)90007-j

Walter, H., 1939. Grasland, Savanne und Busch der arideren Teile Afrikas in ihrer ökologischen Bedingtheit.

Wang, S., Zhang, M., Hughes, C.E., Zhu, X., Dong, L., Ren, Z., Chen, F., 2016. Factors controlling stable isotope composition of precipitation in arid conditions: An observation network in the Tianshan Mountains, central Asia. Tellus, Series B: Chemical and Physical Meteorology 68. https://doi.org/10.3402/tellusb.v68.26206

Wang, X.F., Yakir, D., 2000. Using stable isotopes of water in evapotranspiration studies. Hydrological Processes 14, 1407–1421. https://doi.org/10.1002/1099-1085(20000615)14:8<1407::AID-HYP992>3.0.CO;2-K

Wanke, H., 2005. Abschätzung der Grundwasserneubildung in Namibia mittels der Chlorid-Bilanz-Methode: Ist die trockene Deposition vernachlässigbar? Hydrogeology und Umwelt 33, 1–14.

Wanke, H., Beyer, M., Hipondoka, M., Hamutoko, J., Gaj, M., Koeniger, P., Himmelsbach, T., 2018a. The long road to sustainability: integrated water quality and quantity assessments in the Cuvelai-Etosha Basin, Namibia. In: Climate change and adaptive land management in southern Africa – assessments, changes, challenges, and solutions, in: Revermann, R., Krewenka, K.M., Schmiedel, U., Olwoch, J.M., Helmschrot, J., Jürgens, N. (Eds.), Biodiversity & Ecology. Klaus Hess Publishers, Göttingen & Windhoek, pp. 75–83. https://doi.org/10.7809/b-e.00307

Wanke, H., Dünkeloh, A., Udluft, P., 2008. Groundwater recharge assessment for the Kalahari catchment of north-eastern Namibia and north-western Botswana with a regional-scale water balance model. Water Resources Management 22, 1143–1158. https://doi.org/10.1007/s11269-007-9217-5

Wanke, H., Dünkeloh, A., Udluft, P., Wanke, A., 2013. A distributed water balance model to estimate direct groundwater recharge : A case study from the Nhoma and. Int. Sci. Technol. J. Namibia ISTJN 2, 11–32.

Wanke, H., Gaj, M., Beyer, M., Koeniger, P., Hamutoko, J.T., 2018b. Stable isotope signatures of meteoric water in the Cuvelai-Etosha Basin, Namibia: Seasonal characteristics, trends and relations to southern African patterns. Isotopes in Environmental and Health Studies 54, 588–607. https://doi.org/10.1080/10256016.2018.1505724

Wanke, H., Nakwafila, A., Hamutoko, J.T., Lohe, C., Neumbo, F., Petrus, I., David, A., Beukes, H., Masule, N., Quinger, M., 2014. Hand dug wells in Namibia: An underestimated water source or a threat to human health? Physics and Chemistry of the Earth 76–78, 104–113.

https://doi.org/10.1016/j.pce.2015.01.004

White, J.W.C., Cook, E.R., Lawrence, J.R., Wallace S., B., 1985. The D H ratios of sap in trees: Implications for water sources and tree ring D H ratios. Geochimica et Cosmochimica Acta 49, 237–246. https://doi.org/10.1016/0016-7037(85)90207-8

Wood, W.W., 1999. Use and Misuse of the Chloride-Mass Balance Method in Estimating Ground Water Recharge. Ground water. https://doi.org/https://doi.org/10.1111/j.1745-6584.1999.tb00949.x

Wrabel, J., 1999. Ermittlung der Grundwasserneubildung im semiariden Bereich Namibias mittels der Chlorid-Bilanz-Methode. Universität Würzburg.

Yeh, H.F., Lin, H.I., Lee, C.H., Hsu, K.C., Wu, C.S., 2014. Identifying seasonal groundwater recharge using environmental stable isotopes. Water (Switzerland) 6, 2849–2861. https://doi.org/10.3390/w6102849

Zarch, M.A., Sivakumar, B., Ashish, S., 2015. Assessment of global aridity change. Journal of Hydrology 520, 300–313.

Zencich, S.J., Froend, R.H., Turner, J. V., Gailitis, V., 2002. Influence of groundwater depth on the seasonal sources of water accessed by Banksia tree species on a shallow, sandy coastal aquifer. Oecologia 131, 8–19. https://doi.org/10.1007/s00442-001-0855-7

APPENDICES

APPENDIX 1: Ethical clearance

UNAM
UNIVERSITY OF NAMIBIA

ETHICAL CLEARANCE CERTIFICATE

Ethical Clearance Reference Number: FOS/164/2017 **Date: 28 March, 2017**

This Ethical Clearance Certificate is issued by the University of Namibia Research Ethics Committee (UREC) in accordance with the University of Namibia's Research Ethics Policy and Guidelines. Ethical approval is given in respect of undertakings contained in the Research Project outlined below. This Certificate is issued on the recommendations of the ethical evaluation done by the Faculty/Centre/Campus Research & Publications Committee sitting with the Postgraduate Studies Committee.

Title of Project: Estimation of Groundwater recharge Along the Precipitation Gradient for Savanna Aquifers In Namibia

Nature/Level of Project: Doctorate

Researcher: S. Uugulu

Student Number: 200326244

Faculty: Faculty of Science

Supervisors: Dr Heike Wanke (Main) Dr Paul Koeniger (Co)

Take note of the following:

(a) Any significant changes in the conditions or undertakings outlined in the approved Proposal must be communicated to the UREC. An application to make amendments may be necessary.

(b) Any breaches of ethical undertakings or practices that have an impact on ethical conduct of the research must be reported to the UREC.

(c) The Principal Researcher must report issues of ethical compliance to the UREC (through the Chairperson of the Faculty/Centre/Campus Research & Publications Committee) at the end of the Project or as may be requested by UREC.

(d) The UREC retains the right to:

(i) Withdraw or amend this Ethical Clearance if any unethical practices (as outlined in the Research Ethics Policy) have been detected or suspected,

(ii) Request for an ethical compliance report at any point during the course of the research.

UREC wishes you the best in your research.

Prof. P. Odonkor: UREC Chairperson

Ms. P. Claassen: UREC Secretary

APPENDIX 2: Research/Collecting permit

MINISTRY OF ENVIRONMENT AND TOURISM

RESEARCH/COLLECTING PERMIT

Permit Number 2112/2016
Valid from 1 January 2016 to 31 December 2016

Permission is hereby granted in terms of the Nature Conservation Ordinance 1975 (Ord. 4 of 1975) to:

Name: **Dr. K. Geissler**
Address: **University of Potsdam**
Maulbeerallee 3
Potsdam
14469
Germany
Coworkers: **I. Mapaure, B. Mapani, D. Lohmannn, A. Marquart, H. Wanke, C. Nesongano, K. Tielborgen, F. Kakombe, C. Nesongano, D. Joubert, M. Hauptfleisch, N. Blaum, A. Marquart, S. Uugulu and R. Ihula**

To conduct a study on OPTIMASS Subproject 1 and Subproject 2(a): Ecohydrological feedback analyses and establishment constraints of vegetation-environmental feedbacks at farms Kizikus, Etameko, Tsumore, Seismic station, Hoba meteorite and Waterberg P.P., subject to attached conditions.

IMPORTANT: This permit is not valid if altered in any way.

MINISTRY OF ENVIRONMENT AND TOURISM
REPUBLIC OF NAMIBIA
06 JAN 2016
WINDHOEK
Private Bag 13306, Windhoek
Tel: 2842111 • Fax: 258861

Authorising Officer

IMPORTANT
This permit is subject to the provisions of the Nature Conservation Ordinance, 1975 (Ordinance 4 of 1975) and the regulations promulgated thereunder, and the holder is subject to all such conditions and regulations.

Enquiries: Conservation Scientist, email imatheus@met.na Private Bag 13306, Windhoek, Namibia

MINISTRY OF ENVIRONMENT AND TOURISM

RESEARCH/COLLECTING PERMIT

Permit Number 2227/2016
Valid from 1 January 2017 to 31 December 2017

Permission is hereby granted in terms of the Nature Conservation Ordinance 1975 (Ord. 4 of 1975) to:

Name: **Dr. K. Geissler**
Address: **University of Potsdam**
Maulbeerallee 3
Potsdam
14469
Germany
Coworkers: **I. Mapaure, B. Mapani, D. Lohmannn, A. Marquart, H. Wanke, C. Nesongano, K. Tielborgen, F. Kakombe, N. Blaum, M. Hauptfleisch, D. Joubert, R. Ihul and S. Uugulu**

Ecohydrological feedback analyses and establishment constraints of vegetation-environmental feedbacks at farms Kizikus, Etameko, Tsumore, Seismic station. Hoba meteorite and Waterberg P.P. (OPTIMASS Subproject 1 and Subproject 2(a)). subject to attached conditions.

IMPORTANT: This permit is not valid if altered in any way.

20 DEC 2016
Private Bag 13306, Windhoek
Tel: 2842111 • Fax: 258861

Authorising Officer

IMPORTANT
This permit is subject to the provisions of the Nature Conservation Ordinance, 1975 (Ordinance 4 of 1975) and the regulations promulgated thereunder, and the holder is subject to all such conditions and regulations.

Enquiries: Conservation Scientist, email ita.matheus@met.gov.na
Private Bag 13306, Windhoek, Namibia

APPENDIX 3: Field work and laboratory work pictures.

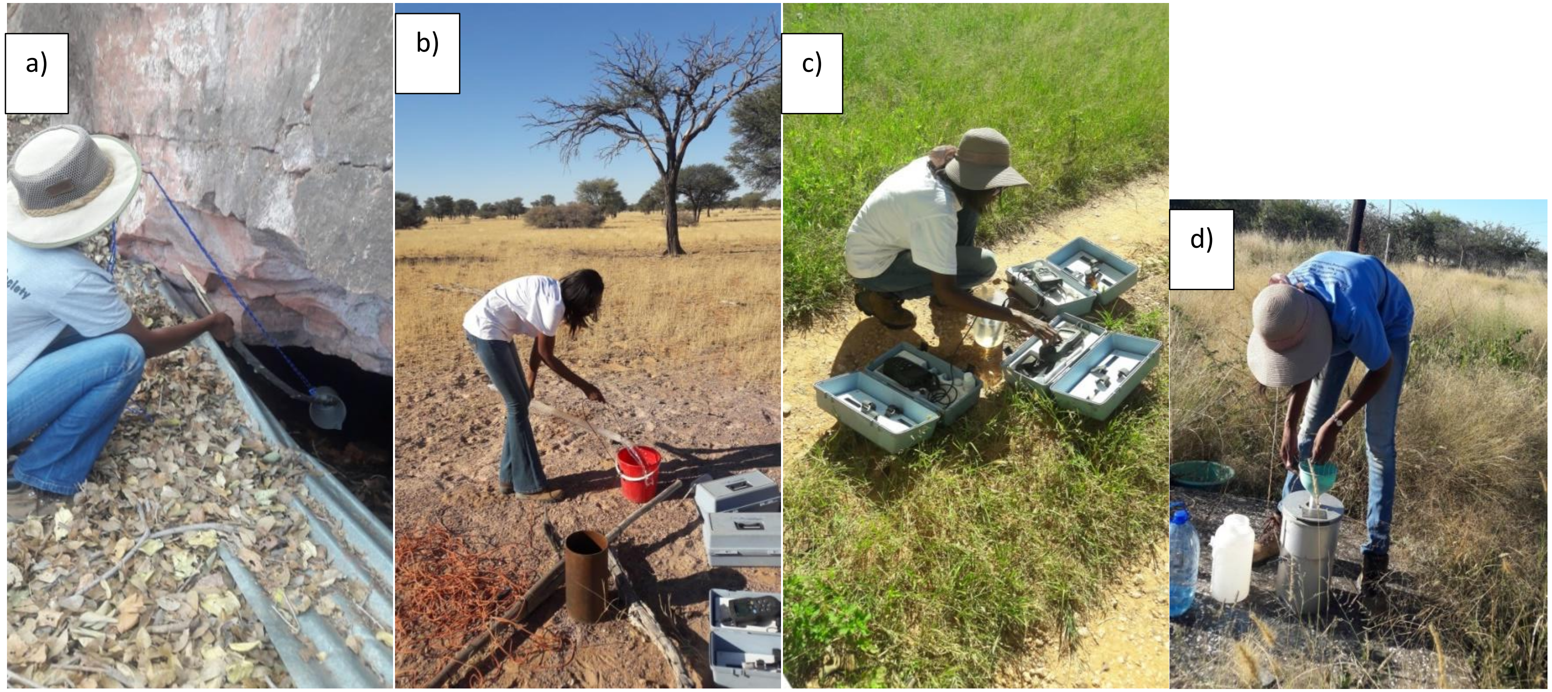

The pictures from a-e show work done both in the field and in the laboratory for Chapter 4.

a) Sampling of groundwater from a spring at Waterberg.
b) Sampling of groundwater from one of the boreholes in Ebenhaezer farm.
c) Measuring of groundwater onsite parameters such as pH, redox potential, electrical conductivity and temperature.
d) Collection of monthly precipitation.
e) Measuring chloride content in groundwater and rainwater at UNAM hydro-lab.

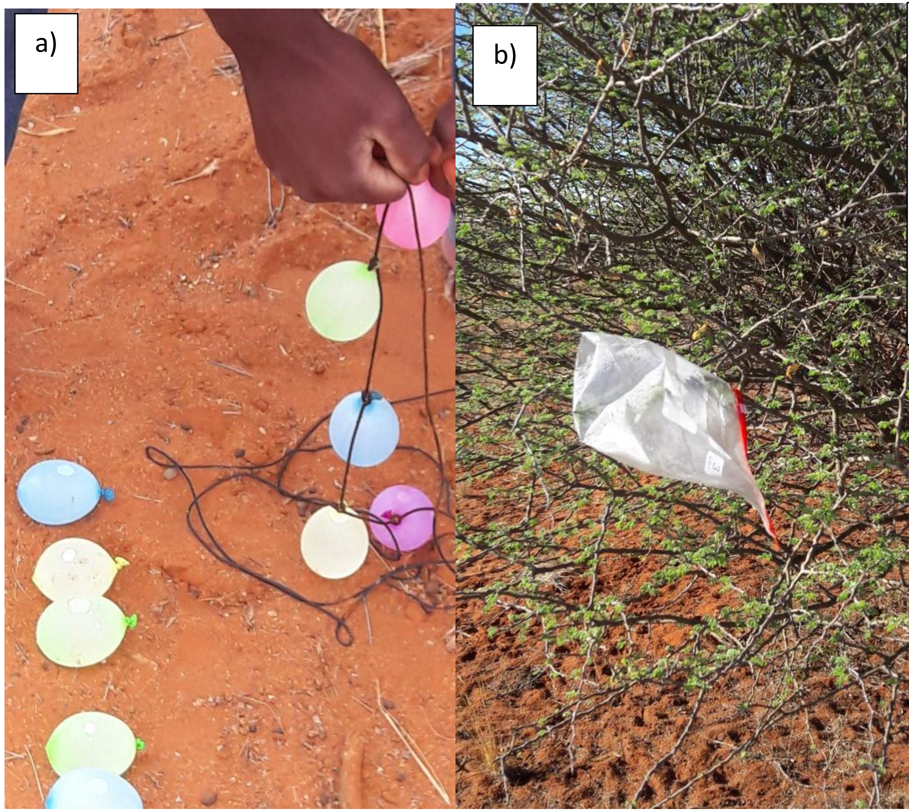

The pictures show some part of field work done at Ebenhaezer farm for Chapter 5.

a) A deuterium tracer was filled in small balloons tied together and inserted to the target depth.
b) A bag collecting transpired water from *S. mellifera* leaves.
c) Xylem sampling from *S. mellifera*.

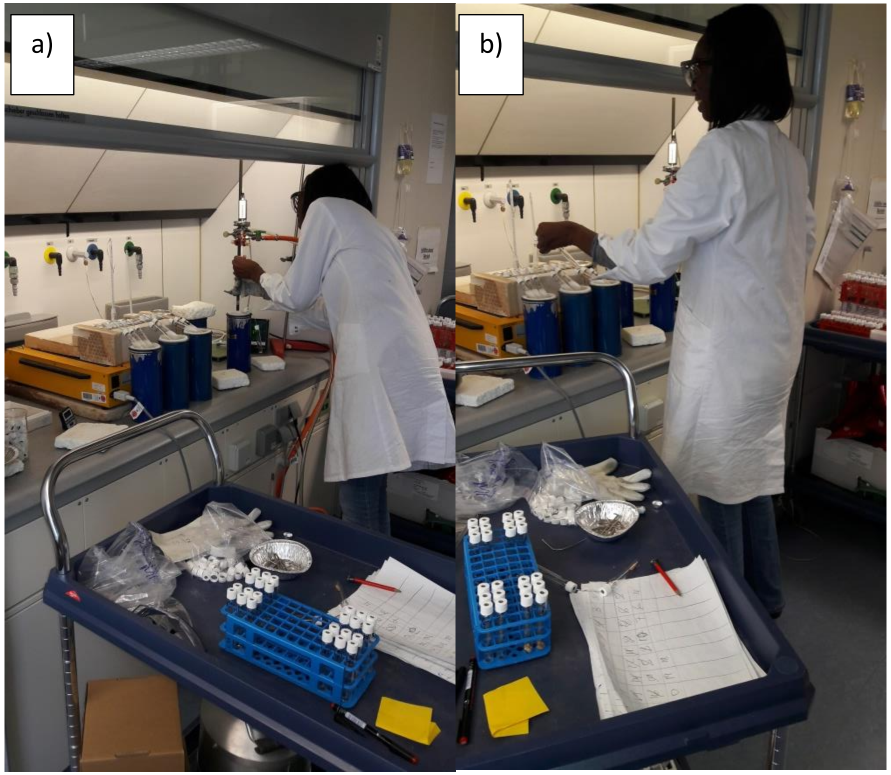

The pictures show laboratory work done at BGR Lab in Hannover. Xylem and soil water were extracted using a cryogenic vacuum extraction method.

a) A sample is being placed on a sucking station to ensure vacuum before extraction.
b) Monitoring the extraction process.

APPENDIX 4: Precipitation data used in Chapter 3.

Site	Date	P. amount [mm]	$\delta^{18}O$		SD	$\delta^{2}H$		SD	d-excess
Kuzikus/Ebenhaezer	14/04/14	65	-12.54	-815.15	0.34	-79.8	-5185.6	0.7	20.55
Kuzikus/Ebenhaezer	5&6-Apr-14	3	2.42	7.27	0.58	33.7	101.2	1.5	14.34
Kuzikus/Ebenhaezer	24/03/14	13	-4.21	-54.70	0.07	-22.5	-292.3	1.0	11.17
Kuzikus/Ebenhaezer	17/12/14	28	-3.38	-94.72	0.10	-12.1	-338.9	0.5	14.96
Kuzikus/Ebenhaezer	07/12/14	18	-2.31	-41.51	0.05	-5.4	-97.4	0.3	13.04
Kuzikus/Ebenhaezer	07/12/14	15	-2.21	-33.15	0.10	-5.7	-85.8	0.3	11.96
Kuzikus/Ebenhaezer	14/12/14	12	-3.35	-40.22	0.16	-10.7	-128.9	1.7	16.08
Kuzikus/Ebenhaezer	17/12/14	17	-4.02	-68.39	0.09	-14.0	-238.4	1.4	18.16
Kuzikus/Ebenhaezer	14/12/14	12	-3.34	-40.12	0.10	-10.5	-125.8	0.5	16.26
Kuzikus/Ebenhaezer	06/10/14	25	-1.85	-46.30	0.10	1.7	41.4	0.4	16.47
Kuzikus/Ebenhaezer	06/10/14	25	-1.58	-39.61	0.03	5.0	125.8	0.5	17.71
Kuzikus/Ebenhaezer	06/10/14	25	-1.65	-41.21	0.03	5.1	127.0	0.3	18.27
Kuzikus/Ebenhaezer	02/11/14	3.3	3.35	11.06	0.07	40.7	134.4	0.3	13.92
Kuzikus/Ebenhaezer	02/11/14	3	4.75	14.25	0.05	47.8	143.3	0.1	9.75
Kuzikus/Ebenhaezer	10/11/14	22	-1.58	-34.70	0.13	1.3	29.5	0.3	13.96

Kuzikus/Ebenhaezer	10/11/14	21	-1.22	-25.62	0.09	4.7	98.2	0.1	14.43
Kuzikus/Ebenhaezer	16/12/14	16.8	-4.92	-82.66	0.06	-20.4	-342.7	0.5	18.97
Kuzikus/Ebenhaezer	12/01/15	10	1.63	16.33	0.10	20.1	201.3	0.7	7.07
Kuzikus/Ebenhaezer	13/01/15	0.5	1.94	0.97	0.16	29.0	14.5	1.2	13.42
Kuzikus/Ebenhaezer	14/01/15	1	3.43	3.43	0.21	27.1	27.1	0.6	-0.35
Kuzikus/Ebenhaezer	25&26-Jan-15	10.5	1.43	15.06	0.04	31.1	326.8	0.4	19.66
Kuzikus/Ebenhaezer	23/03/15	3	1.84	5.51	0.12	16.4	49.2	0.5	1.68
Kuzikus/Ebenhaezer	11/04/15	35	-6.27	-219.51	0.07	-39.0	-1365.1	0.9	11.17
Kuzikus/Ebenhaezer	02/04/15	55	-11.10	-610.42	0.19	-82.5	-4538.3	0.8	6.27
Kuzikus/Ebenhaezer	01/04/15	23	-5.51	-126.77	0.30	-33.6	-771.9	1.9	10.53
Kuzikus/Ebenhaezer	24/03/15	12	-0.63	-7.53	0.15	3.5	42.2	0.6	8.54
Kuzikus/Ebenhaezer	21/03/15	3	1.97	5.90	0.06	26.7	80.0	0.2	10.93
Kuzikus/Ebenhaezer	06/12/14	19	-4.58	-86.93	0.04	-28.1	-534.7	0.4	8.46
Kuzikus/Ebenhaezer	13/12/14	13	-2.37	-30.80	0.07	-6.6	-86.0	0.2	12.34
Kuzikus/Ebenhaezer	16/12/14	12	-4.30	-51.66	0.05	-19.8	-237.5	0.7	14.65
Waterberg	04/12/17	2	-2.23	-4.46	0.13	-17.5	-35.1	1.0	0.29
Waterberg	21/3/2018	17	-15.96	-271.39	0.13	-117.5	-1997.5	0.7	10.21
Waterberg	29/3/2018	10	-7.36	-73.56	0.04	-50.3	-502.6	1.0	8.58

Waterberg	20/3/2018	17	-11.84	-201.21	0.11	-81.8	-1390.8	0.6	12.88
Waterberg	04/07/18	3	-6.25	-18.75	0.09	-48.0	-144.1	1.2	1.95
Waterberg	17/4/2018	6	-6.41	-38.49	0.13	-35.6	-213.8	0.5	15.69
Waterberg	19/3/2018	12	-9.78	-117.33	0.15	-80.5	-966.5	0.9	-2.32
Waterberg	16/04/2018	8	-9.71	-77.69	0.05	-63.6	-508.7	0.5	14.10
Waterberg	12/08/17	13	3.15	40.90	0.04	27.3	355.5	0.3	2.18
Waterberg	19/01/2018	3.6	2.09	7.53	0.09	20.9	75.3	0.7	4.17
Waterberg	23/11/2017	4	-2.44	-9.74	0.04	-8.6	-34.4	0.9	10.88
Waterberg	11/01/17	5	-1.77	-8.83	0.03	-7.0	-35.0	0.8	7.13
Waterberg	02/02/18	2	4.46	8.92	0.10	31.8	63.5	0.4	-3.93
Waterberg	28/01/2018	25	-0.62	-15.38	0.09	8.2	205.1	0.7	13.12
Waterberg	22/2/2018	4	-6.65	-26.61	0.22	-39.9	-159.6	0.3	13.31
Waterberg	17/12/2017	2.3	-3.27	-7.52	0.09	-21.6	-49.8	0.5	4.52
Waterberg	12/05/17	7	-8.24	-57.67	0.12	-52.4	-367.1	0.6	13.47
Waterberg	02/07/18	0.2	-7.51	-1.50	0.05	-47.8	-9.6	0.2	12.21
Waterberg	26/2/2018	3	1.07	3.21	0.11	-0.9	-2.7	0.6	-9.46
Waterberg	17/3/2018	4	-7.58	-30.34	0.11	-51.3	-205.1	0.7	9.39
Waterberg	16/01/18	6.5	-1.00	-6.52	0.05	3.5	23.0	1.3	11.56

Waterberg	04/02/18	12	-4.37	-52.47	0.06	-23.0	-275.7	1.2	12.01
Waterberg	02/04/18	12	-4.71	-56.57	0.10	-22.0	-264.4	0.7	15.68
Waterberg	04/03/18	12	-2.39	-28.71	0.13	-4.5	-53.9	0.7	14.65
Waterberg	11/10/18	1	-9.96	-9.96	0.04	-66.8	-66.8	0.6	12.86
Waterberg	02/03/18	9	-2.95	-26.59	0.16	-3.3	-29.7	0.8	20.33
Waterberg	04/04/18	8	-2.37	-18.96	0.19	-4.6	-36.8	1.3	14.37
Waterberg	15/1/18	1	5.06	5.06	0.21	40.6	40.6	1.0	0.12
Waterberg	03/07/18	30	-8.44	-253.17	0.12	-55.1	-1652.4	0.6	12.43
Waterberg	03/01/18	2	-2.70	-5.40	0.14	-19.2	-38.3	1.0	2.43
Tsumeb	11/10/18	1.4	5.19	7.27	0.07	46.7	65.4	1.0	5.19
Tsumeb	12/04/17	3	-1.63	-4.89	0.08	-16.1	-48.2	1.2	-3.03
Tsumeb	28/10/17	1.8	4.17	7.50	0.12	30.6	55.0	1.0	-2.79
Tsumeb	16/2/18	19	-6.46	-122.79	0.12	-35.1	-667.1	0.6	16.59
Tsumeb	24/11/17	3	-0.03	-0.08	0.12	-4.5	-13.5	0.7	-4.27
Tsumeb	20/12/17	1	-5.94	-5.94	0.02	-45.8	-45.8	0.3	1.68
Tsumeb	24/1/18	7	1.31	9.18	0.16	22.4	157.1	1.6	11.95
Tsumeb	30/10/17	6	-3.30	-19.82	0.05	-21.4	-128.3	0.6	5.03
Tsumeb	02/10/18	14	-3.22	-45.11	0.12	-15.5	-217.1	0.6	10.27

Tsumeb	21/12/17	16	-8.74	-139.78	0.06	-55.8	-892.5	0.2	14.11
Tsumeb	30/1/18	8	-2.47	-19.73	0.08	-0.4	-2.9	0.3	19.37
Tsumeb	02/06/18	5	-9.08	-45.42	0.10	-73.3	-366.3	1.1	-0.60
Tsumeb	14/1/18	7	-1.82	-12.75	0.05	-7.3	-51.4	1.2	7.23
Tsumeb	12/07/17	12.5	-3.81	-47.57	0.15	-16.5	-205.8	1.0	13.98
Tsumeb	02/04/18	14	-4.69	-65.67	0.20	-27.4	-383.3	1.0	10.14
Tsumeb	11/01/17	20	-0.97	-19.36	0.09	2.6	52.8	0.7	10.39
Tsumeb	25/1/28	20	0.00	-0.08	0.07	7.9	157.7	0.7	7.92
Tsumeb	31/12/17	20	-7.77	-155.35	0.26	-59.4	-1187.5	0.3	2.77
Tsumeb	22/12/17	4	-8.62	-34.48	0.05	-61.1	-244.6	0.6	7.82
Tsumeb	03/02/18	12	-6.37	-76.50	0.11	-47.9	-574.3	0.4	3.14
Tsumeb	28/1/18	15	-1.44	-21.65	0.14	7.1	107.0	0.7	18.68

APPENDIX 5: Isotopic composition and chloride content of groundwater and precipitation Data used in Chapter 4.

Tsumeb

Tsumeb site	Date	Cl (mg/l)	$\delta^{18}O$	SD	δ2H	SD
Tsumeb BH1	Feb/March 2016	13	-9.73	0.23	-64.2	1.6
Tsumeb BH3	Feb/March 2016	29.8	-8.86	0.16	-56.7	0.7
Tsumeb BH5	Feb/March 2016	14.2	-9.94	0.14	-63.4	0.8
Tsumeb BH4	Feb/March 2016	19.4	-9.19	0.29	-64.5	0.3
Tsumeb BH7	Feb/March 2016	14.1	-9.44	0.05	-63.2	0.6
Oslean pos	01/03/2017		-6.27	0.27	-47.7	1.0
Tsumeb BH4	01/03/2017		-8.81	0.20	-64.6	0.9
Tsumeb BH5	01/03/2017		-9.36	0.01	-63.3	0.6
Tsumeb lake Otjikoto	01/03/2017		-7.26	0.16	-57.4	0.6
Tsumeb BH1	01/03/2017		-8.40	0.09	-61.1	0.2
Tsumeb BH2	01/03/2017		-8.76	0.08	-63.7	0.4
Tsumeb BH3	01/03/2017		-7.71	0.09	-60.4	0.5
Tsumeb BH3	01/07/2016		-7.92	0.16	-56.8	1.1
Tsumeb Lake Otjikoto	01/07/2016		-7.03	0.13	-55.1	0.6
Tsumeb BH1	01/07/2016		-8.62	0.12	-62.4	0.6
Tsumeb BH2	01/07/2016		-8.92	0.15	-64.2	1.2
Tsumeb BH5	01/07/2016		-8.61	0.07	-62.3	0.4
Tsumeb BH4	01/07/2016		-9.01	0.28	-64.0	1.2
Tsumeb Lake Otjikoto	01/05/2017		-6.99	0.15	-56.0	0.6
Tsumeb BH4	01/05/2017		-7.92	0.07	-59.8	0.4
Tsumeb BH3	01/05/2017		-7.99	0.11	-60.9	0.3

Tsumeb BH1	01/05/2017		-8.34	0.13	-61.1	0.7
Tsumeb BH5	01/05/2017		-8.69	0.16	-62.4	1.2
Tsumeb BH2	01/05/2017		-8.90	0.05	-64.4	0.7
Tsumeb Lake Otjikoto	Nov/Dec 2016		-5.35	0.14	-46.7	1.0
Tsumeb BH1	Nov/Dec 2016		-9.42	0.26	-64.2	0.5
Tsumeb BH2	Nov/Dec 2016		-9.84	0.09	-65.6	0.3
Tsumeb BH3	Nov/Dec 2016		-8.65	0.28	-59.1	1.2
Tsumeb BH4	Nov/Dec 2016		-9.59	0.21	-65.1	1.2
Tsumeb BH5	Nov/Dec 2016		-9.39	0.18	-65.0	1.1
Ebehaezer rain	April/May 2017		-1.96	0.17	-4.7	0.7
Ebenhaezer rain	10/03/2017		-10.28	0.20	-66.2	0.9
Ebenhaezer rain	Jan 2017		-6.83	0.11	-45.7	0.7
Ebenhaezer rain	Nov/Dec 2017		0.77	0.14	25.4	0.4
Ebenhaezer rain	Nov/Dec 2017		0.70	0.20	11.9	0.9
Ebenhaezer rain	Nov/Dec 2017		6.10	0.20	42.1	1.0
Waterberg rain	12/03/2017		-9.02	0.23	-59.3	2.0
Waterberg rain	March 2017		-5.38	0.12	-27.2	0.9
Waterberg rain	April 2017		-2.86	0.14	-3.6	0.3
Waterberg rain	May 2017		0.98	0.08	20.9	0.1
Waterberg rain	Nov/Dec 2017		-1.62	0.09	-5.6	1.2
Tsumeb rain	Jan 2017		-10.70	0.09	-72.7	0.7

Tsumeb rain	Feb 2017		-9.08	0.11	-59.5	0.8
Tsumeb rain	March/April 2017		-0.79	0.09	-3.5	0.6
Tsumeb rain	April/May 2017		-0.85	0.03	-4.6	0.7
Tsumeb rain	14/03/2017		-7.64	0.30	-48.5	1.5
Tsumeb rain	Nov/Dec 2016		-0.33	0.10	6.5	0.3

Waterberg

Waterberg site	**Date**	**Cl (mg/l)**	**$\delta^{18}O$**	**SD**	**δ2H**	**SD**
Okatjikona BH/spring	Feb/March 2016	10.9	-10.40	0.16	-66.5	0.3
Okatjikona spring	Feb/March 2016	11.5	-10.41	0.15	-67.0	0.4
Onyoka BH1	Feb/March 2016	10.4	-10.00	0.11	-65.6	0.6
Onyoka spring	Feb/March 2016	11.4	-10.18	0.09	-65.1	0.3
NWR Waterberg spring 1	Feb/March 2016	10.1	-10.85	0.13	-69.4	0.8
NWR Waterberg spring 2	Feb/March 2016	8.8	-10.82	0.18	-69.2	0.9
NWR spring	01/03/2017		-10.03	0.13	-70.7	1.2
Onyoka spring	01/03/2017		-9.27	0.07	-64.3	0.5
Okatjikona spring	01/03/2017		-10.18	0.08	-68.2	0.3
Okatjikona BH/spring	01/03/2017		-9.98	0.22	-66.5	1.0

Onyoka BH	01/03/2017		-9.78	0.28	-67.3	1.7
Kahengombe & sons stud	01/03/2017		-8.60	0.10	-61.2	1.2
Okatijikona spring	01/07/2016		-9.56	0.35	-65.0	1.4
NWR spring	01/07/2016		-9.60	0.16	-67.2	0.9
Onyoka BH	01/07/2016		-9.39	0.15	-65.6	0.7
Onyoka spring	01/07/2016		-9.27	0.06	-64.8	0.6
Okatjikona spring/BH	01/05/2017		-9.68	0.37	-66.4	1.3
Okatjokona BH/spring	01/05/2017		-9.48	0.05	-66.0	0.5
Okatjokona spring	01/05/2017		-9.46	0.06	-66.2	0.4
NWR spring	01/05/2017		-9.74	0.22	-69.7	1.1
Onyoka spring	01/05/2017		-8.99	0.09	-64.6	0.4
Onyoka BH	01/05/2017		-9.23	0.15	-66.2	0.4
Onyoka spring	Nov/Dec 2016		-9.90	0.29	-66.8	0.6
Onyoka BH	Nov/Dec 2016		-9.91	0.07	-67.7	0.9
NWR spring	Nov/Dec 2016		-10.26	0.15	-69.9	0.4
Okatjikona BH/spring	Nov/Dec 2016		-9.67	0.16	-65.2	0.4
Okatjikona spring	Nov/Dec 2016		-10.04	0.13	-67.1	0.9

Ebehaezer rain	April/May 2017		-1.96	0.17	-4.7	0.7
Ebenhaezer rain	10/03/2017		-10.28	0.20	-66.2	0.9
Ebenhaezer rain	Jan 2017		-6.83	0.11	-45.7	0.7
Ebenhaezer rain	Nov/Dec 2017		0.77	0.14	25.4	0.4
Ebenhaezer rain	Nov/Dec 2017		0.70	0.20	11.9	0.9
Ebenhaezer rain	Nov/Dec 2017		6.10	0.20	42.1	1.0
Waterberg rain	12/03/2017		-9.02	0.23	-59.3	2.0
Waterberg rain	March 2017		-5.38	0.12	-27.2	0.9
Waterberg rain	April 2017		-2.86	0.14	-3.6	0.3
Waterberg rain	May 2017		0.98	0.08	20.9	0.1
Waterberg rain	Nov/Dec 2017		-1.62	0.09	-5.6	1.2
Tsumeb rain	Jan 2017		-10.70	0.09	-72.7	0.7
Tsumeb rain	Feb 2017		-9.08	0.11	-59.5	0.8
Tsumeb rain	March/April 2017		-0.79	0.09	-3.5	0.6
Tsumeb rain	April/May 2017		-0.85	0.03	-4.6	0.7
Tsumeb rain	14/03/2017		-7.64	0.30	-48.5	1.5
Tsumeb rain	Nov/Dec 2016		-0.33	0.10	6.5	0.3

Kuzikus/Ebenhaezer

Kuzikus/Ebenhaezer site	**Date**	**Cl (mg/l)**	**$\delta^{18}O$**	**SD**	**$\delta^{2}H$**	**SD**
SUE02-01	14/03/2015		-6.87	0.11	-51.4	0.3
SUE02-02	14/03/2015		-7.23	0.39	-52.5	0.2
SUE02-03	14/03/2015		-7.10	0.08	-53.2	0.3
SUE02-04	14/03/2015		-6.49	0.15	-50.1	0.3
SUE02-05	14/03/2015		-7.43	0.15	-53.8	0.3
SUE02-06	14/03/2015		-8.24	0.38	-54.2	0.5
SUE02-07	14/03/2015		-6.72	0.09	-50.8	0.4
SUE02-08	14/03/2015		-7.25	0.52	-51.0	0.5
Kuzikus Farmouse 80 m	25/02/2016	29.6	-6.92	0.10	-51.6	0.6
Kuzikus Farmouse 40 m	25/02/2016	47.6	-6.71	0.10	-50.9	1.0
Kuzikus Farmouse Windmotor	25/02/2016	42.2	-6.87	0.16	-51.3	0.3
Schakal	25/02/2016	71.4	-7.34	0.06	-54.4	0.6
Fohlen 1	25/02/2016	24	-7.13	0.13	-53.3	0.8
Fohlen 2	25/02/2016	40	-4.26	0.08	-39.5	0.5
Geier	25/02/2016	63.4	-7.33	0.15	-54.1	0.4
SUE05-2	25/02/2016	27.1	-7.31	0.09	-53.9	0.6
SUE05-7	25/02/2016	19	-7.30	0.09	-54.1	0.1
SUE05-10	25/02/2016	26.7	-7.42	0.04	-54.0	0.2
SUE05-1	01/03/2016	32.1	-7.09	0.14	-53.0	0.6
SUE05-3	01/03/2016	21.7	-7.59	0.11	-53.6	0.5
SUE05-4	01/03/2016	15	-6.72	0.14	-50.2	0.7
SUE05-5	01/03/2016	14.8	-7.45	0.10	-54.5	0.3
SUE05-6	01/03/2016	16	-7.63	0.22	-57.1	0.9
SUE05-8	01/03/2016	13	-7.07	0.22	-53.9	0.6
Oslean pos	01/03/2017		-6.27	0.27	-47.7	1.0

Rosinki	01/03/2017		-5.05	0.30	-43.2	1.0
Fohlen2	01/03/2017		-7.38	0.28	-53.6	1.3
Schakal	01/03/2017		-7.33	0.13	-53.9	0.5
Kuzikus Framhouse deep	01/03/2017		-6.94	0.08	-49.8	0.8
Geier	01/03/2017		-7.39	0.11	-53.3	0.4
SUE08-10	01/03/2017		-7.19	0.10	-52.5	0.8
SUE08-5	01/03/2017		-7.53	0.16	-53.8	0.8
SUE08-4	01/03/2017		-6.70	0.18	-50.1	0.7
SUE08-2	01/03/2017		-7.36	0.17	-53.2	1.0
SUE08-1	01/03/2017		-7.22	0.05	-52.2	0.3
Fohlen2	01/03/2017		-7.06	0.11	-53.2	0.4
Gemsbock	01/03/2017		-7.25	0.06	-52.3	1.1
Solarpumpe	01/03/2017		-1.56	0.21	-22.7	0.5
Flugfeld	01/03/2017		-4.94	0.26	-40.5	0.9
Wachtel	01/03/2017		-6.29	0.15	-48.5	0.3
SUE09-1	01/05/2017		-6.72	0.13	-52.1	0.8
SUE09-2	01/05/2017		-6.68	0.10	-51.8	0.7
SUE09-3	01/05/2017		-6.79	0.09	-52.8	0.3
SUE09-4	01/05/2017		-6.32	0.07	-49.7	0.6
SUE09-5	01/05/2017		-7.00	0.19	-53.5	0.4
SUE09-9	01/05/2017		-6.80	0.19	-51.8	0.8
SUE03-01	April/May15		-6.74	0.15	-53.6	0.3
SUE03-02	April/May15		-6.92	0.10	-55.6	0.2
SUE03-03	April/May15		-7.11	0.09	-56.6	0.2
SUE03-04	April/May15		-6.25	0.12	-52.8	0.5
SUE03-05	April/May15		-7.17	0.10	-57.4	0.6
SUE03-06	April/May15		-7.50	0.08	-59.0	0.7

SUE03-07	April/May15		-6.69	0.12	-55.5	0.5
SUE03-08	April/May15		-6.72	0.08	-55.8	1.0
SUE03-09	April/May15		-6.52	0.14	-54.6	0.4
Kuzikus farmhouse	April/May15		-6.17	0.10	-52.7	0.8
SUE07-07	Nov/Dec 2016		-6.93	0.08	-51.8	0.3
SUE07-01	Nov/Dec 2016		-7.23	0.16	-52.7	0.5
Flugfeld	Nov/Dec 2016		-4.73	0.23	-41.8	1.3
Wachtel	Nov/Dec 2016		-6.24	0.24	-46.0	1.5
Schakal	Nov/Dec 2016		-6.95	0.10	-50.8	0.6
Fohlen2	Nov/Dec 2016		-7.03	0.07	-51.2	0.9
Ochsen	Nov/Dec 2016		-6.47	0.06	-48.6	1.0
Solarpumpe	Nov/Dec 2016		-6.55	0.16	-48.8	0.9
Kuzikus Farmhaus shallow	Nov/Dec 2016		-6.37	0.12	-47.6	1.1
Rosinki	Nov/Dec 2016		-4.96	0.14	-41.9	1.2
Geier	Nov/Dec 2016		-7.02	0.25	-52.3	1.1
Fohlen1	Nov/Dec 2016		-6.95	0.15	-51.0	1.2
Gemsbock	Nov/Dec 2016		-6.90	0.19	-50.8	1.3
Kuzikus Farmhaus deep	Nov/Dec 2016		-6.57	0.14	-48.7	1.6
SUE07-02	Nov/Dec 2016		-7.19	0.19	-52.6	0.6

SUE07-03	Nov/Dec 2016		-7.38	0.11	-53.5	0.5
SUE07-04	Nov/Dec 2016		-6.66	0.15	-50.0	0.4
SUE07-05	Nov/Dec 2016		-7.42	0.11	-54.2	0.7
SUE07-06	Nov/Dec 2016		-7.62	0.07	-55.0	0.4
SUE07-010B	Nov/Dec 2016		-7.19	0.21	-52.7	1.2
SUE07-08	Nov/Dec 2016		-7.16	0.13	-52.6	0.9
SUE07-02	Nov/Dec 2016		-7.06	0.14	-51.9	0.6
SUE07-03	Nov/Dec 2016		-7.22	0.13	-52.5	0.6
SUE07-04	Nov/Dec 2016		-6.62	0.09	-50.5	0.4
SUE07-05	Nov/Dec 2016		-7.51	0.12	-54.3	0.4
SUE07-06	Nov/Dec 2016		-7.84	0.09	-55.9	0.8
SUE07-010B	Nov/Dec 2016		-7.15	0.07	-52.1	0.6
SUE07-08	Nov/Dec 2016		-7.24	0.13	-52.5	0.7
Ebehaezer rain	April/May 2017		-1.96	0.17	-4.7	0.7
Ebenhaezer rain	01/03/2017		-10.28	0.20	-66.2	0.9
Ebenhaezer rain	Jan 2017		-6.83	0.11	-45.7	0.7
Ebenhaezer rain	Nov/Dec 2017		0.77	0.14	25.4	0.4
Ebenhaezer rain	Nov/Dec 2017		0.70	0.20	11.9	0.9

Ebenhaezer rain	Nov/Dec 2017		6.10	0.20	42.1	1.0
Waterberg rain	12/03/2017		-9.02	0.23	-59.3	2.0
Waterberg rain	March 2017		-5.38	0.12	-27.2	0.9
Waterberg rain	April 2017		-2.86	0.14	-3.6	0.3
Waterberg rain	May 2017		0.98	0.08	20.9	0.1
Waterberg rain	Nov/Dec 2017		-1.62	0.09	-5.6	1.2
Tsumeb rain	Jan 2017		-10.70	0.09	-72.7	0.7
Tsumeb rain	Feb 2017		-9.08	0.11	-59.5	0.8
Tsumeb rain	March/April 2017		-0.79	0.09	-3.5	0.6
Tsumeb rain	April/May 2017		-0.85	0.03	-4.6	0.7
Tsumeb rain	14/03/2017		-7.64	0.30	-48.5	1.5
Tsumeb rain	Nov/Dec 2016		-0.33	0.10	6.5	0.3

APPENDIX 6: Estimated biometric parameters of the traced woody plants for Chapter 5

Plot name	**Selected woody plants**	**Trunk diameter**	**Crown diameter (m)**	**Height (m)**	**Distance from the injected holes to the traced woody plants**
1	*S. mellifera*	25 cm (7 branches)	5	2.5	10
	B. albitrunca	1.6 m	1.33	5	8
2	*S. mellifera*	32 cm (3 branches)	5.5	3.5	2.3
	S. mellifera shrub	20 cm (4 branches)	2.4	2	2
	B. albitrunca	1.5 m	3.5	5.5	2.8
3	*S. mellifera*	33 cm (4	4	2.8	4.4

		branched)			
	S. mellifera	30 cm (5 branches)	3.5	3	3.14
	B. albitrunca	1.12 m	5	4	3.15
4	*S. mellifera*	23 cm (9 branches)	3.5	3	3.2
	B. albitrunca	1.1	5	4.5	2.4
5	*S. mellifera*	29 cm (6 branches)	5	3	3
	S. mellifera shrub	10 cm (3 branches)	1	1.1	0.5
	B. albitrunca	1.6	5	5.5	3.5
	B. albitrunca shrub	32 cm (2 branches)	1.5	2.5	1
6	*S. mellifera (small)*	39 cm (6 branches)	5.5	3	3
	S. mellifera (big)	50 cm (13 branches)	12	8	3.4

APPENDIX 7: The distance from the injected holes to the traced woody plants for Chapter 5

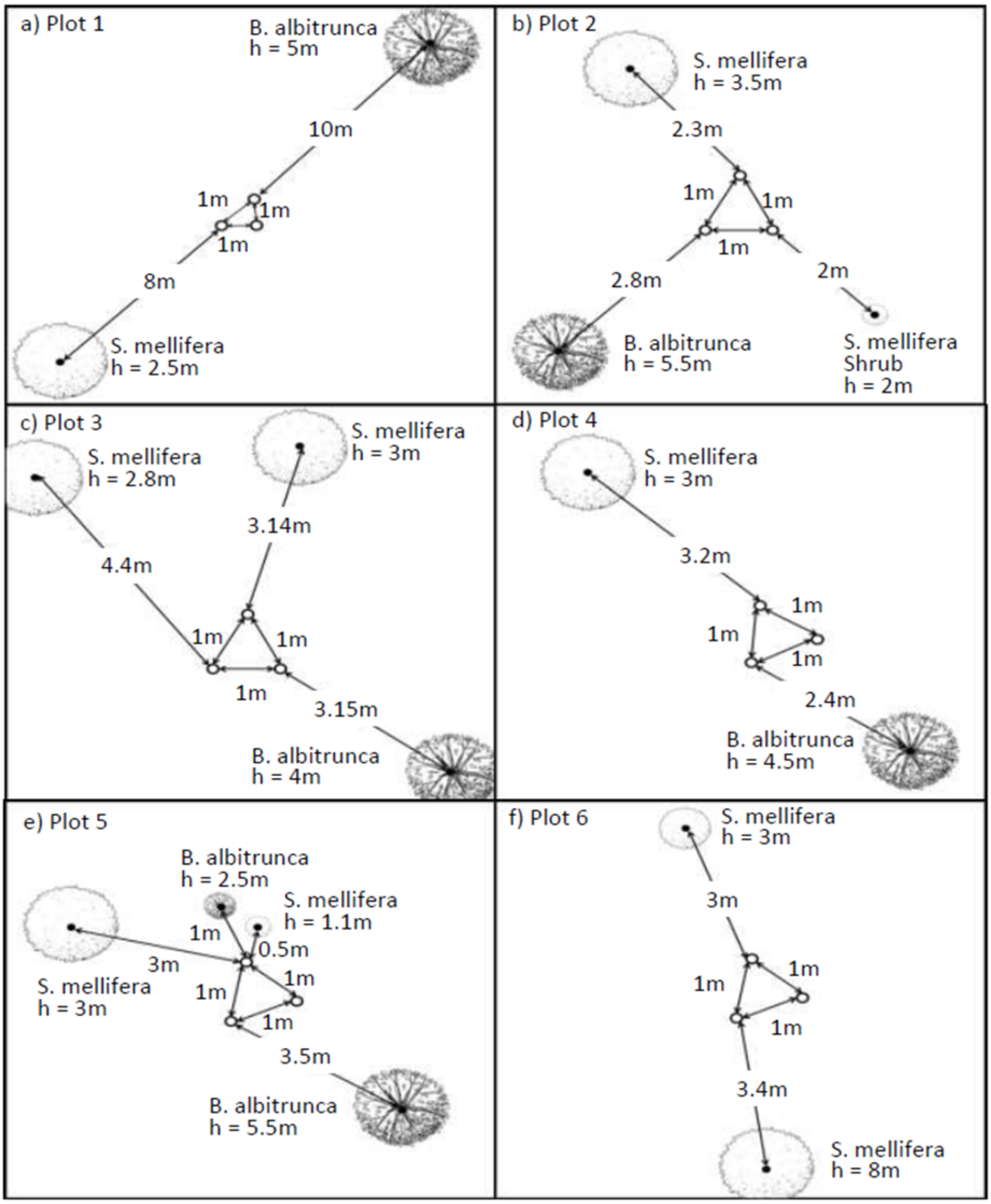

Appendix 8: Deuterium tracer data used in Chapter 5.

Transpired water

Sample ID	**δ^{18}O**	**SD**	**δ^{2}H**	**SD**
S. mellifera 5-1	-0.55	0.26	-16.3	1.5
S. mellifera 5-2	3.51	0.19	-0.7	0.8
S. mellifera 1-2	3.38	0.11	-5.4	0.9
S. mellifera 1-1	2.12	0.12	-4.6	1.0
S. mellifera 2-1	2.57	0.23	0.7	1.8
S. mellifera 3-1	5.96	0.10	14.6	0.6
B. albitrunca 3-2	0.79	0.25	-13.8	2.2
B. albitrunca 3-3	1.91	0.11	-7.1	0.2
B. albitrunca 3-4	7.29	0.60	-0.9	3.6
B. albitrunca 3-5	2.62	0.10	-15.1	0.8
B. albitrunca 3-6	-0.46	0.17	-17.2	0.6
B. albitrunca 3-7	1.15	0.14	-16.9	0.6
B. albitrunca 3-8	-0.05	0.07	-20.3	0.5
B. albitrunca 3-9	3.42	0.09	12.8	2.1
B. albitrunca 3-10	0.70	0.05	-15.9	1.5
S. mellifera 3-2	0.27	0.07	-17.7	1.0
S. mellifera plot5 10/12/16	2.33	0.46	-12.5	2.5
S. mellifera plot1 10/12/2016	2.12	0.96	-12.5	9.9
S. mellifera plot2 10/12/2016	2.28	0.06	-17.2	0.1
S. mellifera plot2 10/12/2016	2.24	0.16	-11.0	0.3
S. mellifera plot 2 10/12/2016	-17.63	13.91	515.9	237.0
S. mellifera plot3 10/12/2016	4.51	0.23	-4.3	0.7
S. mellifera plot3 drilled 10/12/2016	-0.96	0.18	-22.0	0.5
S. mellifera plot4 10/12/2016	1.68	0.14	-19.9	0.1
B. albitrunca plot1 10/12/2016	6.29	0.21	-7.7	0.8
B. albitrunca plot2 10/12/2016	8.62	0.16	11.4	0.8
B. albitrunca plot3 10/12/2016	4.57	0.09	-5.5	0.4
B. albitrunca plot1 10/12/2016	-1.86	0.07	-28.6	0.4
B. albitrunca plot5 10/12/2016	3.80	0.21	-10.7	1.1
S. mellifera plot1 11/12/2016	1.77	0.01	-13.3	0.6
S. mellifera plot1 2 11/12/2016	0.64	0.16	-17.5	1.2
S. mellifera plot2 shrub1 11/12/2016	-0.32	0.43	-16.3	7.8
S. mellifera plot2 shrub2 11/12/2016	4.67	0.33	14.1	1.6
S. mellifera plot1 3 11/12/2016	-0.12	0.17	-21.4	0.8
S. mellifera plot2 3 11/12/2016	2.26	0.06	-9.6	0.5
S. mellifera plot4 11/12/2016	0.53	0.11	-21.2	0.7
S. mellifera plot5 11/12/2016	1.27	0.26	-17.6	0.8
B. albitrunca plot1 11/12/2016	5.22	0.14	-6.1	0.8
B. albitrunca plot 2 11/12/2016	1.81	0.16	-14.3	0.3
B. albitrunca plot 3 11/12/2016	1.53	0.12	-17.3	0.7
B. albitrunca plot 4 11/12/2016	1.48	0.20	-17.0	1.3

B. albitrunca plot 5 11/12/2016	4.39	0.12	-9.6	0.8
S. mellifera plot 1 12/12/2-16	2.80	0.40	-12.1	1.6
S. mellifera 1 plot 2 12/12/2-16	1.26	0.13	-9.6	0.1
S. mellifera shrub1 plot 2 12/12/2-16	1.85	0.20	-6.0	0.9
S. mellifera shrub2 plot 2 12/12/2-16	-0.28	0.29	-19.3	0.6
S. mellifera 1 plot 3 12/12/2-16	0.73	0.27	-17.7	1.1
S. mellifera plot 3 12/12/2-16	3.78	0.37	-4.1	0.8
S. mellifera plot 4 12/12/2-16	1.12	0.15	-19.9	1.5
S. mellifera plot 5 12/12/2-16	3.34	0.17	-12.8	1.0
B. albitrunca plot 1 12/12/2016	0.92	0.13	-20.3	0.9
B. albitrunca 1 plot 4 12/12/2016	1.12	0.31	-14.4	1.3
B. albitrunca 1 plot 4 12/12/2016	2.52	0.18	-12.1	0.4
B. albitrunca plot 5 12/12/2016	1.89	0.14	-20.0	0.8
B. albitrunca shrub plot 5 12/12/2016	1.26	0.21	-19.9	1.1

Soil and Xylem water

Sample-ID	Vial-ID	Description	depth	comments	weight soil vial [g]	weight soil vial + soil wet [g]	weight soil vial + soil dry [g] After extraction	weight oven dry [g]	diff weight after extraction/oven dry [g]	water content after extraction [mass - fraction]	water content oven dry [mass-fraction]	Vial-ID	**d18O**	**s.d. d18O**	**d2H**	**s.d. d2H**
Plot 2-0.5	**SU1**	Ebenhaezer soil	0.5	Tracer inserted at 2.5 m	12.8899	25.3533	25.2143	25.207	-0.007	0.011	0.012	SU1	-3.72	0.06	-32.6	0.2
Plot 2-0.5	SU2	Ebenhaezer soil		**Tracer inserted at 2.5 m**	12.5896	24.2276	24.1077	24.0963	-0.011	0.010	0.011	SU2	-2.66	0.03	-29.9	0.3
Plot 2-0.5	SU3	Ebenhaezer soil		Tracer inserted at 2.5 m	12.7281	25.4354	25.3228	25.3075	-0.015	0.009	0.010	SU3	-2.34	0.05	-28.9	0.2
Plot 2-1	**SU4**	Ebenhaezer soil	**1**	**Tracer inserted at 2.5 m**	12.3821	24.0749	23.9246	23.9323	0.008	0.013	0.012	SU4	-2.99	0.05	1.8	0.2
Plot 2-1	SU5	Ebenhaezer soil		Tracer inserted at 2.5 m	12.3198	24.1733	23.9815	23.9716	-0.010	0.016	0.017	SU5	-2.31	0.05	4.5	0.1
Plot 2-1	SU6	Ebenhaezer soil		**Tracer inserted at 2.5 m**	12.8159	24.9603	24.8322	24.8359	0.004	0.011	0.010	SU6	-2.68	0.02	3.1	0.1
Plot 2-1.5	**SU7**	Ebenhaezer soil	1.5	Tracer inserted at 2.5 m	12.2799	24.0388	23.8775	23.8843	0.007	0.014	0.013	SU7	-3.17	0.07	974.6	1.7
Plot 2-1.5	SU8	Ebenhaezer soil		**Tracer inserted at 2.5 m**	12.637	24.8662	24.6883	24.6943	0.006	0.015	0.014	SU8	-3.54	0.05	963.8	2.6
Plot 2-1.5	SU9	Ebenhaezer soil		Tracer inserted at 2.5 m	12.2075	25.1335	24.992	24.9902	-0.002	0.011	0.011	SU9	-2.66	0.09	979.8	1.0
Plot 2-2	**SU10**	Ebenhaezer soil	**2**	**Tracer inserted at 2.5 m**	12.2915	25.3589	25.1737	25.1794	0.006	0.014	0.014	SU10	-1.38	0.10	8032.4	14.7
Plot 2-2	SU11	Ebenhaezer soil		Tracer inserted at 2.5 m	12.5676	24.327	24.1804	24.1844	0.004	0.012	0.012	SU11	-1.77	0.00	8131.4	33.7
Plot 2-2	SU12	Ebenhaezer soil		**Tracer inserted at 2.5 m**	12.2668	24.5236	24.3614	24.3649	0.003	0.013	0.013	SU12				
Plot 2-2.5	**SU13**	Ebenhaezer soil	2.5	Tracer inserted at 2.5 m	12.4692	25.0803	24.8998	24.9026	0.003	0.014	0.014	SU13	5.16	0.26	24602.5	15.1
Plot 2-2.5	SU14	Ebenhaeze		**Tracer**	12.501	25.162	24.9632	24.960	-0.003	0.016	0.016	SU14	4.16	0.22	24531.	82.6

		r soil		**inserted at 2.5 m**	7	7		5							3	
Plot 2-2.5	SU15	Ebenhaezer soil		Tracer inserted at 2.5 m	12.5229	24.8371	24.6596	24.6596	0.000	0.014	0.014	SU15	5.13	0.31	24823.9	35.7
Plot 2-3	**SU16**	Ebenhaezer soil	**3**	**Tracer inserted at 2.5 m**	12.4673	24.2671	24.0937	24.1008	0.007	0.015	0.014	SU16	1.89	0.03	14553.8	16.6
Plot 2-3	SU17	Ebenhaezer soil		Tracer inserted at 2.5 m	12.4864	24.2054	24.0466	24.0499	0.003	0.014	0.013	SU17	1.13	0.18	14624.7	35.0
Plot 2-3	SU18	Ebenhaezer soil		**Tracer inserted at 2.5 m**	12.5562	24.7666	burst			#VALUE!	2.028	SU18				
Plot 3-0.5	**SU19**	Ebenhaezer soil	0.5	Tracer inserted at 3 m	12.5032	24.3021	24.1385	24.1424	0.004	0.014	0.014	SU19	-4.81	0.11	-27.9	0.5
Plot 3-0.5	SU20	Ebenhaezer soil		**Tracer inserted at 3 m**	12.5003	23.4264	23.2723	23.2783	0.006	0.014	0.014	SU20	-3.89	0.09	-22.5	0.4
Plot 3-0.5	SU21	Ebenhaezer soil		Tracer inserted at 3 m	12.5241	23.7111	23.6026	23.5651	-0.037	0.010	0.013	SU21	-4.42	0.06	-23.5	0.5
Plot 3-1	**SU22**	Ebenhaezer soil	**1**	**Tracer inserted at 3 m**	12.4903	24.3867	24.2306	24.2253	-0.005	0.013	0.014	SU22	-3.37	0.09	1039.9	4.1
Plot 3-1	SU23	Ebenhaezer soil		Tracer inserted at 3 m	12.6195	25.8544	25.6777	25.6651	-0.013	0.013	0.014	SU23	-3.45	0.06	1007.8	3.3
Plot 3-1	SU24	Ebenhaezer soil		**Tracer inserted at 3 m**	12.5425	24.7313	24.5714	24.5711	0.000	0.013	0.013	SU24	-3.35	0.04	1031.0	1.6
Plot 3-1.5	**SU25**	Ebenhaezer soil	1.5	Tracer inserted at 3 m	12.784	25.399	25.2216	25.2219	0.000	0.014	0.014	SU25	-1.34	0.11	9284.7	4.8
Plot 3-1.5	SU26	Ebenhaezer soil		**Tracer inserted at 3 m**	12.1471	24.0771	23.9333	23.8859	-0.047	0.012	0.016	SU26	-1.96	0.05	9220.8	14.7
Plot 3-1.5	SU27	Ebenhaezer soil		Tracer inserted at 3 m	12.4098	23.5782	23.451	23.4193	-0.032	0.011	0.014	SU27	-1.99	0.06	9147.5	6.0
Plot 3-2	**SU28**	Ebenhaezer soil	**2**	**Tracer inserted at 3 m**	12.3852	24.9191	24.7468	24.7401	-0.007	0.014	0.014	SU28	-0.38	0.05	13872.3	2.2
Plot 3-2	SU29	Ebenhaezer soil		Tracer inserted at 3 m	12.9558	24.7595	24.5799	24.5864	0.007	0.015	0.015	SU29	-1.29	0.15	13860.8	11.3
Plot 3-2	SU30	Ebenhaeze		**Tracer**	12.647	25.675	25.5181	25.522	0.004	0.012	0.012	SU30	0.31	0.04	14109.	35.6

		r soil		**inserted at 3 m**	1	8		4							8	
Plot 3-2.5	**SU31**	Ebenhaezer soil	2.5	Tracer inserted at 3 m	12.7086	26.5836	26.3926	26.3973	0.005	0.014	0.013	SU31	-2.47	0.03	5564.6	26.3
Plot 3-2.5	SU32	Ebenhaezer soil		**Tracer inserted at 3 m**	12.6617	26.0966	25.8983	25.8714	-0.027	0.015	0.017	SU32	-2.11	0.04	5556.4	19.8
Plot 3-2.5	SU33	Ebenhaezer soil		Tracer inserted at 3 m	12.363	25.7085	25.5195	25.5214	0.002	0.014	0.014	SU33	-2.58	0.05	5565.5	6.9
Plot 3-3	**SU34**	Ebenhaezer soil	**3**	**Tracer inserted at 3 m**	12.7169	26.5185	26.3827	26.3308	-0.052	0.010	0.014	SU34	-5.09	0.08	1203.2	11.1
Plot 3-3	SU35	Ebenhaezer soil		Tracer inserted at 3 m	12.8204	26.8697	26.6806	26.6791	-0.002	0.013	0.014	SU35	-3.38	0.07	1231.4	18.0
Plot 3-3	SU36	Ebenhaezer soil		**Tracer inserted at 3 m**	12.7389	25.8207	25.6411	25.6315	-0.010	0.014	0.014	SU36	-4.54	0.05	1185.9	8.1
Plot 4-0.35	**SU37**	Ebenhaezer soil	0.35	Tracer inserted at 1 m	12.3423	24.25	24.1201	24.111	-0.009	0.011	0.012	SU37	-1.64	0.05	218.5	0.1
Plot 4-0.35	SU38	Ebenhaezer soil		**Tracer inserted at 1 m**	12.3886	23.4304	23.3824	23.3042	-0.078	0.004	0.011	SU38				
Plot 4-0.35	SU39	Ebenhaezer soil		Tracer inserted at 1 m	12.7796	25.4504	25.2947	25.2988	0.004	0.012	0.012	SU39	-1.69	0.05	219.3	1.5
Plot 4-0.70	**SU40**	Ebenhaezer soil	**0.7**	**Tracer inserted at 1 m**	12.261	25.6795	25.5233	25.5278	0.005	0.012	0.011	SU40	-4.67	0.09	2053.8	1.9
Plot 4-0.70	SU41	Ebenhaezer soil		Tracer inserted at 1 m	12.6862	24.7584	24.5952	24.6002	0.005	0.014	0.013	SU41	-4.61	0.03	2080.2	9.4
Plot 4-0.70	SU42	Ebenhaezer soil		**Tracer inserted at 1 m**	12.7625	25.3993	25.2479	25.2298	-0.018	0.012	0.013	SU42				
Plot 4-1	**SU43**	Ebenhaezer soil	1	Tracer inserted at 1 m	12.6588	25.7547	25.6222	25.5867	-0.035	0.010	0.013	SU43	-3.24	0.09	5461.7	6.4
Plot 4-1	SU44	Ebenhaezer soil		**Tracer inserted at 1 m**	12.7067	25.3168	25.1909	25.1444	-0.046	0.010	0.014	SU44	-3.30	0.19	5501.1	24.4
Plot 4-1	SU45	Ebenhaezer soil		Tracer inserted at 1 m	12.7153	26.7323	26.5851	26.5431	-0.042	0.011	0.013	SU45	-1.93	0.06	5535.0	11.9
Plot 4-1.5	**SU46**	Ebenhaeze	**1.5**	**Tracer**	12.901	25.712	25.576	25.543	-0.032	0.011	0.013	SU46	-2.62	0.05	7139.8	8.7

		r soil		**inserted at 1 m**	9	4		9								
Plot 4-1.5	SU47	Ebenhaezer soil		Tracer inserted at 1 m	12.2751	24.2616	24.0987	24.0761	-0.023	0.014	0.015	SU47	-1.58	0.02	7082.2	23.2
Plot 4-1.5	SU48	Ebenhaezer soil		**Tracer inserted at 1 m**	12.755	25.1559	24.9619	24.9635	0.002	0.016	0.016	SU48	-1.75	0.07	7119.7	9.9
Plot 4-2	**SU49**	Ebenhaezer soil	2	Tracer inserted at 1 m	12.2182	25.4858	25.3044	25.3061	0.002	0.014	0.014	SU49	-5.36	0.06	1533.3	7.2
Plot 4-2	SU50	Ebenhaezer soil		**Tracer inserted at 1 m**	12.5517	24.2807	24.0954	24.0994	0.004	0.016	0.015	SU50	-5.35	0.08	1544.7	1.3
Plot 4-2	SU51	Ebenhaezer soil		Tracer inserted at 1 m	12.2335	24.0403	23.8848	23.8783	-0.006	0.013	0.014	SU51	-4.92	0.07	1553.6	1.0
Plot 5-0.25	**SU52**	Ebenhaezer soil	**0.25**	**Tracer inserted at 0.5 m**	12.3118	23.8332	23.685	23.6809	-0.004	0.013	0.013	SU52	0.70	0.10	299.4	2.3
Plot 5-0.25	SU53	Ebenhaezer soil		Tracer inserted at 0.5 m	12.2363	23.4159	23.2786	23.2628	-0.016	0.012	0.014	SU53	0.81	0.14	207.6	1.8
Plot 5-0.25	SU54	Ebenhaezer soil		**Tracer inserted at 0.5 m**	12.3576	23.0778	22.9283	22.9347	0.006	0.014	0.013	SU54	1.38	0.04	267.7	0.8
Plot 5-0.5	**SU55**	Ebenhaezer soil	0.5	Tracer inserted at 0.5 m	12.3563	24.1746	24.0193	24.0178	-0.002	0.013	0.013	SU55	-4.90	0.06	885.7	7.4
Plot 5-0.5	SU56	Ebenhaezer soil		**Tracer inserted at 0.5 m**	12.3512	24.7979	24.6222	24.6266	0.004	0.014	0.014	SU56	-4.34	0.08	672.2	1.3
Plot 5-0.5	SU57	Ebenhaezer soil		Tracer inserted at 0.5 m	12.547	24.553	24.3915	24.3834	-0.008	0.013	0.014	SU57	-4.68	0.04	763.1	0.5
Plot 5-0.75	**SU58**	Ebenhaezer soil	**0.75**	**Tracer inserted at 0.5 m**	12.2175	24.3456	24.1825	24.1772	-0.005	0.013	0.014	SU58	-6.09	0.03	1413.5	2.1
Plot 5-0.75	SU59	Ebenhaezer soil		Tracer inserted at 0.5 m	12.2291	24.0355	23.9042	23.8763	-0.028	0.011	0.013	SU59	-7.48	0.03	1397.2	3.5
Plot 5-0.75	SU60	Ebenhaezer soil		**Tracer inserted at 0.5 m**	12.3575	25.0302	24.8943	24.8604	-0.034	0.011	0.013	SU60	-6.40	0.08	1978.6	3.7
Plot 5-1	**SU61**	Ebenhaezer soil	1	Tracer inserted at 0.5 m	12.2766	24.1286	23.9606	23.9613	0.001	0.014	0.014	SU61	-3.61	0.05	3324.4	16.4
Plot 5-1	SU62	Ebenhaeze		**Tracer**	12.802	24.819	24.6501	24.654	0.005	0.014	0.014	SU62	-3.51	0.07	3346.8	8.4

		r soil		**inserted at 0.5 m**	7	5		6								
Plot 5-1	SU63	Ebenhaezer soil		Tracer inserted at 0.5 m	12.6836	24.6694	24.5154	24.5156	0.000	0.013	0.013	SU63	-3.86	0.04	3322.5	23.4
Plot 5-1.5	**SU64**	Ebenhaezer soil	**1.5**	**Tracer inserted at 0.5 m**	12.5532	25.6173	25.4512	25.4519	0.001	0.013	0.013	SU64	-4.00	0.06	3285.2	12.8
Plot 5-1.5	SU65	Ebenhaezer soil		Tracer inserted at 0.5 m	12.4198	25.0733	24.9263	24.9181	-0.008	0.012	0.012	SU65	-4.50	0.04	3286.8	3.1
Plot 5-1.5	SU66	Ebenhaezer soil		**Tracer inserted at 0.5 m**	12.707	24.984	24.8173	24.8077	-0.010	0.014	0.014	SU66	-5.15	0.08	3276.1	2.4
BH3-13/03/2017a	**SU67**	Tsumeb xylem		*S. mellifera*	12.625	12.9635	12.8428		-12.843	0.357	38.297	SU67	-8.03	0.21	-66.3	0.7
BH3-13/03/2017a	SU68	Tsumeb xylem		*S. mellifera*	12.8914	13.1343	13.035		-13.035	0.409	54.073	SU68	-7.31	0.07	-63.8	0.4
BH3-13/03/2017b	**SU69**	Tsumeb xylem		*B. albitrunca*	12.9181	13.2003	13.0961		-13.096	0.369	46.776	SU69	-5.93	0.05	-57.0	0.6
BH3-13/03/2017b	**SU70**	Tsumeb xylem		*B. albitrunca*	12.6246	12.8486	12.7622		-12.762	0.386	57.360	SU70	-5.02	0.06	-55.5	0.5
BH2-14/03/2017a	**SU71**	Tsumeb xylem		*S. mellifera*	12.241	12.5273	12.401		-12.401	0.441	43.756	SU71	-6.55	0.08	-57.1	0.6
BH2-14/03/2017a	**SU72**	Tsumeb xylem		*S. mellifera*	12.884	13.2446	13.1103		-13.110	0.372	36.729	SU72	-8.00	0.02	-5.2	0.5
BH2-14/03/2017b	**SU73**	Tsumeb xylem		*B. albitrunca*	12.6716	12.9485	12.8575		-12.858	0.329	46.762	SU73	-6.97	0.11	-58.5	0.4
BH2-14/03/2017b	**SU74**	Tsumeb xylem		*B. albitrunca*	12.3833	12.6792	12.5836		-12.584	0.323	42.850	SU74	-7.03	0.08	-59.6	0.6
BH2-14/05/2017a	**SU75**	Tsumeb xylem		*S. mellifera*	12.7849	13.117	12.9779		-12.978	0.419	39.497	SU75	-3.72	0.09	-34.3	0.5
BH2-14/05/2017a	**SU76**	Tsumeb xylem		*S. mellifera*	12.644	13.0631	12.8948		-12.895	0.402	31.169	SU76	-5.29	0.06	10.8	0.6
BH2-14/05/2017b	**SU77**	Tsumeb xylem		*B. albitrunca*	12.4654	12.8466	12.7061		-12.706	0.369	33.700	SU77	-5.47	0.08	-51.6	0.6
BH2-14/05/2017b	**SU78**	Tsumeb xylem		*B. albitrunca*	12.8203	13.1792	13.0383		-13.038	0.393	36.721	SU78	-4.64	0.09	-48.1	0.2
Driefontain-14/05/2017a	**SU79**	Tsumeb xylem		*S. mellifera*	12.4458	12.6856	12.5792		-12.579	0.444	52.901	SU79	-3.06	0.07	-26.7	0.6
Driefontain-14/05/2017a	**SU80**	Tsumeb xylem		*S. mellifera*	12.8314	13.2391	13.0962		-13.096	0.351	32.473	SU80	-3.32	0.10	-31.5	0.3

Driefontain-14/05/2017b	**SU81**	Tsumeb xylem		*B. albitrunca*	12.9228	13.2167	13.1027		-13.103	0.388	44.970	SU81	-2.83	0.09	-42.3	0.4
Driefontain-14/05/2017b	**SU82**	Tsumeb xylem		*B. albitrunca*	12.7018	13.0038	12.8805		-12.881	0.408	43.059	SU82	-3.70	0.09	-44.1	0.6
Okatjikona-12/03/2017a	**SU83**	Waterberg xylem		*S. mellifera*	12.4373	12.8408	12.6902		-12.690	0.373	31.824	SU83	-4.88	0.12	-50.8	0.4
Okatjikona-12/03/2017a	**SU84**	Waterberg xylem		*S. mellifera*	12.7723	13.0911	12.969		-12.969	0.383	41.064	SU84	-4.52	0.06	-51.4	0.2
Okatjikona-12/03/2017b	**SU85**	Waterberg xylem		*B. albitrunca*	12.7159	13.0354	12.9111		-12.911	0.389	40.799	SU85	-4.63	0.06	-51.6	0.2
Okatjikona-12/03/2017b	**SU86**	Waterberg xylem		*B. albitrunca*	12.7923	13.0658	12.9572		-12.957	0.397	47.773	SU86	-5.34	0.09	-52.4	0.5
NWR-12/03/2017a	**SU87**	Waterberg xylem		*S. mellifera*	12.2937	12.4994	12.3936		-12.394	0.514	60.765	SU87	-5.19	0.11	-44.7	0.4
NWR-12/03/2017a	**SU88**	Waterberg xylem		*S. mellifera*	12.6691	12.7821	12.7302		-12.730	0.459	113.116	SU88	-4.68	0.12	-45.7	0.3
NWR-12/03/2017b	**SU89**	Waterberg xylem		*B. albitrunca*	12.7055	12.9394	12.8488		-12.849	0.387	55.320	SU89	-8.25	0.14	-60.2	0.7
NWR-12/03/2017b	**SU90**	Waterberg xylem		*B. albitrunca*	12.8911	13.1587	13.0439		-13.044	0.429	49.173	SU90	-7.28	0.08	-55.9	0.3
Okatjikona-15/05/2017a	**SU91**	Waterberg xylem		*S. mellifera*	12.4913	12.7793	12.6587		-12.659	0.419	44.373	SU91	-4.52	0.14	-47.8	0.5
Okatjikona-15/05/2017a	**SU92**	Waterberg xylem		*S. mellifera*	12.5954	12.8676	12.764		-12.764	0.381	47.273	SU92	-5.39	0.04	-50.7	0.4
Okatjikona-15/05/2017b	**SU93**	Waterberg xylem		*B. albitrunca*	12.5713	12.8531	12.7081		-12.708	0.515	45.611	SU93	-4.84	0.20	-38.1	0.5
Okatjikona-15/05/2017b	**SU94**	Waterberg xylem		*B. albitrunca*	12.7872	12.8939	12.8487		-12.849	0.424	120.843	SU94				
NWR-15/05/2017a	**SU95**	Ebenhaezer xylem		*S. mellifera*	12.3984	12.625	12.5415		-12.542	0.368	55.715	SU95	-4.80	0.08	-46.8	0.6
NWR-15/05/2017a	**SU96**	Ebenhaezer xylem		*S. mellifera*	12.8461	13.0266	12.9511		-12.951	0.418	72.170	SU96	-5.70	0.10	-47.2	0.2
NWR-15/05/2017b	**SU97**	Ebenhaezer xylem		*S. mellifera*	12.6876	12.9192	12.8387		-12.839	0.348	55.782	SU97	-5.54	0.12	-50.2	0.3
NWR-15/05/2017b	**SU98**	Ebenhaezer xylem		*S. mellifera*	12.3726	12.5537	12.4842		-12.484	0.384	69.319	SU98	-7.00	0.14	-57.2	0.3
SUE08-02-10/03/2017a	**SU99**	Ebenhaezer xylem		*S. mellifera*	12.5905	12.7748	12.7608		-12.761	0.076	69.315	SU99				
SUE08-02-10/03/2017a	**SU100**	Ebenhaezer xylem		*S. mellifera*	12.8047	12.989	12.8996		-12.900	0.485	70.477	SU100	-7.53	0.00	-62.3	0.3

SUE09-02-17/05/2017a	**SU101**	Ebenhaezer xylem		*S. mellifera*	12.8664	13.2369	13.1018		-13.102	0.365	35.727	SU101	-1.57	0.15	-25.4	0.7
SUE09-02-17/05/2017a	**SU102**	Ebenhaezer xylem		*S. mellifera*	12.6303	12.9945	12.8821		-12.882	0.309	35.680	SU102	-1.86	0.00	-25.3	0.5
SUE01-09/12/2016a	**SU103**	Ebenhaezer xylem		*B. albitrunca*	12.6862	13.0636	12.9771		-12.977	0.229	34.615	SU103				
SUE01-09/12/2016a	**SU104**	Ebenhaezer xylem		*B. albitrunca*	12.7481	13.0439	12.959		-12.959	0.287	44.097	SU104	-1.69	0.03	34.9	0.2
plot1-07/12/2016a	**SU105**	Ebenhaezer xylem		*S. mellifera*	12.7046	13.1854	13.0465		-13.047	0.289	27.424	SU105	-2.03	0.18	-23.4	0.0
plot1-07/12/2016a	**SU106**	Ebenhaezer xylem		*S. mellifera*	12.9085	13.2394	13.1289		-13.129	0.334	40.010	SU106	-3.16	0.25	-35.3	1.4
Plot1-07/12/2016b	**SU107**	Ebenhaezer xylem		*B. albitrunca*	12.9403	13.3692	13.2075		-13.208	0.377	31.171	SU107	-2.95	0.01	-37.7	1.1
Plot1-07/12/2016b	**SU108**	Ebenhaezer xylem		*B. albitrunca*	12.6499	13.0193	12.8786		-12.879	0.381	35.244	SU108	-2.86	0.25	-32.1	0.6
Plot1-07/12/2016o	**SU109**	Ebenhaezer xylem		*Omupopo*	12.9878	13.312	13.1496		-13.150	0.501	41.061	SU109	-3.08	0.02	-29.5	0.5
Plot1-07/12/2016o	**SU110**	Ebenhaezer xylem		*Omupopo*	12.529	12.8115	12.6586		-12.659	0.541	45.350	SU110	-2.45	0.24	-26.3	0.2
Plot2-07/12/2016a	**SU111**	Ebenhaezer xylem		*S. mellifera*	12.2737	12.6088	12.4752		-12.475	0.399	37.627	SU111	-3.12	0.26	-24.6	0.8
Plot2-07/12/2016a	**SU112**	Ebenhaezer xylem		*S. mellifera*	12.7174	13.1178	13.0456		-13.046	0.180	32.762	SU112				
Plot2-07/12/2016b_a	**SU113**	Ebenhaezer xylem		*B. albitrunca* next to *S. mellifera*	12.3388	12.5767	12.4739		-12.474	0.432	52.865	SU113	-1.37	0.06	-25.6	0.4
Plot2-07/12/2016b_a	**SU114**	Ebenhaezer xylem		*B. albitrunca* next to *S. mellifera*	12.6545	12.8452	12.7663		-12.766	0.414	67.358	SU114	-1.41	0.34	-28.8	2.1
Plot2-07/12/2016b_o	**SU115**	Ebenhaezer xylem		*B. albitrunca* next to *Omupopo*	12.6019	13.0845	12.9518		-12.952	0.275	27.113	SU115	-3.44	0.24	-37.8	0.5
Plot2-07/12/2016b_o	**SU116**	Ebenhaezer xylem		*B. albitrunca* next to *Omupopo*	12.4988	13.0786	12.8564		-12.856	0.383	22.557	SU116	-2.13	0.00	-36.7	0.1
Plot2-07/12/2016o	**SU117**	Ebenhaezer xylem		*Omupopo*	12.6984	12.958	12.9037		-12.904	0.209	49.915	SU117				

Plot2-07/12/2016o	**SU118**	Ebenhaezer xylem		*Omupopo*	12.7068	12.9615	12.8627		-12.863	0.388	50.889	SU118	-2.29	0.09	-27.5	0.4
Plot3-07/12/2016a	**SU119**	Ebenhaezer xylem		*S. mellifera*	12.806	13.2605	13.0769		-13.077	0.404	29.176	SU119	-2.56	0.21	-30.6	0.3
Plot3-07/12/2016a	**SU120**	Ebenhaezer xylem		*S. mellifera*	12.5823	12.9812	12.8347		-12.835	0.367	32.542	SU120	-3.55	0.20	-32.0	0.9
Plot3-07/12/2016as	**SU121**	Ebenhaezer xylem		*S. mellifera* shrub	12.7894	13.5935	13.2336		-13.234	0.448	16.905	SU121	-2.99	0.03	-40.1	0.9
Plot3-07/12/2016as	**SU122**	Ebenhaezer xylem		*S. mellifera* shrub	12.5692	13.4106	13.0357		-13.036	0.446	15.938	SU122	-1.83	0.09	-29.7	0.1
Plot3-07/12/2016b1	**SU123**	Ebenhaezer xylem		*B. albitrunca* 1	12.5572	12.8561	12.748		-12.748	0.362	43.011	SU123	-1.62	0.12	-34.9	0.5
Plot3-07/12/2016b1	**SU124**	Ebenhaezer xylem		*B. albitrunca* 1	12.8367	13.1789	13.0367		-13.037	0.416	38.512	SU124	-1.96	0.05	-30.9	1.2
Plot3-07/12/2016b2	**SU125**	Ebenhaezer xylem		*B. albitrunca* 2	12.8844	13.7599	13.439		-13.439	0.367	15.717	SU125	-3.90	0.12	-41.9	0.2
Plot3-07/12/2016b2	**SU126**	Ebenhaezer xylem		*B. albitrunca* 2	12.8047	13.3929	13.1692		-13.169	0.380	22.769	SU126	-4.70	0.32	-51.9	3.9
Plot4-07/12/2016a	**SU127**	Ebenhaezer xylem		*S. mellifera*	12.5155	12.7812	12.7642		-12.764	0.064	48.104	SU127				
Plot4-07/12/2016a	**SU128**	Ebenhaezer xylem		*S. mellifera*	12.5326	12.7568	12.6841		-12.684	0.324	56.899	SU128	-1.16	0.03	-31.2	0.9
Plot4-07/12/2016as	**SU129**	Ebenhaezer xylem		*S. mellifera* shrub	12.5139	13.5102	13.093		-13.093	0.419	13.560	SU129	-1.14	0.15	-30.5	0.7
Plot4-07/12/2016as	**SU130**	Ebenhaezer xylem		*S. mellifera* shrub	12.4523	13.5385	13.0658		-13.066	0.435	12.464	SU130	0.59	0.31	-15.9	1.7
Plot4-07/12/2016b1	**SU131**	Ebenhaezer xylem		*B. albitrunca* 1	12.4981	12.9295	12.7437		-12.744	0.431	29.971	SU131	-2.24	0.27	-30.4	2.0
Plot4-07/12/2016b1	**SU132**	Ebenhaezer xylem		*B. albitrunca* 1	12.5019	12.8399	12.6919		-12.692	0.438	37.988	SU132	-1.68	0.47	-27.5	1.0
Plot4-07/12/2016b2	**SU133**	Ebenhaezer xylem		*B. albitrunca* 2	12.5187	12.8713	12.7864		-12.786	0.241	36.504	SU133				
Plot4-07/12/2016b2	**SU134**	Ebenhaezer xylem		*B. albitrunca* 2	12.5588	12.9493	12.8001		-12.800	0.382	33.161	SU134	-2.86	0.31	-46.7	3.3
Plot5-07/12/2016a1	**SU135**	Ebenhaezer xylem		*S. mellifera*	12.5317	13.0644	12.9261		-12.926	0.260	24.525	SU135	-3.06	0.32	-34.8	0.7

				1												
Plot5-07/12/2016a1	**SU136**	Ebenhaezer xylem		*S. mellifera* 1	12.5499	13.0695	12.8827		-12.883	0.360	25.153	SU136	-2.90	0.27	-37.3	1.5
Plot5-07/12/2016a2	**SU137**	Ebenhaezer xylem		*S. mellifera* 2	12.5768	12.9559	12.8294		-12.829	0.334	34.175	SU137	-2.76	0.15	-32.3	0.8
Plot5-07/12/2016a2	**SU138**	Ebenhaezer xylem		*S. mellifera* 2	12.5561	12.9477	12.7999		-12.800	0.377	33.064	SU138	-3.49	0.36	-33.1	0.0
Plot5-07/12/2016b	**SU139**	Ebenhaezer xylem		*B. albitrunca*	12.5822	12.8187	12.7412		-12.741	0.328	54.202	SU139	-4.42	0.07	-41.2	1.0
Plot5-07/12/2016b	**SU140**	Ebenhaezer xylem		*B. albitrunca*	12.5763	12.9155	12.8014		-12.801	0.336	38.076	SU140	-3.37	0.17	-31.2	0.2
Plot3-08/12/2016a	**SU141**	Ebenhaezer xylem		*S. mellifera*	12.5445	12.9492	12.8381		-12.838	0.275	31.997	SU141	-2.61	0.08	32.1	3.1
Plot3-08/12/2016a	**SU142**	Ebenhaezer xylem		*S. mellifera*	12.5695	13.0766	12.8952		-12.895	0.358	25.787	SU142	-2.42	0.13	29.2	1.0
Plot3-08/12/2016b	**SU143**	Ebenhaezer xylem		*B. albitrunca*	12.5226	13.1398	12.8676		-12.868	0.441	21.289	SU143	-2.68	0.27	-9.9	1.4
Plot3-08/12/2016b	**SU144**	Ebenhaezer xylem		*B. albitrunca*	12.5323	13.007	12.8037		-12.804	0.428	27.400	SU144	-3.79	0.35	-11.5	2.0
Plot6-09/12/2016asm	**SU145**	Ebenhaezer xylem		*S. mellifera* small	12.5544	12.788	12.7134		-12.713	0.319	54.743	SU145	-2.89	0.10	-35.1	0.5
Plot6-09/12/2016asm	**SU146**	Ebenhaezer xylem		*S. mellifera* small	12.5502	12.6796	12.6313		-12.631	0.373	97.988	SU146	-0.96	0.10	-33.5	0.4
Plot6-09/12/2016abi	**SU147**	Ebenhaezer xylem		*S. mellifera* big	12.5007	12.8674	12.7926		-12.793	0.204	35.090	SU147				
Plot6-09/12/2016abi	**SU148**	Ebenhaezer xylem		*S. mellifera* big	12.5092	12.9033	12.824		-12.824	0.201	32.741	SU148	-1.64	0.03	-27.7	0.1
Plot1-09/12/2016a	**SU149**	Ebenhaezer xylem		*S. mellifera*	12.51	12.9525	12.7995		-12.800	0.346	29.271	SU149	-6.20	0.08	-55.5	0.7
Plot1-09/12/2016a	**SU150**	Ebenhaezer xylem		*S. mellifera*	12.5389	13.0895	12.8909		-12.891	0.361	23.773	SU150	-6.22	0.03	-55.8	0.4
Plot1-09/12/2016b	**SU151**	Ebenhaezer xylem		*B. albitrunca*	12.5874	12.7205	12.6587		-12.659	0.464	95.571	SU151	-3.34	0.03	-56.4	0.1
Plot1-09/12/2016b	**SU152**	Ebenhaezer xylem		*B. albitrunca*	12.5822	12.7807	12.7099		-12.710	0.357	64.386	SU152	-5.45	0.08	-78.2	0.7

Plot2-09/12/2016a	**SU153**	Ebenhaezer xylem		*S. mellifera*	12.5778	13.0305	12.9085		-12.909	0.269	28.784	SU153	0.96	0.06	-26.2	0.6
Plot2-09/12/2016a	**SU154**	Ebenhaezer xylem		*S. mellifera*	12.644	13.1607	13.0256		-13.026	0.261	25.471	SU154	-4.82	0.10	-59.1	1.1
Plot2-09/12/2016b	**SU155**	Ebenhaezer xylem		*B. albitrunca*	12.4724	13.6523	13.2527		-13.253	0.339	11.571	SU155	-7.63	0.03	-63.8	0.5
Plot2-09/12/2016b	**SU156**	Ebenhaezer xylem		*B. albitrunca*	12.4571	13.2593	12.9815		-12.982	0.346	16.529	SU156	-5.85	0.05	-60.4	0.4
Plot3-09/12/2016a	**SU157**	Ebenhaezer xylem		*S. mellifera*	12.5047	13.1394	13.0164		-13.016	0.194	20.702	SU157	-10.46	0.00	-95.5	0.2
Plot3-09/12/2016a	**SU158**	Ebenhaezer xylem		*S. mellifera*	12.532	13.069	12.8939		-12.894	0.326	24.337	SU158	-4.41	0.05	-53.7	0.7
Plot3-09/12/2016b	**SU159**	Ebenhaezer xylem		*B. albitrunca*	12.5229	13.0919	12.8507		-12.851	0.424	23.009	SU159	-6.55	0.03	-66.2	0.7
Plot3-09/12/2016b	**SU160**	Ebenhaezer xylem		*B. albitrunca*	12.5251	13.0891	12.8869		-12.887	0.359	23.208	SU160	-6.62	0.06	-66.4	0.3
Plot4-09/12/2016a	**SU161**	Ebenhaezer xylem		*S. mellifera*	12.5195	12.8258	12.767		-12.767	0.192	41.873	SU161	-0.46	0.19	-29.9	2.9
Plot4-09/12/2016a	**SU162**	Ebenhaezer xylem		*S. mellifera*	12.5323	12.8679	12.801		-12.801	0.199	38.343	SU162	-2.89	0.10	-50.5	0.6
Plot4-09/12/2016as	**SU163**	Ebenhaezer xylem		*S. mellifera* shrub	12.5638	13.5679	13.1764		-13.176	0.390	13.512	SU163	-15.10	0.14	-132.4	0.0
Plot4-09/12/2016as	**SU164**	Ebenhaezer xylem		*S. mellifera* shrub	12.4468	13.4856	13.0625		-13.063	0.407	12.982	SU164	-13.03	0.07	-117.7	0.7
Plot4-09/12/2016b	**SU165**	Ebenhaezer xylem		*B. albitrunca*	12.5544	13.4681	13.1418		-13.142	0.357	14.740	SU165	-3.91	0.18	-49.3	0.7
Plot4-09/12/2016b	**SU166**	Ebenhaezer xylem		*B. albitrunca*	12.549	13.6225	13.2429		-13.243	0.354	12.690	SU166	-3.93	0.04	-48.8	0.5
Plot5-09/12/2016a	**SU167**	Ebenhaezer xylem		*S. mellifera*	12.5898	13.133	12.9771		-12.977	0.287	24.177	SU167	-5.82	0.03	-47.9	0.6
Plot5-09/12/2016a	**SU168**	Ebenhaezer xylem		*S. mellifera*	12.4757	13.0905	12.887		-12.887	0.331	21.292	SU168	-5.36	0.03	-47.1	0.1
Plot5-09/12/2016b	**SU169**	Ebenhaezer xylem		*B. albitrunca*	12.4703	12.8384	12.6885		-12.689	0.407	34.877	SU169	-5.56	0.06	-58.5	0.4
Plot5-09/12/2016b	**SU170**	Ebenhaezer xylem		*B. albitrunca*	12.5291	12.9299	12.7612		-12.761	0.421	32.260	SU170	-5.25	0.03	-52.5	0.5
Plot5-09/12/2016bs	**SU171**	Ebenhaezer xylem		*B. albitrunc*	12.4603	13.6024	13.1711		-13.171	0.378	11.910	SU171	-24.42	0.09	-199.7	2.2

				a shrub												
Plot5-09/12/2016bs	**SU172**	Ebenhaezer xylem		*B. albitrunca* shrub	12.4979	13.6552	13.1665		-13.167	0.422	11.799	SU172	-20.94	0.06	-176.7	1.8
Plot6-09/12/2016asme	**SU173**	Ebenhaezer xylem		*S. mellifera* small evening	12.4882	12.954	12.8218		-12.822	0.284	27.810	SU173	-5.76	0.06	-56.4	1.2
Plot6-09/12/2016asme	**SU174**	Ebenhaezer xylem		*S. mellifera* small evening	12.6181	13.0966	12.9636		-12.964	0.278	27.370	SU174	-3.50	0.09	-48.9	0.5
Plot6-09/12/2016abie	**SU175**	Ebenhaezer xylem		*S. mellifera* big evening	12.5375	13.2164	12.9929		-12.993	0.329	19.467	SU175	-3.75	0.10	-50.0	0.7
Plot6-09/12/2016abie	**SU176**	Ebenhaezer xylem		*S. mellifera* big evening	12.5122	13.1403	13.0246		-13.025	0.184	20.921	SU176	-6.85	0.09	-64.9	0.5
Plot1-10/12/2016a	**SU177**	Ebenhaezer xylem		*S. mellifera*	12.5388	12.9644	12.8314		-12.831	0.312	30.461	SU177	-7.26	0.11	-72.3	0.6
Plot1-10/12/2016a	**SU178**	Ebenhaezer xylem		*S. mellifera*	12.4942	12.9334	12.7842		-12.784	0.340	29.448	SU178	-6.21	0.05	-59.1	0.3
Plot1-10/12/2016b	**SU179**	Ebenhaezer xylem		*B. albitrunca*	12.4902	12.8192	12.7083		-12.708	0.337	38.964	SU179	-5.14	0.07	-61.8	0.7
Plot1-10/12/2016b	**SU180**	Ebenhaezer xylem		*B. albitrunca*	12.5747	13.0238	12.893		-12.893	0.291	29.000	SU180	-4.94	0.03	-51.4	0.6
Plot2-10/12/2016a	**SU181**	Ebenhaezer xylem		*S. mellifera*	12.5956	13.0299	12.9151		-12.915	0.264	30.002	SU181	-4.25	0.04	-38.5	0.8
Plot2-10/12/2016a	**SU182**	Ebenhaezer xylem		*S. mellifera*	12.5108	12.957	12.8302		-12.830	0.284	29.039	SU182	-4.61	0.08	-48.5	0.5
Plot2-10/12/2016b	**SU183**	Ebenhaezer xylem		*B. albitrunca*	12.5222	12.7754	12.6743		-12.674	0.399	50.456	SU183	-7.31	0.16	-79.9	0.9
Plot2-10/12/2016b	**SU184**	Ebenhaezer xylem		*B. albitrunca*	12.53	12.8984	12.7698		-12.770	0.349	35.012	SU184	-7.37	0.08	-76.0	0.6
Plot3-10/12/2016a	**SU185**	Ebenhaezer xylem		*S. mellifera*	12.5236	13.0015	12.8757		-12.876	0.263	27.205	SU185	-5.06	0.05	-59.1	0.6
Plot3-10/12/2016a	**SU186**	Ebenhaezer xylem		*S. mellifera*	12.5168	12.9016	12.7815		-12.782	0.312	33.528	SU186	-5.47	0.09	-59.2	0.3
Plot3-10/12/2016b	**SU187**	Ebenhaezer xylem		*B. albitrunca*	12.5139	12.9945	12.8259		-12.826	0.351	27.038	SU187	-6.85	0.07	-70.6	0.6
Plot3-	**SU18**	Ebenhaeze		*B.*	12.423	12.934	12.7328		-12.733	0.395	25.317	SU18	-6.15	0.06	-65.8	0.5

10/12/2016b	**8**	r xylem		*albitrunca*	8	7						8				
Plot4-10/12/2016a	**SU189**	Ebenhaezer xylem		*S. mellifera*	12.5081	12.7956	12.7166		-12.717	0.275	44.506	SU189	-2.56	0.09	-38.4	0.9
Plot4-10/12/2016a	**SU190**	Ebenhaezer xylem		*S. mellifera*	12.5065	12.7482	12.6821		-12.682	0.273	52.744	SU190	-3.02	0.04	-38.3	0.1
Plot4-10/12/2016b	**SU191**	Ebenhaezer xylem		*B. albitrunca*	12.5557	13.1824	12.9485		-12.949	0.373	21.035	SU191	-6.50	0.09	-63.2	0.5
Plot4-10/12/2016b	**SU192**	Ebenhaezer xylem		*B. albitrunca*	12.5491	13.3878	13.0639		-13.064	0.386	15.963	SU192	-5.86	0.02	-62.1	0.3
Plot5-10/12/2016a	**SU193**	Ebenhaezer xylem		*S. mellifera*	12.5982	13.2436	13.1235		-13.124	0.186	20.520	SU193	-5.32	0.04	-50.2	0.3
Plot5-10/12/2016a	**SU194**	Ebenhaezer xylem		*S. mellifera*	12.5058	13.0909	12.9393		-12.939	0.259	22.374	SU194	-2.78	0.05	-45.9	0.6
Plot5-10/12/2016b	**SU195**	Ebenhaezer xylem		*B. albitrunca*	12.48	12.7557	12.6591		-12.659	0.350	46.267	SU195	-5.59	0.06	-62.3	0.0
Plot5-10/12/2016b	**SU196**	Ebenhaezer xylem		*B. albitrunca*	12.5874	12.8149	12.7379		-12.738	0.338	56.329	SU196	-5.12	0.07	-62.6	0.4
Plot5-10/12/2016bs	**SU197**	Ebenhaezer xylem		*B. albitrunca* shrub	12.5359	13.3567	13.0478		-13.048	0.376	16.273	SU197	-24.47	0.02	-222.0	2.0
Plot5-10/12/2016bs	**SU198**	Ebenhaezer xylem		*B. albitrunca* shrub	12.5129	13.5764	13.2352		-13.235	0.321	12.766	SU198	-39.98	0.05	-338.5	0.2
Plot6-10/12/2016asm	**SU199**	Ebenhaezer xylem		*S. mellifera* small	12.5223	13.1326	12.9844		-12.984	0.243	21.518	SU199	-4.62	0.10	-53.2	2.4
Plot6-10/12/2016asm	**SU200**	Ebenhaezer xylem		*S. mellifera* small	12.6336	13.1491	13.0013		-13.001	0.287	25.507	SU200	-4.88	0.09	-58.0	0.2
Plot6-10/12/2016abi	**SU201**	Ebenhaezer xylem		*S. mellifera* big	12.4949	13.101	12.9066		-12.907	0.321	21.615	SU201	-7.88	0.10	-80.4	0.7
Plot6-10/12/2016abi	**SU202**	Ebenhaezer xylem		*S. mellifera* big	12.559	13.2679	13.0358		-13.036	0.327	18.716	SU202	-6.19	0.08	-63.0	0.5
Plot1-11/12/2016a	**SU203**	Ebenhaezer xylem		*S. mellifera*	12.5417	13.143	12.9758		-12.976	0.278	21.858	SU203	-4.26	0.06	-47.0	0.3
Plot1-11/12/2016a	**SU204**	Ebenhaezer xylem		*S. mellifera*	12.4782	13.098	12.9101		-12.910	0.303	21.133	SU204	-4.13	0.01	-44.9	0.6
Plot1-11/12/2016b	**SU205**	Ebenhaezer xylem		*B. albitrunca*	12.4877	12.7892	12.7152		-12.715	0.245	42.419	SU205	-4.07	0.02	-62.7	0.5
Plot1-	**SU20**	Ebenhaeze		*B.*	12.484	12.751	12.6656		-12.666	0.321	47.811	SU20	-4.94	0.07	-72.7	0.5

11/12/2016b	**6**	r xylem		*albitrunca*	4	1						6				
Plot1-11/12/2016o	**SU207**	Ebenhaezer xylem		*Omupopo*	12.5839	13.1784	12.9531		-12.953	0.379	22.167	SU207				
Plot1-11/12/2016o	**SU208**	Ebenhaezer xylem		*Omupopo*	12.5684	13.1	12.8336		-12.834	0.501	24.643	SU208	-12.12	0.00	-104.8	0.9
Plot2-11/12/2016a	**SU209**	Ebenhaezer xylem		*S. mellifera*	12.4874	12.9498	12.8114		-12.811	0.299	28.006	SU209	-2.95	0.10	-40.8	0.1
Plot2-11/12/2016a	**SU210**	Ebenhaezer xylem		*S. mellifera*	12.5526	13.0178	12.8678		-12.868	0.322	27.983	SU210	-2.66	0.05	-41.5	0.2
Plot2-11/12/2016as1	**SU211**	Ebenhaezer xylem		*S. mellifera* shrub 1	12.571	13.2583	12.9908		-12.991	0.389	19.290	SU211	-11.82	0.12	-106.6	0.2
Plot2-11/12/2016as1	**SU212**	Ebenhaezer xylem		*S. mellifera* shrub 1	12.5091	13.2034	12.9959		-12.996	0.299	19.017	SU212	-17.15	0.01	-146.7	0.5
Plot2-11/12/2016as2	**SU213**	Ebenhaezer xylem		*S. mellifera* shrub 2	12.6076	13.7145	13.1727		-13.173	0.489	12.390	SU213	-16.42	0.02	-138.3	0.3
Plot2-11/12/2016as2	**SU214**	Ebenhaezer xylem		*S. mellifera* shrub 2	12.4986	13.5462	13.0581		-13.058	0.466	12.931	SU214	-18.86	0.01	-157.0	1.9
Plot2-11/12/2016b	**SU215**	Ebenhaezer xylem		*B. albitrunca*	12.4873	12.8792	12.7561		-12.756	0.314	32.863	SU215	-7.27	0.04	-71.7	1.2
Plot2-11/12/2016b	**SU216**	Ebenhaezer xylem		*B. albitrunca*	12.5057	13.061	12.8568		-12.857	0.368	23.521	SU216	-7.19	0.05	-69.8	0.1
Plot2-11/12/2016o	**SU217**	Ebenhaezer xylem		*Omupopo*	12.4887	12.8978	12.7379		-12.738	0.391	31.527	SU217	-3.48	0.02	-40.2	0.7
Plot2-11/12/2016o	**SU218**	Ebenhaezer xylem		*Omupopo*	12.5176	12.9138	12.7572		-12.757	0.395	32.594	SU218	-3.77	0.06	-48.3	0.5
Plot3-11/12/2016a	**SU219**	Ebenhaezer xylem		*S. mellifera*	12.5295	12.9912	12.9145		-12.915	0.166	28.138	SU219				
Plot3-11/12/2016a	**SU220**	Ebenhaezer xylem		*S. mellifera*	12.5539	13.1452	13.0042		-13.004	0.238	22.231	SU220	-4.32	0.07	-51.5	0.8
Plot3-11/12/2016b	**SU221**	Ebenhaezer xylem		*B. albitrunca*	12.5185	13.1823	12.9228		-12.923	0.391	19.859	SU221	-7.65	0.14	-72.6	0.2
Plot3-11/12/2016b	**SU222**	Ebenhaezer xylem		*B. albitrunca*	12.6177	13.2397	12.965		-12.965	0.442	21.286	SU222	-7.34	0.02	-71.3	0.6
Plot4-11/12/2016a	**SU223**	Ebenhaezer xylem		*S. mellifera*	12.58	13.1734	13.0232		-13.023	0.253	22.200	SU223	-4.07	0.13	-49.6	0.1
Plot4-11/12/2016a	**SU224**	Ebenhaezer xylem		*S. mellifera*	12.5529	12.9897	12.8709		-12.871	0.272	29.738	SU224	-4.23	0.06	-50.1	0.2
Plot4-11/12/2016as	**SU225**	Ebenhaezer xylem		*S. mellifera*	12.5111	14.0712	13.447		-13.447	0.400	9.019	SU225				

				shrub												
Plot4-11/12/2016as	**SU226**	Ebenhaezer xylem		*S. mellifera* shrub	12.6098	14.2352	13.5656		-13.566	0.412	8.758	SU226	-13.78	0.04	-128.9	0.6
Plot4-11/12/2016b1	**SU227**	Ebenhaezer xylem		*B. albitrunca* 1	12.493	12.8793	12.7706		-12.771	0.281	33.340	SU227	-6.04	0.02	-58.9	0.7
Plot4-11/12/2016b1	**SU228**	Ebenhaezer xylem		*B. albitrunca* 1	12.5179	12.9355	12.7841		-12.784	0.363	30.976	SU228	-4.92	0.05	-55.3	0.2
Plot4-11/12/2016b2	**SU229**	Ebenhaezer xylem		*B. albitrunca* 2	12.5243	12.7956	12.7128		-12.713	0.305	47.164	SU229	-6.01	0.06	-69.2	0.2
Plot4-11/12/2016b2	**SU230**	Ebenhaezer xylem		*B. albitrunca* 2	12.542	12.8646	12.7666		-12.767	0.304	39.878	SU230	-5.52	0.06	-67.2	0.4
Plot5-11/12/2016a	**SU231**	Ebenhaezer xylem		*S. mellifera*	12.5249	13.0699	12.9461		-12.946	0.227	23.981	SU231	-0.92	0.02	-35.6	0.6
Plot5-11/12/2016a	**SU232**	Ebenhaezer xylem		*S. mellifera*	12.5312	13.0674	12.9486		-12.949	0.222	24.370	SU232	-0.59	0.06	-30.3	0.1
Plot5-11/12/2016as	**SU233**	Ebenhaezer xylem		*S. mellifera* shrub	12.5183	13.7816	13.293		-13.293	0.387	10.909	SU233	5.43	0.08	-52.1	1.0
Plot5-11/12/2016as	**SU234**	Ebenhaezer xylem		*S. mellifera* shrub	12.5531	14.0817	13.6011		-13.601	0.314	9.212	SU234				
Plot5-11/12/2016b	**SU235**	Ebenhaezer xylem		*B. albitrunca*	12.5424	12.8717	12.7606		-12.761	0.337	39.088	SU235	-5.90	0.04	-60.4	0.4
Plot5-11/12/2016b	**SU236**	Ebenhaezer xylem		*B. albitrunca*	12.4935	13.0081	12.8397		-12.840	0.327	25.278	SU236	-6.85	0.07	-66.2	0.2
Plot5-11/12/2016bs	**SU237**	Ebenhaezer xylem		*B. albitrunca* shrub	12.6332	13.9072	13.4346		-13.435	0.371	10.916	SU237	-20.40	0.02	-176.5	0.3
Plot5-11/12/2016bs	**SU238**	Ebenhaezer xylem		*B. albitrunca* shrub	12.5182	13.6282	13.2238		-13.224	0.364	12.278	SU238	-20.19	0.06	-174.9	0.6
Plot6-11/12/2016asm	**SU239**	Ebenhaezer xylem		*S mellifera* small	12.5172	13.069	12.9094		-12.909	0.289	23.684	SU239	-5.62	0.00	-62.2	1.1
Plot6-11/12/2016asm	**SU240**	Ebenhaezer xylem		*S. mellifera* small	12.5742	13.1099	12.9662		-12.966	0.268	24.472	SU240	-2.73	0.07	-45.8	0.3
Plot6-11/12/2016abi	**SU241**	Ebenhaezer xylem		*S. mellifera* big	12.6193	13.1631	12.9905		-12.991	0.317	24.206	SU241	-3.59	0.04	-45.4	0.3
Plot6-	**SU24**	Ebenhaeze		*S.*	12.627	13.210	13.0135		-13.014	0.338	22.659	SU24	-4.50	0.03	-51.4	0.3

11/12/2016abi	**2**	r xylem		*mellifera* big	4	4						2				
Plot1-12/12/2016a	**SU243**	Ebenhaezer xylem		*S. mellifera*	12.4913	13.218	12.977		-12.977	0.332	18.189	SU243	-11.71	0.10	-105.8	1.0
Plot1-12/12/2016a	**SU244**	Ebenhaezer xylem		*S. mellifera*	12.5181	13.0958	12.9192		-12.919	0.306	22.669	SU244	-13.28	0.08	-116.3	0.5
Plot1-12/12/2016b	**SU245**	Ebenhaezer xylem		*B. albitrunca*	12.5093	12.9259	12.8068		-12.807	0.286	31.027	SU245	-8.70	0.09	-78.0	0.4
Plot1-12/12/2016b	**SU246**	Ebenhaezer xylem		*B. albitrunca*	12.5921	13.0313	12.8993		-12.899	0.301	29.671	SU246	-8.08	0.06	-83.6	0.3
Plot1-12/12/2016o	**SU247**	Ebenhaezer xylem		*Omupopo*	12.5397	13.3564	12.9484		-12.948	0.500	16.354	SU247	-5.73	0.06	-42.5	0.4
Plot1-12/12/2016o	**SU248**	Ebenhaezer xylem		*Omupopo*	12.5067	13.4359	13.1257		-13.126	0.334	14.460	SU248	-7.78	0.08	-58.8	0.6
Plot2-12/12/2016a	**SU249**	Ebenhaezer xylem		*S. mellifera*	12.4596	13.1505	12.9952		-12.995	0.225	19.034	SU249	-1.54	0.05	-30.6	0.3
Plot2-12/12/2016a	**SU250**	Ebenhaezer xylem		*S. mellifera*	12.5323	13.0722	12.962		-12.962	0.204	24.212	SU250	-1.38	0.06	-28.5	0.1
Plot2-12/12/2016as1	**SU251**	Ebenhaezer xylem		*S. mellifera* shrub 1	12.4675	13.641	13.2771		-13.277	0.310	11.624	SU251	-6.89	0.06	-107.3	1.5
Plot2-12/12/2016as1	**SU252**	Ebenhaezer xylem		*S. mellifera* shrub 1	12.4679	13.531	13.1167		-13.117	0.390	12.728	SU252	-1.77	0.05	-69.5	0.3
Plot2-12/12/2016as2	**SU253**	Ebenhaezer xylem		*S. mellifera* shrub 2	12.5014	13.0569	12.7949		-12.795	0.472	23.505	SU253	-16.33	0.02	-137.5	0.4
Plot2-12/12/2016as2	**SU254**	Ebenhaezer xylem		*S. mellifera* shrub 2	12.5843	13.1962	12.9114		-12.911	0.465	21.566	SU254	-15.65	0.01	-134.1	1.4
Plot2-12/12/2016b	**SU255**	Ebenhaezer xylem		*B. albitrunca*	12.5255	13.4866	13.1772		-13.177	0.322	14.032	SU255	-6.25	0.05	-56.4	0.9
Plot2-12/12/2016b	**SU256**	Ebenhaezer xylem		*B. albitrunca*	12.4935	13.55	13.173		-13.173	0.357	12.825	SU256	-6.10	0.05	-61.6	0.1
Plot2-12/12/2016o	**SU257**	Ebenhaezer xylem		*Omupopo*	12.4953	12.8092	12.6878		-12.688	0.387	40.807	SU257	-10.14	0.02	-89.8	0.4
Plot2-12/12/2016o	**SU258**	Ebenhaezer xylem		*Omupopo*	12.6165	12.8959	12.7716		-12.772	0.445	46.156	SU258	-4.20	0.06	-46.0	0.6
Plot3-12/12/2016a	**SU259**	Ebenhaezer xylem		*S. mellifera*	12.4745	12.9767	12.8441		-12.844	0.264	25.840	SU259	-2.95	0.09	-41.1	0.3
Plot3-12/12/2016a	**SU260**	Ebenhaezer xylem		*S. mellifera*	12.5581	13.157	13.0477		-13.048	0.183	21.969	SU260	-6.68	0.02	-59.9	0.5
Plot3-12/12/2016b	**SU261**	Ebenhaezer xylem		*B. albitrunc*	12.5005	13.317	13.0243		-13.024	0.358	16.310	SU261	-7.93	0.08	-67.0	0.1

				a												
Plot3-12/12/2016b	**SU262**	Ebenhaezer xylem		*B. albitrunca*	12.521	13.2631	12.9808		-12.981	0.380	17.872	SU262	-6.97	0.07	-62.7	0.4
Plot4-12/12/2016a	**SU263**	Ebenhaezer xylem		*S. mellifera*	12.5375	13.1998	12.9933		-12.993	0.312	19.930	SU263	-6.27	0.06	-52.9	0.5
Plot4-12/12/2016a	**SU264**	Ebenhaezer xylem		*S. mellifera*	12.6034	13.281	13.1234		-13.123	0.233	19.600	SU264	-8.15	0.04	-64.9	0.5
Plot4-12/12/2016as	**SU265**	Ebenhaezer xylem		*S. mellifera* shrub	12.5446	13.7609	13.3656		-13.366	0.325	11.314	SU265	-15.56	0.17	-138.2	1.9
Plot4-12/12/2016as	**SU266**	Ebenhaezer xylem		*S. mellifera* shrub	12.5247	13.6426	13.2008		-13.201	0.395	12.204	SU266	-11.37	0.00	-110.8	0.6
Plot4-12/12/2016b1	**SU267**	Ebenhaezer xylem		*B. albitrunca* 1	12.5269	12.9596	12.8015		-12.802	0.365	29.951	SU267	-6.25	0.10	-64.2	0.2
Plot4-12/12/2016b1	**SU268**	Ebenhaezer xylem		*B. albitrunca* 1	12.4453	12.8617	12.6975		-12.698	0.394	30.888	SU268	-5.75	0.08	-61.3	0.4
Plot4-12/12/2016b2	**SU269**	Ebenhaezer xylem		*B. albitrunca* 2	12.6078	13.1649	12.9872		-12.987	0.319	23.631	SU269	-4.38	0.08	-52.4	0.4
Plot4-12/12/2016b2	**SU270**	Ebenhaezer xylem		*B. albitrunca* 2	12.4828	12.9002	12.8019		-12.802	0.236	30.906	SU270	-6.08	0.07	-54.6	0.2
Plot5-12/12/2016a	**SU271**	Ebenhaezer xylem		*S. mellifera*	12.4929	13.006	12.8979		-12.898	0.211	25.348	SU271	-7.89	0.04	-74.0	0.7
Plot5-12/12/2016a	**SU272**	Ebenhaezer xylem		*S. mellifera*	12.5067	13.0273	12.9042		-12.904	0.236	25.024	SU272	-5.10	0.08	-57.4	0.2
Plot5-12/12/2016as	**SU273**	Ebenhaezer xylem		*S. mellifera* shrub	12.4907	13.5438	13.2909		-13.291	0.240	12.861	SU273	-7.32	0.15	-151.0	1.0
Plot5-12/12/2016as	**SU274**	Ebenhaezer xylem		*S. mellifera* shrub	12.4873	13.4436	13.0811		-13.081	0.379	14.058	SU274	7.22	0.11	-45.9	0.3
Plot5-12/12/2016b	**SU275**	Ebenhaezer xylem		*B. albitrunca*	12.5121	13.2592	13.0046		-13.005	0.341	17.748	SU275	-5.34	0.08	-54.6	0.8
Plot5-12/12/2016b	**SU276**	Ebenhaezer xylem		*B. albitrunca*	12.5792	13.4451	13.1995		-13.200	0.284	15.527	SU276	-5.93	0.09	-58.3	0.4
Plot5-12/12/2016bs	**SU277**	Ebenhaezer xylem		*B. albitrunca* shrub	12.5373	13.6754	13.2648		-13.265	0.361	12.016	SU277	-24.35	0.09	-205.9	1.5
Plot5-12/12/2016bs	**SU278**	Ebenhaezer xylem		*B. albitrunca* shrub	12.5397	13.7599	13.3113		-13.311	0.368	11.277	SU278	-23.10	0.02	-195.1	0.3

Plot6-12/12/2016asm	**SU279**	Ebenhaezer xylem		*S. mellifera* small	12.5074	13.1787	13.0005		-13.001	0.265	19.632	SU279	-3.05	0.02	-47.9	1.2
Plot6-12/12/2016asm	**SU280**	Ebenhaezer xylem		*S. mellifera* small	12.4934	13.1986	13.0238		-13.024	0.248	18.716	SU280	-4.84	0.05	-55.6	0.2
Plot6-12/12/2016abig	**SU281**	Ebenhaezer xylem		*S. mellifera* big	12.4755	12.9365	12.8317		-12.832	0.227	28.062	SU281	-1.32	0.05	-36.0	0.1
Plot6-12/12/2016abig	**SU282**	Ebenhaezer xylem		*S. mellifera* big	12.5244	13.0022	12.9444		-12.944	0.121	27.213	SU282	-3.62	0.06	-49.0	0.0
Plot 1-11/03/2017a	**SU283**	Ebenhaezer xylem		*S. mellifera*	12.4754	12.7178	12.6832		-12.683	0.143	52.466	SU283	-19.70	0.15	-152.2	2.7
Plot 1-11/03/2017a	**SU284**	Ebenhaezer xylem		*S. mellifera*	12.5386	12.7786	12.6631		-12.663	0.481	53.244	SU284	-10.63	0.07	-80.7	1.4
Plot 1-11/03/2017b	**SU285**	Ebenhaezer xylem		*B. albitrunca*	12.5008	12.7944	12.6705		-12.671	0.422	43.578	SU285	-9.29	0.08	-81.9	0.5
Plot 1-11/03/2017b	**SU286**	Ebenhaezer xylem		*B. albitrunca*	12.4835	12.7988	12.6529		-12.653	0.463	40.592	SU286	-9.34	0.12	-75.8	0.4
Plot 2-11/03/2017a	**SU287**	Ebenhaezer xylem		*S. mellifera*	12.4814	12.7907	12.678		-12.678	0.364	41.354	SU287	-9.77	0.03	-71.6	0.3
Plot 2-11/03/2017a	**SU288**	Ebenhaezer xylem		*S. mellifera*	12.5215	12.9382	12.775		-12.775	0.392	31.049	SU288	-9.72	0.07	-72.0	0.4
Plot 2-11/03/2017b	**SU289**	Ebenhaezer xylem		*B. albitrunca*	12.5716	12.9225	12.7803		-12.780	0.405	36.827	SU289	-8.74	0.09	-75.8	0.6
Plot 2-11/03/2017b	**SU290**	Ebenhaezer xylem		*B. albitrunca*	12.5529	12.9855	12.8244		-12.824	0.372	30.017	SU290	-8.92	0.08	-78.2	0.4
Plot 3-11/03/2017a	**SU291**	Ebenhaezer xylem		*S. mellifera*	12.5568	12.8944	12.7526		-12.753	0.420	38.194	SU291	-9.89	0.09	-77.3	0.6
Plot 3-11/03/2017a	**SU292**	Ebenhaezer xylem		*S. mellifera*	12.5615	12.9089	12.7946		-12.795	0.329	37.159	SU292	-7.80	0.02	-70.3	0.1
Plot 3-11/03/2017b	**SU293**	Ebenhaezer xylem		*B. albitrunca*	12.5632	12.9111	12.7805		-12.781	0.375	37.112	SU293	-8.44	0.06	-38.4	0.5
Plot 3-11/03/2017b	**SU294**	Ebenhaezer xylem		*B. albitrunca*	12.4798	13.0194	12.8134		-12.813	0.382	24.128	SU294	-8.30	0.05	-33.6	0.5
Plot 4-11/03/2017a	**SU295**	Ebenhaezer xylem		*S. mellifera*	12.537	12.7101	12.6373		-12.637	0.421	73.426	SU295	-14.06	0.03	-114.7	0.5
No enough sample	**SU296**	Ebenhaezer xylem			12.4911	no enough			0.000	#VALUE!	#VALUE!	SU296				
Plot 4-11/03/2017b	**SU297**	Ebenhaezer xylem		*B. albitrunc*	12.4411	12.8105	12.6576		-12.658	0.414	34.679	SU297	-9.09	0.05	-79.2	0.7

				a												
Plot 4- 11/03/2017b	**SU29 8**	Ebenhaeze r xylem		*B. albitrunc a*	12.603 2	13.037 5	12.8447		-12.845	0.444	30.020	SU29 8	-7.81	0.17	-70.7	0.8
Plot 5- 11/03/2017a	**SU29 9**	Ebenhaeze r xylem		*S. mellifera*	12.579 5	12.913 1	12.7925		-12.793	0.362	38.708	SU29 9	- 11.14	0.05	-78.3	0.6
Plot 5- 11/03/2017a	**SU30 0**	Ebenhaeze r xylem		*S. mellifera*	12.536 9	12.956 6	12.7859		-12.786	0.407	30.871	SU30 0	- 10.96	0.07	-72.6	0.3
Plot 5- 11/03/2017b	**SU30 1**	Ebenhaeze r xylem		*B. albitrunc a*	12.527 8	12.821 3	12.7168		-12.717	0.356	43.684	SU30 1	-7.56	0.07	-71.7	0.1
Plot 5- 11/03/2017b	**SU30 2**	Ebenhaeze r xylem		*B. albitrunc a*	12.583 9	12.941 6	12.7755		-12.776	0.464	36.180	SU30 2	-7.61	0.07	-68.7	0.5
Plot 6- 11/03/2017asm	**SU30 3**	Ebenhaeze r xylem		*S. mellifera* small	12.463 2	12.708 4	12.5959		-12.596	0.459	51.829	SU30 3	- 11.66	0.10	-90.9	0.6
Plot 6- 11/03/2017asm	**SU30 4**	Ebenhaeze r xylem		*S. mellifera* small	12.558 5	12.806 6	12.7013		-12.701	0.424	51.619	SU30 4	- 12.72	0.09	-94.4	0.3
Plot 6- 11/03/2017abig	**SU30 5**	Ebenhaeze r xylem		*S. mellifera* big	12.531 4	12.863 2	12.7385		-12.739	0.376	38.768	SU30 5	- 11.19	0.03	-86.2	0.3
Plot 6- 11/03/2017abig	**SU30 6**	Ebenhaeze r xylem		*S. mellifera* big	12.544 9	12.940 4	12.7858		-12.786	0.391	32.719	SU30 6	-9.65	0.13	-79.4	0.8
Plot 2- 17/05/2017a	**SU30 7**	Ebenhaeze r xylem		*S. mellifera*	12.543 1	12.897 6	12.7863		-12.786	0.314	36.383	SU30 7	-4.50	0.09	-37.1	0.2
Plot 2- 17/05/2017a	**SU30 8**	Ebenhaeze r xylem		*S. mellifera*	12.486	12.803 4	12.7091		-12.709	0.297	40.338	SU30 8	-3.72	0.07	-44.2	0.4
Plot 2- 17/05/2017b	**SU30 9**	Ebenhaeze r xylem		*B. albitrunc a*	12.494 8	12.852 4	12.7058		-12.706	0.410	35.941	SU30 9	-9.26	0.13	-78.3	0.7
Plot 2- 17/05/2017b	**SU31 0**	Ebenhaeze r xylem		*B. albitrunc a*	12.454 7	12.795 7	12.6622		-12.662	0.391	37.524	SU31 0	-8.93	0.08	-71.0	0.3
Plot 3- 17/05/2017a	**SU31 1**	Ebenhaeze r xylem		*S. mellifera*	12.519 8	12.801 7	12.7076		-12.708	0.334	45.412	SU31 1	-4.44	0.05	-44.2	0.8
Plot 3- 17/05/2017a	**SU31 2**	Ebenhaeze r xylem		*S. mellifera*	12.510 9	12.754 6	12.7086		-12.709	0.189	52.337	SU31 2	-9.27	0.11	-77.3	0.9
Plot 3- 17/05/2017b	**SU31 3**	Ebenhaeze r xylem		*B. albitrunc a*	12.438 4	12.784 6	12.6736		-12.674	0.321	36.928	SU31 3	-8.49	0.05	-27.3	0.9
Plot 3- 17/05/2017b	**SU31 4**	Ebenhaeze r xylem		*B. albitrunc a*	12.560 7	13.003 7	12.7986		-12.799	0.463	29.354	SU31 4	-6.46	0.05	-19.5	0.5
Plot 4- 17/05/2017a	**SU31 5**	Ebenhaeze r xylem		*S. mellifera*	12.522 2	12.750 7	12.6671		-12.667	0.366	55.802	SU31 5	-5.18	0.02	-46.7	0.3

Plot 4-17/05/2017a	**SU316**	Ebenhaezer xylem		*S. mellifera*	12.4757	12.7218	12.6412		-12.641	0.328	51.694	SU316	-4.64	0.04	-47.7	0.2
Plot 4-17/05/2017b	**SU317**	Ebenhaezer xylem		*B. albitrunca*	12.197	12.576	12.4157		-12.416	0.423	33.182	SU317	-7.27	0.12	-62.7	0.6
Plot 4-17/05/2017b	**SU318**	Ebenhaezer xylem		*B. albitrunca*	12.1349	12.6014	12.4122		-12.412	0.406	27.013	SU318	-7.49	0.04	-63.3	0.4
Plot 5-17/05/2017a	**SU319**	Ebenhaezer xylem		*S. mellifera*	12.7429	13.1533	13.0037		-13.004	0.365	32.050	SU319	-4.00	0.05	-41.0	0.6
Plot 5-17/05/2017a	**SU320**	Ebenhaezer xylem		*S. mellifera*	12.6392	13.0062	12.8836		-12.884	0.334	35.439	SU320	-4.23	0.10	-48.2	0.4
Plot 5-17/05/2017b	**SU321**	Ebenhaezer xylem		*B. albitrunca*	12.3629	12.6923	12.5396		-12.540	0.464	38.532	SU321	-6.85	0.09	-63.5	0.6
Plot 5-17/05/2017b	**SU322**	Ebenhaezer xylem		*B. albitrunca*	12.2951	12.7382	12.5469		-12.547	0.432	28.748	SU322	-6.75	0.12	-66.1	0.3
Plot 6-17/05/2017asm	**SU323**	Ebenhaezer xylem		*S. mellifera* small	12.684	13.1295	12.9784		-12.978	0.339	29.471	SU323	-3.84	0.05	-38.0	0.4
Plot 6-17/05/2017asm	**SU324**	Ebenhaezer xylem		*S. mellifera* small	12.2145	12.6137	12.4828		-12.483	0.328	31.597	SU324	-3.94	0.08	-43.1	0.5
Plot 6-17/05/2017abig	**SU325**	Ebenhaezer xylem		*S. mellifera* big	12.6881	13.0358	12.9029		-12.903	0.382	37.492	SU325	-4.22	0.05	-39.5	0.0
Plot 6-17/05/2017abig	**SU326**	Ebenhaezer xylem		*S. mellifera* big	12.3085	12.6331	12.5042		-12.504	0.397	38.919	SU326	-4.78	0.08	-50.0	0.2
Plot5-10/12/2016as	**SU327**	Ebenhaezer xylem		*S. mellifera* shrub	12.8987	13.5629	13.3123		-13.312	0.377	20.420	SU327	0.81	0.04	-60.3	0.8
Plot5-10/12/2016as	**SU328**	Ebenhaezer xylem		*S. mellifera* shrub	12.3231	13.2009	12.8699		-12.870	0.377	15.039	SU328	1.42	0.05	-55.9	0.6
Plot 2-07/12/2016b	**SU329**	Ebenhaezer xylem		*B. albitrunca*	12.6065	12.859	12.7911		-12.791	0.269	50.927	SU329	-0.29	0.03	-30.2	0.5
Plot 2-07/12/2016b	**SU330**	Ebenhaezer xylem		*B. albitrunca*	12.6165	12.847	12.7827		-12.783	0.279	55.735	SU330	0.26	0.07	-28.8	0.2